The Modulation of Synaptic Function by Dopamine in the Lateral Entorhinal Cortex

Laura Harvey

Doctor of Philosophy

Aston University

June 2024

Aston University

The Modulation of Synaptic Function by Dopamine in the Lateral Entorhinal Cortex

Laura Harvey

Doctor of Philosophy, June 2024

Forming new declarative memories requires integrating sensory information in the entorhinal cortex and its transfer through the hippocampal circuit. To understand the entorhinal cortex's role in cognition, factors affecting superficial layer projection neuron excitability and mechanisms of sensory information encoding must be identified. Modulatory neurotransmitter systems shape synaptic processes required for encoding and retaining information and influence membrane excitability. The neurotransmitter dopamine, linked to Schizophrenia and Parkinson's disease also regulates learning and memory. Dopaminergic neurons from the ventral tegmental area project widely, including to the lateral entorhinal cortex, strongly affecting neuron responsiveness and excitability. However, the effects of dopamine on synaptic plasticity remain unclear. To investigate this, intra- and extracellular electrophysiological recordings, pharmacological interventions, and neuronal tracing were used to assess synaptic transmission, plasticity, and cellular morphology in rat lateral entorhinal cortex slices *in vitro*. Results showed that dopamine suppressed sensory inputs to the lateral entorhinal cortex via a D_2 receptor-mediated reduction in glutamate release from sensory afferents projecting to the superficial layers. Dopamine application paired with low-frequency stimulation blocked activity-dependent LTD, but this was reversed by a priming application of dopamine, which triggered clathrin-dependent internalisation of dopaminergic receptors for up to 3 hours. Previous exposure to dopamine affected future responsiveness to the agonist, potentially representing a novel form of metaplasticity in the lateral entorhinal cortex. Blocking metabotropic receptor desensitisation with the β-arrestin inhibitor, barbadin, prevented receptor internalisation and restored the dopamine-mediated block of LTD. Tetanic stimulation intended to induce LTP in sensory inputs to superficial layer II induced LTD instead, mediated partly by stimulation-induced changes in local inhibition and dopaminergic tone. Superficial layer projection neurons are resistant to LTP induction, but methods to boost NMDA receptor activation restored the capacity of these neurons to support short-term potentiation following high frequency stimulation. Together, these data highlight multiple mechanisms by which dopamine exposure can modulate sensory and mnemonic processing in the medial temporal lobe. This modulation occurs through the regulation of basal synaptic transmission and activity-dependent plasticity in the lateral entorhinal cortex.

Key Words: *Synaptic Plasticity, Desensitisation, Metaplasticity, Long-Term Potentiation, Long-Term Depression*

- Acknowledgements -

First, my deepest gratitude goes to my academic supervisors, Dr Douglas Caruana and Professor Gavin Woodhall, for their boundless knowledge, scientific guidance and helpful critiques throughout this project. Particularly, thank you Doug for the copious amount of time and effort you have invested in this project and into my own personal and professional development.

Thank you to Aston University for funding this PhD project and for your generous additional support regarding Coronavirus extensions and bursaries. I would also like to extend thanks to all the project and placement students over the three years for their assistance in preparing solutions and monitoring experiments. A huge thank you to the Biomedical Team, especially Matt and Wayne. Without your extended efforts, going above and beyond for me, this journey would have been substantially more challenging.

Thank you to all the amazing and inspiring people I had the pleasure of studying alongside at Aston University: Ellen, Nicole, Carolina, Idoia, Cristina, Bita, to name a few, I am so proud of all of you. Thank you, also, to my old friends whom, despite the distance, have given me endless laughs and created a fantastic support network around me. Aatikah, Rachel, Haleema, Matt and Mel. I would not be the person I am today without your support.

Above all, thank you to my family for their unwavering support on my journey. Thank you, Mum and Dad, for your patience and understanding, your guidance, and your unconditional love. Thank you, Jack and Ben, for your time and humour. Thank you, Katie, for being my energy and sanity. And Danny, my love, thank you for being the brightest star on my darkest nights. I dedicate this Thesis to you all.

- List of Contents -

List of Abbreviations

A_1/ A_{2A} – adenosine A_1/ A_{2A} receptor

ACSF – artificial cerebral spinal fluid

AMPA – α-amino-3-hydroxy-5-methyl-4-isoxazole propionic acid

ANOVA – analysis of variance

AP2 – adapter protein 2

AP5 – (2R)-amino-5-phosphonovaleric acid

BAPTA – 1,2-bis(o-aminophenoxy)ethane-N,N,N′,N′-tetraacetic acid

BDNF – brain derived neurotropic factor

Ca^{2+}/K^+/Mg^{2+}/Na^+ – calcium/potassium/magnesium/ sodium ion

CaCl – calcium chloride

CaMKII – calcium–calmodulin dependent protein kinase II

cAMP – cyclic adenosine monophosphate

CA1/2/3 – *cornu ammonis 1/2/3*

CMPD101 – compound 101

CsCl – ceasium chloride

D_1 - D_5 – dopamine 1-5 receptor

D_1-/ D_2-like – D_1 & D_5/ D_2, D_3 & D_4 receptors

DA – dopamine

DAPI – 4′,6-diamidino-2-phenylindole

DC – direct current

EC_{50} – half maximal effective concentration

EGTA – ethylene glycol-bis (β-aminoethyl ether)-N,N,N′,N′-tetraacetic acid

E/IPSC – excitatory/inhibitory postsynaptic current

fEPSP – field excitatory postsynaptic potential

FSL – flinders sensitive line

GABA – gamma-aminobutyric acid

GPCR – g-protein-coupled receptor

GRK2/3/5 – g-protein-coupled receptor kinase2/3/5

HEPES – 4-(2-hydroxyethyl)-1-piperazineethanesulfonic acid

HFS – high frequency stimulation

HPLC – high performance liquid chromatography

i/mGlu – ionotropic/metabotropic glutamate receptor

IPI – interpulse interval

KCl – potassium chloride

K-gluconate – potassium gluconate

KYNA – kynurenic acid

LTD/P –long-term depression/potentiation

Mdm2 – murine double minute 2

MgCl – magnesium chloride

mGluR – metabotropic glutamate receptor

Na^+-ATP – sodium-adensosine triphosphate

Na^+-GTP – sodium-glycine triphosphate

$NaHCO_3$ – sodium carbonate

NaH_2PO_4 – monosodium phosphate

Nedd4 – neural precursor cell expressed developmentally down-regulated 4

NMDA – n-methyl-d-aspartate

PBS – phosphate buffered solution

PET (imaging) – positron emission tomography

PKA – protein kinase A

PP1/2B – protein phosphatase 1/2B

PP-LFS – paired-pulse low-frequency stimulation

R_m – membrane resistance

R_s – series resistance

SEM – standard error of the mean

TEA-Cl – tetraethylammonium chloride

TBS – theta burst stimulation

V_h – membrane holding voltage

List of Figures

Chapter 1: General Introduction

Memory

It is undeniable that the fundamental cognitive processes of memory formation, consolidation, storage, and retrieval are complex. Within the scientific community, it is generally accepted that humans have at least two major types of memory that vary in terms of their temporal properties: short-term memory and long-term memory (Waugh and Norman, 1965; Glanzer and Cunitz, 1966; Cowan, 2008). These differ based on the encoding format, capacity and duration of information. The former helps us to make decisions and perform common tasks in day-to-day life but holds only 5 to 9 different, predominantly auditory, pieces of information for less than eighteen seconds (Atkinson and Shiffrin, 2024). Long-term memory, in contrast, serves as a 'data bank' of information comprised of persistent representations of previous events, encounters and acquired skills lasting minutes, hours, years, or a lifetime encoding for all types – visual, auditory, semantic, etc. – of information with unlimited capacity (Broadbent, 1958; Ward, 2020; Atkinson and Shiffrin, 2024). In this way, long-term memory exists as an amalgamation of several different variants that collectively adhere to the multiple memory systems approach (Nyberg and Tulving, 1996). According to this, information is not stored long-term as a single and distinct unit of information but as an overlap of qualitatively different types of persistent experiences or memories (Nyberg and Tulving, 1996). For example, an experience recalled in a conscious manner, like supporting your favourite team at an important football match would be classed as a declarative (also known as explicit) memory, whilst non-declarative (or implicit) memories are often unconsciously retrieved, and manifest in the form of skills or learned behaviours (Dickerson and Eichenbaum, 2010). Declarative memory can consist of both episodic and semantic components, a distinction which was first proposed and described by Endel Tulving (Tulving and Donaldson, 1972; Nyberg, McIntosh and Tulving, 1998). Episodic memory consists of personal experiences that are unique to an individual, whereas semantic memory is comprised of general knowledge and facts. These two forms of memory involve overlapping brain regions for their acquisition and consolidation, but not necessarily for their long-term retention (Nyberg, McIntosh and Tulving, 1998). The encoding and consolidation of declarative memories occurs within the hippocampal formation and parahippocampal cortices, of which the entorhinal cortex is a critical component that is instrumental in orchestrating the flow of sensory information destined for processing by the hippocampus (for review see Hasselmo, 2006; Canto, Wouterlood and Witter, 2008; Nilssen *et al.* 2019).

The Medial Temporal Lobe

In the mammalian brain, the hippocampal formation and parahippocampal cortices are situated bilaterally, occupying a significant proportion of the medial temporal lobe (see **Figure 1.1**). The hippocampal formation is comprised of the dentate gyrus, area *cornu ammonis* 1 (CA1), CA2, CA3 and the subicular complex

(subiculum proper; pre- and parasubiculum) (Andersen *et al*., 2007). The surrounding parahippocampal cortices contain the perirhinal, postrhinal and entorhinal (lateral and medial) cortices (Agster and Burwell, 2013; for review see Witter *et al*., 2017). The relevance of these areas to the formation of a set of interconnected structures critical for long-term memory acquisition and consolidation was made evident following detailed analyses of patients with significant bilateral trauma to the medial temporal lobe, such as the anterograde amnesia observed in patient H.M. This case involved a bilateral medial temporal lobe resection that involved the separation and removal of a large section of the medial temporal lobe including but not limited to parts of the amygdala, hippocampus and entorhinal cortex, commonly referred to as a temporal lobectomy. The key element here is the *post-hoc* finding that, as with many of the other patients receiving temporal resections, the ability to form new episodic memories was severely impaired, H.M. was unable to form new autobiographical memories. Interestingly, memories for previously learned semantic information – understanding the meaning of words, for example – was not significantly affected in follow-up cognitive examinations (Milner, 1972; Corkin, 2014), and the inability to recall any novel semantic formation did not appear to affect his capacity to have 'normal' conversations and understand complex sentences using preoperatively formed semantic memory (Dossani, Missios and Nanda, 2015). Another notable outcome of the operation was H.M.'s unaffected ability to improve upon tasks following practice, showing intact procedural memory, most notably examined using mirror drawing tasks (Milner, Corkin and Teuber, 1968). Although this procedure is extreme, it was only to reduce the severity of epileptic seizures in patients with debilitating symptoms, including H.M. Less invasive and more tailored approaches are used more commonly today, for example, patients with severe forms of epilepsy are more thoroughly screened and examined to provide a more accurate view of where the epileptic regions are allowing for a more precise and selective resection of damaged tissue (Scoville and Milner, 1957; for review see Boling, 2018).

Patient H.M.'s case is notable due to the 'frankly experimental' (Scoville and Milner, 1957, pg. 11) nature of the procedure and the profound anterograde amnesia that ensued. In the intervening years following surgery, H.M. underwent repeated assessment and testing to determine the precise structures resected during the surgery. Speculation arose that it was not only a large portion of the hippocampal formation that was resected from H.M.'s brain, but also part of the surrounding parahippocampal cortices, including the entorhinal cortex. Subsequent analysis of images of patient H.M.'s brain indicated that the entire entorhinal cortex was disconnected from the hippocampus in both hemispheres, likely rendering the remaining posterior third of the hippocampus non-functional (Corkin *et al.*, 1997; Annese *et al.*, 2014; Dossani, Missios and Nanda, 2015). This, along with studies looking into the medial temporal lobe memory system of monkeys, (Zola-Morgan *et al.*, 1989; Meunier *et al.*, 1993; Suzuki *et al.*, 1993; Zola-Morgan *et al.*, 1993), has helped to elucidate the intricate and complex interconnectivity and cooperativity of the temporal lobe in regards to long-term declarative memory acquisition, consolidation and storage (for review see Eichenbaum, Yonelinas and Ranganath, 2007; Squire, Stark and Clark, 2004). These findings suggest that medial temporal lobe structures – perirhinal, entorhinal and hippocampal regions – show a cooperative role in memory processing and consolidation. Studies indicate that perirhinal lesions result in severe deficits in visual recognition and long-term memory, while the entorhinal

cortex is crucial for connectivity with the hippocampus acting as an input and relay for memory storage (Zola-Morgan *et al.*, 1989; Meunier *et al.*, 1993; Zola-Morgan *et al.*, 1993; Eichenbaum, Yonelinas and Ranganath, 2007).

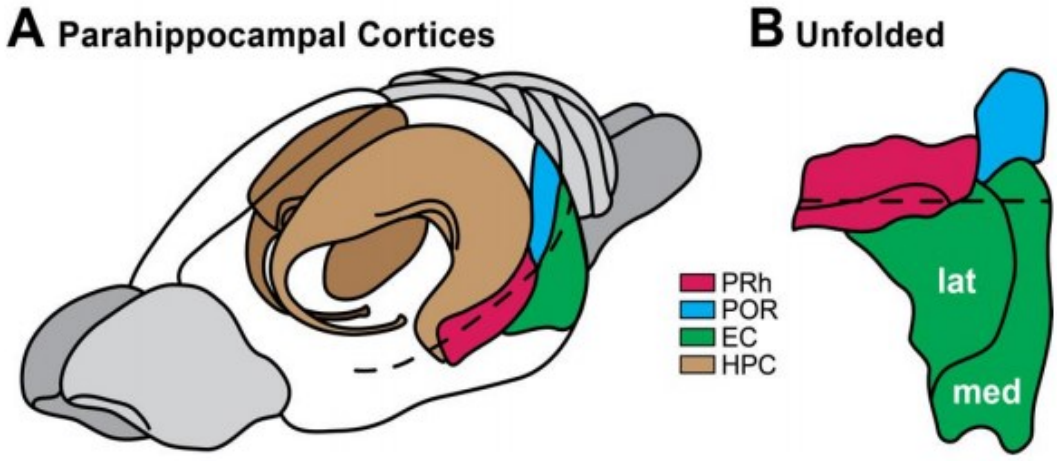

Figure 1.1. The hippocampal formation is located adjacent to the parahippocampal cortices. *The anatomical proximity shared between the hippocampus and the parahippocampal cortices is critical to the formation and consolidation of declarative memory. (**A**) The hippocampus (HPC) is flanked laterally by the parahippocampal cortices, including the entorhinal cortex (EC, green), perirhinal cortex (PRh, pink) and postrhinal cortex (POR, blue). (**B**) The medial (med) and lateral (lat) areas of the entorhinal cortex are highlighted in the unfolded view of the parahippocampal cortices. Data in (**A**) is adapted from Amaral and Witter (1995) and data in (**B**) is adapted from Burwell and Amaral (1998b).*

Both the hippocampus and entorhinal cortex (among others) are critical to the formation (or encoding) of new memories, formatting the information in a way that can be 'read' by the hippocampus, as well as for the consolidation of this information required for the conversion of short-term memory to long-term memory storage. Indeed, the entorhinal cortex is uniquely positioned to provide the hippocampus with an array of multimodal sensory information, integrating that of olfactory, auditory and visual cues, originating from major cortical sensory systems outside the hippocampal formation (Burwell *et al.*, 2004). It is believed that the entorhinal cortex acts as a gate to regulate the flow of sensory signals: originating from the piriform cortex carrying olfactory-rich information directly to the entorhinal cortex; direct signals from visual association areas (inferior temporal cortices in primates, parietal and occipital areas in rodents) for object recognition and interpretation; connections from prefrontal cortex adding contextual salience (attention-based); as well as the vast connectivity between entorhinal and the adjacent perirhinal and postrhinal cortices known for sensory (olfactory dominant) and spatial (visual dominant) information (Burwell, 2000; Knierim, Neunuebel and Deshmukh, 2014; Schroder *et al.*, 2015). These signals enter the hippocampus where they are integrated further with associated contextual and temporal cues (Canto and Witter, 2012a; Witter *et al.*, 2017).

Brodmann was the first to refer to the ventroposterior portion of the parahippocampal cortices as the '*entorhinal*' area, and this nomenclature was based largely on the location of the entorhinal cortex relative to the rhinal sulcus (for review see Canto, Wouterlood and Witter, 2008). The word '*ento*' is derived from Latin roots to mean '*within*' giving the word 'entorhinal' the literal meaning '*within the rhinal sulus*.' The entorhinal cortex itself can be divided into two main parts: the lateral division and the medial division. Both regions of the entorhinal cortex innervate the hippocampus, and these robust projections carry diverse types of sensory information, olfactory and visual, via divergent paths to different targets within the hippocampus proper (see **Figure 1.2**). Area CA3 and the dentate gyrus are innervated by layer II neurons of both the medial division and lateral division of the entorhinal cortex to form the perforant path (Vyleta and Snyder, 2021; for review see Jones and McHugh, 2011). Both superficial layers II and III of the medial division and lateral division of the entorhinal cortex also have a direct path to area CA2 (for review see Jones and McHugh, 2011; Burwell, 2000). The temporoammonic path is formed of parallel but distinct projections from layer III of the lateral and medial entorhinal cortex to neurons in area CA1 of the hippocampus (for review see Jones and McHugh, 2011; see also **Figure 1.2**). These four main inputs originating from the entorhinal cortex terminate at different locations in the hippocampus: two distinct perforant path projections to area CA3 and the dendate gyrus, the direct projection to area CA2 and the temporoammonic path projecting to area CA1, are thought to carry qualitatively distinct types of sensory information (Stanton and Sejnowski, 1989; Christie and Abraham, 1992; for review see Burwell, 2000; Knierim *et al*., 2014)

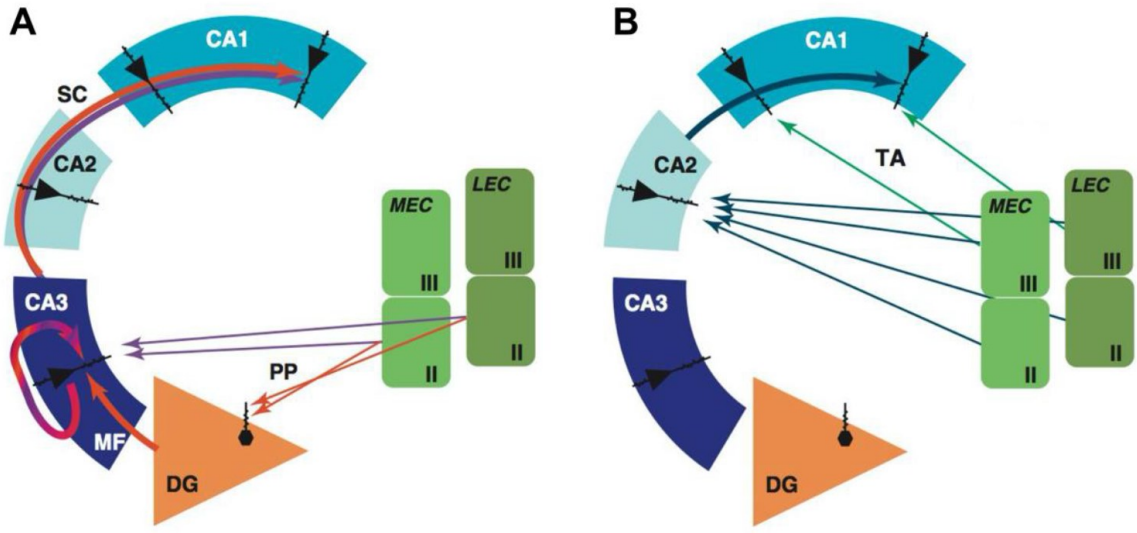

Figure 1.2. There are multiple parallel pathways entering the hippocampus from the entorhinal cortices. *(**A**) Area CA3 and the dentate gyrus (DG) are innervated by layer II neurons of both the medial and lateral entorhinal cortices (MEC and LEC, respectively), and these separated axons are referred to as the medial or lateral perforant path (PP), respectively. (**B**) Layer II and layer III neurons of the medial and lateral entorhinal cortex also have a direct cortical path to area CA2. Layer III neurons of the medial and lateral entorhinal cortices synapse with neurons in area CA1 via neighbouring but distinct projections known as the temporoammonic path (TA). These four output pathways from the entorhinal cortex directly connect with four separate targets within the hippocampus. MF, mossy fibres; SC, Schaffer collaterals. Figure adapted from the review by Jones and McHugh (2011).*

The medial division of the entorhinal cortex is believed to convey spatial sensory information to the hippocampus proper, whereas the lateral division is thought to provide non-spatial sensory signals. In particular, the medial entorhinal cortex contains spatially-tuned cells known as 'grid cells', suitably named for their role in firing in a 'grid-like' tessellating pattern to help create an internal map of the external environment (Hargreaves *et al*., 2005; Iwase, Kitanishi and Mizuseki, 2020; for review see Moser, Kropff and Moser, 2008; Moser *et al*., 2014; Fukawa *et al*., 2020).

The lateral entorhinal cortex, in contrast, has not received as much attention in the literature as the medial division over the last two decades, despite the close anatomical proximity and interconnectivity shared by the two regions (Vandrey *et al.*, 2022). Decline in interest in the lateral entorhinal cortex during this time may be attributed to the discovery of grid cells in the medial division by Fyhn, Moser and Moser in 2004 (Fyhn *et al.*, 2004). Following this discovery, intensive research focused specifically on uncovering links between entorhinal grid cells and hippocampal place cells (O'Keefe and Dostrovsky, 1971; O'Keefe and Nadel, 1978) in spatial processing and spatial navigation. Indeed, this work earned Edvard Moser, May-Britt Moser and John O'Keefe the Nobel Prize in Physiology or Medicine in 2014, after which research into the role of the medial entorhinal cortex and spatial memory only grew more intense. In fact, between 2012 and 2021 over 160 papers mentioning 'medial entorhinal cortex' in the title were published, whereas 'lateral entorhinal cortex' was noted in less than 60 publications during the same period (Source: National Library of Medicine; see **Appendix A**). Although the nature of the non-spatial information innervating the lateral entorhinal cortex was not as widely studied, research into the lateral division persevered (Agster and Burwell, 2013; Basu *et al.*, 2016). In the rodent brain, non-spatial information reaching the lateral entorhinal cortex is predominantly olfactory, originating from the piriform (primary olfactory) cortex (for a review, see Burwell, 2000). Additionally, olfactory cues from accessory olfactory systems reach the entorhinal cortex via the amygdala, where signals from these two systems are thought to be compared, playing a key role in social and reproductive behaviours in rodents. (Liu *et al.*, 2024). Within the temporal lobe, the lateral entorhinal cortex is highly interconnected with the perirhinal cortex, a structure that plays a key role in the identification and recognition of objects in the environment (Bashir *et al.*, 1993a; Warburton *et al.*, 2003; Warburton *et al.*, 2005; Agster and Burwell, 2013). Lateral entorhinal cortex projections supply the hippocampus with neuronal inputs coding for odour (Igarashi *et al.*, 2014), object novelty (Deshmukh and Knierim, 2011), object-place associations (Tsao, Moser and Moser, 2013), contextual salience (Basu *et al.*, 2016), time-point associations (Tsao *et al.*, 2018) and cue-reward associations (Lee *et al.*, 2021).

The Entorhinal Cortex and Brain Disease

Knowledge of memory formation and consolidation is critical to furthering our understanding of brain pathophysiology, including schizophrenia. Experimental work conducted by Otmakhova and Lisman (1999)

suggested that the salience of sensory cues in the formation of new memories is mediated, in part, by the entorhinal cortex. It is important to note, this path is referred to as the perforant pathway in the study described but is now commonly termed the 'temporoammonic' pathway (Vago, Bevan and Kesner, 2007). This study by Otmakhova and Lisman (1999) assessed synaptic transmission in area CA1 to measure the salience of temporoammonic path inputs against inputs via Schaffer collaterals. In their slice preparation, axons between areas CA3 and CA1 were cut to prevent any indirect inputs via the perforant path from the entorhinal cortex influencing recordings. During the experiments, dopamine, or specific dopamine receptor antagonists, such as broad-spectrum clozapine, D_1/D_5 receptor specific SCH-23390, and D_2 receptor specific eticlopride, were applied to the slices and changes in fEPSP amplitude in area CA1 were measured. They demonstrated that dopamine selectively affects inputs to the distal part of the stratum lacunosum-moleculare in area CA1, suppressing direct inputs from the entorhinal cortex while sparing indirect inputs from Schaffer collaterals via area CA3, which may influence the encoding of specific olfactory and visual information. (Otmakhova and Lisman, 1999). They also proposed that dopamine *hyperfunction* in area CA1 could isolate sensory inputs from the entorhinal cortex entering area CA1 from those originating in CA3 or the dentate gyrus leading to potential errors in comparisons between new sensory signals and existing long-term memories. The comparison of these inputs are thought to provide a basis for whether new sensory information is novel enough to be encoded as a new memory, or if it is simply much too similar to preexisting information to warrant encoding (Otmakhova and Lisman, 1999). In the brains of schizophrenic patients, information processing within the hippocampus is altered leading to incorrect associations and an increase in random memory associations propagating from the entorhinal cortex to area CA1: specifically, delusions (Lisman *et al.*, 2010). This could be mediated by the presence of excessive dopaminergic tone in area CA1 (Otmakhova and Lisman, 1999). An imaging study by Baiano *et al.* (2008) scanned the brains of control and schizophrenic patients using MRI and compared the cortical volumes of the hippocampus and the entorhinal cortex between the two groups. They found that the entorhinal cortex of schizophrenic patients was significantly smaller in volume compared to control patients, though, hippocampal volume was consistent between the groups. It was suggested that the shrinkage of the entorhinal cortex in schizophrenic patients may contribute to the cognitive abnormalities associated with the disease (Baiano *et al.*, 2008). However, more recent findings by Ho *et al.* (2011) suggest that chronic use of various antipsychotic medications, including clozapine and haloperidol, underlies the reduction in cortical volume in the entorhinal and not the progression of disease itself (for review see Zipursky *et al*., 2013). These medications target a range of receptors. For example, haloperidol is a first-generation antipsychotic known for its efficacy in antagonising D_2-like dopaminergic receptors. In contrast, clozapine, a second-generation antipsychotic, antagonises both D_2 and serotoninergic 2A receptors and is therefore believed to exert its therapeutic effects through these mechanisms. (Li, Snyder and Vanover, 2016). However, both clozapine and haloperidol also bind to every other dopamine receptor subtypes (D_1 to D_5), multiple serotonin receptors and several adrenergic receptors, including the histaminergic H_1 and muscarinic M_1 receptor at different affinities with unknown downstream effects (Li, Snyder and Vanover, 2016). Despite this, decreases in the volume of medial temporal lobe structures, like the entorhinal cortex, are still correlated with symptoms of schizophrenia and psychosis such as altered spatial

memory (Roalf *et al.*, 2017; Guo, Ragland and Carter, 2019). This is likely due to the role of the entorhinal cortex within the medial temporal lobe in integrating spatial and non-spatial information. Without this integration, aspects of spatial memory may become inaccurate or entirely absent when received by the hippocampus for further processing and storage (for review see Hasselmo, 2006; Canto, Wouterlood and Witter, 2008; Guo, Ragland and Carter, 2019; Nilssen *et al.* 2019).

Schizophrenia is not the only neurological disorder that has been linked to entorhinal cortex dysfunction. Specifically, major depressive disorder, chronic stress and Alzheimer's disease have all been linked to impaired functioning of the lateral entorhinal cortex (Sunanda, Meti and Raju, 1997; Schultz *et al.*, 2018; Li *et al.*, 2023). In Alzheimer's disease, the pathology begins in the entorhinal cortex before spreading to other regions of the brain (Schultz *et al.,* 2018; for review see Fu, Hardy and Duff, 2018). Interestingly, impairments in olfactory processing are among the first symptoms reported in early Alzheimer's dementia, as well as throughout the progression of psychosis and cognitive decline in schizophrenic patients (Yoo *et al.*, 2018). In Alzheimer's disease, impairments in olfactory function are likely the result of neurofibrillary tangles: intracellular aggregates of the micro-tubule associated protein, tau, into an insoluble hyperphosphorylated structure. These form in both the entorhinal cortex and area CA1 during the early phases of disease progression (Yoo *et al.*, 2018). The exact cause leading to the emergence of these tangles has yet to be fully elucidated. However, there is emerging evidence suggesting a mutation of the amyloid-β precursor protein leading to a build-up in excessive production of amyloid-β in the intracellular environment, specifically within the hippocampal and entorhinal regions of the medial temporal lobe. This build-up of amyloid-β into plaques appears prior to the neurofibrillary tau tangles leading to speculation regarding the influence of amyloid-β-plaque build-up to the rapid increase of neurofibrillary tangles. (Sheppard and Coleman, 2020; Roda *et al.*, 2022). The appearance of amyloid-β plaques and neurofibrillary tangles in the entorhinal cortex likely accounts for altered olfactory function since it is this region of the medial temporal lobe that is responsible for the integration of olfactory signals to the hippocampus for memory consolidation and storage (Igarashi *et al.*, 2014). Interestingly, other neurodegenerative diseases, relating to Alzheimer's disease, also encounter early-stage olfactory disturbance, specifically olfactory discrimination (Franco, Garrigos and Lillo, 2024). In Parkinson's disease, olfactory receptor expression is altered within the frontal cortex even before any hallmark motor symptoms occur, like tremors (Ferrer, 2009). As with Huntington's disease, deterioration of the entorhinal cortex was directly correlated with the olfactory deficits regarding this disease (Barrios *et al.*, 2007).

A recent study by Li *et al.* (2023) showed that functional connectivity between the entorhinal cortex and surrounding brain regions, including the hippocampus, was reduced following chronic restraint stress to induce anxiety- and depressive-like behaviours in rats. It is thought that both chronic stress and depression can lead to neuronal cell death so the reduced functional connectivity within the temporal lobe observed by Li *et al.* (2023) could reflect a loss of neurons in the entorhinal cortex that innervate nearby regions, including the hippocampus. Furthermore, Sunanda, Meti and Raji (1997) showed significant atrophy of CA3 neurons following chronic restraint stress, but if perforant path axons were ablated prior to the stress then the atrophy of CA3 neurons

was significantly reduced. This suggests that periods of chronic stress alter activity in entorhinal cortex projections to the hippocampus in a way that results in the atrophy of targets in area CA3, possibly through stress-induced elevations in glutamate release from perforant path terminals (Sunanda, Meti and Raju, 1997). Interestingly, the release of glutamate in the entorhinal cortex is regulated by local fluctuations in levels of extracellular dopamine (Caruana *et al.*, 2006; Harvey, 2020), and this may be a co-factor contributing to the atrophy of both hippocampal and entorhinal neurons observed following periods of chronic stress.

Principle Neurons in the Superficial Layers of the Entorhinal Cortex

A unique feature of the entorhinal cortex is that it receives input from a variety of different sensory modalities like olfactory, visual and auditory, but the density of the input to the entorhinal cortex differs considerably depending on the sensory system (see **Figure 1.3**). Critically, the inputs also differ in terms of how strongly they innervate the medial or the lateral division of the entorhinal cortex, specifically. For example, the lateral entorhinal cortex receives predominantly olfactory signals either directly via a robust monosynaptic projection originating from the piriform cortex, the main olfactory system in the rat brain, or via polysynaptic relays through the perirhinal cortex (Burwell and Amaral, 1998; for review see Burwell, 2000). Regardless of the sensory modality and whether the input terminates in the medial or lateral division, it is neurons in the *superficial layers* (layers II and III) of the entorhinal cortex that receive these sensory signals. This information is then propagated to the hippocampus via the multiple parallel streams: including the perforant and temporammonic pathways, discussed earlier in this Chapter (see also **Figure 1.2**). Once processed by the hippocampus, information is then returned once more to the entorhinal cortex, but these efferent projections are sent to the deep layers (layers V and VI) where it is relayed back to the original cortical and subcortical sensory regions. This forms a loop whereby the entorhinal cortex acts as a gate serving as both the entrance point and exit point for a vast amount of sensory information into and out of the hippocampus (for review see Canto, Wouterlood and Witter, 2008; Witter *et al*., 2017; Nilssen *et al*., 2019). Another sensory system to consider is the vestibular system, which provides a major source of idiothetic cues related to self-motion in rats and other mammals. Damage to the peripheral vestibular system can result in deficits across various spatial tasks, including navigation based on idiothetic cues and object recognition tasks. This highlights a critical functional interaction between vestibular input and the entorhinal cortex network, which processes spatial information and supports navigation (for review see Jacob *et al*., 2014). Interestingly, sensory input to the hippocampus can be modulated by feedback originating from deep layer collaterals to superficial layer projection neurons. In this way, hippocampal output has the capacity to regulate its own input by modulating the excitability of superficial layer projection neurons directly (Kloosterman, van Haeften and Lopes da Silva, 2004). It is important to note that although there are projections returning to the deep layers of the entorhinal cortex from the hippocampus, these are not the only efferent connections originating from the hippocampus. The hippocampus, along with the entorhinal cortex, is also part of a well-known system named the Papez circuit. This network includes projections that connect the fimbria, fornix, mammillary body, anterior nucleus of the

thalamus and the cingulate gyrus (Chauhan *et al.*, 2021). At the level of the hippocampus, projections from the perforant path in the entorhinal cortex synapse onto granule neurons in the dentate gyrus, which then send mossy fibres to the apical dendrites of pyramidal neurons in area CA3. Further projections extend from area CA3 to area CA1 via Schaffer collaterals and then to the subiculum. Additionally, CA3 pyramidal cells give rise to white matter fibres known as the alveus, which continue as the fimbria before forming the fornix. White matter tracts from the subiculum also contribute to this fibre pathway, ultimately forming the major hippocampal output. (Chauhan *et al.*, 2021). This white matter tract connects the hippocampus to the mammillary bodies, the thalamus and the cingulate gyrus in sequence (Chauhan *et al.*, 2021). It is widely believed this circuit recruits regions responsible for emotional memory.

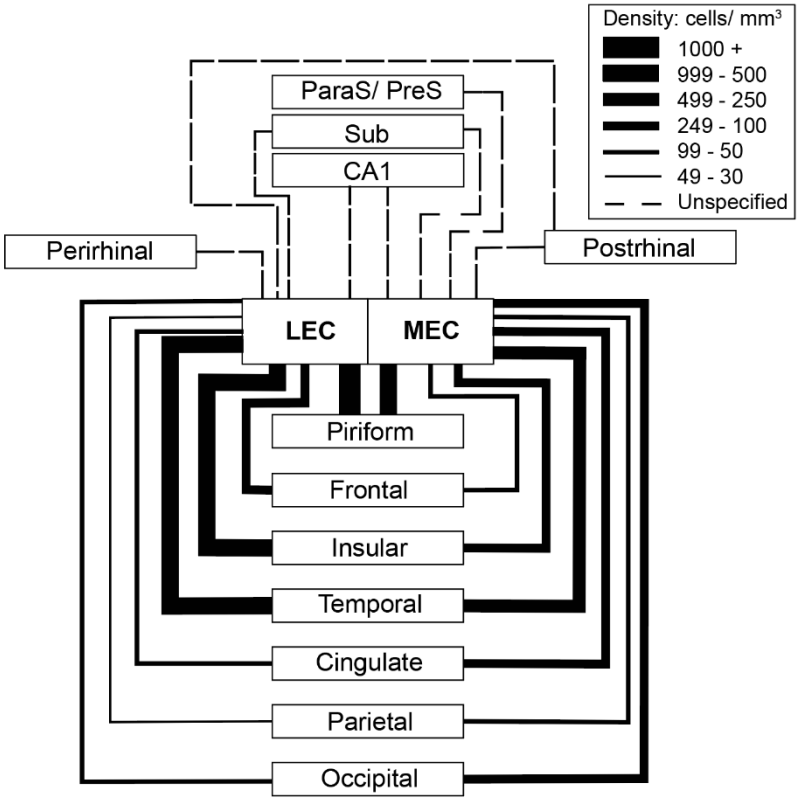

Figure 1.3. Multimodal sensory information converges in the entorhinal cortex*. A plethora of connections carrying a variety of sensory modalities project directly to the entorhinal cortex and these projections terminate with varying densities in either the lateral or medial division. Primary olfactory (piriform), primary visual (occipital), primary auditory (temporal), gustatory (insular), vestibular (insular) and somatosensory (parietal) information all converge in the entorhinal cortex prior to reaching the hippocampus. Projections from the cingulate cortex consist of information related to emotional and behavioural processing as well as navigation, planning and imagination whilst the frontal lobe projections are providing the entorhinal cortex with information related to rewards/punishment and behaviour. The density, or strength, of connections are represented by the thickness of the lines. Any dashed lines represent known afferent connections of unquantified neuronal density in relation to the ones shown. CA1, area CA1 in the hippocampus; L/MEC, lateral/medial entorhinal cortex; ParaS, parasubiculum; PreS, presubiculum; Sub, subiculum; Data in image taken from Burwell and Amaral (1998a, pg. 184) and Nilssen et al. (2019, pg. 1240).*

Superficial layer neurons are separated from deep layer neurons by the *lamina dissecans* (layer IV), which is a thin region of the entorhinal cortex that is completely devoid of any neurons. Throughout most of the cortex, input neurons tend to reside within the *deep layers*, but in the entorhinal cortex, input neurons are found solely in the *superficial layers* instead (Lingenhohl and Finch, 1991; Solodkin and Van Hoesen, 1996). In the

medial division of the entorhinal cortex, these input neurons are known to play a role in spatial processing (Fyhn *et al.*, 2004; Moser, Kropff and Moser, 2008; Deshmukh and Knierim, 2011), but in the lateral division less is known about what role superficial layer projection neurons play in declarative memory (but see Vandrey *et al.,* 2020). One of the distinguishing features of the entorhinal cortex is how the somata of neurons in the superficial layers tend to be grouped together into tiny clusters or 'cell islands.' Early descriptions of these cell islands are from studies of Nissl-stained brain sections in fish (Breathnach and Goldby, 1954), guinea pigs (Lohman and Lammers, 1963) rats (Price and Powell, 1971) and primates (Carboni and Lavelle, 2000). By analysing the catecholaminergic fibres that innervate the entorhinal cortex using tyrosine-hydroxylase immunoreactivity, Akil and Lewis (1994) also found the same clustering of cell islands; a pattern which differs considerably from how neurons tend to be organised in other cortical regions. The functional significance of this clustering in layer II of the entorhinal cortex is not currently known. However, a study by Kitamura *et al.* (2014) suggested that the properties of the neurons that comprise the cell islands differed considerably from those in the inter-island regions in terms of the type of information processed. More specifically, cells surrounding an island were shown to process contextual information whereas cells directly within an island processed temporal association and non-spatial information. Together, island and inter-island cells are thought to contribute significantly to the encoding of new episodic memories (Kitamura *et al.*, 2014). Further investigation found that these two proximally close but distinct populations of projection neurons synapse onto different targets in the hippocampus: contextual information is carried to area CA3 and the dentate gyrus, and temporal information to area CA1 (Kitamura *et al.*, 2014). Also, immunolabeling of neurons across layer II of the lateral entorhinal cortex suggests that some cell types expressing specific molecular characteristics are not evenly distributed throughout the layer, but instead, cluster together in the same cell islands. Markers such as: cholera toxin subunit B (CTB), a retrograde tracer used to show connections with the dentate gyrus; Wfs1, the insertion gene for the Cre construct in the C57BL/6J mouse module responsible for regulating cellular calcium; and calbindinD-28K, a major calcium-binding and calcium buffering protein used for maintaining calcium homeostasis (Kitamura *et al.*, 2014; Kook *et al.*, 2014). The cell islands were distinguishable from other cell types by the absence or presence of these markers, specifically the absence of CTB and the presence of both Wsf1 and calbindinD-28K. Other distinct cell types spread more evenly around these island cells showed opposite molecular expression of these markers (Kitamura *et al*., 2014; for review see Witter *et al*., 2017). As well as expressing different molecular characteristics, lateral entorhinal cortex neurons exhibit distinct morphological and electrophysiological properties, defined in detail below, but in summary these are related to the neuronal branching patterns and spread as well as the spiking patterns found from I-V tests. Further knowledge of the differences between the various types of superficial projection neurons in the entorhinal cortex may be critical in understanding the role these neurons play in memory formation and memory consolidation.

Characterisation of layer II and layer III projection neurons in the lateral entorhinal cortex, carried out initially by Tahvildari and Alonso (2005), demonstrated that a diverse array of different cell types, each with unique morphological features and electrophysiological properties, were present in the superficial layers of the lateral entorhinal cortex (see also Canto and Witter, 2012) . Specifically, layer II of the lateral entorhinal cortex

contains a heterogeneous population of neurons, including pyramidal neurons, fan neurons and multiform neurons (see **Figure 1.4**). Fan neurons, for example, are the most abundant cell types in layer II and exhibit a polygon-shaped soma with thick, spine-dense dendrites that extend upwards into layer I and laterally into layer II, forming a characteristic semi-circle shape (see **Figure 1.4A**, Fan Neurons). Fan neurons loosely resemble stellate neurons located in layer II of the medial entorhinal cortex as they share a similar morphology, though, stellate neurons have larger ascending apical dendrites than fan neurons, and it is this prominent morphological feature that endows stellate neurons with their characteristic star-like appearance (Tahvildari and Alonso, 2005; Canto and Witter, 2012a; 2012b). Stellate neurons also display strong inward rectification in response to hyperpolarising direct current injection that produces a prominent sag in the voltage response during a current-voltage (I-V) test (Dickson *et al.*, 2000). Fan neurons, in contrast, show very little sag in response to similar protocols (Tahvildari and Alonso, 2005; Canto and Witter, 2012a).

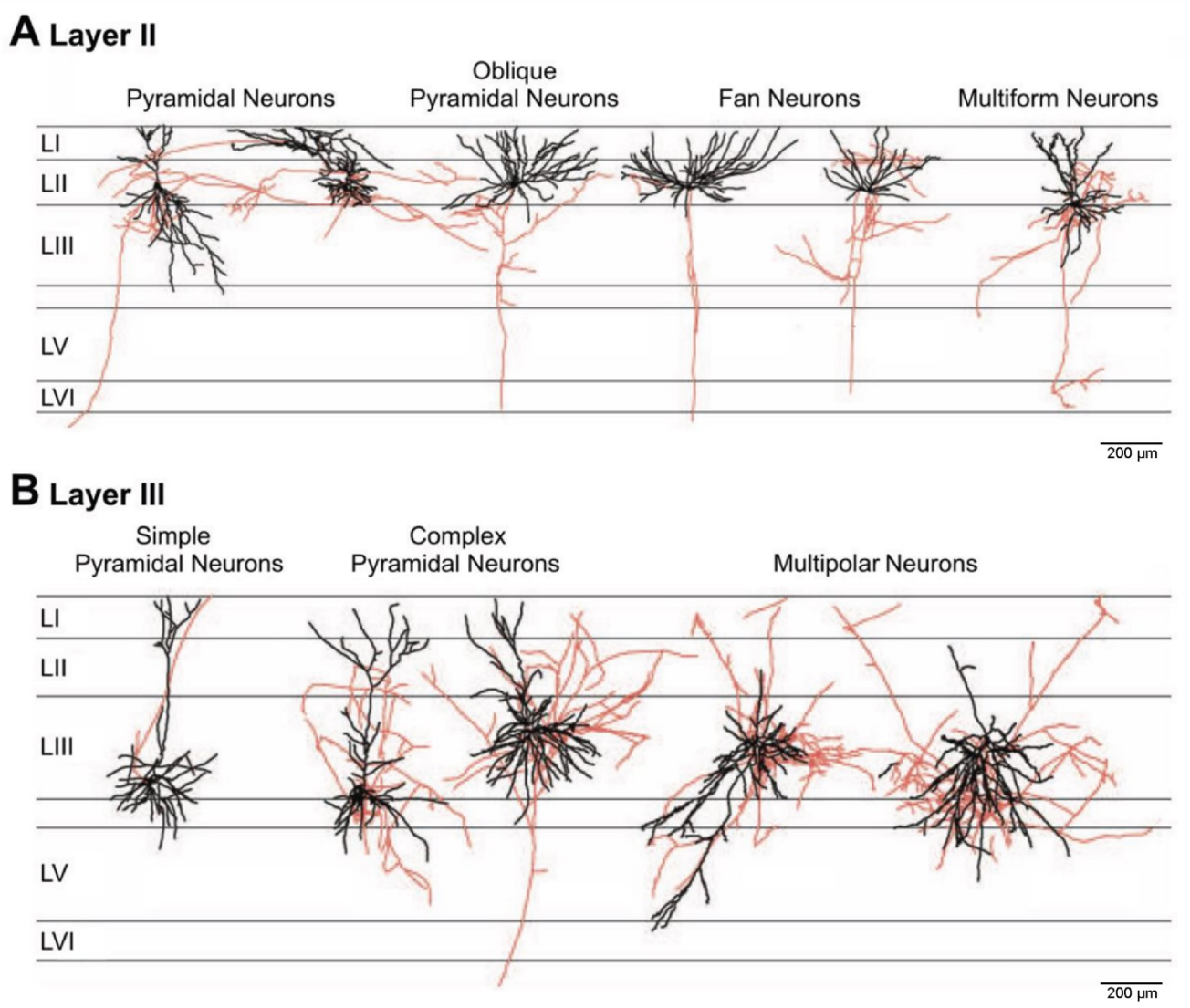

Figure 1.4. Branching of projection neurons in layer II and III of the lateral entorhinal cortex*. (**A**) The main neuron types in the lateral entorhinal cortex are pyramidal, fan, multiform and multipolar neurons. Dendritic trees of layer II fan cells are confined mostly to layers I and II, whereas the wider branching patterns observed in pyramidal and multiform neurons tend to arborise deep into layer III. (**B**) Pyramidal neurons in layer III branch into layers I, II and III, whereas multipolar neurons in layer III have wider branching across layer III and into layer V. Together, this indicates possible synaptic communication within and between cells in layers I, II and III as well as deep layers V and VI. Dendrites are shown in black*

and axonal arbours in red. Grey horizontal lines demarcate the cortical layers (L, layer). Image adapted from Canto and Witter (2012a). Scale bar: 200 µm.

Pyramidal neurons in layer II of the lateral entorhinal cortex have triangular, or 'pyramid'-shaped, cell bodies that are much smaller than those of fan neurons (see **Figure 1.4A**, Pyramidal Neurons, Oblique Pyramidal Neurons). A feature characteristic of these cells is how the apical dendrite bifurcates in layer II before crossing into layer I and spreading laterally (Canto and Witter, 2012a). Typically, the complete dendritic tree forms a rectangular shape, further augmented by the spine-containing basal dendrites that protrude and ramify deep into layer III. Electrophysiological characteristics of these cells, such as the prominent spiking doublet at low depolarisation intensities (Tahvildari and Alonso, 2005), is not consistent with other pyramidal cells in area CA1 of hippocampus, which does not show a spiking doublet in response depolarisation (Chapman and Lacaille, 1999; Staff *et al.*, 2000; Milior *et al.*, 2016) or the prefrontal cortex, where a select few subtypes (regular spiking and adapting) of layer V pyramidal neurons show evidence of a spiking doublet at higher current injections that elicit more than five action potentials (Yang, Seamans and Gorelova, 1996; van Aerde and Feldmeyer, 2015) that share the same morphology. A large proportion of superficial layer neurons are multiform and multipolar cells, especially in layer III, though, these neurons are less uniform in terms of their morphological characteristics (Canto and Witter, 2012a; 2012b).

Pyramidal neurons are the most prominent cell type in layer III of the lateral entorhinal cortex and share similar morphology and electrophysiology with neurons in layer II of the lateral division and layer III of the medial division of the entorhinal cortex (Tahvildari and Alonso, 2005; Canto and Witter, 2012a). However, the apical dendrites of layer III pyramidal neurons that branch into layer II are thicker than the basal ones, and these basal dendrites are much longer, reaching into layer V, but have fewer arbours than the layer II neurons (Tahvildari and Alonso, 2005). These distinct differences in morphology and spread of dendrites has led to the idea that each projection neuron may carry out specific and unique computational functions (Witter and Amaral, 2004; van Strien, Cappaert and Witter, 2009).

The interconnectivity between principal neurons in the superficial layers of the medial and lateral divisions of the entorhinal cortex is complex and extends beyond simply monosynaptic or recurrent connections between the various principal cell types. In particular, interneuron networks help to regulate information salience in sensory afferents to the entorhinal cortex (for review see Witter *et al*., 2017). For example, odour-responsive inhibitory GABAergic interneurons in layer II of the lateral entorhinal cortex are preferentially targeting other GABAergic interneurons, and they are more broadly tuned to odour stimuli than excitatory neurons in this layer (Leitner *et al.*, 2016). This suggests that these interneurons are contributing to the odour tuning of principal cells in layer II of the lateral entorhinal cortex by essentially reducing inhibitory control during odour representation (Leitner *et al.*, 2016). Interneurons across the entorhinal cortex are subdivided by their chemical expression of parvalbumin (PV), somatostatin (SOM) or 5-HT3a with PV-expressing neurons making up about 50% of the interneuron subtypes (Leitner *et al.*, 2016). The PV-expressing interneurons are not evenly

spread across the entorhinal cortex, in fact, they are most prominent in layer II of the medial entorhinal cortex where they reside closer to the rhinal fissure and have a relatively smaller presence in the lateral entorhinal cortex. Instead, 5-HT3a-expressing interneurons are most prevalent in layer II of the lateral entorhinal cortex (Leitner *et al.*, 2016). Interestingly, different interneuron subtypes may synapse onto specific principal neurons based on their distinct molecular characteristics, for instance principal neurons that express reelin or calbindin (Leitner *et al*., 2016; for review see Witter *et al*., 2017). Additional research is needed in terms of understanding the complex inhibitory-excitatory circuits formed in the lateral division of the entorhinal cortex.

Principal neurons in layer II and layer III of the lateral entorhinal cortex receive sensory information from various cortical sensory regions, including the piriform cortex (see **Figure 1.3**). This information is then integrated with other afferent sensory signals and transmitted to different targets in the hippocampus and dentate gyrus (see **Figure 1.2**).

Processed signals from the hippocampus return to the entorhinal cortex, this time to its deep layers, where they are relayed back to the cortical regions from which they originated (for a review, see Canto et al., 2008; Witter et al., 2017; Nilssen et al., 2019). The complex bidirectional flow of signals through the entorhinal cortex suggests that this circuit requires a high degree of regulation, particularly given the crosstalk between deep and superficial layer neurons (Kloosterman, van Haeften, and Lopes da Silva, 2004), the anatomical segregation of spatial and non-spatial inputs, and the diverse array of projection neurons in the superficial layers. Modulatory neurotransmitters appear well-suited for this regulatory control. Indeed, the physiological functions of the entorhinal cortex and hippocampus are finely tuned by multiple modulatory neurotransmitters. Glutamate modulates excitatory neurotransmission via AMPA receptor activation and regulates synaptic plasticity through NMDA receptors and metabotropic glutamate receptors (mGluRs). Acetylcholine facilitates the encoding of new episodic memories by increasing the likelihood of synaptic modification, particularly by supporting long-term potentiation via nicotinic receptor activation (Buccafusco et al., 2005; for a review, see Hasselmo, 2006). Adenosine regulates neuronal excitability by inhibiting spontaneous glutamate release from presynaptic sites via A1 receptor activation, mediated by voltage-dependent calcium channels and extracellular calcium levels (Li et al., 2011). Serotonin influences the synchrony of excitatory synaptic transmission by hyperpolarising excitatory neurons through potassium channel activation, a mechanism particularly relevant in the pathophysiology of epilepsy (for a review, see Schmitz et al., 1998). Dopamine plays a key role in regulating the encoding of new episodic memories by modulating the salience of sensory inputs and outputs of the entorhinal cortex (Caruana et al., 2006; Caruana and Chapman, 2008; Glovaci, Caruana, and Chapman, 2014; Liu, 2020). Of all the modulatory neurotransmitters that are known to contribute to the complex functions of the entorhinal cortex, perhaps the least understood is the role of dopamine in modulating the intrinsic and synaptic excitability of projection neurons in the superficial layers.

Dopamine

The neurotransmitter dopamine plays a central role in mediating numerous cognitive functions via four main pathways: the tuberoinfundibular, mesocortical, nigrostriatal and mesolimbic pathways. The tuberoinfundibular pathway originates in the hypothalamus, and dopamine release from these axons influence downstream mechanisms to regulate prolactin secretion from the pituitary gland where this path terminates (Meriney and Fanselow, 2019, pp. 384; for review see Qi-Lytle, Sayers & Wagner, 2023). The mesocortical pathway contains dopaminergic neurons originating in the ventral tegmental area (VTA) and projecting to multiple regions of the cortex to regulate motivation, reward and addiction (for review see Luo & Huang, 2015), as well as both working and verbal memory, and general executive function (for review see Hirano, 2021). Dopaminergic projections from the substantia nigra that terminate in the basal ganglia and striatum, forming the nigrostriatal pathway, help to control voluntary movement (Hattori *et al.*, 1991; Chen *et al.*, 2022). These projections degenerate in patients presenting with the characteristic motor symptoms of Parkinson's disease. The mesolimbic pathway is, perhaps, the most intensely studied starting at the ventral tegmental area (VTA) and terminating in the nucleus accumbens. These projections are involved in reward circuits, a pathway that is hijacked in addiction (Meriney and Fanselow, 2019, pp. 384). Moreover, the mesolimbic pathway sends branches to many other forebrain areas, including the prefrontal cortex and hippocampus (for review see Alcaro, Huber & Panksepp, 2007).

Dopaminergic Innervation of the Lateral Entorhinal Cortex

Of all the midbrain dopaminergic projections described above, axons from neurons in the A10 cell group of the ventral tegmental area innervate both the medial and lateral divisions of the entorhinal cortex (Swanson, 1982; Taber *et al*., 2012; for review see Oades and Halliday, 1987). Interestingly, the organisation and topography of these inputs is conserved across many mammalian species including humans, primates and rodents (for review see Oades and Halliday, 1987). This projection is considered a branch of the mesocortical pathway, which also includes dopaminergic efferents to the prefrontal cortex (Swanson, 1982). Although these axons typically project towards the basal forebrain, some of them bifurcate at the medial forebrain bundle and synapse onto superficial layer entorhinal cortex neurons (Lindvall *et al.*, 1974). Dopaminergic axons terminating in the entorhinal cortex form synaptic contacts with both excitatory and inhibitory neurons, similar to the patterns observed in the prefrontal cortex of primates. Notably, dopaminergic terminals frequently oppose GABA-containing dendrites, despite local differences in overall innervation patterns and the distribution and density of dopaminergic fibres in these regions (Erickson, Sesack and Lewis, 2000). Early anatomical studies (Fuxe, 1965; Lindvall *et al.*, 1974; Swanson, 1982) presented compelling evidence for the formation of direct and deliberate dopaminergic projections to specific cortical areas, including the entorhinal cortex. A study by Fuxe (1965) utilised a novel fluorescence imaging technique, first described by Falck *et al.* (1962), to determine the localisation of monoaminergic cells in the brain and was one of the first reports demonstrating that dopamine, noradrenaline and serotonin are released from specific terminal regions and function as neurotransmitters. Subsequent work by Lindvall *et al.* (1974) found much richer dopaminergic innervation in the entorhinal cortex

than anything reported previously, and this was later corroborated by Swanson (1982) who utilised a combination of anti-tyrosine hydroxylase immunofluorescent labelling and fluorescent retrograde tracing methods to quantify dopaminergic projections to multiple regions in the rat brain, including the entorhinal cortex.

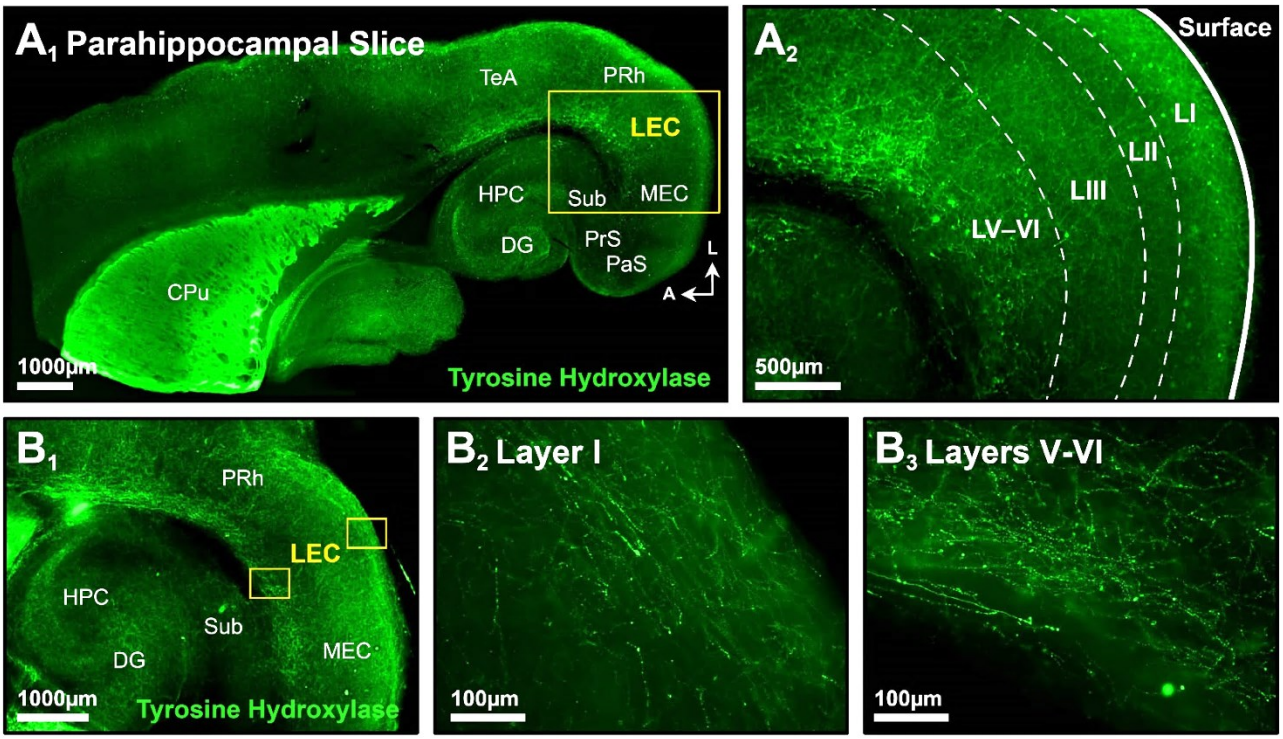

Figure 1.5. Fluorescent tyrosine hydroxylase immunolabelling in the parahippocampal region*. (**A₁, B₁**) Tyrosine hydroxylase, a rate-limiting enzyme required for dopamine synthesis, is not evenly expressed in dopaminergic projections terminating in the hippocampus and parahippocampal regions. (**A₂**) Dopaminergic fibres have a different laminar expression profile across the lateral entorhinal cortex with fibres in layer I (**B₁**) and layers V-VI (**B₂**) being the most dense. CPu, caudate putamen; DG, Dentate gyrus; HPC, hippocampus; LEC, lateral entorhinal cortex; MEC, medial entorhinal cortex; PaS, parasubiculum; PRh, perirhinal cortex; PrS, presubiculum; Sub, subiculum; TeA, tegmental area. Adapted from Harvey (2020).*

Although it has been known for decades that dopaminergic projections from the ventral tegmental area innervate the entorhinal cortex, surprisingly little has been done to investigate the cognitive, behavioural or physiological relevance of these inputs. Not only are dopaminergic fibres present in both the medial and lateral divisions of the entorhinal cortex (see **Figure 1.5**) they also show striking specificity in terms of the layers in which they innervate. Dense immunolabeling for tyrosine hydroxylase is most prominent in superficial layer I, as well as in deep layers V and VI (see **Figure 1.5**), with only moderate labelling in layers II and III. It is tempting to speculate, then, that it is not mere coincidence the densest dopaminergic projections to the entorhinal cortex also happen to overlap with the main input and output layers of the structure. Exploring the exact dopamine receptor subtype configurations, interactions and distributions present on the principal neurons of the lateral entorhinal cortex (and even in sensory afferent terminals), may aid in determining the functional role of dopamine in the structure.

All dopaminergic receptors are metabotropic and consist of seven transmembrane spanning alpha helices. Five subtypes of dopamine receptors have been identified (D_1 to D_5), but they differ in terms of their function and associated G-protein. In general, dopaminergic receptors are typically grouped into two distinct families: D_1-like receptors (D_1 and D_5) and D_2-like receptors (D_2, D_3 and D_4). When activated, D_1-like receptors trigger downstream signalling cascades that increase activity of adenylyl cyclase. The opposite is true for D_2-like receptors as these, when activated, lead to the suppression of adenyl cyclase (see **Figure 1.6A**)(Glovaci and Chapman, 2015; 2019). The D_2, D_3 and D_4 receptors also have a longer third cytoplasmic loop but shorter carboxyl tail compared to D_1 and D_5 receptors, and this is down to the genome sequencing of each receptor subtype (i.e., the addition or absence of amino acids common among receptors affecting the same downstream G-proteins)(for review see Missale *et al*., 1998). When D_1-like receptors are homo-oligomeric, they modulate adenylyl cyclase activity through $G_{s/Olf}$ proteins to upregulate adenylyl cyclase production and subsequent cyclic adenosine monophosphate (cAMP). D_2-like receptor homo-oligomers act via the $G_{i/o}$ proteins to suppress adenylyl cyclase and therefore cAMP activity (Hasbi, O'Dowd and George, 2010). Within the entorhinal cortex, D_1 receptors are located *only* in layers II, V and VI whereas D_2 receptors are found in all layers of the entorhinal cortex, but they are most abundant in layers I and III (Köhler, Ericson and Radesäter, 1991). Interestingly, D_1-receptors are three times more prominent overall, despite their lower affinity for dopamine (Boyson, McGonigle and Molinoff, 1986; Richfield, Penney and Young, 1989). Moreover, the mode of dopamine release in the synapse can influence receptor binding affinity. Tonic dopamine release, characterised by continuous, prolonged exposure often regarded as 'background' or 'low-level' signalling, tends to favour D2-like receptor binding. In contrast, phasic release, which occurs in short but intense bursts, preferentially promotes D1-like receptor binding (for review see Subramaniyan and Danni, 2015).

The opposing release paradigms described above are often driven by distinct firing patterns of dopaminergic projections. For example, burst firing can lead to a rapid and large phasic release of dopamine, which primarily activates D1-like receptors due to their low affinity. In contrast, population firing of dopaminergic neurons elicits a slower, tonic release of dopamine, which preferentially targets D2-like receptors, likely due to their higher affinity for dopamine (Floresco et al., 2003; Grieder et al., 2012). Grace (1991) proposed that prefrontal afferent projections to subcortical regions regulate tonic dopamine release, setting the 'background' levels necessary for further activity at subcortical targets. Relevant behavioural stimuli would then reach these subcortical regions and induce burst firing of dopaminergic projections, resulting in phasic dopamine release. Changes in tonic dopamine levels, particularly the strength of prefrontal cortex dopaminergic projections, would therefore influence the salience of phasically released dopamine. This dynamic balance is crucial when considering the pathophysiology of brain disorders such as schizophrenia, which disrupts the finely tuned dopamine signalling system (Grace, 1991).

Dopaminergic Modulation of the Lateral Entorhinal Cortex

Dopamine as a modulatory neurotransmitter in the medial entorhinal cortex was explored following initial reports that dopaminergic fibres innervate the structure (for review see Oades and Halliday, 1987). These early studies assessed the effects of bath-applied dopamine, replicating tonic release, on glutamate-mediated synaptic transmission in layers II and III of the medial entorhinal cortex. Application of 100 and 500 µM dopamine was shown to alter the membrane resistance of principal neurons resulting in a strong suppression of synaptic responses in layer II fan neurons (Pralong and Jones, 1993). A similar suppressive effect of dopamine on synaptic transmission was also observed in layer III, and this was attributed to a coincidental change in the release probability of glutamate as evidenced by a dopamine-mediated increase in paired-pulse ratios (Stenkamp, Heinemann and Schmitz, 1998). These two studies were the first to suggest that dopamine could regulate the flow of sensory input to the hippocampus by suppressing synaptic transmission in the entorhinal cortex. Exact concentrations of dopamine found extracellularly at the synaptic cleft are unknown, however, studies looking into transient changes in dopaminergic tone related to reward associations have made predictions based on microdialysis and electrochemistry at mesolimbic dopamine projections from ventral tegmental area to the nucleus accumbens. Here, it has been shown that dopaminergic afferents synapse onto the neck of spines on medium spiny neurons (Schultz, 1998), where they predominantly contain D1-like receptors in their low-affinity state (KD: 1.6 µM) but not in their high-affinity state (KD: 0.02 µM). In contrast, only a few D2-like receptors are present, and these are primarily found in their high-affinity state (KD: 0.02–0.05 µM) (Richfield, Penney and Young, 1989). Interestingly, medium spiny neurons in the nucleus accumbens are likely exposed to tonic concentrations of dopamine at around 20 - 50 nM (Richfield, Penney and Young, 1989) which would theoretically be enough to occupy dopaminergic receptors in their high-affinity state. During phasic release, however, the amount of dopamine released has concentration-dependent bidirectional consequences. Evoked release of dopamine to concentrations up to 600 nM at striatal neurons results in increase excitation, however further increases in dopamine concentration, elicits inhibitory effects (Gonon, 1997; for review see Wightman and Robinson, 2002). Although not much is known about regional specificity of dopamine receptor subtype affinities for dopamine, these subtypes are believed to follow a similar trend in other areas of the brain with D_2-like receptors (D_2, D_3 and D_4) having a 10 to 100 times higher affinity for dopamine than those in the D_1 family (D_1 and D_5) (Martel and Gatti McArthur, 2020).

Further studies have corroborated the initial findings of Pralong and Jones (1993), as well as Stenkamp, Heinemann and Schmitz (1998), but in the lateral division on the entorhinal cortex, demonstrating that, indeed, dopamine acts as a powerful suppressor of synaptic transmission. Dopamine at high concentrations (bath-applied; 50 to 100 µM) has been shown to significantly attenuate the amplitude of synaptic responses *in vitro* via a D_2 receptor-mediated decrease in presynaptic glutamate release (Caruana *et al.*, 2006; Caruana and Chapman, 2008). Interestingly, the effects on basal synaptic transmission were also shown to be both concentration-dependent *and* bidirectional. Dopamine at low concentrations (1 to 10 µM) was then shown to *increase* the amplitude of synaptic responses in layer II of the lateral entorhinal cortex (Caruana *et al.*, 2006; Caruana and Chapman, 2008; Glovaci, Caruana and Chapman, 2014). This enhancement of synaptic transmission is believed to be dependent on the activation of the G_q-coupled protein at the D_1 receptor leading to an increase

in phospholipase C (PLC) activity. PLC with phosphoinositide 2 (PIP_2) triggers the production of diacylglycerol (DAG) and inositol 1,4,5-trisphosphate ($InsP_3$) which subsequently enhances release of internal calcium via $InsP_3$ receptors from within superficial layer projection neurons directly. This increase in cytosolic calcium and DAG can activate protein kinase C leading to subsequent phosphorylation of AMPA receptor subunit $Ser^{831/818}$ to increase channel conductance (Glovaci and Chapman, 2019). The concentration of dopamine used in studies of the entorhinal cortex are based on estimated levels of dopamine at release sites. Since vesicular release of dopamine at an active site generates an area with a steep concentration gradient, the closer a dopamine receptor is to its release site, the higher the dopamine concentration effectively targeting it. It has been estimated that only receptors within 1 µm of the vesicular release would be effectively activated following to vesicular release (Cragg and Rice, 2004). In regions such as the striatum, dopaminergic release sites are estimated to be densely clustered, innervating neighbouring projections in a manner that facilitates sustained signalling. Given a tonic firing rate of approximately 5 Hz and a dopamine clearance rate of around 25 ms via dopamine transporters, it is likely that a steady concentration of dopamine is maintained. This results from the summation of approximately 25 to 50 individual release events, producing a background, or tonic, dopamine concentration measured at around 30 nM (Arbuthnott and Wickens, 2007). Phasic release of dopamine is more complex. Most microdialysis probes used for measurement are significantly larger than the release sites they are assessing. Combined with the likelihood that dopamine reuptake is overwhelmed by repeated agonist release at 5 Hz, as well as the rapid diffusion and reuptake kinetics, this means that recorded values will always underestimate the actual dopamine concentration achieved. Despite these limitations, estimations of vesicular dopamine concentration in midbrain neurons suggest levels of approximately 300 mM (Pothos, Davila, and Sulzer, 1998). At the site of release, this high concentration of dopamine rapidly diffuses across the synaptic cleft, following a steep concentration gradient as it disperses (Scimemi and Beato, 2009). Based on these reasonable assumptions, it is physiologically plausible that dopamine reaches micromolar concentrations at dopamine receptors, given the narrow width of synaptic clefts (less than 1 µm) (Cragg and Rice, 2004).

Dopaminergic signalling in layers II and III of the lateral entorhinal cortex is complex. Projection neurons respond to dopamine in various ways depending not only on the layer in which they reside (II versus III), but also in relation to both the timing and the magnitude of the dopamine signal itself. Projection neurons in layer II respond more strongly to bath application of a high 100 µM concentration of dopamine relative to layer III neurons (Unpublished observation, by Harvey, 2020). Specifically, layer II neurons hyperpolarise in response to dopamine via a dopamine-mediated change in membrane resistance to attenuate spiking (Unpublished observation, by Harvey, 2020). In contrast, layer III neurons respond preferentially to transient ‘puffs’ of dopamine applied directly to the soma relative to layer II neurons. In these experiments, spiking activity is abolished in layer III neurons for a short period of time immediately following a puff of 100 µM dopamine before recovering completely (Unpublished observation, by Harvey, 2020), an effect that is completely absent in layer II projection neurons. These findings suggest that the timing and strength of the dopamine signal can affect the propagation of sensory afferents to the hippocampus by differentially affecting the excitability of superficial layer II and layer III projection neurons.

One reason for the variable responsiveness of layer II and layer III projection neurons to dopamine may be due to the distribution patterns of different dopaminergic receptor subtypes across the superficial layers of the lateral entorhinal cortex. D_1 and D_2 receptors are found in many dopamine-rich cortical areas with some of the highest densities in the entorhinal cortex (Savasta, Dubois and Scatton, 1986; Weiner *et al.*, 1991). More specifically, in studies utilising autoradiography with ligand binding in the entorhinal cortex of rats, higher densities of D_1 receptors were found in layer II compared to D_2 receptors, however, layer III neurons had little to no ligand binding to D_1 receptors but much more D_2 receptor binding than in layer II (Köhler, Ericson and Radesäter, 1991). As such, the higher density of inhibitory D_2-like receptors in layer III neurons may underlie the sensitivity of these cells to transient puffs of dopamine (Harvey, 2020).

Dopaminergic receptors are known to dimerise with each other to form complexes that work via an array of intracellular signals to affect the release of calcium from internal stores, or to provide both short- and long-term changes in membrane excitability (for review see Martel and Gatti, 2020). There is evidence to suggest that D_1 receptors can form heteromers with D_2 receptors, and in this configuration the dimer has the potential to increase neuronal excitability by upregulating levels of phospholipase C and inositol triphosphate (Glovaci and Chapman, 2019). The upregulation of inositol triphosphate triggers the liberation of calcium from intracellular stores (**Figure 1.6B**), thereby providing the putative signal underlying the increased synaptic excitability in layer II fan neurons in response to application of low concentrations of dopamine (Glovaci and Chapman, 2019). Moreover, D3 dopaminergic receptors signal via an alternative cAMP-independent pathway involving calcium/calmodulin-dependent protein kinase II (CaMKII). Here, CaMKII activates ERK proteins leading to the downregulation of CREB phosphorylation: CREB protein activation (by phosphorylation) is responsible for the induction of early- and late-response genes required for short- and long-term excitability as well as cell survival (Bozzi and Borrelli, 2013). Unfortunately, very little is known about the dopamine-mediated intracellular signals that regulate both the synaptic and intrinsic excitability of superficial layer projection neurons in the lateral entorhinal cortex.

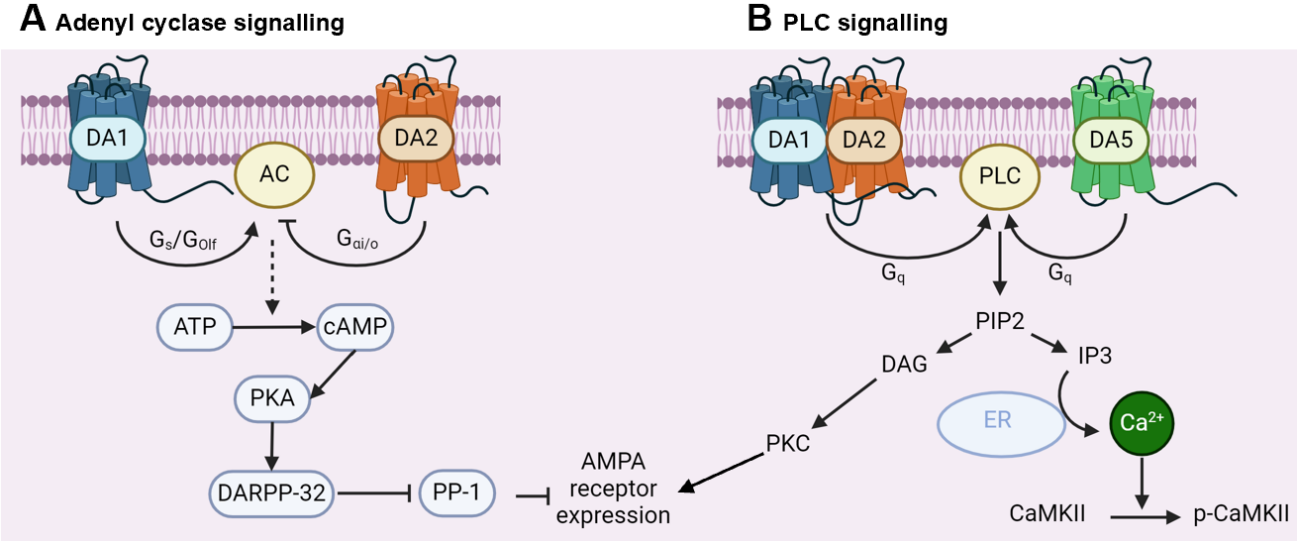

Figure 1.6. Intracellular signalling pathways linked to activation of dopamine receptors*. D_1 receptors have a longer carboxylic acid tail and shorter cytoplasmic loop compared to D_2 receptors. (**A**) Both D_1 and D_2 receptors can affect the surface expression of AMPA receptors via an increase (mediated by $G_{s/Olf}$) or decrease (mediated by $G_{\alpha i/o}$) in protein phosphorylation mediated by PKA. (**B**) Activation of the D_1-D_2 receptor heteromer, or D_5 receptor, can also lead to an increase in AMPA receptor expression, but via activation of the protein PLC. The subsequent activation of PIP2 leads to a signalling cascade affecting AMPA receptor expression, as well as the release of calcium from intracellular stores via IP3 actions on ryanodine receptors on endoplasmic reticulum. This results in phosphorylation of CaMKII to p-CaMKII. AC, adenyl cyclase; ATP, adenosine triphosphate; Ca2+, calcium ion; CaMKII, calcium/ calmodulin-stimulated protein kinase II; cAMP, cyclic adenosine monophosphate; $DA_{1/2/5}$; dopamine $_{1/2/5}$ receptor; DAG, diacylglycerol; DARPP-32, dopamine- and cAMP-regulated phosphoprotein 32; ER, Endoplasmic reticulum; Gs/Olf,αi/o,q, G-protein; IP3, inositol 1,4,5-triphosphate; p-CaMKII, phosphorylated CaMKII; PIP2, phosphatidylinositol 4,5-biphosphate; PKA, protein kinase A; PKC, protein kinase C; PLC, phospholipase C; PP-1, protein phosphatase 1. Adapted from Hasbi, O'Dowd and George (2010), Glovaci and Chapman (2015), and reviews by Neve, Seamans and Trantham-Davidson (2004), and Beaulieu, Espinoza and Gainetdinov (2015).*

The dense presence of dopamine receptors in the entorhinal cortex led to the assumption that they have a role in neuromodulation of synaptic transmission and/or plasticity (Savasta, Dubois and Scatton, 1986; Köhler, Ericson and Radesäter, 1991; Weiner *et al.*, 1991; Pralong and Jones, 1993; Stenkamp, Heinemann and Schmitz, 1998; Caruana *et al.*, 2006; Caruana *et al.*, 2007; Caruana and Chapman, 2008; Glovaci, Caruana and Chapman, 2014). However, as with most other metabotropic receptors, they can desensitise in the presence of high concentrations of agonists. A function which may be innately protective or ultimately detrimental for the synapse (for review see Beaulieu and Gainetdinov, 2011).

Dopaminergic Receptor Desensitisation

As noted above, all dopaminergic receptors are metabotropic and signal via their association with different G-proteins. Additionally, metabotropic receptors are known to desensitise in response to prolonged exposure to high concentrations of their endogenous ligand or an exogenous agonist (Kim *et al.*, 2004; Al-Hasani *et al.*, 2011; Sander *et al.*, 2016). Desensitisation of G-protein-coupled receptors (GPCRs) can be defined as the lack of a response to an agonist following prolonged or repeated exposure/activation (for review see Hausdorff, Caron & Lefkowitz, 1990). GPCR desensitisation occurs due to the phosphorylation of the G-protein via a mechanism requiring G-protein-coupled receptor kinases (GRKs) (for review see Premont & Gainetdinov, 2007) and regulatory proteins called arrestins (Lohse *et al.*, 1990). These arrestins have a high binding affinity to GRK-phosphorylated GPCRs that prevents G-protein-mediated activation of downstream signals leading to an attenuated – or desensitised – response (for review see Kelly, Bailey & Henderson, 2008). This is the case for both D_1-like (Kim *et al.*, 2004) and D_2-like receptors (Sander *et al.*, 2016). Previous research has shown that D_2 receptors are desensitised initially by phosphorylation of the GPCR, but this effect is only transient and typically reverses within several minutes (Williams *et al.*, 2013). However, dopamine-induced desensitisation can last for hours – or even days – thereby suggesting that this long-lasting desensitisation may reflect receptor internalisation, or even receptor degradation (Sander *et al.*, 2016). Given the potent suppressive effects high concentrations of dopamine have on the excitability of superficial layer projection neurons in the lateral

entorhinal cortex (Caruana *et al.*, 2006; Caruana and Chapman, 2008), it remains to be determined whether any dopamine-induced desensitisation effects influenced these initial experiments.

Metabotropic receptors are not the only group of receptors known to desensitise. Ionotropic glutamate receptors (iGluRs), for example AMPA, NMDA and kainate receptors, also have this ability. A critical difference between metabotropic and ionotropic receptor desensitisation is the mechanism by which they become desensitised. In particular, AMPA receptors are shown to desensitise rapidly following glutamate binding due to the relative instability of the activated receptor conformation. To resolve this, the channel closes with glutamate remaining bound and the transmembrane helices are repositioned rendering the AMPA receptor desensitised (Hansen *et al.*, 2021). AMPA receptors are also the fastest iGluRs to deactivate, desensitise and recover following glutamate binding, regardless of the subunit (GluA1, 2, 3 and 4). The average time to achieve this is 1 ms, 5 ms and 100 ms, respectively. This is a much faster receptor recycling time compared to the few NMDA receptor subunits (GluN1/2A,B,C and GluN1/3A) that show deactivation, desensitisation and recovery following glutamate binding (2 s, 200 ms, and 1.2 s respectively) as well as many kainate receptor subunits (GluK1, 2 and 3) in response to glutamate binding (5 ms, 20 ms and 25 s respectively) (Hansen *et al.*, 2021). The mechanism of kainate receptor desensitisation is very similar to AMPA receptors, the agonist binds to the ligand binding site after which a conformational change occurs to retain the bound ligand and close the channel. Thus, although the receptors remain on the cell surface, they are functionally inactive (Meyerson *et al.*, 2016). This differs from NMDA receptors, which can enter desensitised states through two distinct mechanisms, depending on the concentration of agonist present at the time of activation. When fully saturated by glutamate and/or glycine, NMDA receptors can transition into a long-lasting non-conducting state. Residues in the GluN2 subunit play a key role in regulating the extent of this desensitisation, which can occur both in the presence and absence of calcium ions (Nahum-Levy *et al.*, 2001). Alternatively, if only a sub-saturation of NMDA receptors is achieved, the ligand binding affinity is reduced, effectively reducing the number of occupied binding sites and desensitising the receptor to its agonist (Nahum-Levy *et al.*, 2001). In summary, the major differences between metabotropic glutamate receptors (mGluRs) and ionotropic glutamate receptors (iGluRs) lie in the speed of their kinetics, particularly regarding deactivation, desensitisation, and recovery, with iGluRs exhibiting much faster dynamics than mGluRs. This difference is likely due to the distinct mechanisms of desensitisation. Metabotropic receptors undergo internalisation of active receptors, requiring more time and cellular energy for removal, degradation, and recycling of receptor components. In contrast, iGluRs undergo conformational changes in response to agonist binding, enabling a closed state without necessitating receptor internalisation, making this form of desensitisation more time efficient.

The differences in desensitisation and recovery speed may be functionally significant. Ionotropic glutamate receptors generally require rapid kinetics to support fast excitatory synaptic transmission and the rapid burst firing of synapses, necessitating quick receptor cycling. Conversely, mGluRs are functionally adapted to mediate longer-lasting changes in synaptic efficacy, often contributing to long-term synaptic plasticity. This is frequently achieved through the regulation of iGluRs, such as NMDA receptors, via G-protein-coupled receptor

(GPCR) signalling. (Nahum-Levy *et al.*, 2001; Meyerson *et al.*, 2016; Hansen *et al.*, 2021). A noteworthy point to consider is possible interactions between iGlu and mGlu receptor activity. For example, group I mGluRs are known to reduce the probability of NMDA receptors opening in response to glutamate at Schaffer collateral synapses in area CA1 of the hippocampus. The proposed mechanism likely involves the lateral movement of NMDA receptors away from the synapse following the activation of group I mGluRs (Ireland and Abraham, 2009). Interestingly, kainate receptors can function as iGluRs or mGluRs and this usually depends on where they are situated within the synapse. Presynaptic kainate receptors can function as metabotropic receptors to modulate glutamate release. When facilitating glutamate release via presynaptic kainate receptor activation, the calcium/calmodulin-dependent protein kinase pathway is typically recruited. In contrast, downregulation of glutamate release is generally mediated through a G-protein–protein kinase A pathway, as observed in Schaffer collateral projections synapsing onto pyramidal neurons in area CA1 (Vesikansa *et al.*, 2007; Falcon-Moya and Rodriguez-Moreno, 2021).

Activity-Dependant Synaptic Plasticity

The strength of synaptic connections between neurons is highly modifiable and considered to be 'plastic'. As such, the term synaptic plasticity is used to highlight the ability of neurons to modify the strength of their connections resulting from experience. Synapses can be strengthened (Bliss and Gardner-Medwin, 1973; Bliss and Lomo, 1973) or weakened (Stanton and Sejnowski, 1989; Dudek and Bear, 1992; Chen *et al.*, 1995), and these modifications can be temporary (or short-term), lasting in the order of milliseconds to minutes, or persistent (or long-term), lasting several hours to several months or even years (for review see Malenka, 1994; Malenka and Bear, 2004; Sigurdsson *et al.*, 2007; Citri and Malenka, 2008; O'Dell *et al.*, 2010; Kumar , 2011; Bassi *et al.*, 2019). Some forms of short-term plasticity, such as paired-pulse facilitation, can result in enhanced or 'potentiated' synaptic efficacy via a transient elevation in presynaptic calcium to affect glutamate release. Longer lasting forms of synaptic plasticity require persistent changes in the surface expression of postsynaptic glutamate receptors and changes in gene transcription (Dasgupta *et al.*, 2020; France *et al.*, 2022). Synaptic depression, on the other hand, reduces the number of neurotransmitter-containing vesicles available for exocytosis in response to an action potential. As a result, less neurotransmitter is released into the synaptic cleft, leading to decreased excitation of the synapse. Long-lasting forms of plasticity, such as long-term potentiation (LTP) and long-term depression (LTD), initially involve modifications to molecular mechanisms, including glutamate receptor trafficking and the alteration of existing proteins. However, in later stages, these processes also induce changes in gene expression and the synthesis of new proteins. Long-term plasticity can lead to lasting modifications in the brain, contributing to the formation of both positive and negative emotional memories, language acquisition, and the consolidation of motor skills through repeated practice (Purves, 2018). Experimentally, long-term depression and potentiation can be induced using specific electrical stimulation protocols, however, *in vivo*, the release of neuromodulators in fast, specific and repeating patterns are required to elicit activity-dependent forms of synaptic plasticity.

Ionotropic Glutamate Receptors: AMPA and NMDA Receptors

Initially, ionotropic glutamate (iGlu) receptors were thought to belong to the nicotinic receptor superfamily of receptors due to their similar four transmembrane spanning alpha helical structure (for review see Wyllie and Bowie, 2022). After considerable debate and continued research, iGlu receptors have been shown to belong to their own family of receptors comprised of a similar tetrameric structure (for review see Hansen *et al*., 2021). It is important to note that the expression of iGlu receptors in the developing rat hippocampus does not reach full maturation until postnatal day 10-20 (Behuet *et al*., 2019; for review see Egbenya, Aidoo and Kyei, 2021). One of the key iGlu receptors essential for excitatory transmission between neurons is the ∝-amino-3-hydroxyl-5-methyl-4-isoxazole-propionate, or AMPA, receptor. These tetrameric complexes respond to glutamate and are responsible for opening a cation-selective channel in the membrane, permeable to the influx of sodium ions (Na^+; at rest) and efflux of potassium ions (K^+; when depolarised). AMPA receptors can be comprised of different subunits, each with specific properties, leading to unique AMPA receptor function (for review see Kamalova and Nakagawa, 2020). For example, in the hippocampus, the GluA1 and GluA2 receptor subunits are implicated in hippocampal long-term synaptic plasticity and memory (Ran *et al.*, 2013). AMPA receptors open in the presence of high concentrations (100 µM or above) of glutamate in the synaptic cleft, very rapidly (8 to 24 pS; Andersen, 2007; for review see Coombs and Cull-Candy, 2021). In the presence of chronic glutamate, AMPA receptors desensitise rapidly (2-3 ms) but often require much longer (300 ms) to fully recover (Aittoniemi *et al.*, 2023). In most instances, where the amino acid arginine (R) displaces glutamine (Q) at the Q/R site in the GluA2 subunit of the AMPA receptor, it becomes impermeable to calcium ions (Ca^{2+}). If this edited subunit is not present, however, like in some hippocampal interneurons, the AMPA receptor is largely permeable to Ca^{2+}. As such, an AMPA receptor permeable to Ca^{2+} could potentially play a role in synaptic facilitation since Ca^{2+} would enter the into the cell soma, however, in dentate gyrus basket cells, these Ca^{2+}-permeable AMPA receptors have an innate polyamine block that is voltage-dependent (Rozov *et al.*, 1998), perhaps in a similar way to the voltage-dependent block of N-methyl-D-aspartate (NMDA). These receptors could play an important role in synaptic plasticity due to the modulation of conductance and opening probability when phosphorylated (Andersen *et al.*, 2007). The modifiable AMPA receptor subunit, GluA2, has been identified in the hippocampal and parahippocampal regions of both humans and rodents. However, the entorhinal cortex exhibited the lowest density of GluA2 staining compared to areas CA2 and CA3 of the hippocampus, as determined using fluorescent immunohistochemistry and western blotting techniques (Yeung *et al.*, 2021). A similar pattern of expression was shown for the GluN1 subunit of NMDA receptors, which suggests primary localisation to dendritic processes in area CA1 and similar patterns of staining in areas CA2 and CA3 with less densely labelled fibres found in the entorhinal cortex (Yeung *et al.*, 2021). However, staining for the NMDA receptor subunit GluN2A revealed high density labelling in predominantly the superficial layers of the entorhinal cortex in what is described to be a 'glia-like' pattern of expression; since co-labelling of GluN2A with neuronal nuclear protein (NeuN), a protein present in the vast majority of neurons (Gusel'nikova and

Korzhevskiy, 2015), revealed no co-localisation of expression (Yeung *et al*., 2021, pp. 10). The presence of GluN2A at the synapse has been linked to neuroprotective properties in rodent studies due to its role in the regulation of calcium influx (for review see Zhang and Luo, 2013). Also, upregulation of NMDA receptors containing GluN1 and GluN2 subunits in the hippocampus have been directly linked to spatial working memory and spatial memory consolidation (Cercato *et al.*, 2016). A study by Wong et al. (2019) investigated the cognitive effects of centella asiatica on learning and memory. Their findings demonstrated that novel object recognition memory was enhanced in rodents following increased expression of the AMPA receptor subunits GluA1 and GluA2, as well as the NMDA receptor subunit GluN2B, in the entorhinal cortex and hippocampal region at the highest dose (600 mg/kg). In contrast, spatial learning and memory, assessed using the Morris Water Maze test, improved following increased expression of GluA1 and GluA2 but not GluN2B at a centella asiatica dose of 300 mg/kg (Wong *et al.*, 2019).

Work by Beneyto et al. (2007) investigated changes in glutamate receptor expression in schizophrenia and mood disorders and established a baseline level for receptor expression in the medial temporal lobe of humans. Using receptor autoradiography and in situ hybridisation techniques, the study examined all NMDA, AMPA, and kainate receptor subunits. The findings showed that under normal conditions, all seven NMDA receptor subunits (GluN1, GluN2A-D, and GluN3A-B) were present in bands corresponding to layers II, III, V, and VI of the entorhinal cortex. Among these, GluN1 and GluN2B exhibited the highest concentrations, while GluN2A, GluN2C, and GluN2D showed lower optical densities across each band (Beneyto et al., 2007). In contrast, all AMPA receptor subunits were found in the entorhinal cortex but did not display a laminar distribution. Instead, each subunit was expressed throughout the region, with GluA3 showing the highest expression compared to the other three subunits (GluA1, GluA2, and GluA4) (Beneyto et al., 2007). Similarly, all kainate receptor subunits (GluK1-5; referred to in this study as GluR5-7, KA1, and KA2) were identified in the entorhinal cortex, though their distribution patterns varied. The highest density was observed for GluK3, followed by GluK4 and GluK5, while GluK1 and GluK2 exhibited the lowest optical densities (Beneyto et al., 2007). Overall, kainate and AMPA receptors were more localised to layers V/VI and II, whereas NMDA receptors displayed a more widespread distribution across all layers of the entorhinal cortex (Beneyto et al., 2007).

Another critical iGlu receptor involved in excitatory synaptic transmission is the NMDA receptor. These receptors are expressed differently depending on their location and stage of development (Andersen *et al.*, 2007). NMDA receptors are found in many different tetrameric configurations to elicit unique functions depending on their subunit composition (GluN1, N2A-D, N3A and B), with the most common and physiologically relevant configurations being the ones containing the GluN1/GluN2 subunits (Collingridge *et al*., 2013; for review see Vyklicky *et al*., 2013; Adell, 2020). Each tetrameric structure making up the NMDA receptor consists of two obligatory GluN1 subunits with two regulatory subunits (GluN2A-D, GluN3A and B). These NMDA receptors require two glycine and two glutamate molecules for activation. Glycine is naturally occurring and abundantly available in cerebral spinal fluid (Iijima *et al.*, 1978). It is typically found already bound to NMDA receptors (in advance of a glutamate transient or signal) or occupied by the glycine agonist, D-serine (Papouin *et al.*, 2012).

Basal synaptic transmission at excitatory synapses does not require NMDA receptors, but instead they regulate synaptic plasticity at these synapses. At resting membrane potentials, a magnesium ion (Mg^{2+}) blocks the channel pore and prevents the flow of ions (like Ca^{2+}, Na^{+} or K^{+}) across the membrane. This Mg^{2+} block is alleviated following sufficient depolarisation of the membrane; depolarisation typically provided by nearby AMPA receptors. If the exocytosis of glutamate is timed with coincident depolarisation of the postsynaptic membrane, then the Mg^{2+} block is removed and Ca^{2+}, for which NMDA receptors have a high permeability, enters the postsynaptic cell. This influx of Ca^{2+} is critical intracellular signal that triggers long-lasting changes in synaptic strength (Blanke and Van Dongen, 2009). In the hippocampus, prefrontal cortex and entorhinal cortex, GluN2A and GluN2B are the major regulatory subunits of the NMDA receptor (Beneyto *et al.*, 2007; Baez, Cercato and Jerusalinsky, 2018; Wong *et al.*, 2019; Kovalenko *et al.*, 2021). Indeed, GluN2B has been implicated in the induction of long-term depression in hippocampal and perirhinal regions, with both GluN2A and B required for long-term potentiation (Wyllie, Livesey and Hardingham, 2013). However, it is still important to note that the influx in Ca^{2+} is what ultimately induces long-term changes in synaptic efficacy.

Long-Term Synaptic Depression

Long-term depression (or LTD) is a form of synaptic plasticity expressed throughout the brain, yet it differs in subtle ways depending on the brain region investigated. In brain slices maintained *in vitro*, LTD is often induced by low frequency electrical stimulation delivered to excitatory afferents over a prolonged period (Dudek and Bear, 1992; Chen *et al.*, 1995). LTD induction can be via the NMDA or mGlu receptor, which can be dependent on the induction protocol used. For NMDA receptor-dependent LTD, a low frequency stimulation typically 900 pulses at 1-3 Hz is needed. As shown at Schaffer collateral projections synapsing onto area CA1 of the hippocampus in adolescent rodents, for example, NMDA receptors must be activated to allow Ca^{2+} to flow across the membrane and into the postsynaptic neuron following low frequency stimulation of these inputs (Dudek and Bear, 1992). Alternatively, paired-pulse low-frequency stimulation (PP-LFS) has been shown to require the activation of mGlu receptors as well as AMPA/kainate receptors for successful induction of LTD in area CA1 of the hippocampus (Bashir *et al.*, 1993b; Kemp and Bashir, 1999) via a novel signalling cascade involving protein tyrosine kinases (Moult *et al.*, 2008).The amount of Ca^{2+} entering the postsynaptic cell is a key regulator of the type of activity-dependent plasticity that is induced and is controlled by the affinity of calcium binding to regulatory proteins: small increases in postsynaptic calcium are enough to recruit downstream protein phosphatase signalling pathways to induce LTD whereas larger transients are required for protein kinase-dependent long-term potentiation (for review see Citri and Malenka, 2008). The influx of modest amounts of postsynaptic calcium typically activates protein phosphatases, such as protein phosphatase 1 (PP1) or protein phosphatase 2B (PP2B; also known as calcineurin), which dephosphorylate key target proteins, including AMPA receptor subunits required for basal excitatory synaptic transmission (Andersen *et al*., 2007; for review see Collingridge *et al*., 2010). The dephosphorylation of AMPA receptor subunits can lead to their internalisation resulting in reduced efficacy at the synapse (for review see Citri and Malenka, 2008).

Long-Term Synaptic Potentiation

Excitatory synapses activated by short bursts of high-frequency and high-intensity electrical stimulation, traditionally referred to as a tetanus, can initiate a cascade of postsynaptic signalling events that strengthen synapses through a process known as long-term potentiation (LTP). One widely used protocol for inducing LTP is theta burst stimulation (TBS), which has been shown to induce LTP at CA1 pyramidal neurons synapsing with afferent Schaffer collateral projections by delivering repeated short bursts of stimulation (Larson and Munkacsy, 2015). This was a key discovery, demonstrating that when appropriately timed, spontaneous bursts of neuronal firing occurring during behaviour (four spikes at 100 Hz, repeated at 200 ms intervals) can successfully induce LTP (Larson and Lynch, 1986; Larson, Wong and Lynch, 1986). In the same region, LTP can be induced reliably in Schaffer collateral projections from area CA3 that synapse with the apical dendrites of pyramidal neurons in the *stratum radiatum* in area CA1 of the hippocampus but via high-frequency stimulation: 30 spikes at 100 Hz repeated 4 times with 5 min intervals (Kemp and Manahan-Vaughan, 2004). LTP at these synapses is input specific, meaning only those synapses that receive the tetanic stimulation are affected. Despite the ability to induce LTP following a brief tetanus, the effects are extremely long-lasting, hence why it is such an excellent candidate mechanism to underlie memory storage in the brain (Abraham *et al.*, 2002). In most instances, for LTP to occur, the postsynaptic membrane must be depolarised, usually by strong activation of AMPA receptors following a high frequency stimulation (Bliss, Lancaster and Wheal, 1983; for review see Citri and Malenka, 2008). In area CA1 of the hippocampus, the induction of activity-dependent LTP is mediated by glutamate receptors – particularly, NMDA receptors – in a manner similar to induction of LTD. When NMDARs are activated by glutamate and the magnesium ion block has been alleviated due to AMPA receptor-driven depolarisation of the postsynaptic membrane, calcium ions are driven into the postsynaptic cell by the concentration gradient following the removal of the magnesium ion blockade on NMDA receptors and the channel pore opening to allow calcium ions to flow through. This calcium influx is critical to induce a series of biochemical cascades that upregulate AMPA receptor activity and/or initiate the addition of further AMPA receptors into the postsynaptic membrane (Malenka and Nicoll, 1999; Malinow and Malenka, 2002). Calcium-dependent kinases (and not phosphatases, like with LTD induction), such as CaMKII, are required for this process (for review see O'Dell *et al*., 2009). The net result of LTP is an increase in synaptic efficacy so that when another action potential arrives at the potentiated synapse, a much greater postsynaptic response is observed (for review see Citri and Malenka, 2008).

Synaptic Plasticity in the Entorhinal Cortex

Action potentials form the basis for neural communication across synapses. The driving force elicited by action potentials on postsynaptic membranes is controlled, in part, by synaptic plasticity. Synapses can be up- or down-regulated to form new synaptic connections or silence spurious or irrelevant associations, respectively. In the entorhinal cortex, changes in synaptic efficacy are a mechanism thought to underlie how sensory inputs are encoded or integrated within networks in the superficial layers of both the medial and the lateral divisions

of the entorhinal cortex. Many studies have reported that synapses in the medial entorhinal cortex are capable of supporting glutamate-mediated forms of activity-dependent synaptic plasticity (Alonso, de Curtis and Llinas, 1990; Kourrich and Chapman, 2003; Deng and Lei, 2007), and that activation of NMDA receptors is a key requirement for both LTP and LTD in sensory inputs to the superficial layers. Induction of synaptic plasticity, both LTP and LTD, has also been observed in the superficial layers of the medial entorhinal cortex to affect the propagation of sensory afferents to hippocampus, as well as in the deep layers of the medial entorhinal cortex to influence the salience of processed sensory efferents from hippocampus (Solger *et al*., 2004; for review see Witter *et al*., 2017). Much of the literature on the medial division of the entorhinal cortex has shown that induction of LTP is possible using acetylcholine receptor agonist carbachol (Yun *et al.*, 2000) or via various high frequency stimulation protocols (Yun, Mook-Jung and Jung, 2002). For example, application of the acetylcholine receptor agonist carbachol at concentrations >5 μM has been shown to induce a reversible short-term depression of synaptic transmission, or at lower concentrations (0.25 μM) the long-lasting potentiation of baseline synaptic transmission (Yun *et al.*, 2000). This chemically-mediated form of plasticity, dependent on activation of cholinergic receptors, has been observed in area CA1 of the hippocampus using carbachol at various concentrations (LTP at <1 μM, LTD at >5 μM) (Yun *et al.*, 2000) and in the prefrontal cortex using carbachol concentrations of 1, 10 and 100 μM to induce concentration-dependent long-term depression by varying amounts (Caruana, Warburton & Bashir, 2011). This induction of LTD by applications of carbachol likely involves pharmacological activation of metabotropic acetylcholine receptors which enhances glutamate transmission (Caruana, Warburton and Bashir, 2011), leading to increased postsynaptic activation of AMPA and therefore NMDA receptors and a larger calcium influx – enough to trigger LTD, but not enough for LTP. Of the relatively little data available on synaptic plasticity in the lateral division of the entorhinal cortex, there is evidence to show that activity-dependent forms of long-lasting plasticity are, indeed, supported in sensory afferents to the superficial layers. In particular, the robust monosynaptic projection from the piriform cortex that carries olfactory information to the superficial layers of the lateral entorhinal cortex supports both LTP and LTD *in vivo* (Caruana *et al.*, 2007). Interestingly, preventing reuptake of dopamine by blocking the actions of the dopamine transporter (DAT) with GBR12909 in rats prior to induction blocks activity-dependent synaptic plasticity in the lateral entorhinal cortex (Caruana *et al.*, 2007). Not only do these findings demonstrate that synapses in the superficial layers of the lateral entorhinal cortex support LTP and LTD, but they also highlight how modulatory neurotransmitters, such as dopamine, can dramatically regulate the expression of plasticity in olfactory sensory inputs to the structure. Surprisingly, the role of synaptic plasticity in sensory afferents to the lateral division of the entorhinal cortex has been largely overlooked.

Activity-dependent synaptic potentiation can be induced at excitatory synapses in many brain regions. Hippocampal plasticity, particularly NMDA receptor-dependent long-term potentiation in area CA1, has been extensively studied. (Bliss, Lancaster, and Wheal, 1983; Collingridge, Kehl, and McLennan, 1983; Larson, Wong, and Lynch, 1986; Dudek and Bear, 1992; Chapman, Perez, and Lacaille, 1998). However, interconnected regions such as the anterior cingulate cortex and the infralimbic cortex of the prefrontal region also exhibit increased excitation 25 days after hippocampal LTP induction following a spatial learning task (Bontempi et al., 1999).

Additionally, in the ventral tegmental area, burst firing of dopaminergic neurons induces LTP in adjacent dopamine neurons through the activation of endocannabinoid CB1 and dopamine D2 receptors co-localised on astrocytes, as well as presynaptic mGluR1 receptor activation (Requie et al., 2022). Area CA2 of the hippocampus is a notable exception, as it does not support LTP, particularly at the Schaffer collateral inputs from CA3 that synapse onto the apical dendrites of CA2 pyramidal neurons. These synapses lack the ability to support activity-dependent LTP under basal conditions (Zhao et al., 2007; for a review, see Caruana et al., 2012). This innate resistance to LTP is partly due to the rapid removal and buffering of calcium within CA2 postsynaptic spines during induction (Simons et al., 2009). The loss of the calcium signal during a tetanus prevents the induction of LTP via conventional mechanisms. In fact, the only way to potentiate CA2 synapses was through inhibition of plasma membrane calcium ATPase (PMCA) using carboxyeosin, ensuring Ca^{2+} availability at the synapse when administering an intensified tetanising stimulation (eight bursts of eight pulses at 200 Hz with a 2 s inter-train interval) (Simons et al., 2009).

Dopaminergic Modulation of Synaptic Plasticity

In many brain regions, basal synaptic transmission and the ability to induce activity-dependent synaptic plasticity are both regulated by modulatory neurotransmitters, including dopamine and acetylcholine. For example, in the dentate gyrus, administration of a D_1 receptor agonist blocks induction of LTP (Yanagihashi and Ishikawa, 1992). Similarly, LTD is prevented in area CA1 by activating D_1 and D_5 receptors (Mockett *et al.*, 2007). In the prefrontal cortex, the effects of modulatory neurotransmitters on plasticity are more complex and nuanced. In a study by Matsuda *et al*. (2006) induction of LTP results only when levels of extracellular dopamine are raised in tandem with the delivery of subthreshold tetanic stimulation. This is particularly unusual since a weak tetanus typically induces LTD at the same synapses. It appears, however, that by priming synapses with dopamine in the prefrontal cortex produces a long-lasting upregulation of synaptic transmission (Otani *et al.*, 1998). It is important to note that although the exact mechanisms contributing to this form of plasticity are unknown, NMDA receptor activation during the priming phase with dopamine and activation of metabotropic glutamate receptors were both critical to induce LTP at these synapses in the prefrontal cortex. In the superficial layers of the lateral entorhinal cortex, Caruana *et al.* (2007) showed that an increase in dopaminergic tone in the superficial layers during the delivery of patterned stimulation to induce either LTP or LTD blocks plasticity, though, the exact mechanism remains elusive (Caruana *et al.*, 2006; Caruana and Chapman, 2008).

Excitation and Inhibition in the Entorhinal Cortex

Fast excitatory synaptic transmission in the entorhinal cortex is largely dependent on the neurotransmitter glutamate acting via activation of AMPA receptors (Andersen *et al*., 2007; for review see Coombs and Cull-Candy, 2021; Kamalova and Nakagawa, 2021). Glutamate-mediated transmission has been the focus of most studies discussed so far as it is a crucial component required for basal synaptic function and neuronal communication. Excitatory transmission can also be affected by many additional factors, including the probability of presynaptic glutamate release, modulatory effects of metabotropic receptors, and induction and expression of activity-dependent forms of synaptic plasticity (Koles *et al.*, 2016). For example, the release probability of glutamate at presynaptic terminals in the lateral entorhinal cortex can be influenced by the presence of dopamine resulting in bidirectional effects on synaptic transmission (Caruana *et al.*, 2006; Caruana and Chapman, 2008). Excitatory synapses are also constrained by local inhibitory circuits that can have powerful effects on both basal synaptic transmission and plasticity (Wouterlood , Mugnaini and Nederlof, 1985; for review see Barron, 2020). This form of signalling is largely mediated by ɣ-aminobutyric acid (GABA)-gated ion channels that transport chloride ions through the cell membrane in order to reduce or to constrain excitatory transmission (for review see Barron, 2020). The opposing effects glutamate and GABA have on one another are permissive in terms of allowing finite control over circuits responsible for the integration of non-spatial sensory signals in the lateral entorhinal cortex and the subsequent propagation of these signals to the hippocampal formation. Fan cells in layer II of the lateral entorhinal cortex are influenced by a large and interconnected network of inhibitory cells, in a manner similar to inhibitory circuits regulating stellate cells in the medial entorhinal cortex. GABA-mediated inhibition dramatically affects spatial processing in the medial entorhinal cortex, and it is possible that inhibitory control of layer II fan neurons in the lateral entorhinal cortex influences the processing of non-spatial sensory information, such as olfactory inputs originating from the piriform cortex (Nilssen *et al.*, 2018). As noted earlier in the Introduction, dopamine receptors exert powerful bidirectional effects on excitatory synaptic transmission in the lateral entorhinal cortex, but it is unknown whether dopamine influences local inhibitory circuits in a similar way. The emergence of network oscillations often depends on pacing provided by local inhibitory circuits to synchronise the timing and propagation of activity across disparate neural networks. Any perturbations to the balance of inhibition and excitation within these networks can lead to disorganised brain activity and manifest, in extreme cases, in disorders like medial temporal lobe epilepsy (Bragin *et al.*, 1999). As such, it may be important to explore dopamine as a potential regulator of inhibitory transmission and plasticity in the entorhinal cortex.

Aims and Objectives

The primary aim of this research is to deepen our understanding of how dopamine modulates synaptic function in the superficial layers of the lateral entorhinal cortex. To achieve this, we have set the following objectives:

- Confirm and expand existing knowledge on the effects of dopamine on basal synaptic transmission in the superficial layers of the lateral entorhinal cortex.
- Characterise a novel dopamine-mediated desensitisation of metabotropic receptors in these layers.
- Investigate the properties of long-term depression and long-term potentiation in the superficial layers.
- Examine the role of dopamine in modulating activity-dependent synaptic plasticity.
- Explore interactions between dopamine-mediated desensitisation of metabotropic receptors and activity-dependent plasticity.

Chapter 2: General Methods

Animals and Ethics

Male or female Wistar rats aged between postnatal days 14 and 21 were used for all experimental work (n = 495; 95% male) described in this thesis, except for biocytin-streptavidin imaging (n = 43) which was undertaken in male Sprague Dawley rats aged between postnatal days 14 to 21. Pre-weaned pups were housed as single litters with their dams in the Biomedical Facility at Aston University. Animals had access to food and water *ad libitum* and were kept on a 12-hour light-dark cycle. Prior to euthanasia, every attempt was made to minimise distress in experimental animals, and all procedures adhered strictly to the guidelines mandated by the Home Office and outlined in the UK Animal (Scientific Procedures) Act 1986.

One rat brain was sliced on the morning of every test day. The brain was sliced such that the posteroventral part of the temporal lobe from each hemisphere was present that included both the hippocampal formation and parahippocampal cortices. As such, a substantial portion of the lateral division of the entorhinal cortex was preserved within about 6 to 8 bilateral slice pairs obtained from a single brain (Paxinos and Watson, 2007).

Tissue Slices

Tissue was collected and prepared according to methods described previously (Caruana and Chapman, 2008; Caruana, Warburton and Bashir, 2011; Caruana and Dudek, 2020). At the start of each experimental test day, a single rat was euthanised in the Biomedical Facility by cervical dislocation (Schedule 1). The brain was removed rapidly and placed in ice cold (~4 °C) oxygenated (95% O_2 and 5% CO_2) and sucrose-substituted artificial cerebrospinal fluid (ACSF) comprised of (in mM): 2 KCl, 1.25 NaH_2PO_4, 1 $MgCl_2$, 1 $CaCl_2$, 26 $NaHCO_3$, 240 sucrose, and 10 D-glucose. Here the sucrose is substituting 124 mM NaCl and 7 mM D-glucose from 'normal' ACSF since a high sucrose-low sodium environment acts to protect the newly cut brain slice by removing sodium from the extracellular solution thereby reducing the likelihood of sodium influx into cells which would be followed by water entry and cell swelling, which can lead to cell death (Ting *et al.*, 2014). All chemicals were obtained from Merck-SA unless stated otherwise. Once back in the laboratory, the brain was placed on ACSF-soaked filter paper atop a glass petri dish filled with crushed ice and sectioned using a single-edged razor blade. Blocking the brain began with two coronal cuts to detach the most rostral portion of the frontal lobes followed by removal of the cerebellum. Next, a single horizontal cut was made to remove the dorsal part of the cerebral cortex to allow the brain to sit flat when flipped upside down for mounting and slicing. Lastly, a single cut along the longitudinal fissure in the sagittal plane separated the two hemispheres. Slices were cut using a vibrating blade microtome (VT1000S, Leica Systems). The two blocks of brain tissue, each containing the medial temporal lobe from both the left and the right hemisphere, were superglued to a mounting plate in front of a SYLGARD elastomer

(SYLGARD 184, Dow Corning) support block. The mounting plate was then secured to the bottom of the buffer tray and the entire assembly was affixed to the main bolt of the microtome. The buffer tray was filled with ice cold (~4 °C) oxygenated (95% O_2 and 5% CO_2) and sucrose-substituted ACSF to fully submerge the tissue, and the cold temperature was maintained by packing the outer cooling bath with crushed ice. Horizontal sections were cut at a thickness of 340 µm. Only slices that contained both the medial and lateral divisions of the entorhinal cortex, including the hippocampus, were used for experiments included in this thesis (see **Figure 2.1A and 2.1B**). Slices rested for at least 60 minutes atop an elevated nylon net in individual wells positioned in a Pyrex dish (i.e., the holding chamber) filled with oxygenated (95% O_2 and 5% CO_2) ACSF containing (in mM): 124 NaCl, 2.5 KCl, 1.25 NaH_2PO_4, 2 $MgCl_2$, 2 $CaCl_2$, 26 $NaHCO_3$, and 17 D-glucose. Oxygenation was provided by two bubbling stones (repurposed stainless steel HPLC intake filters) placed in the ACSF. The holding chamber was positioned atop a hot plate to maintain the slices between 30 to 33 °C, a near-physiological temperature given that physiological temperatures for *in vitro* experiments range between 33 to 35 °C (Huang and Uusisaari, 2013; Dorst and Vervaeke, 2024). A digital thermometer was used to monitor the temperature of the ACSF via feedback from a probe positioned beneath the nylon net, and the settings on the hot plate were adjusted manually to ensure a consistent temperature.

Stimulation and Recording

Field Potential Recordings

Following a 60-minute recovery period, a single brain slice was transferred to the recording chamber using a glass transfer pipette and placed atop a nylon net submerged in ACSF. Oxygenated (95% O2 and 5% CO_2) ACSF was warmed initially to 36 °C in a water bath (JBA12, Grant Instruments Ltd.) before it was pumped into the recording chamber. A bath temperature of 30 to 32 °C was maintained within the recording chamber itself via an automated temperature controller (TC-324C, Warner Instruments) connected to a feedback thermistor positioned in the chamber. ACSF was pumped into a small reservoir using a peristaltic pump (Minipuls 3, Gilson) where it dripped under negative pressure through an in-line heating assembly (SH-27B, Warner Instruments) just prior to entering the recording chamber. Slices were held down via two small segments of thin twisted silver wire (see **Figure 2.1B**). A needle connected to a vacuum pump (Dymax 5, Charles Austin Pumps Ltd.) maintained the bath volume at a fixed level within the chamber keeping the slice fully submerged in the ACSF. The flow rate was maintained at a constant rate of 1.6 mL/min (Caruana *et al.*, 2006) via the peristaltic pump. Given the slice thickness, bath temperature and surface level recording of field potentials, a flow rate of 1.6 mL/min provides adequate oxygenation to the surface of the brain slice (Lipton *et al.*, 1995; Hajos *et al.*, 2009; Voss, George and Sleigh, 2012).

To evoke field excitatory postsynaptic potentials (fEPSPs) a bipolar tungsten stimulating electrode (WE3ST30.5A10, 250 µm tip separation, MicroProbes) was positioned in the slice under visual guidance (via a dissection microscope, UZ1-Boom, GT Vision Ltd.) to span the superficial layers (I to III) of the lateral entorhinal

cortex (see **Figure 2.1A and 2.1B**). Sharp recording electrodes were prepared from borosilicate glass capillaries (1.5 mm OD, Harvard Apparatus) using a horizontal micropipette puller (P-1000, Sutter Instruments). Electrodes were filled with ACSF and placed in a Perspex microelectrode holder containing a thin chloride-coated silver wire connected to the headstage of the recording amplifier. Forceps were used to carefully break the sharp tip of the pipette prior to insertion into a slice. The recording electrode was positioned caudal to the stimulating electrode (approximately 200 µm away) along the layer I/II border (see **Figure 2.1A and 2.1B**; Caruana & Chapman, 2006). Precise placement of the electrodes within the lateral division of the entorhinal cortex was made relative to prominent surface features of the slice (e.g., the rhinal sulcus) verified against corresponding plates from a stereotaxic atlas (Paxinos and Watson, 2007). All electrophysiological recordings were made in reference to a silver chloride ground pellet (AgCl, E200, 1.5 mm D; Harvard Apparatus) positioned in the bath.

Basal synaptic responses were evoked by delivering single test pulses (0.1 msec in duration) of electrical stimulation to the slice once every 20 seconds using a constant current stimulus isolator (DS3, Digitimer Ltd.). Stimulation intensity was adjusted to evoke fEPSPs approximately 75% of maximal amplitude (range; 20 to 280 µA). Recordings were obtained using an EXT-02F extracellular amplifier (gain set to 100x; npi electronic GmbH). Responses were filtered at 700 Hz (low pass band) and digitised at 20 kHz (PCIe-6321 X-Series DAQ, National Instruments) for storage on the hard drive of the primary data acquisition computer. Additional 50 Hz electrical interference was eliminated using a Hum Bug (Quest Scientific). At the end of a test day, the raw data were backed-up to an external storage array connected to the primary data acquisition PC, as well as uploaded to a cloud-based storage provider (Box) for added redundancy. If the amplitude of evoked fEPSPs was below 0.3 mV (see **Figure 2.1D**) or was unstable during the baseline period prior to an experiment, then the recording was terminated and the electrodes were either repositioned elsewhere in the same slice, or the slice was changed outright for another. All extracellular recording experiments were programmed and controlled using the software package, WinLTP (version 2.20b, WinLTP Ltd.). Measures of DC offset, latency to fEPSP peak, and peak amplitude of evoked responses (measured relative to the prestimulus baseline; **Figure 2.1D**) were plotted in real-time and visualised within the main acquisition window of WinLTP during an experiment. Each individual sweep evoked as part of an experimental protocol was saved to a file in a separate and unique folder on the acquisition PC for later offline analysis (or for conversion to a different file format, like .ABF), and the results of the real-time analysis (for offset, latency and peak) were written to an Excel worksheet and saved in the same folder as the corresponding sweeps.

Control recordings were interleaved regularly throughout all data collection, and each experimental protocol and manipulation was associated with an appropriate time-matched control experiment. Recordings were stable for periods lasting as short as 90 minutes up to a maximum of 330 minutes. Control recordings helped to monitor the stability of both the recording equipment and the experimental preparation during testing, as well as to provide an untreated and time-matched set of control data for statistical comparisons. Multiple sets of interleaved control experiments were obtained throughout testing to match the duration of all experimental protocols included in this thesis.

Multiple pharmacological and electrophysiological protocols were administered during data collection. Experiments were interleaved, and the same protocol was never repeated in more than one slice from a single animal. Typically, the amplitude of fEPSPs was assessed before, during and after one of these experimental manipulations. During pharmacological experiments, synaptic responses were evoked by delivering either single test pulses of electrical stimulation or *pairs* of stimulation pulses. For paired-pulse experiments, interpulse intervals (IPIs) of 10, 30, 100, 300 and 1000 msec were used, and paired-pulse ratios calculated for each IPI were compared at multiple time points during an experiment. In some experiments, activity-dependent forms of synaptic plasticity were induced in the lateral entorhinal cortex either on their own or together with various pharmacological interventions. To induce long-term synaptic depression (LTD), 900 pairs of stimulation pulses (with a 30 msec IPI) were delivered to sensory afferents at a frequency of 1 Hz for 15 minutes since single pulse LFS (900 pulses at 1Hz) is not enough to induce LTD at postsynaptic sites of the medial and lateral perforant path in the dentate gyrus (Abraham and Bear, 1996; Abraham, Mason-Parker and Logan, 1996; Gonzalez *et al.*, 2014) but pairs of pulses (900 pulses at 1 Hz, 25 ms IPI) does induce a short-term depression lasting 60-90 mins (Strauch and Manahan-Vaughan, 2020). Additionally, multiple stimulation protocols were used to induce long-term synaptic potentiation (LTP). Specifically, high frequency stimulation (a single train of 100 or 200 pulses delivered at either 100 or 200 Hz, respectively) or theta burst stimulation (10 trains of 10 pulses at 100 Hz; inter-train interval of 200 msec; repeated 3 times once every minute) were delivered to sensory afferents in slices of lateral entorhinal cortex, since it has been shown that TBS (10 trains of 4 pulses at 100 Hz; repeated at 5 H) and HFS (long HFS: 1 sec train of pulses at 100Hz) is suitable for inducing LTP at medial entorhinal cortex principle neurons in the superficial input layers II/III (Yun, Mook-Jung and Jung, 2002). Also, TBS consisting of more than 4 pulses (100 > pulses > 10) in each train leads to greater induction of LTP in *stratum radiatum* of area CA1 (Larson and Munkacsy, 2015).

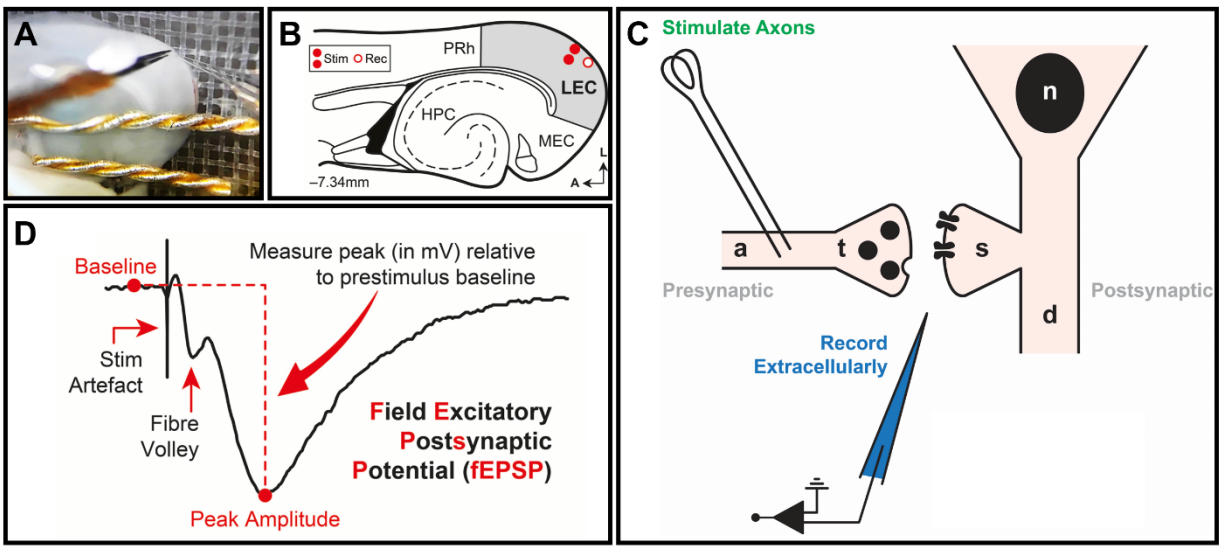

Figure 2.1. Recording evoked field excitatory postsynaptic potentials (fEPSPs) in the lateral entorhinal cortex*. Only slices that contained a large portion of lateral entorhinal cortex were used for all experiments in this thesis. (**A**) A photograph captured by a camera pointing down the main objective of the dissection microscope highlights the position of the stimulating and recording electrodes in a typical slice recording setup. The bipolar stimulating electrode is visible*

*in the top centre of the frame and the glass recording pipette can be seen just off to the right of the stimulating electrode. (**B**) Schematic diagram of the rat brain slice (at a position -7.34 mm relative to Bregma) indicating the target positions for stimulating and recording electrodes in horizontal slices containing the lateral entorhinal cortex. A bipolar stimulating electrode was positioned in the superficial layers of the lateral entorhinal cortex (layers I to III; filled red circles; Stim) and a recording electrode was positioned nearby along the layer I/II border (open circle; Rec). (**C**) Schematic diagram highlighting a simplified view of the recording setup to evoke extracellular fEPSPs in the lateral entorhinal cortex. A stimulating electrode is positioned in cortical sensory afferents to evoke glutamate release from terminals in the entorhinal cortex. Activity at multiple synapses is recorded simultaneously via an extracellular recording electrode positioned nearby (a, axon; t, terminal; n, nucleus; s, spine; and d, dendrite). (**D**) Evoked fEPSPs in the lateral entorhinal cortex typically consist of multiple components, including a stimulation artifact, a presynaptic fibre volley, and a postsynaptic response. The primary dependent measure used for all field recording experiments was the peak amplitude of evoked fEPSPs measured relative to the prestimulus baseline.*

Whole-Cell Recordings

Whole-cell experiments began following a one-hour recovery period post-slicing. Individual slices were transferred to a recording chamber and visualised using an upright microscope (BX51WI, Olympus-Keymed) equipped with a 40x water-immersion objective, a near-infrared camera (IR-1000E, Dage-MTI), and differential interference contrast optics connected to a reference monitor. Slices were secured with either a small segment of twisted silver wire or a stainless steel and Lycra slice anchor (SHD-42/15, World Precision Instruments) and submerged in warmed, oxygenated ACSF (or ACSF containing 1 mM kynurenic acid to isolate inhibitory currents) perfused at a rate of 2 mL/min. The composition of the ACSF was the same as the ACSF used for field potential recordings (see above). A thermistor positioned in the bath was connected to an automatic temperature controller (TC-324C, Warner Instruments) used to maintain the bath at around 30 °C by heating the ACSF via an inline solution heater (SH-27B, Warner Instruments) just prior to entering the recording chamber. A 4-channel gravity perfusion system (Valve Commander VC3, ALA Scientific Instruments Inc.) facilitated manual solution changes during an experiment. A control pad was used to trigger the opening or closing of a series of pinch valves that permitted rapid changes to the bathing medium and the perfusion of ACSF mixed with specific drugs. The flow rate was regulated by a pinch-clamp and thumb screw assembly attached to the main perfusion line adjusted manually at the start of an experiment to ensure a final flow rate of 2 mL/min. A suction tube connected to a vacuum pump (Dymax 5, Charles Austin Pumps Ltd.) was also used to maintain a consistent bath level during experiments.

Methods used to obtain whole-cell patch clamp recordings were similar to those used previously (Caruana and Chapman, 2008; Caruana, Warburton and Bashir, 2011; Caruana and Dudek, 2020). Recording electrodes were pulled from borosilicate glass capillaries (1.5 mm OD; 3-8 MΩ; Harvard Apparatus) using a horizontal micropipette puller (P-1000, Sutter Instruments, USA) and filled with a solution containing (in mM): 120 K-gluconate, 10 KCl, 3 $MgCl_2$, 0.5 EGTA, 40 HEPES, 2 Na^{2+}-ATP, and 0.3 Na^{2+}-GTP (270-280 mOsm) unless stated otherwise. For streptavidin labelling of individual neurons (described below; final osmolarity of 270-280 mOsm), the patch solution also contained 5 mg/mL of the cell tracer, biocytin. During experiments to isolate and record inhibitory synaptic currents, an alternative, caesium-based (Cs^+), patch solution containing (in mM): 100 CsCl, 1 QX-314, 10 TEA-Cl, 5 $MgCl_2$, 0.6 EGTA in CsOH, 40 HEPES, 4 Na^{2+}-ATP, and 0.3 Na^{2+}-GTP (270-280 mOsm)

was used. With this internal solution, both voltage-gated sodium and voltage-gated potassium channels were blocked, by QX-314 and tetraethylammonium (TEA), respectively, thereby preventing cells from spiking when depolarised suprathreshold to 0 mV. QX-314 is a quaternary derivative of lidocaine known to block voltage-gated sodium channels and acts as a local anaesthetic (Lee, Goodchild and Ahern, 2012), it works by intracellularly blocking the inner pore of the voltage-gated sodium channels in the same way lidocaine does: blocking the inner pore whilst its permanent positive charge provides electrostatic attraction to the carbonyl backbone of the pore in position *p48,* thus enabling a channel specific inhibition (Tikhonov and Zhorov, 2017). TEA, however, is a voltage-gated channel blocker specific to potassium channels. The specificity arises from its innate ability to inhibit key pore-forming subunits of the voltage gated potassium channels via the gene; KCNQ3, KCNA1, KCNA3 and KCNA5 (Zhou *et al.*, 2024)

To accurately pinpoint the lateral entorhinal cortex (see **Figure 2.2B**), slices were visualised under 4x magnification and prominent anatomical features (such as the rhinal fissure) were identified in relation to corresponding horizontal plates from a stereotaxic atlas (Paxinos and Watson, 2007; see **Figure 2.2A**). The objective was then switched to the 40x water-immersion objective and suitable neurons in layer II of the lateral entorhinal cortex were identified for whole-cell experiments. Once a cell was selected, the recording electrode was lowered into the slice under negative pressure and placed into contact with the target neuron's soma (see **Figure 2.2D**). The negative pressure was released, and gentle suction was applied under voltage clamp to form a tight seal (≥ 1 GΩ). Whole-cell configuration was achieved by increased suction, and experiments began after cells stabilised (typically within 5 to 10 min following break-in). Voltage clamp recordings (V_h of -70 mV, though, in some experiments V_h was set to 0 mV) were obtained using a MultiClamp 700B amplifier (Molecular Devices, LLC) and displayed on a computer monitor using the software package WinLTP (version 2.20b, WinLTP Ltd.). Recordings were filtered at 10 kHz and digitized at 20 kHz (Digidata 1550A, Molecular Devices, LLC) for storage on the hard drive of the primary data acquisition PC. Data were also backed-up to external media and online to Box at the end of each test day. No correction was applied to compensate for liquid junction potentials. Only cells with a series resistance (R_s) < 25 MΩ and a < 20% change in R_s from baseline during an experiment were included for analysis. In addition, cells with a baseline resting membrane potential > -50 mV or requiring more than 100 pA of direct current injection to reach a holding potential of -70 mV at the start of an experiment were also excluded. All electrophysiological recordings were made in reference to a silver chloride ground pellet (AgCl, E200, 1.5 mm D; Harvard Apparatus) positioned in the bath. Measures of holding current, R_s, membrane resistance (R_m), and peak amplitude of evoked synaptic currents (measured relative to the prestimulus baseline; **Figure 2.2D**) were plotted in real-time and visualised within the main acquisition window of WinLTP during an experiment. Each individual sweep evoked as part of an experimental protocol was saved to a file in a separate and unique folder on the acquisition PC for later offline analysis (or for conversion to a different file format, like .ABF), and the results of the real-time analysis were written to an Excel worksheet and saved in the same folder.

Synaptic responses were evoked with 0.1 msec duration constant current pulses delivered using a stimulus isolation unit (Model DS3, Digitimer Ltd., Hertfordshire, UK), and stimulation intensity was adjusted to

evoke synaptic currents approximately 75% of maximal amplitude (range; 20 to 200 µA). Single test pulses or pairs of stimulation pulses (with a 30 msec IPI) were delivered once every 60 seconds (or in some instances, once every 120 seconds) using a bipolar tungsten stimulating electrode (WE3ST30.5A5, 125 µm tip separation, MicroProbes) positioned in layers I-II of the lateral entorhinal cortex (see **Figure 2.2A**). Protocols to induce activity-dependent forms of plasticity in sensory inputs to the superficial layers of the lateral entorhinal cortex were the same as those outlined above for field potential recording experiments. As with field recordings, interleaved control experiments were obtained regularly throughout data collection, and every experimental protocol was associated with a time-matched and interleaved control. Experimental interventions were also interleaved, and the same protocol was never repeated in more than one slice from a single animal.

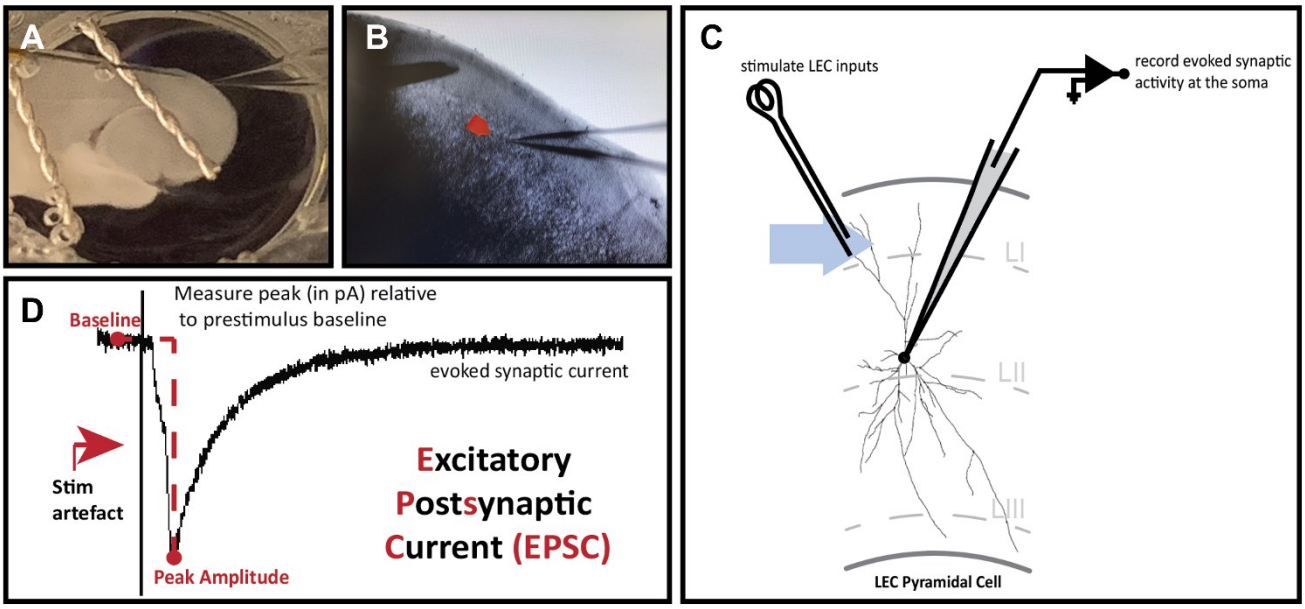

Figure 2.2. Recording evoked synaptic currents from single neurons in the lateral entorhinal cortex*. Slices containing a larger portion of the lateral entorhinal cortex were used for these experiments. (**A**) A photograph showing the position of a slice in the recording chamber. Note the twisted silver wire used to keep the slice submerged and stationary in the ACSF. It is also possible to see the location of the bipolar stimulating electrode in the top centre of the frame, and the nearby recording pipette slightly off to the right. (**B**) A DIC image of the lateral entorhinal cortex taken at 4x magnification. The stimulating electrode is positioned to span layers I-II under this level of magnification. (**C**) Schematic diagram highlighting a simplified view of the recording setup to evoke intracellular synaptic currents in a single projection neuron in the lateral entorhinal cortex. A stimulating electrode is positioned to span layers I-II to activate cortical sensory afferents and trigger glutamate release from these terminals. The recording electrode detects the sum of all evoked synaptic activity at the soma of the patched cell. (**D**) An example excitatory synaptic current recorded from a single lateral entorhinal cortex neuron (located in layer II). The peak amplitude of the current (or EPSC) is measured relative to the prestimulus baseline.*

Neuronal Morphology

Biocytin-Streptavidin Labelling

In some of the whole-cell recording experiments described above, the intracellular solution contained the cell tracer, biocytin (5 mg/mL). Note: a separate cohort of layer III neurons were filled separately and used

just for morphological comparison with layer II neurons. Depending on the access (or R_s), biocytin in the patch solution was expected to dialyse into the patched neuron so that the morphological features of the cell could be identified, and the neuron classified. Only neurons located on the surface of the slice and visible under DIC optics were accessible for whole-cell recordings. Therefore, only these cells were filled with biocytin and included in the morphological analysis. At the end of a successful 60-minute experiment, the recording electrode was slowly retracted from the cell, and the brain slice placed in a pre-labelled well plate and submerged in 4% paraformaldehyde (PFA). The slice was left in the dark for 12 to 24 hours at 4 °C. The following day, slices were washed in 4% phosphate buffered saline (PBS) three times and allowed to develop in a solution containing 4% PBS, 1% Triton X-100 and 0.2% streptavidin [Alexa Fluor 594 (red) and 488 (green) conjugates; Invitrogen] for 18 hours in the dark at 4 °C. Afterwards, slices were washed three more times in 4% PBS, mounted on slides using an Antifade Mounting Medium with DAPI (Vectashield; Vector Laboratories), and coverslipped. The conjugates of streptavidin used were fluorescent and detected biotinylated molecules, of which biocytin is one. This made the labelled cells easy to visualise using a fluorescent microscope as their signal was amplified.

Data Analysis

Electrophysiology and Pharmacology

Evoked synaptic responses (fEPSPs, EPSCs and IPSCs) were measured and analysed using a range of specialised electrophysiology software applications, including WinLTP, Clampfit (Molecular Devices, LLC) and AxoGraph X (AxoGraph Scientific). In addition, Excel (Microsoft Corporation) and Prism (GraphPad) were used extensively for data triage, analysis and plotting, and final figures for this thesis were prepared using Illustrator (Adobe Inc.). Peak amplitudes of synaptic responses (fEPSPs, EPSCs and IPSCs) were measured relative to the prestimulus baseline (8 to 2 msec period before stimulation pulse) and paired-pulse facilitation was determined by expressing the amplitude of the second response as a proportion of the amplitude of the first response. For whole-cell experiments, R_s was calculated by measuring the peak amplitude of the fast capacitive transient observed at the onset of a −5 mV voltage step (50 msec duration) delivered 100 msec prior to test stimulation. Responses were averaged every minute or every 2-minutes (for some whole-cell experiments) and then normalised to the baseline period for plotting. The effects of bath- or intracellularly applied drugs during pharmacological experiments were assessed on the amplitude of averaged synaptic responses (fEPSPs, EPSCs and IPSCs) obtained during 5- or 10-min epochs recorded at different times during an experiment (latencies specified below). In some instances, the peak change in response amplitude was used, and this was determined manually, within a two-minute window a peak drug effect was determined, for each individual experiment as the latency varied. The peak amplitude of fEPSPs in the entorhinal cortex was measured in this study as opposed to the more commonly used analysis of slope in medial temporal lobe regions. Regions such as area CA1 of the hippocampus for example exhibit more fast and temporally precise synaptic transmission attributing to the fast fEPSP responses measured as well as a strong feedforward inhibitory potential, thus requiring rising phase slope analysis for an accurate depiction of excitatory synaptic efficacy (Marder and Buonomano, 2003). Measuring

peak amplitude of fEPSPs in entorhinal cortex, however, ensures all the far reaching and temporally unique synaptic inputs that are integrated here are represented cumulatively reducing the risk of leaving slower or later stage excitatory potentials out of analysis paradigms (Burwell and Amaral, 1998a; Nilssen *et al.*, 2019). Concentration-response curves were generated with Prism (inhibitor versus response; variable slope with four parameters) and fit using the least squares (ordinary) method. Curves were constrained to 100% at the top, which is the theoretical maximum level of inhibition possible using the compounds tested. Comparisons of curve-fits were made using sum-of-squares F-Tests. Additional curve fitting (nonlinear regression, polynomial modelling, LOWESS curves, and others), when required, was also performed using Prism (see below). All data were expressed as the mean ± SEM and were normalised to the baseline period for plotting. Drug- or stimulation-induced changes in response properties were assessed with Prism using (where appropriate) paired or unpaired samples t-tests, one-way ANOVAs or repeated measures ANOVAs. Post-hoc comparisons were made using the Bonferroni method with an alpha level of $P < 0.05$.

Biocytin-Streptavidin Labelling

Slides containing brain slices with the biocytin-streptavidin labelled neurons were imaged using an epifluorescence microscope (DMI400B, Leica Systems) fitted with a camera (DFC360 FX, Lecia Systems). Neuron morphology was then visualised using either a 10x (for neurons that were highly branched, or with longer reaching dendrites), or a 40x (for neurons with smaller dendritic arborisations) objective, and visual frames captured using the Lecia Application Suite for Advanced Fluorescence (Lecia Systems). Captured images were enhanced and saved (along with relevant metadata) to the hard drive of the imaging PC in both ND2 and JPG formats. Later, individual images were loaded into the open-source image editor, FIJI (Schindelin *et al.*, 2012), and adjusted for brightness and contrast so that all labelled neuropil was visible. In addition, the scale bar was calibrated from the raw image to ensure accurate dendritic branch measurements were obtained from each individual neuron. Images were then loaded into the program, SNT, from the Fiji plugin, Neuroanatomy, in order to reconstruct a digital representation of the traced neuron (Arshadi *et al.*, 2021). A Sholl analysis was performed on each reconstructed neuron using FIJI. This involved superimposing concentric circles at regular intervals over the entire surface area of the cell (distance between rings was set to 5 µm) with the centre point starting at the middle of soma. The number of intersections between each concentric circle and individual dendritic branches was measured, as well as the distance from the soma at which they occurred, and this was used to determine the distance from the soma the level of branching was most prominent. Measures of intersections and peak distance (where the most branching occurred) were compiled for each individual neuronal phenotype in layer II and layer III of the lateral entorhinal cortex and compared using one-way ANOVAs in Prism. Since trace reconstructions were performed on filled neurons from 340 µm-thick sections, some neuropil was likely cropped, making size comparisons between different neuronal phenotypes challenging. Additionally, due to dialysis effects associated with whole-cell recordings, somata were not compared between neurons.

Pharmacology

All drugs and compounds used for pharmacological experiments reported in this thesis (see Table 2.1) were obtained from either Merck-SA, Bio-Techne Ltd. (Tocris), or Hello Bio Inc. and prepared as concentrated stock solutions (typically 10 to 50 mM) by dilution in (where appropriate) either distilled water or dimethyl sulfoxide and stored at -20 °C until required. In some instances, like when using dopamine hydrochloride and kynurenic acid, experimental solutions had to be prepared fresh at the time of use.

To examine the effects of dopamine on basal synaptic transmission and synaptic plasticity in the lateral entorhinal cortex, dopamine hydrochloride was used. It should be noted that this drug is extremely light-sensitive. In order to maintain maximum potency and viability of dopamine-containing solutions, all ambient lighting was reduced when preparing them in the laboratory and when administering them during an experiment (Pralong and Jones, 1993; Stenkamp, Heinemann and Schmitz, 1998; Caruana *et al.*, 2006; Rosenkranz and Johnston, 2006; Caruana and Chapman, 2008; Glovaci, Caruana and Chapman, 2014). As well as reducing ambient lighting, all beakers and graduated cylinders used to prepare solutions containing dopamine hydrochloride were covered in aluminium foil to further prevent light exposure and subsequent oxidation of the active drug. Dopamine hydrochloride was stored, in powder form, in the dark at 4 °C until required, and dopamine stock solutions were prepared 5 to 10 minutes prior to experimental use. Additionally, the antioxidant sodium metabisulfite (50 µM) was added to the dopamine to further reduce oxidation (Yang, Seamans and Gorelova, 1996; Stenkamp, Heinemann and Schmitz, 1998)(see **Figure 2.8**). An initial stock solution of 2 mM dopamine in ACSF was prepared fresh just prior to use, from which further serial dilutions in ACSF provided the desired working concentrations of dopamine (1, 3, 10, 30, 100, 300 or 1000 µM, depending on the experiment). An antioxidant was also added to the dopamine to help prevent oxidation (sodium metabisulfite, 50 µM, see below).

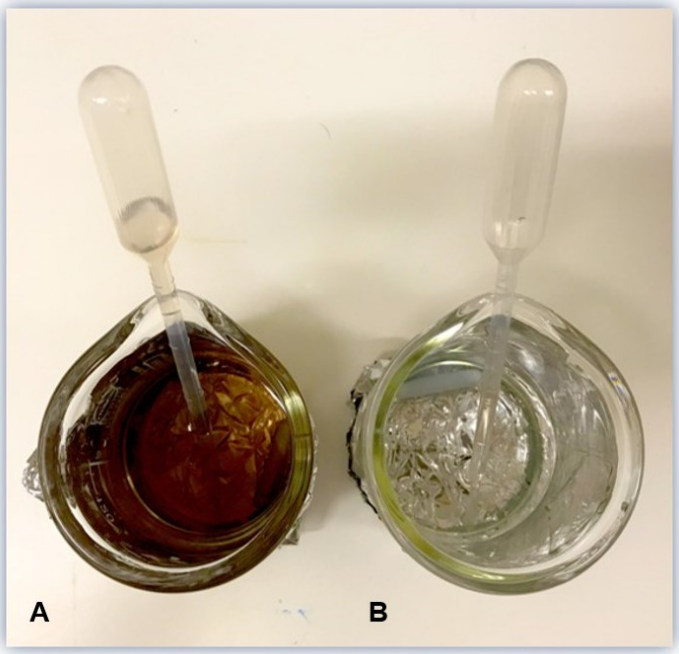

***Figure 2.3. Dopamine hydrochloride oxidises in ACSF alone**. (**A**) Preparing dopamine in an environment with natural and/or artificial light causes rapid oxidation denoted by the brown colouration from a once clear solution. (**B**) When sodium metabisulfite (50 µM) is added to ACSF prior to the dopamine, oxidation is prevented, and the solution remains clear and transparent. Note the beakers are wrapped in foil to further limit light exposure.*

In some experiments, the broad-spectrum dopamine receptor agonist apomorphine was utilised as a potential and more stable alternative to dopamine hydrochloride (Arroyo-Garcia *et al.*, 2018). Using apomorphine reduced the likelihood of the agonist oxidising over time when exposed to ambient light and oxygen (Ang *et al.*, 2016). Multiple concentrations of apomorphine were tested (10, 30, 100 and 300 µM). As noted, the antioxidant, sodium metabisulfite (50 µM), was used to prevent oxidation of drugs sensitive to light and air exposure, including both dopamine and apomorphine. To examine contributions of individual dopamine receptor subtypes, both the D_1-like receptor antagonist SCH-23390 (50 µM) and the D_2-like receptor antagonist sulpiride hydrochloride (50 µM) were used (Savasta, Dubois and Scatton, 1986; Pralong and Jones, 1993; Caruana *et al.*, 2006; Glovaci, Caruana and Chapman, 2014). Contributions of N-methyl-D aspartate receptors (NMDARs) to dopamine-mediated changes in synaptic function were examined using D-(-)-2-Amino-5-phosphonopentanoic acid (AP5; 10 µM). The role of intracellular calcium in activity-dependent forms of plasticity in the lateral entorhinal cortex was assessed by loading cells with 10 mM 1,2-Bis(2-aminophenoxy)ethane-N,N,N',N'-tetraacetic acid (BAPTA). The effects of dopamine on inhibitory transmission were explored by co-applying dopamine together with the $GABA_A$ receptor antagonist, picrotoxin (50 µM), and in some experiments, the effects of dopamine were assessed on isolated inhibitory currents directly. Inhibitory postsynaptic currents (or IPSCs) were isolated using the broad-spectrum glutamate receptor antagonist, kynurenic acid (1 mM), that is known to act as a competitive antagonist at NMDA receptors (Majlath *et al.*, 2016), as well as both AMPA and kainate receptors (Erhardt, Olsson and Engberg, 2009). Mechanisms underlying the dopamine-mediated desensitisation of dopamine receptors was assessed using the clathrin adapter protein (AP2) and β-arrestin-mediated G protein-coupled receptor endocytosis inhibitor, barbadin (30 µM) (Sundqvist *et al.*, 2020), as well as the membrane-permeable G protein-coupled receptor kinase (GRK) inhibitor, compound 101 (CMPD101, 10 µM). Compound 101 is highly effective at preventing the desensitisation of G-protein coupled receptors on neuronal membranes by targeting GRK2 and GRK3 (Lowe *et al.*, 2015). Finally, in some experiments, the effects of the nonselective adenosine receptor antagonist, caffeine (300 µM), was used to assess putative adenosinergic contributions to activity-dependent plasticity in the entorhinal cortex.

Drug/Compound	*Concentration*	*Target Affinity*	*Solvent used in stocks*
DL-AP5	10 µM	IC_{50} (µM) = 0.28, 0.46 and 1.6 for NMDA receptor subunits N2A-C, respectively[1]	Distilled water
Apomorphine	10 µM 30 µM 100 µM 300 µM	K_i values (nM) = 484, 52, 26, 4 and 189; 2523 and 120; and 1995, 679, 65, 141, 66 and 36 for binding to D_1 to D_5; 5-HT_{1A} and 5-HT_2; $\alpha_{1A,B,D}$ and α_{2A-C} receptors, respectively[2,3,4]	Distilled water
BAPTA	10 mM	K_D value (nM) = 160 for Ca^{2+} chelation[5]	-
Barbadin	30 µM	IC_{50} values (µM): 19.1 and 15.6 for β-arrestin1 and 2, respectively[6]	Dimethyl sulfoxide
Caffeine[A]	300 µM	K_D values (µM): 12, 2.4, 13 and 80 for adenosine A_1, A_{2A}, A_{2B} and A_3 receptors respectively[7]. Concs. > 250 µM increases calcium release from internal stores (ER and SR)[8] and concs. < 100 µM caffeine alters Cl^- transport function of $GABA_A$ receptors[9]	Distilled water
Compound 101	10 µM	IC_{50} values (nM): 32 and 54 for GRK2/3, respectively to selectively reduce the internalisation of µ-opioid receptors[10]	Dimethyl sulfoxide
Dopamine[B]	1 µM 3 µM 10 µM 30 µM 100 µM 300 µM 1000 µM	K_i values (nM): 3400, 600-4000, 32-16, 28-40, 228, 67-6000, 40-32000 and 422 for D_{1-5} receptors, DAT, NAT and TAAR1 respectively[2] K_i value of 10 µM for serotonin 1A, 1B, 1D, 2A, 2C, 3, 5, 6 and 7, adrenergic α_A and β, cannabinoid CB1[2]	- - - - - - -
Kynurenic acid	1 mM	IC_{50} values (µM): 70 and 500 for NMDA and kainate receptors, respectively Known to interact with the α7-nicotine acetylcholine receptor at 7 µM, and the adrenoceptor α_{2B}[12]	-
Picrotoxin	50 µM	IC_{50} value (µM): 0.6 and 1.7 for the $GABA_c$ and Cl^- linked GABA receptor, repectively[13,14], IC_{50} value (nM): 240 for $GABA_A$ receptors[15]	Dimethyl sulfoxide
SCH-23390	50 µM	K_i values (nM): 0.2, 0.3 and 6.3-9.3 for D_1 and D_5, and 5-HT_{2C} receptors respectively. Also, blocks GIRK currents with EC_{50} of 268 nM[16]	Distilled water
Sulpiride	50 µM	K_i values (nM): 4786, 5011, 5011, 9.8, 8.05 and 54 for 5-HT_{2A}, 5-HT_6, 5-HT_7 and D_{2-4} receptors respectively. Also, K_i values >10 µM for DAT and 5-HT_{1A}, 5-HT_3, α_1, α_2, D_1, H_1 and V_3 receptors[2]	Dimethyl sulfoxide

Table 2.1. Summary of drugs and compounds used in this study. *Drugs exhibit concentration-dependent targets; therefore, all potential drug targets are listed above. Note: -, not applicable; [A], heteromeric receptors formed of adenosine*

and dopamine subtypes enables caffeine to indirectly affect dopaminergic signalling via adenosine receptor binding; 5-HT, serotonin receptor; α receptor, adrenergic receptor; AP5, 5-phosphonopentanoic acid; BAPTA, 1,2-Bis(2-aminophenoxy)ethane-N,N,N',N'-tetraacetic acid; ^{B}, heterooligomers formed with multiple receptor subtypes enable dopamine to act indirectly via alternate adenosine, adrenergic and ghrelin signalling due to receptor interactions; Cl^-, chloride ion; concs., concentrations; DAT, dopamine transporter; ER, endoplasmic reticulum; GIRK, G protein-coupled inwardly rectifying potassium channel; GPCR, G protein-coupled receptor; NAT, noradrenaline transporter; SR, sarcoplasmic reticulum; TAAR1, trace amine-associated receptor 1; V, vasopressin receptor. Refs: 1, Feuerbach et al. (2010); 2, Besnard et al. (2012); 3, Newman-Tancredi et al. (2002a); 4, Newman-Tancredi et al. (2002b); 5, Sneyers et al. (2024); 6, Beautrait et al. (2017); 7, Froestl, Muhs and Pfeifer (2012); 8, Reddy et al. (2024); 9, Lopez et al. (1989); 10, Harding et al. (2024); 11, Miller (2011); 12, Bertolino, Vicini and Costa (1989); 13, Goutman and Calvo (2004); 14, Akaike et al. (1985); 15, Qian and Dowling (1994); 16, Bourne (2001), Briggs et al. (1991), Millan et al. (2001) and Kuzhikandathil and Oxford (2002).

Chapter 3: Effects of Dopamine on Synaptic Transmission in the Superficial Layers of the Lateral Entorhinal Cortex

Introduction

Gross characterisation of network connectivity within the entorhinal cortex was carried out many years ago using techniques such as Nissl-staining (Price and Powell, 1971; Carboni and Lavelle, 2000), Falck and Hillard staining (Falck *et al.*, 1962; Fuxe, 1965) and retrograde immunolabelling using antibodies against tyrosine-hydroxylase (Swanson, 1982; Akil and Lewis, 1994). More recently, a study by Tahvildari and Alonso (2005) used whole-cell patch clamp recording methods combined with post-hoc fluorescence imaging to characterise – in unprecedented detail – the morphology and electrophysiological properties of the diverse array of cell types found in superficial layers II and III of the lateral entorhinal cortex. Further characterisation of neuronal morphology within *every* cortical layer of the lateral entorhinal cortex has since been carried out by Canto and Witter (2012a), and similar morphological features were observed in superficial layer projection neurons as those outlined in previous work (Tahvildari and Alonso, 2005). For example, layer II and III pyramidal neurons exhibit thick apical dendrites that bifurcate within the same layer as their cell soma, while layer II fan cells typically extend their apical dendrites extensively within layer II and into layer I but rarely into layer III. There are some inconsistencies, however, as Canto and Witter (2012a) found the dendrites of some layer II and layer III principal neurons tended to branch much further into the deeper layers than demonstrated previously. As a result, some of the basic morphological characteristics for several neuronal phenotypes within the lateral entorhinal cortex had to be revised (Tahvildari and Alonso, 2005), but there was still significant overlap in terms of the basic cell types found in the lateral division, as well as in their overall pattern of distribution and total numbers reported within each cortical layer. Canto and Witter (2012a) speculated that some of the inconsistencies may have been due to the previous study (Tahvildari and Alonso, 2005) inadvertently recording from stellate neurons in the medial entorhinal cortex found close to the border with the lateral division that have a similar morphology to lateral division fan neurons, yet a very different electrophysiological profile. It was also noted that the age difference between animals (P14-32 vs P42-60 by Canto and Witter (2012a) and Tahvildari and Alonso (2005), respectively, used in each study (for review see McCutcheon and Marinelli, 2009) may have contributed to some of the variability in overall morphology, and this may have been further compounded by subtle differences in recording equipment used (i.e., recording electrodes). Generally, the distinct morphological and electrophysiological properties of principal cells in layer II of the lateral entorhinal cortex allow them to be clustered into four distinct populations of excitatory neurons comprised mainly of pyramidal, oblique pyramidal, fan and multiform neurons. The principal cells residing in layer III of the lateral entorhinal cortex fall into one of three distinct morphologies comprised of simple pyramidal, complex pyramidal and multipolar neurons (Tahvildari and Alonso, 2005; Canto and Witter, 2012a). Taken together, the results of these studies highlight that principal neurons in the superficial layers of the lateral entorhinal cortex are

morphologically and physiologically heterogeneous and likely contribute to distinct network functions both within and between cortical layers. Further, it is these principal neurons within the superficial layers that receive innervation from sensory association areas and output directly to the hippocampus (Bashir *et al*., 1993; Solodkin and Van Hoesen, 1996; Igarashi *et al*., 2014; for review see Burwell, 2000).

Principle neurons in the superficial layers of the lateral entorhinal cortex receive multimodal sensory information that is non-spatial in nature (Burwell, 2000). This sensory information is integrated within superficial layer circuits and relayed via separate input streams to different targets in the hippocampus, including the dentate gyrus and area CA3 (the perforant path), area CA1 (the temporoammonic path) and area CA2 (the direct pathway and indirect perforant path projections from area CA3 or dendate gyrus, both synapsing onto apical dendrites of the *stratum lacunosum-moleculare* layer) ((Dudek, Alexander and Farris, 2016; Lopez-Rojas *et al.*, 2022) and see **Figure 1.2**). It is thought this information is integrated further with other sensory and non-sensory signals within hippocampal circuits and then encoded and consolidated (Otmakhova and Lisman, 1999; Deshmukh and Knierim, 2011; Igarashi *et al.*, 2014; Basu *et al.*, 2016; Lee *et al.*, 2021). Despite the major output of processed hippocampal information being distributed to the mammillary bodies, thalamus and cingulate cortex via white matter tracks known as the fimbria and fornix (Chauhan *et al.*, 2021), there is also processed information from the hippocampus that is returned, once more, to the entorhinal cortex, but this time to the deep layers (V and VI). Deep layer neurons then relay information back to the original sensory association regions that innervated the entorhinal cortex initially (Canto, Wouterlood and Witter, 2008; Witter *et al.*, 2017; Nilssen *et al.*, 2019). It is known that changes in synaptic function at multiple points through this input and output circuit are essential for the integration, encoding and consolidation of sensory signals essential to declarative memory (Meunier *et al.*, 1993; Zola-Morgan *et al.*, 1993; Winters and Bussey, 2005; Vandrey *et al.*, 2020). Modulatory neurotransmitters, such as acetylcholine (for review see Hasselmo *et al*., 2000; Hasselmo, 2006), are known to play a pivotal role in this process, but surprisingly little is known about the role of dopamine in modulating sensory and mnemonic function in the lateral division of the entorhinal cortex.

Dopaminergic neurons from the VTA target few cortical regions, most notably the prefrontal cortex (Oades and Halliday, 1987; Mingote *et al.*, 2015) where dopamine is essential to working memory function (for review see Goldman-Rakic, 1996; Goldman-Rakic and Selemon, 1997; Goldman-Rakic, 1999). However, there is a branch of the mesocortical dopaminergic pathway that innervates the entorhinal cortex, yet it is unknown how dopamine contributes to the cognitive and mnemonic functions of both the medial and lateral divisions. In the few studies that have explored dopaminergic modulation of principal neurons in the superficial layers of the lateral entorhinal cortex it has been shown that dopamine appears to act predominantly as a *suppressor* of synaptic transmission and neuronal excitability in sensory inputs to superficial layer projection neurons (Caruana *et al.*, 2006; Caruana and Chapman, 2008; Glovaci, Caruana and Chapman, 2014; Batallan-Burrowes and Chapman, 2018; Liu, 2020; Gao *et al.*, 2022). However, the effects of dopamine have also been shown to be concentration-dependent as low concentrations of dopamine (1 to 10 µM) enhance the excitability of layer II neurons (Caruana *et al.*, 2006; Glovaci, Caruana and Chapman, 2014; Glovaci and Chapman, 2015; Mingote *et al.*, 2015). It has been proposed that this bidirectional effect is due to the presence and distribution of different

dopamine receptor subtypes in the membranes of both afferent sensory terminals and superficial layer projection neurons in the lateral entorhinal cortex. Dopamine receptor subtypes can be grouped by their genome sequencing (for review see Missale *et al*., 1998) and associated G-protein leading to specific downstream effects on synaptic function (Hasbi, O'Dowd and George, 2010). D_1-like receptors (D_1 and D_5) upregulate the production of adenyl cyclase via the $G_{s/Olf}$ proteins whereas D_2-like receptors (D_2, D_3 and D_4) downregulate adenyl cyclase via $G_{i/o}$ proteins. Interestingly, a study done by Glovaci, Caruana and Chapman (2014) suggested that the facilitation of excitatory currents in layer II projection neurons is attributed to activation of D_1-like receptors. Further work by Köhler, Ericson and Radesäter (1991) showed that the laminar distribution of D_1 receptors in the superficial layers of the lateral entorhinal cortex is limited to *only* layer II, whereas D_2 receptors are found distributed more heterogeneously in layers I, II and III with little expression in layer II. It is important to note that dopamine receptor subtypes have different binding affinities for dopamine: D_1 receptors have a lower binding affinity for dopamine compared to D_2 receptors, despite D_1 receptors being much more prominent throughout the lateral entorhinal cortex overall (Boyson, McGonigle and Molinoff, 1986; Richfield, Penney and Young, 1989). There are also disparities between receptor types and their response to the mode of dopamine application. Specifically, it has been suggested that D_2-like receptors respond more preferably to tonic release of dopamine compared to D_1-like receptors whereas D_1-like receptors respond better to phasic (or interrupted sequential) dopamine release (for review see Subramaniyan and Danni, 2015; Harvey, 2020).

In the medial entorhinal cortex, the suppressive effect of high concentrations (> 100 µM) of dopamine on synaptic transmission of layer II stellate cells has been attributed to a change in membrane resistance (Pralong and Jones, 1993). In layer III principal neurons, this suppression caused by dopamine has instead been linked to coincidental alteration of glutamate release probability, as suggested by Stenkamp, Heinemann and Schmitz (1998) from analysis of paired-pulse ratios in the presence of dopamine. For the lateral division of the entorhinal cortex, however, relatively little is known about the mechanism by which dopamine elicits its suppressive effects on layer II and layer III principal neurons (but see Caruana and Chapman, 2008; Harvey, 2020).

Materials and Methods

Biocytin-Streptavidin Labelling

During whole-cell experiments, some neurons were patched using an internal solution filled with the cell tracer, biocytin (5 mg/ml). To determine the morphology (or identity) and precise location of recorded neurons within the lateral entorhinal cortex, cells were patched for 60 minutes and immediately transferred into a pre-labelled well plate and submerged in 4% paraformaldehyde. The well plate was stored in the dark at 4 °C for 12 to 24 hours before being washed three times in 4% phosphate buffered saline (PBS). Slices containing biocytin-filled neurons were then developed in a solution containing: 4% PBS, 1% triton X-100 and 0.2% streptavidin for 18 hours in the dark at 4 °C. Once the slices were washed for a final three times in 4% PBS, they were then mounted on glass slides using a DAPI-based mounting medium and coverslipped for fluorescence imaging.

Electrophysiology

For all field recording experiments, slices were rested in warmed and oxygenated ACSF for at least 60 minutes after slicing just prior to experimental testing. Following the rest period, slices were transferred to the recording chamber and a bipolar stimulating electrode and glass recording electrode were placed carefully in the superficial layers (stimulating electrode positioned to span the layer I-II border; recording electrode positioned along the layer I border with layer II; see **Figure 3.3A**) and responses were elicited once every 20s. To obtain time-matched and untreated control data the amplitude of evoked fEPSPs was recorded for a minimum of 60 minutes up to a maximum of 330 minutes whilst perfused continually with warmed and oxygenated ACSF. Control experiments were interleaved throughout all experimental testing, and each treatment condition had its own time-matched control data to compare to. Additional control experiments were conducted to assess the effects of the antioxidant, sodium metabisulfite, that was added together with several drugs to prevent oxidation of the experimental drugs. Experiments that required application of dopamine or apomorphine were always performed together with sodium metabisulfite. In some instance, calcium was removed from the ACSF to confirm that evoked responses were, in fact, synaptically driven. Experiments typically proceeded following a stable period of baseline evoked synaptic responses for a minimum of 30 minutes. Experimental drugs were bath-applied for 30 min followed by a washout period of at least 60 minutes. For paired-pulse experiments, paired-pulse rations were calculated based on the average of three responses evoked at each IPI (10, 30, 100, 300 and 1000 msec) and compared at three different time points during an experiment (baseline, peak of drug effect, and washout).

For all whole-cell patch clamp experiments, brain slices rested for at least 60 minutes after slicing just prior to testing. For experiments measuring excitatory postsynaptic currents (EPSCs), slices were transferred to the recording chamber and a stimulating electrode was placed in layer I and a glass recording electrode, containing the potassium gluconate-based patch solution (sometimes with added biocytin), was lowered carefully into layer II and sealed onto a pre-selected neuron. Layer II neurons were preferred for these

experiments to ensure consistency with experimental work published previously (Caruana *et al.*, 2006; Caruana and Chapman, 2008; Glovaci, Caruana and Chapman, 2014; Glovaci and Chapman, 2019). EPSCs were evoked once every 60 seconds, and experiments began following 10 minutes of stable baseline recordings. Drugs were bath applied for 10 minutes followed by a 40-minute wash in normal ACSF. In some instances, pairs of stimulation pulses (with a 30 msec IPI) were delivered instead of single pulses. For experiments measuring evoked IPSCs, slices were pre-treated in ACSF containing 1 mM kynurenic acid (KYNA) for 15 min prior to being transferred to the recording chamber. These same slices were then perfused continually with normal ACSF also containing 1 mM KYNA. Initially, neurons were held at -70 mV to ensure the absence of any excitatory response, but the holding potential was changed to 0 mV to better visualise and record isolated IPSCs. Experimental protocols and timelines were similar to those used for EPSC recordings described above.

Data Analysis

All imaging data were captured using a camera attached to an epifluorescence microscope and later enhanced, edited, and traced using several applications as described previously in Chapter 2 (Data Analysis: *Biocytin-Streptavidin Labelling).* The effects of bath- or intracellularly applied drugs during pharmacological experiments were assessed on the amplitude of averaged synaptic responses (fEPSPs, EPSCs and IPSCs) obtained during 5- or 10-min epochs recorded at different times during an experiment (latencies specified below). In some instances, the peak change in synaptic efficacy was used, and this was determined manually for each individual experiment as the latency varied due to temporally complex inputs from multimodal sensory cortices as described previously (see **Figure 1.3**). Concentration-response curves were generated with Prism (inhibitor versus response; variable slope with four parameters) and fit using the least squares (ordinary) method. Curves were constrained to 100% at the top, which is the theoretical maximum level of inhibition possible using the compounds tested in this thesis. Comparisons of curve-fits were made using sum-of-squares F-Tests. Additional curve fitting used throughout this thesis (e.g., third-order polynomial modelling, LOWESS curves, and others), when required, was also performed using Prism (see below). All data were expressed as the mean ± SEM and were normalised to the baseline period for plotting. Drug-induced changes in response properties were assessed with Prism using (where appropriate) paired or unpaired samples t-tests, one-way ANOVAs or repeated measures ANOVAs. Post-hoc comparisons were made using the Bonferroni method with an alpha level of $P < 0.05$.

Results

Morphological Characterisation of Superficial Layer Projection Neurons

A total of 43 neurons across both superficial layer II and layer III of the lateral entorhinal cortex were filled sufficiently with biocytin to allow for adequate digital reconstruction of a large proportion of the neuropil to facilitate accurate classification of the cells. There were 24 neurons total that were reconstructed from layer II and another 19 neurons from layer III. Each reconstructed neuron was categorised as having a specific neuronal phenotype based on a visual comparison with the morphological features and methods described previously by Canto and Witter (2012a). Neurons in layer II were classified as either fan, pyramidal, oblique pyramidal or multiform, whereas layer III neurons were classified as either simple pyramidal, complex pyramidal or multipolar. This classification was based largely on the shape and features of the dendritic arbours radiating from the somata of reconstructed neurons as outlined in Canto and Witter (2012a). Portions of the apical and basal dendrites of analysed neurons were likely cropped or missing, as reconstructions were based on fills limited to a 340 µm-thick tissue section. Additionally, although there was insufficient resolution to distinguish between axon and dendrite, the morphological features, overall, were *extremely* consistent with those published previously. A Sholl analysis was performed on each individual neuron, and this provided measures for the peak number of dendritic branch intersections at 5 µm intervals from the soma, as well as the peak distance from the soma the highest level of branching occurred, and the overall number of peak intersections measured. Overall, similar results were obtained to previous reports in that a heterogeneous population of principal excitatory neurons are found in the superficial layers of the lateral entorhinal cortex that fall into one of the main neuronal phenotypes outlined by both Canto and Witter (2012a) and Tahvildari and Alonso (2005).

Layer II Neurons

The largest proportion of labelled and reconstructed cells in layer II were fan neurons (*n* = 11), followed next by pyramidal neurons (*n* = 6), then multiform neurons (*n* = 4), and finally oblique pyramidal neurons (*n* = 3). **Figure 3.1A** highlights a digital reconstruction of each of these neuronal phenotypes found in layer II. As shown in **Figure 3.1B$_1$**, each distinct neuronal phenotype in layer II of the lateral entorhinal cortex showed a similar morphological profile in that the number of branch intersections peaked at around the same distance from the soma. The peak typically fell within 40 to 80 µm from the soma (see **Figure 3.1B$_2$**), and there was no statistical difference between the various cell types in terms of the distance where this branching peaked. As shown in **Figure 3.1B$_2$**, the mean peak distance was highest for oblique pyramidal neurons (81.67 ± 18.33 µm), followed by multiform neurons (61.25 ± 13.90 µm), then pyramidal neurons (61.25 ± 13.90 µm), and finally fan neurons (49.55 ± 4.071 µm). **Figure 3.1B$_3$** highlights the mean number of peak intersections overall for each neuronal phenotype in layer II the lateral entorhinal cortex. This was highest for oblique pyramidal neurons (20.0 ± 4.04), followed by fan neurons (15.18 ± 2.00), then pyramidal neurons (13.67 ± 2.68), and finally multiform neurons (13.00 ± 2.74). However, there was no statistical difference between phenotypes. These results

demonstrate that although each neuron type found in layer II is morphologically distinct, the neurons do not differ significantly in terms of the overall non-directional branch densities of their dendritic arbours.

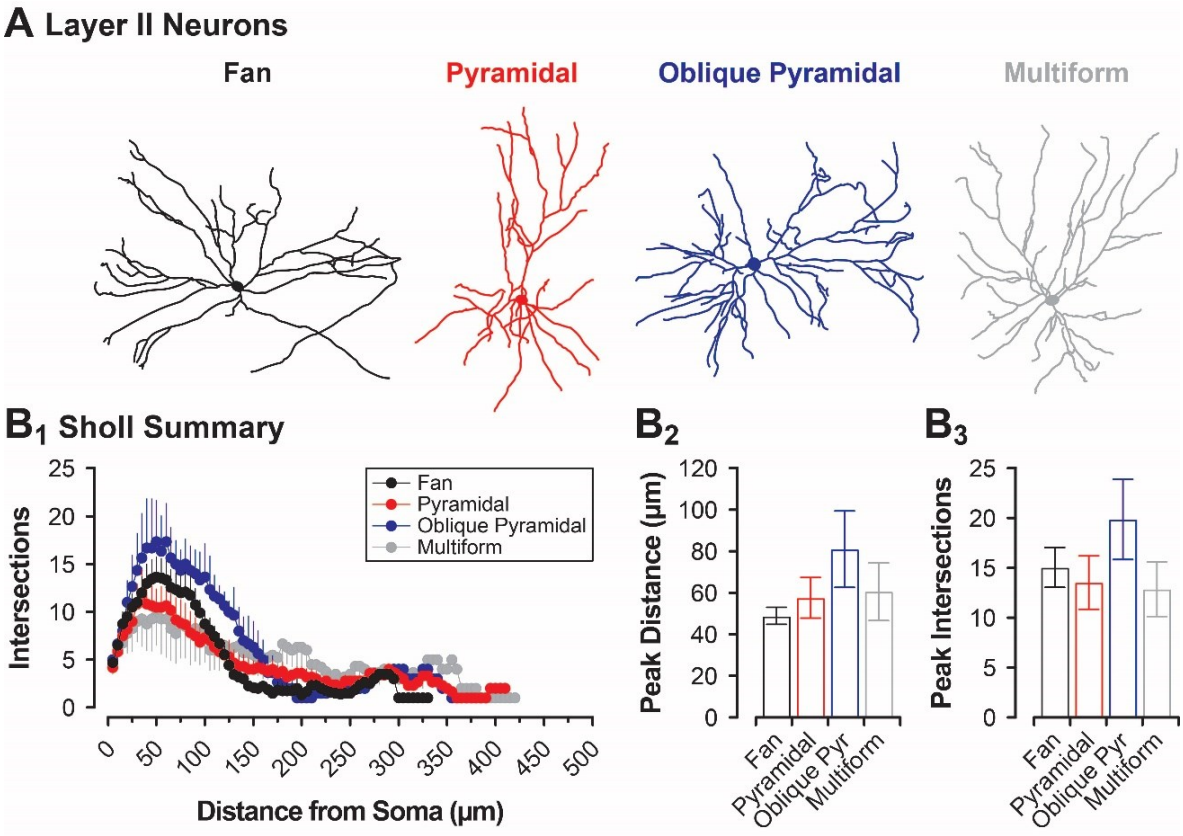

Figure 3.1. Branching characteristics of neurons in layer II of the lateral entorhinal cortex*. (**A**) Representative example reconstructions of each neuronal phenotype found in layer II of the lateral entorhinal cortex. (**B₁**) Summary of the Sholl analysis highlighting the mean number of dendritic intersections plotted as a function of the distance from the soma (in µm). (**B₂**) Summary bar plot highlighting the mean peak distance (in µm) from the soma in which the most dendritic intersections occur. (**B₃**) A bar plot summarising the mean peak number of intersections for each neuronal phenotype.*

Layer III Neurons

In layer III of the lateral entorhinal cortex, the most abundant cell type labelled and reconstructed was the multipolar phenotype (*n* = 10), followed by simple pyramidal phenotype (*n* = 6), and finally the complex pyramidal phenotype (*n* = 3). **Figure 3.2A** highlights a representative example of each of these neuronal phenotypes found in layer III. As shown in **Figure 3.2B₁**, each distinct neuronal phenotype in layer III also shared a similar morphological profile in that the number of branch intersections peaked at roughly the same distance from the soma. The peak typically fell within roughly 40 to 50 µm from the soma (see **Figure 3.2B₂**), and there was no statistical difference between the various cell types in terms of the distance where this branching peaked. As shown in **Figure 3.2B₂**, the mean peak distance was highest for multipolar neurons (47.00 ± 3.18 µm), followed by simple pyramidal neurons (45.83 ± 3.52 µm), and then complex pyramidal neurons (40.00 ± 10.41 µm). Interestingly, although branching drops to around 5 intersections after 150 µm for multipolar and simple pyramidal neurons, complex pyramidal neurons show a second peak of nearly 10 intersections at around 160 µm (**Figure 3.2B₁**; blue circles). This likely reflects the apical dendritic tuft of these cells that ramify in more superficial layers (see example trace reconstruction in **Figure 3.2A** for the Complex Pyramidal phenotype).

Figure 3.2B$_3$ highlights the mean number of peak intersections overall for each neuronal phenotype in layer III the lateral entorhinal cortex. This was highest for complex pyramidal neurons (20.33 ± 0.33), followed by multipolar neurons (18.00 ± 2.50), and then simple pyramidal neurons (12.83 ± 1.01), though, there was no statistical difference between phenotypes. Similar to principal neurons in layer II, these results demonstrate that although each neuron type found in layer III is morphologically distinct, the neurons generally do not differ significantly in terms of the overall branch patterns of their dendritic arbours. It should be noted, however, that peak intersections appear to occur closer to the soma for layer III neurons than for layer II neurons (compare Sholl profiles for **Figure 3.1B$_1$** and **Figure 3.2B$_1$**).

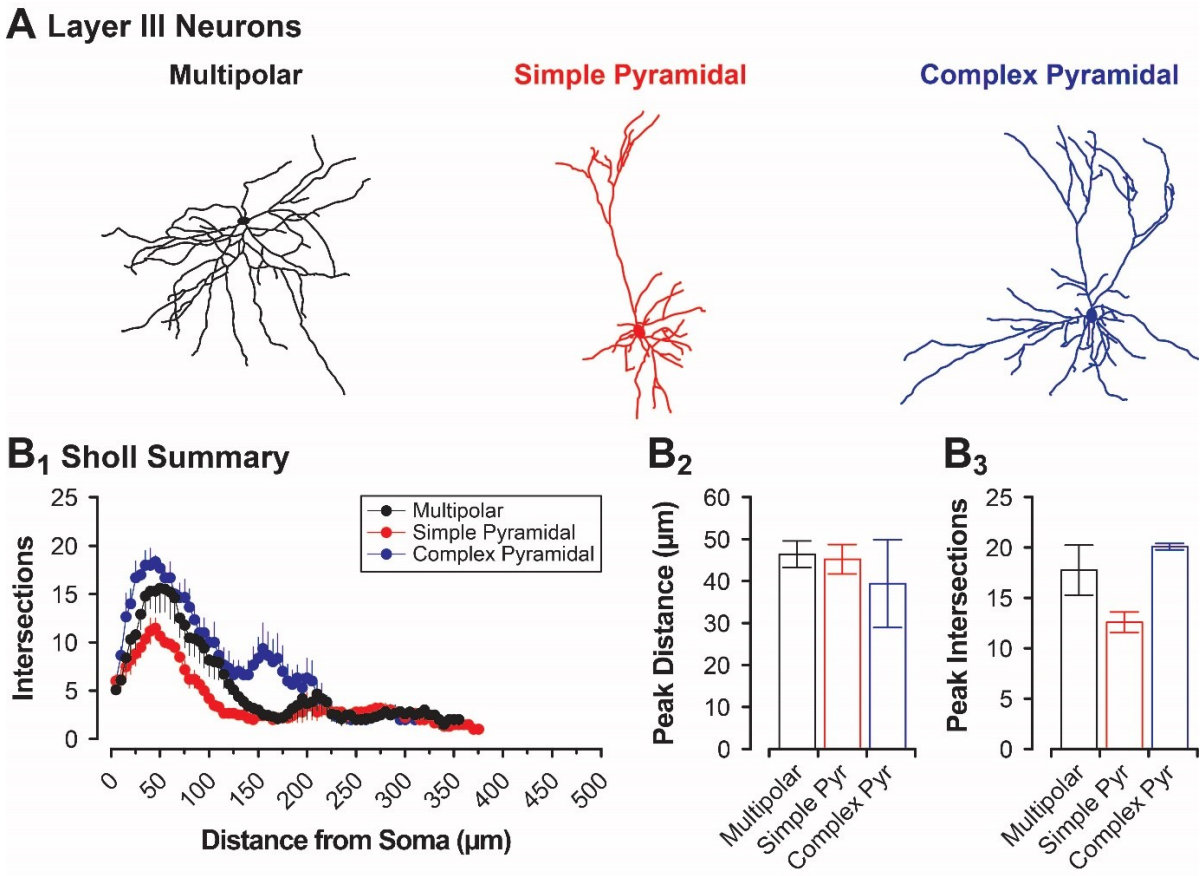

***Figure 3.2. Branching characteristics of neurons in layer III of the lateral entorhinal cortex**. (**A**) Representative example reconstructions of each neuronal phenotype found in layer III of the lateral entorhinal cortex. (**B$_1$**) Summary of the Sholl analysis highlighting the mean number of dendritic intersections plotted as a function of the distance from the soma (in µm). (**B$_2$**) Summary bar plot highlighting the mean peak distance (in µm) from the soma in which the most dendritic intersections occur. (**B$_3$**) A bar plot summarising the mean peak number of intersections for each neuronal phenotype.*

Control Recordings of fEPSPs

Field EPSPs recorded from the superficial layers of the lateral entorhinal cortex (**Figure 3.3A**) were extremely stable and permitted recording for extended periods of time lasting between 90 minutes and 120 minutes (last 5-min; 102.1 ± 2.6 % of baseline, t_5 = 0.52, P = 0.63, n = 6; **Figure 3.3B$_2$**) up to 330 minutes (see Chapter 4). The responses evoked during these experiments were most likely fEPSPs as the postsynaptic component disappeared when the perfusate was changed to calcium free ACSF ($[Ca^{2+}]_0$ vs 100 ± 3.4 % depression; t_{10} = 2.20, P = 0.052, n = 6; **Figure 3.3B$_1$**). Additionally, the amplitude of fEPSPs was not affected by

the addition of 50 μM sodium metabisulfite to the bathing medium for 30 minutes (**Figure 3.3C**). Responses were depressed to 90.0 ± 7.1% of baseline in the presence of the vehicle (n = 10), but this was not statistically significant from responses evoked in time matched and untreated controls (n = 8, t_{16} = 1.450, P = 1.666). As such, the dopamine- and apomorphine-induced changes in basal synaptic transmission described below do not reflect and changes in transmission mediated by inclusion of the antioxidant during these experiments.

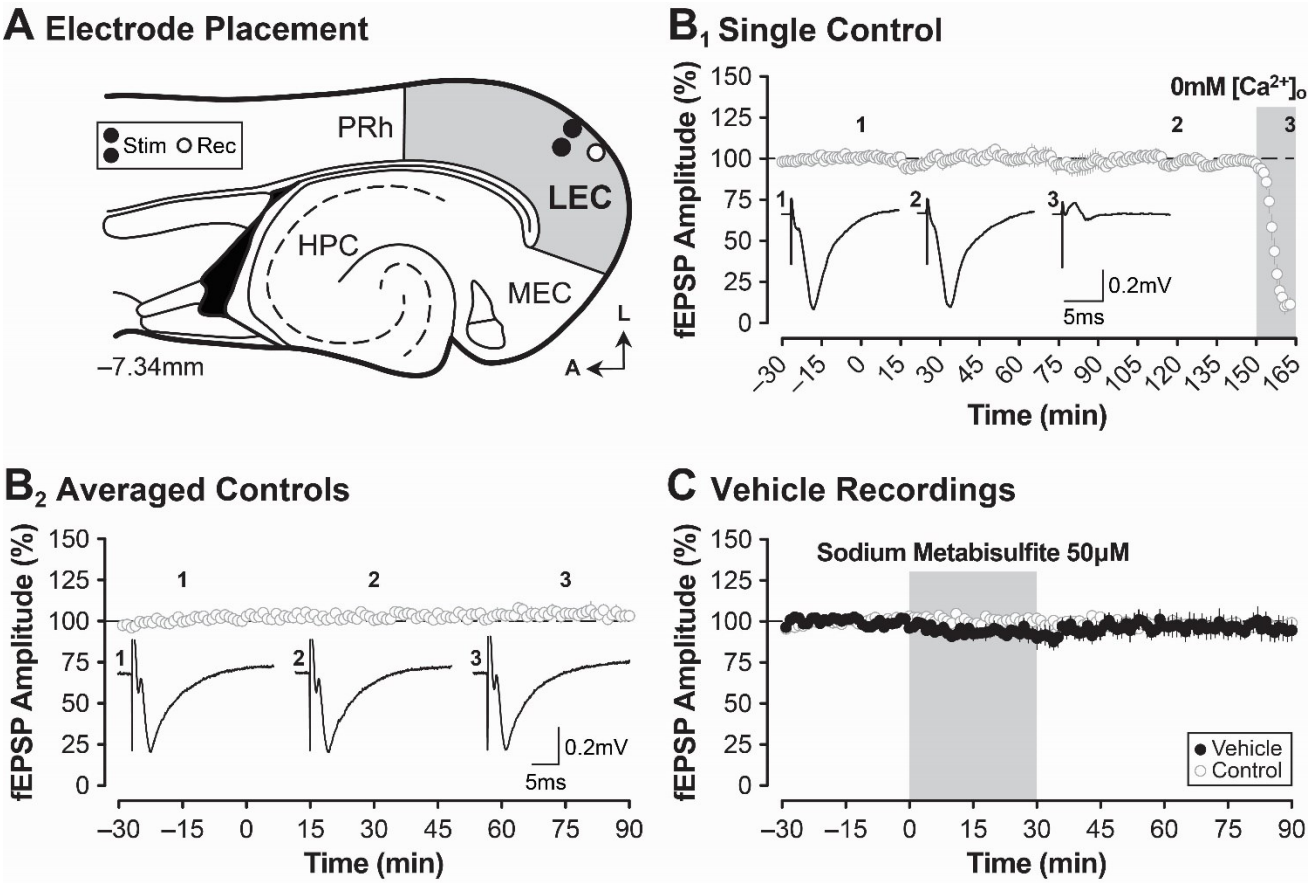

Figure 3.3. Control and vehicle recordings of fEPSPs in the lateral entorhinal cortex. *(**A**) Schematic diagram of the rat brain slice (at a position -7.34 mm relative to Bregma) indicating the target positions for stimulating and recording electrodes in horizontal slices containing the lateral entorhinal cortex. A bipolar stimulating electrode was positioned in the superficial layers of the lateral entorhinal cortex (layers I to III; filled circles; Stim) and a recording electrode was positioned nearby along the layer I/II border (open circle; Rec). (**B₁**) A single control experiment before and after calcium was removed from the bathing medium. Note the rapid disappearance of the postsynaptic component. Numbers indicate the time in which the representative traces inset were recorded. (**B₂**) Results of an averaged set of interleaved control experiments highlighting the stability of the preparation over 120 min of recording. (**C**) Bath-application of the antioxidant, sodium metabisulfite, had no effect on evoked synaptic responses.*

Dopaminergic Modulation of Basal Excitatory Synaptic Transmission in the Lateral Entorhinal Cortex

To confirm the results of previous experimental reports (Caruana *et al*., 2006; Caruana and Chapman, 2008; Glovaci *et al*., 2014), multiple concentrations of dopamine were bath-applied to slices for 30 minutes and the effects on basal synaptic transmission observed in sensory inputs to the superficial layers. Dopamine was applied at concentrations of 1 (*n* = 4), 3 (*n* = 8), 10 (*n* = 5), 30 (*n* = 11), 100 (*n* = 9), 300 (*n* = 4) and 1000 (*n* = 7) μM (note: for clarity, only data for the 10, 30, 100, 300 and 1000 μM concentrations of dopamine are shown superimposed in **Figure 3.4A₁**, but see **Figure 3.4A₂**). Previously, concentration-dependent and *bidirectional*

effects were observed on evoked responses in the superficial layers, with concentrations of 1 to 10 µM *enhancing* synaptic transmission and concentrations ≥50 µM *suppressing* the amplitude of responses. In the current study, regardless of the concentration tested in the micromolar range, a reliable and reversible suppression of basal synaptic transmission was observed (**Figure 3.4**). As shown in **Figure 3.4A$_1$**, dopamine caused a concentration-dependent suppression of fEPSPs in the lateral entorhinal cortex. The magnitude of the suppression peaked at 100 µM, with concentrations of 300 and 1000 µM failing to produce any significantly stronger suppression of synaptic responses. Synaptic responses were significantly depressed by dopamine relative to time-matched controls ($F_{7,45}$ = 17.65, P < 0.0001; **Figure 3.4A$_2$**; data are renormalised here to the time matched and untreated control condition) following application of 30 (to 70.6 ± 3.6% of baseline, Bonferroni P < 0.05), 100 (to 39.9 ± 4.9% of baseline, Bonferroni P < 0.0001), 300 (to 40.3 ± 9.7% of baseline, Bonferroni P < 0.0001), and 1000 (to 42.1 ± 4.6% of baseline, Bonferroni P < 0.0001) µM dopamine (see **Figure 3.4A$_2$**). The suppression of fEPSPs was only transient, and responses recovered quickly during the washout period except for 300 and 1000 µM dopamine where the amplitude of fEPSPs took significantly longer to return to baseline levels (see **Figure 3.4A$_1$**). A concentration-response curve (**Figure 3.4B**) was calculated from peak suppression data shown in **Figure 3.4A$_2$** for each concentration of dopamine tested using an inhibitor versus response with variable slope model in Prism. As dopamine, or any drug causing a significant suppression of fEPSPs, would not be able to depress transmission beyond 100% in magnitude, data were constrained to 100% at the top end of the curve. The EC_{50} value for dopamine was determined to be 21.4 µM (HillSlope -0.8; 95% CI -1.4 to -0.4; see **Figure 3.4B**).

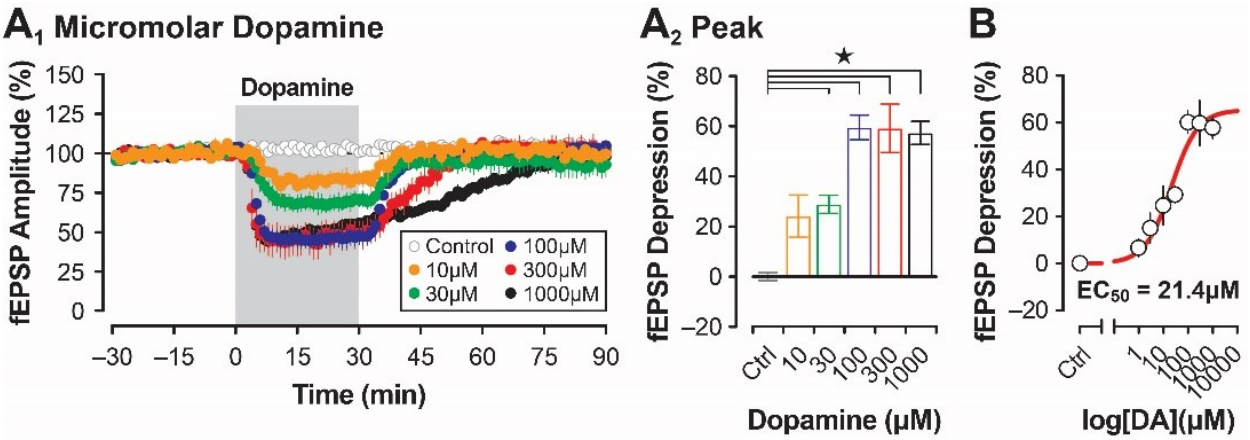

***Figure 3.4. Dopamine suppresses basal synaptic transmission in a concentration-dependent manner**. (**A$_1$**) Averaged results highlighting the suppressive effects of dopamine at different concentrations. Peak suppression is observed at 100 µM dopamine. (**A$_2$**) Quantification of the mean peak fEPSP depression induced by different concentrations of dopamine (star indicates a statistically significant difference between indicated groups; see text for specific P values for this and subsequent figures). Note: data renormalised to control at 'peak' effect. (**B**) A concentration-response curve for dopamine; EC_{50} = 21.4 µM.*

The suppressive effects of dopamine were also confirmed in whole-cell recordings of EPSCs in layer II neurons. Following a 10-minute baseline period, dopamine was bath applied for an additional 10 minutes at a concentration of 100 µM (n = 8) and then washed off for 40 minutes (see **Figure 3.5A-B**). Similar to the results of field recording experiments (summarised above), dopamine significantly depressed the amplitude of EPSCs

to 44.3 ± 4.6% of baseline levels ($F_{6,48}$ = 11.73, P < 0.01, Bonferroni P < 0.01; **Figure 3.5C**), and responses recovered during the initial washout phase (+30 to 36 mins, to 82.0 ± 8.8 % of baseline, Bonferroni P = 0.19) but started to run down by the end of the experiment (last 6-mins, to 75.2 ± 6.3% of baseline, Bonferroni P < 0.01). This run down, however, was not due to a change in electrical access as R_s was stable for the entire duration of the experiment (First 6-mins vs Last 6-mins, t_7 = 2.19, P = 0.06; **Figure 3.5B** bottom panel).

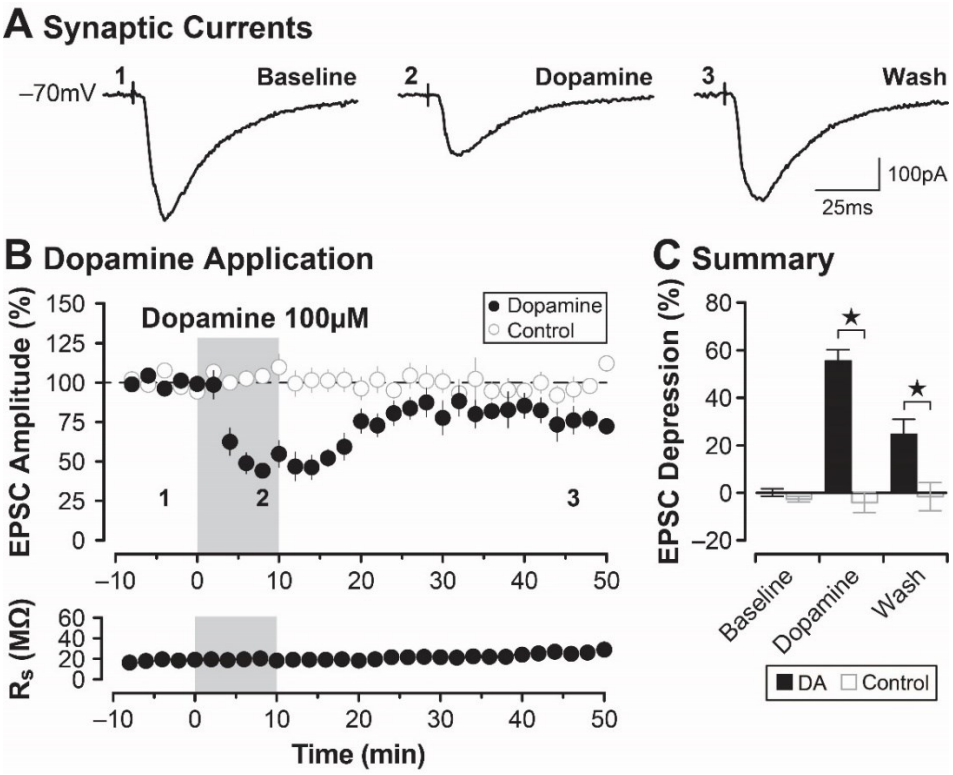

Figure 3.5. Dopamine suppresses excitatory synaptic currents in individual layer II neurons*. (**A**) Representative synaptic currents recorded before, during and after bath-application of 100 µM dopamine. Numbered traces in **A** correspond to the numbers in **B** highlighting the specific times during the experiment when the sample currents were recorded. (**B**) Top: Group data highlighting the dopamine-mediated suppression of EPSCs in layer II neurons (filled circles) relative to untreated controls (open circles). Bottom: R_s was unchanged during the experiment. (**C**) Summary bar plot highlighting the depression of EPSCs induced by dopamine relative to controls at three different time points during the experiment (Baseline, Dopamine and Wash).*

To confirm the effects of dopamine on basal synaptic transmission in the lateral entorhinal cortex, multiple concentrations of the broad-spectrum dopamine receptor agonist, apomorphine, were bath-applied for 30 minutes. Like dopamine, apomorphine caused a significant concentration-dependent suppression of synaptic transmission in sensory inputs to the superficial layers by acting as a full agonist (Isaacson *et al.*, 2023) ($F_{8,62}$ = 10.91, P < 0.01; **Figure 3.6A$_1$-A$_2$**). Effects of apomorphine differed, slightly, from those of dopamine in terms of the onset latency, overall magnitude and time required to wash the effect out. This may be attributed to the differing affinity of apomorphine for dopamine receptor subtypes, as it exhibits a higher affinity for D2 than D5, in contrast to the endogenous agonist dopamine (see **Table 2.1**). The lowest concentration of apomorphine tested (10 µM) did not significantly depress synaptic responses relative to time-matched controls (responses suppressed to only 89.9 ± 7.7% of baseline, Bonferroni P = 0.55, n = 6). However, 30 µM apomorphine significantly depressed transmission to 77.9 ± 10.5 % of baseline (Bonferroni P < 0.01, n = 9), as did 100 µM (to

65.5 ± 7.2% of baseline, Bonferroni $P < 0.01$, $n = 6$) and 300 µM (to 11.9 ± 8.9% of baseline, Bonferroni $P < 0.01$, $n = 6$). In all instances, the amplitude of fEPSPs returned to baseline levels by the end of the experiment (10 µM, to 91.0 ± 1.7% of baseline, Bonferroni $P = 1.00$; 30 µM, to 88.5 ± 3.1% of baseline, Bonferroni $P = 0.43$; 100 µM, to 97.1 ± 3.4% of baseline, Bonferroni $P = 1.00$; 300 µM, to 89.6 ± 12.7% of baseline, Bonferroni $P = 0.94$). A concentration-response curve (**Figure 3.6B**) was calculated from peak suppression data for each concentration of apomorphine tested using an inhibitor versus response with variable slope model in Prism. As with dopamine, data for apomorphine were constrained to 100% at the top end of the curve. The EC_{50} value of apomorphine was determined to be 102.4 µM (HillSlope -1.0; 95% CI -1.8 to -0.6; see **Figure 3.6B**). It is important to note that at the concentrations used in this study, apomorphine binds antagonistically to serotonin (5-$H_{1A,\ 2}$) receptors, as well as adrenergic ($\alpha_{1A,B,D}$ and $\alpha_{2A\text{-}C}$) receptors (see **Table 2.1**).

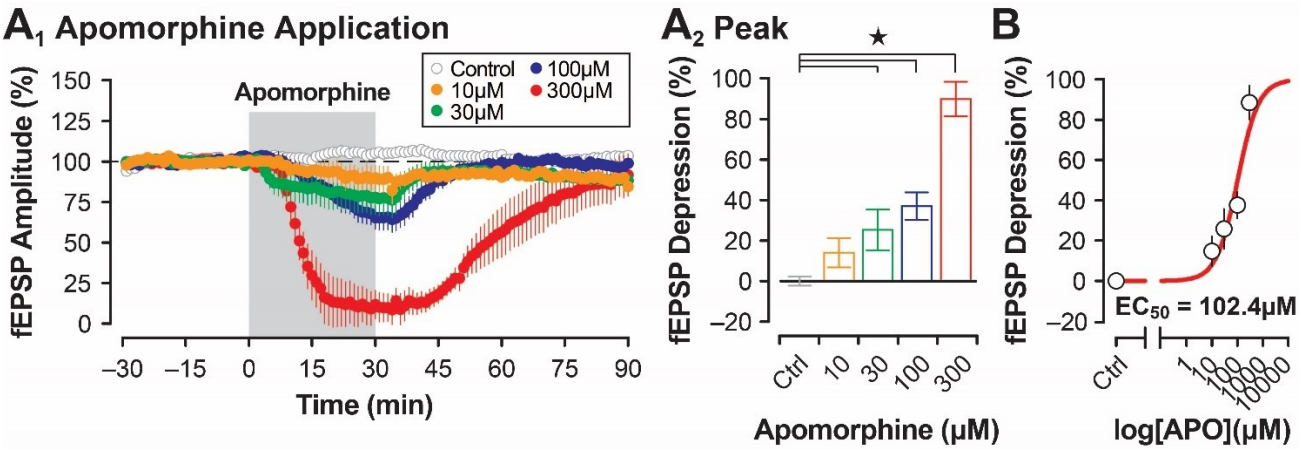

***Figure 3.6. Apomorphine suppresses basal synaptic transmission in a concentration-dependent manner**. (**A_1**) Averaged results highlighting the suppressive effects of the nonselective dopamine receptor agonist, apomorphine, at different concentrations. Peak suppression is observed at 300 µM apomorphine. (**A_2**) Quantification of the mean peak fEPSP depression induced by different concentrations of apomorphine. Note: data renormalised to control. (**B**) A concentration-response curve for apomorphine; EC_{50} = 102.4 µM.*

To assess whether synaptic stimulation was required to induce the dopamine-mediated depression of fEPSPs in the lateral entorhinal cortex, the delivery of test stimulation was paused for 30 minutes at the start of the dopamine application (100 µM for 30 min), and the depression of fEPSPs compared to several different control experiments (e.g., dopamine administered in the presence of continuous test stimulation) in the first minute (+31 minutes) after synaptic stimulation had resumed (**Figure 3.7A_1-A_2**). Synaptic responses were still depressed significantly by dopamine to 65.9 ± 2.6 of baseline in the paused stimulation condition as soon as test stimulation was resumed ($F_{4,\ 29} = 64.26$, P < 0.0001; Bonferroni $P < 0.0001$, $n = 6$), but this depression was significantly *less* than the depression induced by dopamine during the control condition in which test stimulation was delivered continuously (fEPSPs depressed to 47.4 ± 6.0% of baseline, Bonferroni $P < 0.05$, $n = 6$). Interestingly, washout of dopamine and the recovery of responses to baseline took the exact same amount of time in both conditions (see **Figure 3.7B,** black versus red circles). It should also be noted that in a time-matched control experiment in which test stimulation was paused and no dopamine was applied ($n = 5$), responses were about 10% larger in amplitude (to 110.7 ± 1.8% of baseline, n = 5) as soon as synaptic stimulation was resumed,

though this facilitation did not differ significantly from time matched controls (Bonferroni P > 0.999). This suggests that constant synaptic stimulation alone causes a mild suppression of synaptic transmission over time (**Figure 3.7A$_1$&B**, yellow circles). In addition, the dopamine-mediated depression of fEPSPs did not depend on activation of NMDA receptors. Responses were depressed significantly by dopamine to 42.8 ± 4.4% of baseline when applied together with 10 µM AP5, and the magnitude of this depression did not differ significantly from the depression induced by dopamine alone. The only notable difference was the much slower latency required for the amplitude of fEPSPs to recover to baseline when washing AP5 off the slice (**Figure 3.7A$_1$&B**, blue circles). Taken together, these data suggest that constant synaptic drive is not required for the induction of the dopamine-mediated depression of fEPSPs in the lateral entorhinal cortex.

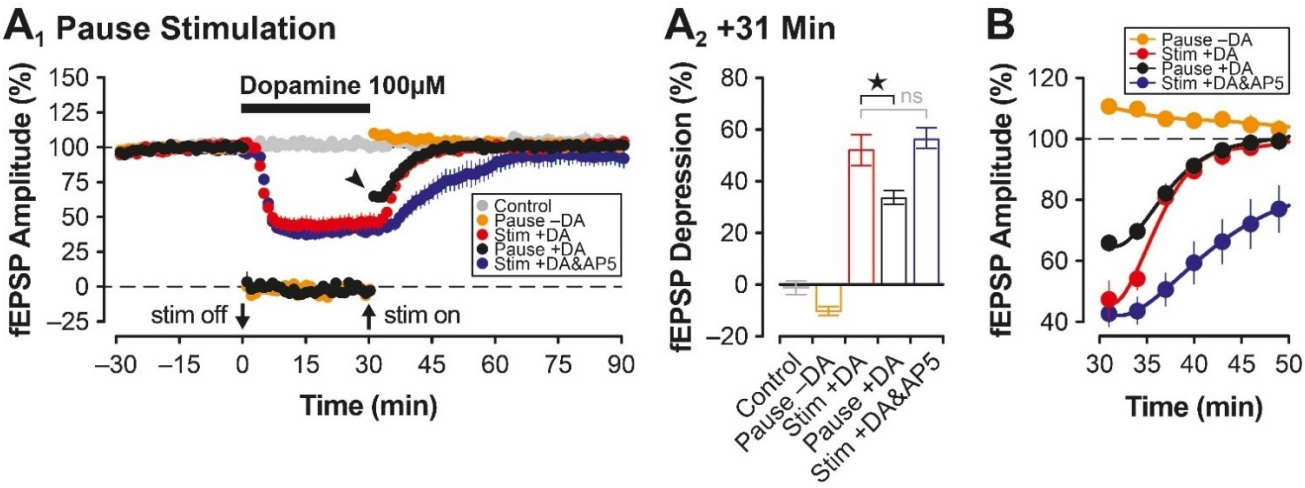

***Figure 3.7. Pausing test stimulation influences dopamine-mediated depression of evoked synaptic responses**. (**A$_1$**) The amplitude of fEPSPs is significantly depressed relative to controls when stimulation is paused (stim off) temporarily during the application of 100 µM dopamine (Pause +DA, black circles; see arrow). Note that the overall magnitude of the effect is significantly less when stimulation is paused compared to when the stimulation is continuous (Stim +DA, red circles versus Pause +DA, black circles at +31 min). Co-application of AP5 together with dopamine has no effect on the magnitude of the dopamine-mediated depression in fEPSPs (Stim +DA&AP5, blue circles versus Stim +DA, red circles). (**A$_2$**) Summary bar plot of data shown in **A$_1$** at the +31-minute time point during the experiment (i.e., the recommencement of test stimulation; stim on in **A$_1$**). (**B**) An expanded view of the first 20 minutes of washout highlighting the recovery of responses to baseline. Note how a pause in test stimulation during untreated control experiments leads to a transient enhancement in synaptic transmission (Pause -DA; yellow circles).*

Paired-pulse tests were used to determine whether dopamine was attenuating synaptic responses via a pre- or a postsynaptic mechanism. These experiments followed a similar protocol to those described above in that following a 30 min baseline period, dopamine (100 µM) was bath-applied for 30-minutes and then washed off the slice for a further 60 minutes of recording. However, during these experiments, separate paired-pulse protocols were tested at three different time points. Specifically, the delivery of test stimulation was paused so that a paired-pulse protocol (three pairs of pulses delivered at the same stimulation intensity with an IPI of 10, 30, 100, 300 and 1000 msec) could be delivered. The paired-pulse protocol was delivered once at the end of the baseline period (PP 1), again during the peak of the dopamine-mediated depression of fEPSPs (10 mins post-application; PP 2), and finally at the end of the washout period (PP 3). Paired-pulse ratios at each IPI were then compared at each of the three time points assessed during the experiment. There was virtually no paired-pulse facilitation or inhibition observed during the baseline period at each IPI tested (PP1; $F_{4,45}$ = 2.48, P = 0.06, n = 10;

see **Figure 3.8B**, Baseline, grey circles). However, paired-pulse ratios increased significantly relative to baseline ($F_{8,90}$ = 32.88, P < 0.0001; n = 10) for the 10 (1.41 ± 0.06, Bonferroni P < 0.0001), 30 (1.49 ± 0.09; Bonferroni P < 0.0001) and 100 msec (1.32 ± 0.06; Bonferroni P < 0.0001) IPIs when assessed during the peak of the dopamine effect (**Figure 3.8B**, Dopamine, blue circles). An important note to consider is the shortest IPI interval, 10 ms, resulted in an overlap of the responses (see **Figure 3.8C**). In this instance, the baseline for the second sweep was taken as close to this overlap as possible and *not* the baseline of the first sweep, before being compared to the second sweeps peak amplitude. Taken together, this increase in paired-pulse ratios suggests that dopamine may act to suppress synaptic responses by reducing the probability of glutamate release from sensory afferents that make synaptic contact with projection neurons in the superficial layers (see also Caruana *et al*., 2006; Caruana and Chapman, 2008). Interestingly, this increase in paired-pulse facilitation was transient, and paired pulse ratios returned to baseline levels by the end of the washout period (see **Figure 3.8B**, Washout, red circles).

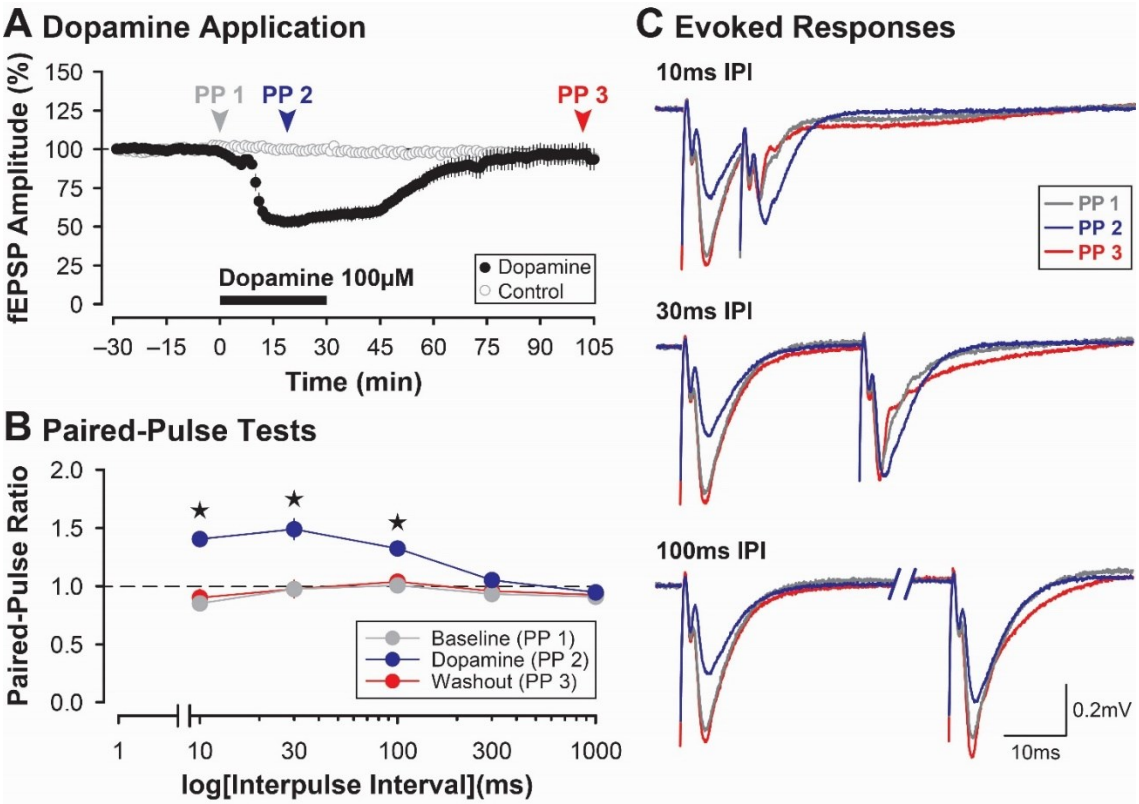

Figure 3.8. The dopamine-mediated depression of fEPSPs is mediated by a change in the release probability of glutamate*. (**A**) Paired-pulse tests were conducted at different times during an experiment to assess the effects of 100 µM dopamine on basal synaptic transmission in the superficial layers of the lateral entorhinal cortex. The paired-pulse tests were conducted before (PP 1), during (PP 2) and after (PP 3) bath-application of dopamine. (**B**) Results of the paired-pulse tests conducted at each time point. Note the significant increase in the paired-pulse ratios for the 10, 30 and 100 msec IPIs during PP 2 (blue circles) conducted in the presence of dopamine. The effect is only transient and returns to baseline levels during washout (PP 3; red circles). (**C**) Representative traces recorded at 10ms IPI, 30ms IPI and 100ms IPI during baseline (PP 1, grey), dopamine application (PP 2, blue) and washout (PP 3, red).*

To further investigate whether dopamine suppressed synaptic transmission in the lateral entorhinal cortex via a presynaptic mechanism to reduce the release probability of glutamate from sensory afferent terminals, paired-pulse experiments were also performed during whole cell recording experiments. During these

experiments, pairs of stimulation pulses with a 30-msec IPI were delivered once every 2-minutes before, during and after bath-application of 100 µM dopamine. As before, a 10-minute application of dopamine significantly depressed the amplitude of EPSCs recorded from layer II neurons (see **Figure 3.9A$_1$**, filled circles; also **Figure 3.9D**). Synaptic responses were reduced significantly to 23.4 ± 3.3% of baseline levels during application, and this was associated with a significant increase in the paired-pulse ratio ($F_{2,28}$ = 13.64, P < 0.01, n = 8). As responses depressed, there was a coincident and significant change in the paired pulse ratio to 1.59 ± 0.22 (Bonferroni P < 0.01, see **Figure 3.9A$_2$**, filled circles; see also **Figure 3.9C$_2$**). And like field potential recording experiments, the change in the paired-pulse ratio returned to baseline levels by the end of the washout (to 0.69 ± 0.09, Bonferroni P = 1.00; **Figure 3.9A$_2$**, filled circles; see also **Figure 3.9C$_2$**). It should be noted that continuous paired-pulse stimulation of sensory afferents to layer II neurons did not cause any change in the amplitude of EPSCs, nor in the paired-pulse ratio, in time-matched control recordings (see **Figure 3.9B$_1$-B$_2$**). Taken together, these results suggest that dopamine acts presynaptically to reduce glutamate release and suppress the amplitude of evoked fEPSPs and EPSCs in the lateral entorhinal cortex.

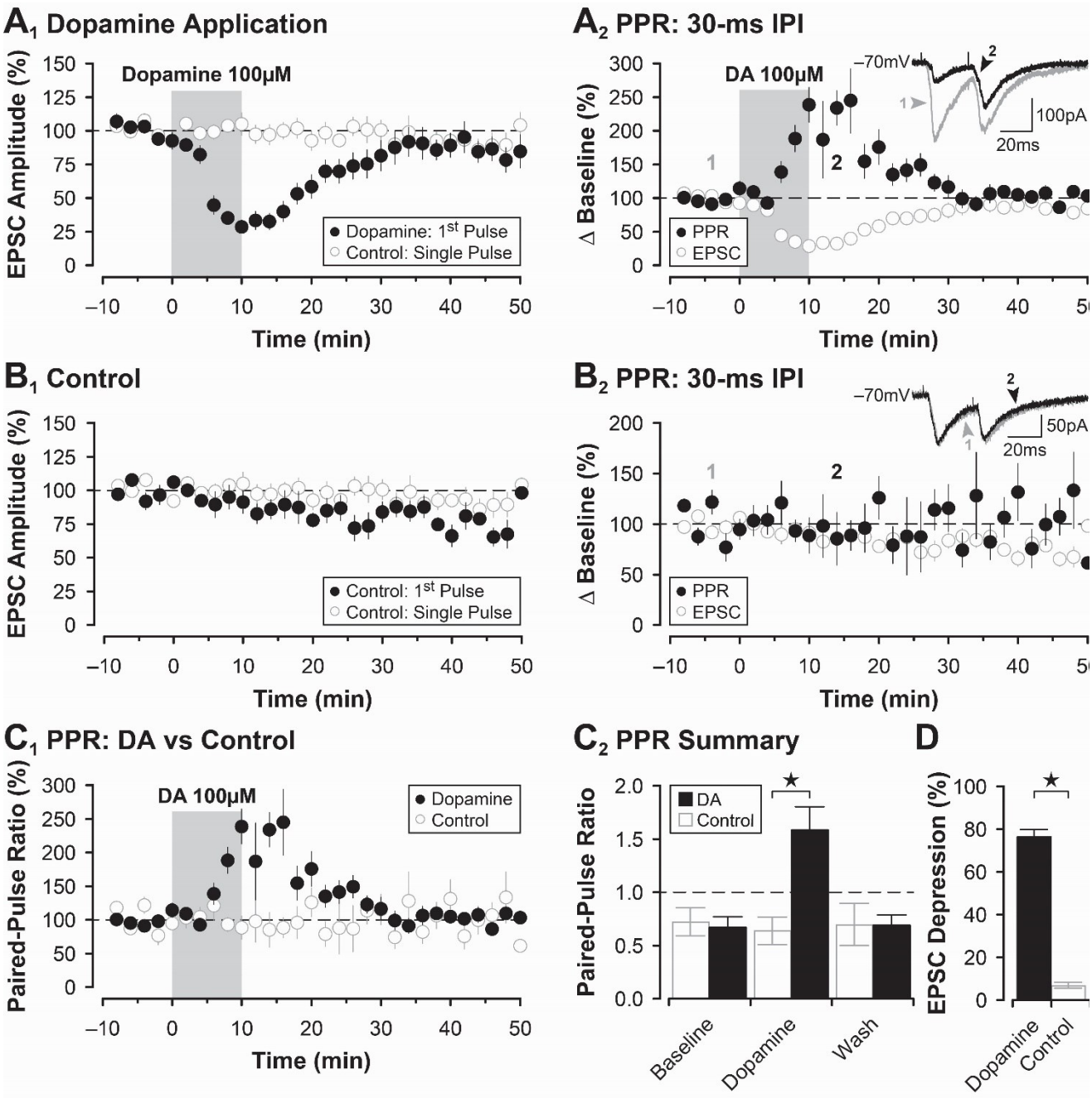

Figure 3.9. Dopamine suppresses EPSCs in layer II neurons whilst simultaneously increasing the paired-pulse ratio*. (**A_1**) Pairs of stimulation pulses with a 30-msec inter-pulse interval (IPI) were delivered once every 2-minutes to the superficial layers of the lateral entorhinal cortex. The amplitude of the first EPSC in the pair (filled circles) is plotted against time matched and untreated control data (open circles) highlighting the transient depression of synaptic responses induced by 100 µM dopamine. (**A_2**) EPSC amplitude data shown in **A_1** is plotted together with measures of the paired-pulse ratio (PPR) for the 30-msec IPI. Inset shows representative traces at 30ms IPI recorded at time points corresponding to numbers on the graph in **A_2**. Note how the increase in the paired-pulse ratio is time-locked to the depression of EPSCs. (**B_1-B_2**) Conventions are the same as **A_1** to **A_2**, but for an untreated control group. (**C_1**) Paired-pulse ratios for treated and untreated conditions are shown superimposed. (**C_2**) Summary bar plot comparing paired pulse-ratios for treated and untreated conditions at three different times during the experiment (Baseline, Dopamine and Wash). (**D**) Bar plot summary quantifying the significant depression of EPSCs induced by 100 µM dopamine relative to untreated controls (summary of data shown in **A_1**).*

Dopamine appears to suppress excitatory synaptic transmission via a presynaptic mechanism, but it is unknown whether dopamine-mediated changes in local inhibitory circuits contribute to this effect. It is possible that dopamine may *enhance* GABAergic transmission in the lateral entorhinal cortex and contribute to the suppression of synaptic responses. As such, experiments were designed to investigate whether dopamine modulates fast inhibitory transmission in the lateral entorhinal cortex to depress the amplitude of fEPSPs. For these experiments, contributions of fast $GABA_A$ receptor-mediated responses were blocked with picrotoxin (50 µM) with an IC_{50} value of 240 nM for $GABA_A$ receptors (Qian and Dowling (1994); see **Table 2.1**). Slices were pre-treated with picrotoxin for 15 min prior to being transferred to the recording chamber under constant perfusion with picrotoxin in ACSF. Like before, following a 30 min baseline, dopamine (100 µM) was added to the perfusate for 30 minutes and then washed off for an additional 60 minutes. As noted, $GABA_A$ receptor-mediated transmission was blocked chronically during these experiments, however it is important to note that at the concentration used, picrotoxin also targets $GABA_C$ receptors with an IC_{50} of 0.6 µM (Goutman and Calvo (2004); see **Table 2.1**) . Results showed that the onset, magnitude and recovery of the dopamine-mediated suppression of fEPSPs in the continuous presence of picrotoxin was identical to control recordings in which dopamine was applied alone in the absence of the antagonist (see **Figure 3.10A₂**). The peak depression of fEPSPs induced by dopamine in the presence of picrotoxin was 53.3 ± 7.6% of baseline (n = 4), and this did not differ significantly from control experiments in which dopamine was applied alone (to 44.1 ± 2.2% of baseline; n = 8; $F_{2,18}$ = 109.2, P < 0.01, Bonferroni P = 0.29; **Figure 3.10B**). Thus, blocking fast inhibitory transmission with picrotoxin does not change the magnitude or time course of the dopamine-mediated suppression of fEPSPs in the lateral entorhinal cortex.

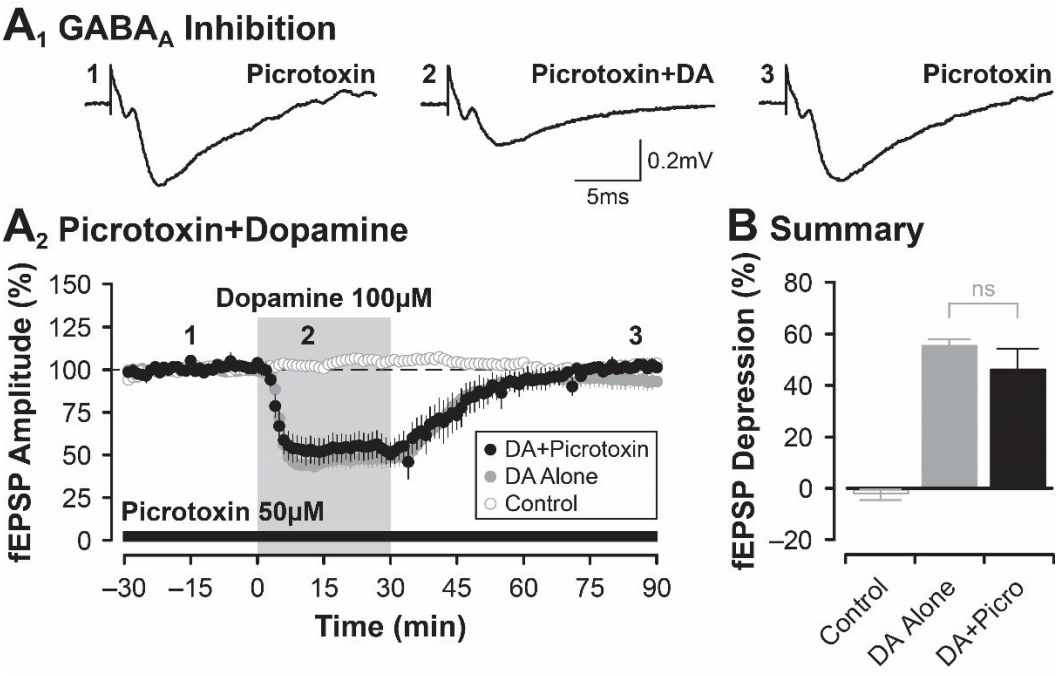

Figure 3.10. Blocking fast inhibitory transmission with picrotoxin does not affect the magnitude or time-course of the dopamine-mediated suppression of fEPSPs. *(**A₁**) Representative fEPSPs recorded before, during and after bath-*

*application of 100 µM dopamine. Numbered traces in **A₁** correspond to the numbers in **A₂** highlighting the specific times during the experiment when the field potentials were recorded. (**A₂**) Group data highlighting the dopamine-mediated suppression of fEPSPs in the presence and absence of picrotoxin (DA+Picrotoxin, black circles versus DA Alone, grey circles) relative to untreated controls (open circles). (**B**) Summary bar plot highlighting the peak depression of EPSCs induced by dopamine during each experimental condition.*

To assess the effects of dopamine on local inhibitory circuits directly, whole cell experiments were performed in which inhibitory synaptic currents were isolated and the effects of bath-applied dopamine on inhibitory synaptic transmission assessed in layer II neurons. For these experiments, the broad-spectrum glutamate receptor antagonist, kynurenic acid (1 mM), was used to block all excitatory transmission in slices of lateral entorhinal cortex (IC_{50} values of 70 and 500 µM for NMDA and kainate receptors, respectively; Bertolino, Vicini and Costa (1989)) so that inhibitory synaptic currents could be isolated and recorded. Cells were voltage clamped at 0 mV in the presence of kynurenic acid to evoke pure IPSCs in layer II neurons (see **Figure 3.11A₁-A₂**). In the presence of a high concentration of dopamine (100 µM), the amplitude of isolated IPSCs was unaffected by the treatment (**Figure 3.11B**). IPSCs remained stable at 106.3 ± 24.3% of baseline relative to time-matched and untreated control IPSCs following bath-application of dopamine ($F_{2, 12}$ = 2.071, P = 0.169, n = 4; **Figure 3.11C**). Interestingly, there was a slight increase in the amplitude of IPSCs during the washout period to 117.3 ± 18.7% of baseline, but this effect was not significant. These results suggest that dopamine has no effect on isolated inhibitory transmission in the lateral entorhinal cortex and that the dopamine-mediated suppression of excitatory synaptic responses results from something other than a change in local inhibition in the superficial layers. However, kynurenic acid at 1 mM also interacts with the α7-nicotine acetylcholine receptor and the adrenoreceptor α_{2B} (Bertolino, Vicini and Costa, 1989).

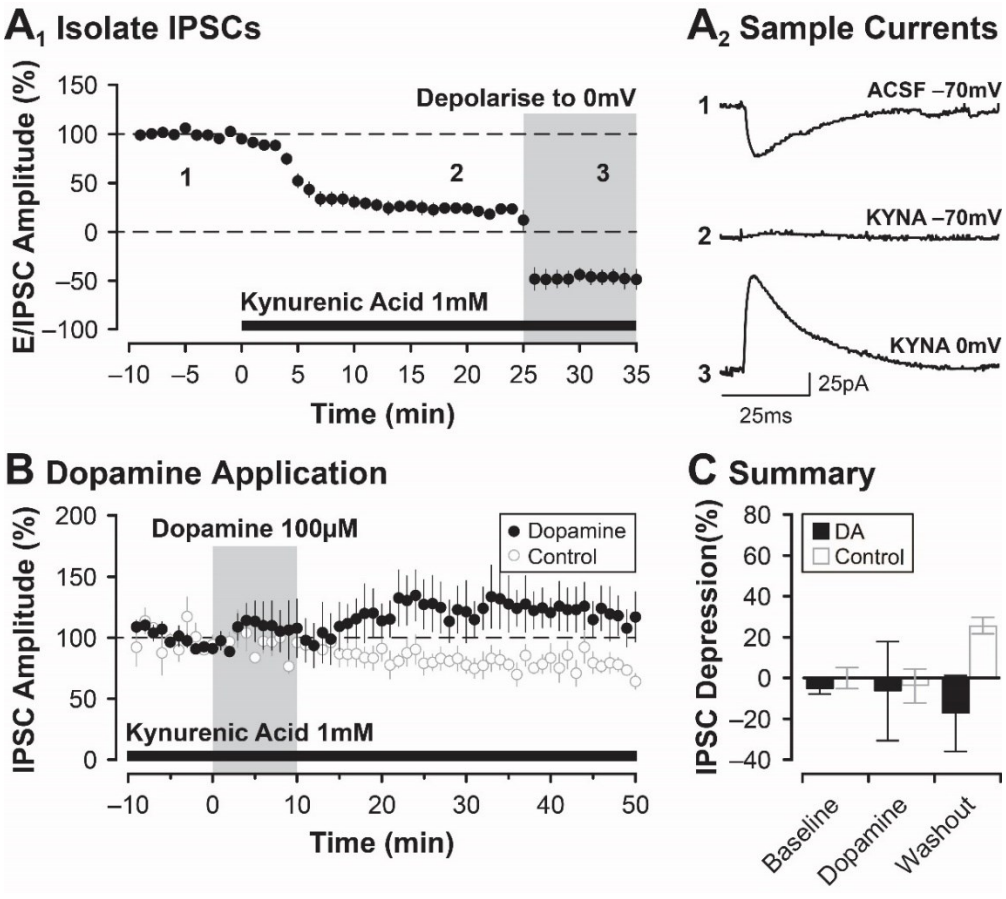

Figure 3.11. Dopamine has no effect on isolated IPSCs in the lateral entorhinal cortex. *(**A₁**) A sample data set highlighting how IPSCs are isolated and recorded from layer II neurons during whole-cell recording experiments. Once stable EPSCs at -70 mV have been recorded for a baseline period lasting 10 minutes, the glutamate receptor antagonist, kynurenic acid (1 mM), is added to the bathing medium. Over time, the EPSC is blocked. Finally, depolarising cells to 0 mV allows for the recording of isolated IPSCs. (**A₂**) Sample currents recorded at three different time points during the experiment shown in **A₁**. Numbers in **A₁** indicate the time points during the when the currents in **A₂** were recorded. (**B**) Inhibitory currents isolated with kynurenic acid (filled circles) are not affected by bath-application of 100 µM dopamine. (**C**) Summary bar plot comparing treated and untreated conditions at three different time points during the experiment (Baseline, Dopamine and Washout).*

Contributions of D_2-Like Dopaminergic Receptors

The receptors for dopamine can be divided into two major groups: D_1-like receptors and D_2-like receptors. In a previous study (Caruana *et al*., 2006), the suppression of excitatory synaptic transmission induced by high concentrations of dopamine (≥ 50 µM) was linked to activation of D_2-like dopaminergic receptors, whereas the facilitation of fEPSPs induced by a lower 10 µM concentration of dopamine was linked to activation of D_1-like receptors. In previous studies, the antagonists for D_1- and D_2-like dopamine receptors were always applied together with dopamine and never on their own. In the current study, antagonists for D_1-like and D_2-like dopaminergic receptors were first tested on their own to determine whether they would have any effect on basal synaptic transmission in the lateral entorhinal cortex. Interestingly, bath-application of the D_1 receptor antagonist, SCH-23390 (50 µM), on its own suppressed synaptic transmission in the lateral entorhinal cortex (see **Figure 3.12A₁-A₂**) however, it is key to note that at the 50 µM concentration used, SCH-23390 also binds to 5-HT_{3C} receptors, and blocks GIRK current with an EC_{50} value of 268 nM (see **Table 2.1**; Briggs *et al.* (1991); Bourne (2001); Millan *et al.* (2001); Kuzhikandathil and Oxford (2002)). Due to the small sample size (n = 2) no statistics were performed here. Responses were reduced to 73.3 ± 4.8% of baseline after 30 minutes of application. In contrast, bath application of the D_2 receptor antagonist, sulpiride (50 µM), appeared to have no effect on transmission (n = 2; see **Figure 3.12B₁-B₂**). Critically, sulpiride has a broad spectrum of receptor binding (see **Table 2.1**), for multiple serotonin, dopamine and adrenergic receptors which would all be targeted at the 50 µM concentration used (Besnard *et al.*, 2012). Given the trend towards a suppression of responses induced by SCH-23390 alone, it was decided to test whether D_2 receptors, specifically, had any effect on the dopamine-mediated suppression of fEPSPs. These data show that co-application of dopamine (100 µM) and sulpiride (50 µM) significantly reduced the magnitude of the dopamine-mediated depression ($F_{2, 19}$ = 61.52, P < 0.0001; **Figure 3.12C₁-C₂**). In control experiments without sulpiride, dopamine significantly depressed the amplitude of synaptic responses to 41.6 ± 5.6% of baseline levels (**Figure 3.12C₁**, grey circles; n = 6). The magnitude of this effect was significantly attenuated in the presence of sulpiride as responses were reduced only to 66.5 ± 3.9% of baseline by dopamine (**Figure 3.12C₁**, black circles; n = 8; Bonferroni P < 0.001; **Figure 3.12C₂**). Although the effects of dopamine were not blocked completely by sulpiride, possibly due to direct competition for the same binding sites, the results may suggest that there is still a significant D_2-like receptor-mediated mechanism that is triggered by high concentrations of dopamine, possibly via a D_2 receptor-mediated change in glutamate release from presynaptic terminals.

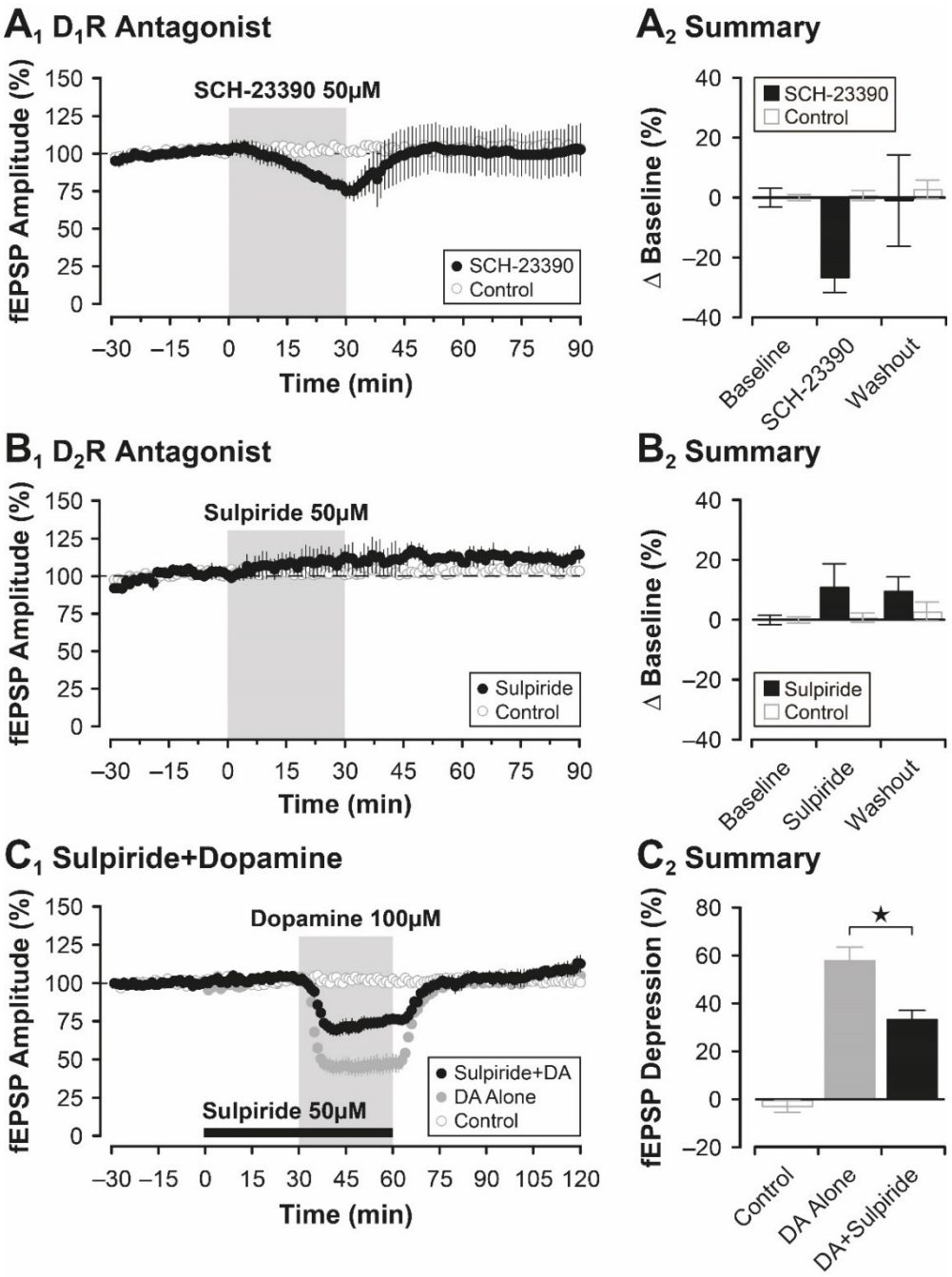

Figure 3.12. Effects of different dopamine receptor antagonists on synaptic transmission in the lateral entorhinal cortex. *(**A₁**) Bath application of the D_1 receptor antagonist, SCH-23390 (50 µM), on its own caused a transient depression in the amplitude of fEPSPs. (**A₂**). Quantification of data shown in A_1 at three different time points during the experiment. (**B₁**) Bath application of the D_2 receptor antagonist, sulpiride (50 µM), on its own had no effect on evoked synaptic responses. (**B₂**) Quantification of data shown in **B₁** at three different time points during the experiment. (**C₁**) Co-application of dopamine together with sulpiride (Sulpiride+DA; black circles) attenuates the dopamine-mediation depression of fEPSPs compared to dopamine alone (DA alone; grey circles) but does not block it. (**C₂**) Quantification of the peak effect of dopamine on synaptic responses for the three conditions tested in **C₁**.*

Discussion

Currently, there is only limited information available on the role of dopamine in modulating both the synaptic and intrinsic excitability of the lateral entorhinal cortex. It has been known for decades that a major branch of the mesocortical dopaminergic system innervates both the medial and lateral divisions of the entorhinal cortex (Fallon, Koziell and Moore, 1978; Swanson, 1982; Oades and Halliday, 1987), yet little progress has been made in terms of understanding how these inputs contribute to the cognitive, sensory and mnemonic functions of the entorhinal cortex. As such, the primary objectives for experiments conducted in this chapter were to confirm and to extend existing knowledge on the responsiveness of principal neurons in layer II of the lateral entorhinal cortex to dopamine, as well as to address some of the shortcomings in the existing literature. To achieve these objectives, a combination of electrophysiological, pharmacological and anatomical methods was employed. In line with what others have shown previously (Canto and Witter, 2012; Tahvildari and Alonso, 2005), the results of this chapter confirm that a heterogeneous population of neurons is present in the superficial layers of the lateral entorhinal cortex, and that these different neuronal phenotypes share many morphological characteristics related to the branch patterns of their dendrites. Further, a thorough assessment of the effects of dopamine on basal synaptic transmission was performed using multiple concentrations of dopamine, as well as using multiple concentrations of the broad-spectrum dopamine agonist, apomorphine. Results show that both dopamine and apomorphine have concentration-dependent and suppressive effects on synaptic responses evoked by stimulating sensory afferents to the superficial layers. Results of paired-pulse tests conducted during both field and whole-cell recording experiments indicate that the suppressive effects of dopamine are linked to a presynaptic change in the release probability of glutamate to affect synaptic transmission. In addition, the suppressive effects of dopamine on synaptic function are not entirely activity-dependent as a temporary pause in the delivery of test stimulation during dopamine application does not prevent the dopamine-mediated depression of fEPSPs when stimulation is resumed. A change in local GABAergic transmission does not seem to contribute to the depression of synaptic responses mediated by dopamine, and activation of D_2-like dopamine receptors is required to trigger the depression in the amplitude of fEPSPs induced by dopamine. Together, these findings expand on previous reports to indicate that dopamine has potent and suppressive effects on synaptic function in the lateral entorhinal cortex.

In this chapter, current knowledge related to the morphology of principal neurons in the superficial layers of the lateral entorhinal cortex was confirmed, as well as *some* of the effects the neurotransmitter dopamine has on basal synaptic function in the lateral division. In terms of morphology, the biocytin-streptavidin labelling methods used in this chapter indicate that a diverse array of neuronal phenotypes is present in both layer II and layer III of the lateral entorhinal cortex similar to what has been reported previously (Tahvildari and Alonso, 2005; Canto and Witter, 2012a). Data show that there are four distinct neuronal phenotypes present in layer II (fan, pyramidal, oblique pyramidal and multiform; **Figure 3.1**) and three phenotypes present in layer III (multipolar, simple pyramidal and complex pyramidal; **Figure 3.2**). Given the complex input-output relationship the entorhinal cortex shares with the hippocampus (Lingenhohl and Finch, 1991; Kloosterman, van Haeften and Lopes da Silva, 2004; for review see Canto, Wouterloud and Witter, 2008; Nilssen *et al*., 2019), it is possible that

different neuronal phenotypes project to distinct anatomical targets in the hippocampus. As noted previously, the entorhinal cortex innervates the hippocampus via several independent pathways (for review see Burwell, 2000; Jones and McHugh, 2011), but it is unknown whether different populations – or subtypes – of entorhinal projection neurons contribute differentially to these inputs. Alternatively, different neuronal phenotypes in the superficial layers of the entorhinal cortex may process qualitatively distinct types of sensory information. Indeed, it has been shown recently that fan cells in layer II, specifically, play a critical role in the discrimination of object-place content configurations (Vandrey, *et al*., 2020). Further, unpublished work from this research group shows that neurons in layer II respond in a different manner to dopamine compared to layer III neurons (Harvey, 2020). Specifically, layer III neurons are sensitive to transient and fast dopaminergic signals whereas layer II neurons respond to slow tonic changes in extracellular dopaminergic tone (Harvey, 2020). Together, these findings highlight the need for more research to uncover the role different neuronal phenotypes play in sensory and mnemonic processing in the lateral entorhinal cortex.

Non-spatial multimodal sensory information converges in the superficial layers of the lateral entorhinal cortex (Burwell and Amaral, 1998b; 1998a; Agster and Burwell, 2013; for review see Burwell, 2000). These excitatory sensory afferents terminate in layer I and make synaptic contact with dendrites belonging to the diverse population of projection neurons that reside in layers II and III. Horizontal slices containing the parahippocampal cortices and hippocampus preserve these glutamatergic input fibres and allow for the synaptic integration of sensory signals in superficial layer networks in the lateral entorhinal cortex to be studied in detail. Previous research has shown that dopamine has concentration-dependent and *bidirectional* effects on evoked responses in the superficial layers, with concentrations of 1 to 10 µM *enhancing* synaptic transmission and concentrations ≥50 µM *suppressing* the amplitude of responses (Caruana *et al*., 2006; Caruana and Chapman, 2008; Glovaci *et al*., 2014). A limitation of these initial reports is that few concentrations of dopaine were tested, and the amount of time dopamine was applied varied from study to study. Here, dopamine was applied for a standard 30-minute duration at multiple concentrations, and this allowed for a concentration-response curve for dopamine to be calculated and the EC_{50} value to be determined. As shown in **Figure 3.4**, dopamine suppressed the amplitude of fEPSPs in a concentration-dependent manner. Dopamine continued to depress responses in a concentration-dependent manner until a concentration of 100 µM, after which no further increase in the peak magnitude of the depression could be induced (**Figure 3.4B**). Interestingly, the effects of dopamine were only transient and responses recovered to baseline levels during washout. The suppressive effects of dopamine at 100 µM were also confirmed in whole-cell recordings (see **Figure 3.5**). These findings differ significantly from those reported previously in that low micromolar concentrations of dopamine (either 1 or 10 µM) were not sufficient to facilitate synaptic responses. A number of key methodological differences may account for the lack of bidirectionality in these findings. In the previous studies, a different strain of rat was used (Long Evans) and slices were prepared from much older animals (≥P35). Additionally, experiments were conducted at room temperature as opposed to a physiological 32 °C. Similar concentration-dependent and suppressive effects of dopamine on synaptic transmission were also found using the broad-spectrum dopamine agonist, apomorphine (**Figure 3.6**). Again, there was no indication of an apomorphine-mediated enhancement

of fEPSPs when using low concentrations of the agonist. Additional work is required to understand why the previous bidirectional effects of dopamine on basal synaptic transmission were not observed in the current study. But consideration should be given to the multiple binding affinities of both dopamine and apomorphine at different receptor types (see **Table 2.1**) which means the resulting fEPSP will reflect a possible combined change in dopaminergic, serotonergic and adrenergic signalling.

Despite a brief pause in the delivery of test stimulation during bath-application of dopamine, synaptic responses were still depressed when test stimulation was resumed at the end of the 30-minute application period (**Figure 3.7**). This suggests that the suppressive effects of dopamine on basal synaptic transmission in the lateral entorhinal cortex are not dependent on constant synaptic stimulation to trigger induction. Activation of NMDA receptors is also not required, as the peak of dopamine-mediated depression of fEPSPs was unaffected by the NMDAR antagonist, AP5, however the recovery to baseline fEPSP magnitude was slower (see **Figure 3.7**). This slow recovery may reflect a washout effect of the AP5, rather than an NMDA effect on dopamine suppression. However, the magnitude of the depression was *smaller* than the depression observed typically with dopamine when test stimulation is delivered continuously during agonist application. Interestingly, during time-matched control experiments in which test stimulation was paused in the absence of any dopamine, responses were about 10% larger in amplitude when synaptic stimulation was resumed (see **Figure 3.7**). These findings suggests that constant synaptic stimulation, on its own, may trigger a mild tonic suppression of synaptic transmission in the lateral entorhinal cortex, and this could account for why the magnitude of the depression induced by dopamine is larger when synaptic stimulation is applied continuously.

Similar to previous reports, the dopamine-mediated suppression of synaptic transmission in the lateral entorhinal cortex is expressed presynaptically via a reduction in the release probability of glutamate from afferent sensory terminals that terminate in layer I. Paired-pulse tests conducted during both field and whole-cell recording experiments show an increase in paired-pulse ratios, and a temporary switch from paired-pulse depression to paired-pulse facilitation in the presence of dopamine. These data suggest that dopamine elicits its effects by restricting glutamate release presynaptically (see **Figures 3.8** and **Figure 3.9**). Although these effects have been alluded to previously (Caruana *et al.*, 2006; Caruana and Chapman, 2008; Liu, 2020), this is the first report to assess paired-pulse ratios before, during and after application of dopamine (see **Figures 3.8**), as well as the first report to demonstrate how dopamine-mediated changes in EPSC amplitude are time-locked to coincident changes in paired-pulse ratios (see **Figure 3.9**).

The superficial layers of the lateral entorhinal cortex consist of complex neural circuits comprised of *both* excitatory *and* inhibitory neurons (Erickson, Sesack and Lewis, 2000). As noted above, the dopamine-mediated suppression of fEPSPs and EPSCs is due largely to a reduction in the release probability of glutamate. However, dopamine-mediated changes in local inhibition may also contribute. In the current study, contributions of fast $GABA_A$ receptor-mediated transmission were investigated by coapplying the $GABA_A$ receptor antagonist, picrotoxin, together with dopamine. Results show that the dopamine-mediated suppression of fEPSPs is not mediated by any change in local $GABA_A$-mediated inhibition in the lateral entorhinal cortex (see **Figure 3.10**), despite the activation of $GABA_A$ having been previously shown to impair associative

learning in superficial layer neurons in this same area (Lee *et al.*, 2021). However, the use of picrotoxin in slice recording experiments has limitations. Picrotoxin is specific to ionotropic GABA receptors ($GABA_A$ and $GABA_C$) and does not bind to metabotropic $GABA_B$ receptors, which are known to be present in the entorhinal cortex (Couve, Moss and Pangalos, 2000; Deng *et al.*, 2009). Activation of $GABA_B$ receptors has been shown to elicit dramatic inhibitory control over neuronal excitability in the superficial layers of the medial entorhinal cortex by activating the bound $G_{\alpha i/o}$-protein and intracellular signalling pathways resulting in the PKA-dependent opening of TREK-2 K^+ channels to hyperpolarise the neuronal membrane (Deng *et al.*, 2009). Also, dopaminergic projections have been shown to contain $GABA_B$ receptors (Schwenk *et al.*, 2016; Porcu *et al.*, 2021). Future work should address the possibility that dopamine may interact with $GABA_B$ receptors to elicit the suppression seen in **Figure 3.10**.

The removal of fast inhibitory control in the lateral entorhinal cortex can sometimes trigger hyperexcitability and seizure activity in slices, and this makes recording stable field responses difficult. To circumvent this, whole-cell experiments were performed on isolated inhibitory currents. Treating slices with the glutamate receptor blocker, kynurenic acid, and depolarising cells to 0 mV, it is possible to isolate and record pure GABA-mediated IPSCs from layer II neurons (see **Figure 3.11**). Dopamine had no significant effect on the amplitude of IPSCs indicating that dopamine-mediated changes in local inhibition do not contribute to the depression of fEPSPs and EPSCs observed.

It has been shown previously that the suppression of synaptic responses by dopamine requires activation of D_2 receptors (Caruana *et al*., 2006; Caruana and Chapman, 2008). Co-application of the selective D_2-like receptor antagonist, sulpiride, together with dopamine was sufficient to reduce the magnitude of the dopamine-mediated depression of fEPSPs by about 50% (see **Figure 3.12C**), a result similar to those reported previously by Caruana *et al*. (2006). It is unclear why sulpiride was unable to fully block the effects of dopamine on synaptic transmission, but it may be due to competition between both drugs at the D_2 receptors themselves. However, it may be due to the alternative binding of sulpiride to serotonergic and adrenergic receptors leading to complex interactions (see **Table 2.1**). Alternatively, these experiments typically involve the application of a relatively high concentration of dopamine (100 µM). As such, dopamine may simply outcompete sulpiride for limited D_2 receptor binding sites leading to only a partial occlusion of the dopamine-mediated depression. It is also possible that D_1-like receptors may contribute. However, initial experiments during which the D_1 receptor antagonist, SCH-23390, was applied alone showed that the antagonist caused a mild depression of fEPSPs on its own in the absence of any dopamine (see **Figure 3.12A**). As such, it was not possible to use this antagonist to assess the role of D_1 receptors in the dopamine-mediated suppression of synaptic responses in the lateral entorhinal cortex.

Chapter 4: Dopamine-Mediated Desensitisation of Metabotropic Receptor Function

Introduction

The results of Chapter 3 demonstrate that dopamine has powerful suppressive effects on synaptic transmission in the lateral entorhinal cortex across a wide range of concentrations. Although the magnitude of the dopamine-mediated suppression of fEPSPs is maximal at a concentration of 100 µM, and no further depression in peak fEPSP amplitude is observed when using 300 or 1000 µM dopamine, an interesting phenomenon was uncovered at the highest concentration tested. When bath-applying 1000 µM dopamine, synaptic responses depress but immediately start to recover to baseline despite the continued presence of the agonist (see **Figure 3.4A$_1$, black circles**). This recovery in the presence of dopamine suggests that the dopaminergic receptors, or dopamine-binding sites on alternative receptors (see **Table 2.1**), that underlie the depression of basal synaptic transmission rapidly desensitise when exposed to high concentrations of an agonist. This is the first evidence of dopamine-mediated desensitisation observed in the lateral entorhinal cortex that can be assayed using standard extracellular recordings of basal synaptic transmission. Given the lack of information available on metabotropic receptor desensitisation in the entorhinal cortex, further characterisation of this phenomenon is needed.

All dopamine receptors are metabotropic and signal via activation of an associated G-protein. Rapid desensitisation of G-protein coupled receptors (GPCRs) is quite common as most isoforms possess an innate ability to internalise when exposed to intense and prolonged exposure to an agonist (for review see Kelly, Bailey and Henderson, 2008). It is generally believed that the rapid desensitisation of GPCRs serves as a fail-safe mechanism to prevent overstimulation and aberrant signalling when the receptors are oversaturated with an agonist. As shown in this study, as well as in previous work (Caruana *et al.*, 2006; Caruana and Chapman, 2008), concentrations of dopamine ≥30 µM reliably induce a stable and reversible suppression of synaptic transmission in the superficial layers of the lateral entorhinal cortex. But throughout this thesis, there is also abundant evidence indicating that receptors can start to desensitise when exposed to concentrations of dopamine ≥100 µM (see **Figure 4.1A**&**B** and **Figure 4.2A$_2$**). It has been shown previously that the desensitisation of dopamine receptors depends, in part, on mechanisms that are receptor subtype-dependent (Kim *et al*., 2001; for review see Beaulieu and Gainetdinov, 2011). This desensitisation is mediated by kinases that regulate the surface expression of dopamine receptors in neuronal membranes. These kinases are known as G-protein-coupled receptor kinases (or GRKs), and phosphorylation of key intracellular targets by GRK2, in particular, has been shown to mediate D_1 receptor (Tiberi *et al.*, 1996), and in some instances D_2 receptor (Iwata *et al.*, 1999; Kim *et al.*, 2001), internalisation. But this is an oversimplification since D_1 receptors can signal via multiple downstream signalling cascades that differ depending on their location and associated second messenger systems. Tiberi *et al.* (1996) have shown that D_1 receptors are modulated by GRK2, but also – depending on where they are

expressed – by GRK3 and GRK5, with each kinase triggering a slightly different downstream signalling pathway to provide a unique response to agonist binding, and ultimately receptor desensitisation.

Regulation of GPCRs in neuronal membranes, including all dopamine receptor subtypes, varies depending on the specific kinases that target the receptor complex itself (Tiberi *et al.*, 1996). D_1 receptors, for example, are known to be targeted by GRK2, GRK3 or GRK5 (Tiberi *et al.*, 1996). In general, GRKs are responsible for phosphorylating activate GPCRs. Excessive binding of an agonist to a metabotropic receptor triggers the repeated activation of the associated G-protein and exposes the active receptor to phosphorylation by GRKs. Phosphorylation of the GPCR by a GRK changes its conformation to promote recruitment of β-arrestin to the receptor complex. The resulting β-arrestin complex mediates downstream receptor desensitisation (for review see Sulon and Benovic, 2021). These first few stages happen within a very short period, typically within 1 to 5 minutes of agonist exposure (for review see Rajagopal and Shenoy, 2018). Upon β-arrestin recruitment, agonist-dependent ubiquitination occurs to allow the new β-arrestin complex to facilitate receptor endocytosis and additional cell signalling mechanisms. Ubiquitination is required for long-lasting receptor desensitisation, whereby these β-arrestins are 'tagged' to direct internalised receptors to lysosomes. Initial conformational changes to the β-arrestin complex also allow it to interact with Nedd4, which removes Mdm2 from the β-arrestin, and this occurs approximately 5 to 15 minutes post-agonist binding. At this point, the β-arrestin complex interacts with clathrin and AP2 to facilitate endocytosis of the GPCR. Once endocytosed, the β-arrestin complex is changed once more, so the modified clathrin-AP2 attachment can be ubiquitinated by Nedd4 at approximately 10 to 15 minutes post-agonist binding. These newly ubiquitinated complexes that are attached to the endocytosed GPCR are then moved into early endosomes. It is not until around 6-hours post-agonist binding that these early endosomes are moved to late endosomes and lysosomes for recycling. It is important to note, however, that receptors can return to the membrane following the early lysosome stages at any time as completely naïve receptors (Shenoy *et al*., 2008; for review see Rajagopal and Shenoy, 2018). As such, the persistence of the desensitisation can vary.

It has been well-established that principal neurons in layer II of the lateral entorhinal cortex express both D_1-like and D_2-like receptors (Köhler, Ericson and Radesäter, 1991), and that these receptors can respond to dopamine in a concentration-dependent manner (see **Figure 3.4**) to restrict the release of glutamate from sensory afferents that terminate in layer I (see **Figure 3.8 & 3.9**). It has also been shown that the dopamine-mediated suppression of fEPSPs is due, in part, to the activation of D_2 receptors (see **Figure 3.12**). Although there is evidence to suggest that metabotropic, dopamine-binding receptors may desensitise in response to high concentrations of dopamine (see **Figure 3.4**), a comprehensive characterisation of this phenomenon is lacking. It is also not clear whether overstimulation of dopamine receptors, or agonist actions at alternative binding sites, in the lateral entorhinal cortex recruits a conserved mechanism for receptor internalisation mediated by GRK phosphorylation, as is shown in other regions of the neocortex (for review see Beaulieu and Gainetdinov, 2011). Given that dopamine has potent suppressive effects on synaptic function in the superficial layers of the lateral entorhinal cortex at high concentrations, it is currently unclear whether a desensitisation of these receptors plays a functional role in cognition, or whether it simply represents a fail-safe mechanism to protect against

aberrant dopaminergic signalling. Indeed, dysregulation of neuromodulatory signalling has been linked to exacerbation of brain disease, including Alzheimer's dementia (Klein *et al.*, 2016), major depressive disorder (Avital *et al.*, 2006) and schizophrenia (Roalf *et al.*, 2017). As such, a greater understanding of the signalling mechanisms triggered by activation of dopamine receptors in the lateral entorhinal cortex could uncover potential therapeutic targets to reduce the debilitating symptoms of brain disease, as well as to further understand the underlying pathophysiology of these disorders.

Materials and Methods

Electrophysiology and Pharmacology

For all field recording experiments, slices were rested in warmed and oxygenated ACSF for at least 60 minutes after slicing just prior to experimental testing. Following the rest period, slices were transferred to the recording chamber and a bipolar stimulating electrode and glass recording electrode were placed carefully in the superficial layers of the lateral entorhinal cortex (stimulating electrode positioned to span the layer I-II border; recording electrode positioned along the layer I border with layer II; see **Figure 3.3A**) and responses were elicited once every 20s. Control experiments were interleaved throughout all experimental testing, and each treatment condition had its own time-matched control data to compare to.

Several experiments were performed to demonstrate dopamine-mediated dopamine receptor desensitisation in the lateral entorhinal cortex. Initially, the desensitisation effect was triggered by using a high concentration of dopamine. Following a 30-minute baseline in normal ACSF, a high concentration of 1000 µM dopamine was bath-applied for 30 minutes. The dopamine was then washed out for a further 60 minutes in normal ACSF. Experiments were also performed to determine if it was possible to desensitise dopamine receptors using a more moderate 100 µM concentration of dopamine. During these experiments, dopamine was applied three times, for 10 minutes each, with a 20-minute wash in between applications. Next, to investigate the persistence of the desensitisation, dopamine (100 µM) was applied twice for 30 minutes with either a 60-minute wash or a 3-hour wash between successive applications.

The mechanism of dopamine-mediated desensitisation of metabotropic receptors was investigated using the GRK inhibitor, compound 101 (CMPD101), as well as the β-arrestin inhibitor, barbadin. These inhibitors are highly selective for their intended targets at the concentrations chosen in the experimental design (see **Table 2.1**). Following a 30-minute baseline in normal ACSF, either CMPD101 (10 µM) or barbadin (30 µM) was applied alone for 30-minutes and then together with dopamine (100 µM) for 30 more minutes. After an initial 60 min wash, a second application of dopamine (100 µM) was bath-applied for 30 minutes followed by a final 60-minute wash.

Data Analysis

The effects of bath-applied drugs during pharmacological experiments were assessed on the amplitude of averaged synaptic responses (fEPSPs) obtained during 5- or 10-min epochs recorded at different times during an experiment (latencies specified below). In instances of comparing peak drug effect over time, the peak change in synaptic efficacy was used, and this was determined manually for each individual experiment as the latency varied. Non-linear regression and curve fitting, when required, was performed using Prism. All data were expressed as the mean ± SEM and were normalised to the baseline period for plotting. Drug-induced changes in response properties were assessed with Prism using (where appropriate) paired or unpaired samples t-tests, one-way ANOVAs or repeated measures ANOVAs. Post-hoc comparisons were made using the Bonferroni method with an alpha level of $P < 0.05$.

Results

Initial attempts to uncover the dopamine-mediated desensitisation were performed using a high 1000 µM concentration of dopamine. As shown in **Figure 4.1A**, synaptic responses were depressed, initially, by dopamine but immediately started to recover to baseline despite the continued presence of the agonist. This recovery in the presence of dopamine suggests that dopamine, or alternative agonist binding, receptors desensitise when exposed to high concentrations of an agonist (in this case, dopamine). To quantify the desensitisation, a regression line was fit through the data points during the application period for 1000 µM dopamine starting at the peak of the fEPSP depression and ending at the start of the washout period. The slope of the regression line differed significantly from zero (y = 0.50x + 40.75, $P < 0.0001$; **Figure 4.1A**) indicating that the magnitude of the dopamine-mediated depression of fEPSPs was not stable nor consistent during the application period.

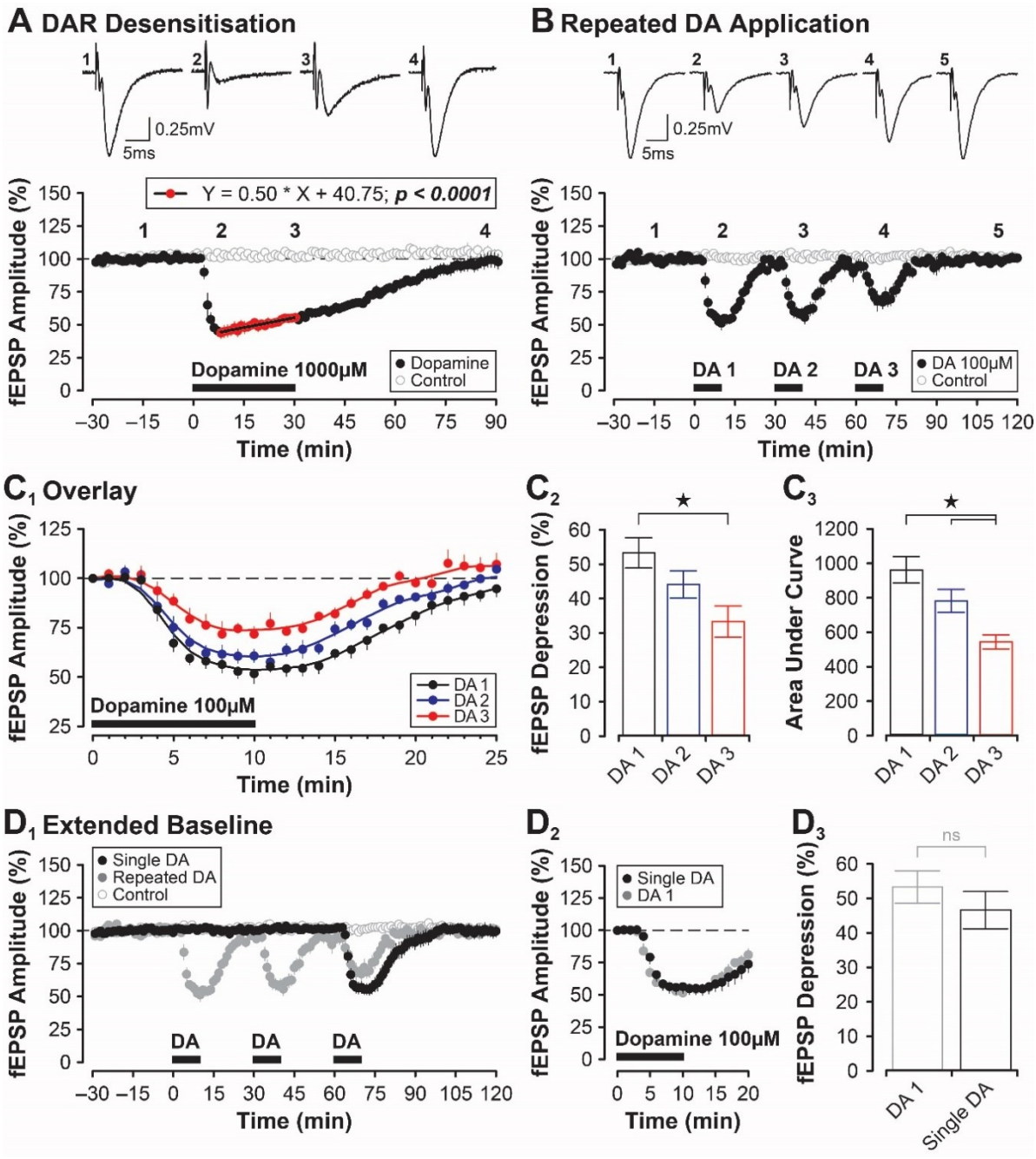

Figure 4.1. Dopamine-mediated desensitisation of metabotropic receptors in the lateral entorhinal cortex can be induced using several different experimental protocols*. (**A**) Field EPSPs are depressed during exposure to a single high concentration of dopamine (1000 µM, black circles), but begin to recover despite the continued presence of the agonist. A regression line fit through the data points during dopamine application deviates significantly from zero (red line) indicating the effect of dopamine is not consistent at this concentration. (**B**) The magnitude of the dopamine-mediated depression of fEPSPs weakens with every successive application of dopamine. Dopamine was applied three times for 10-min once every 30-min (DA 1, DA 2, and DA 3). (**C_1**) Data for each application of dopamine are renormalised and superimposed to show how the impact on transmission weakens with each successive exposure. (**C_2**) Summary bar plot of data shown in **C_1** comparing during the peak suppression of fEPSPs during each application of dopamine. (**C_3**) Summary bar plot of data shown in **C_1** comparing the area under the curve following each successive exposure to dopamine. (**D_1**) Control experiment with an extended, 90-minute, baseline followed by a single application of dopamine (Single DA, black circles) to rule out the possibility that the desensitisation was an artefact due to a time-dependent run-down in transmission. Dopamine had the same suppressive effect on fEPSPs regardless of whether it was applied quickly (after 30 minutes; DA 1) or following an extended 90-minute baseline (Single DA). (**D_2**) Overlay of the extended, 90-minute, baseline single dopamine application (Single DA, black circles) compared to DA 1 from repeated dopamine application experiment in **B** (DA 1, grey circles). (**D_3**) Summary bar plot comparing the peak suppression of fEPSPs for data shown in **D_2**. Note: representative fEPSPs recorded before, during and after bath application of 1000 µM dopamine (**A**) and multiple, short applications of 100 µM dopamine (**B**) are plotted above the respective summary graphs. Numbered traces correspond to numbed labels shown on the summary graphs below to highlight specific times during the experiment when these field recordings were recorded.*

To test whether it was possible to desensitise dopamine-binding receptors using a more moderate 100 µM concentration of dopamine, the agonist was applied three times in rapid succession and the magnitude of the dopamine-mediated depression of fEPSPs in response to each application compared (see **Figure 4.1B-C**). As shown in **Figure 4.1B**, repeated application of 100 µM dopamine for 10 minutes once every 30 minutes (x3; DA 1, DA 2 and DA 3) was sufficient to trigger the desensitisation effect as the magnitude of the dopamine-mediated suppression appeared to lessen with each successive application. And as with other dopamine experiments, responses returned to baseline levels during the 60-minute washout period. Data for a 25-minute window during each application of dopamine (DA 1, DA 2 and DA 3) were renormalised and superimposed to further highlight and quantify the desensitisation (see **Figure 4.1C_1**). The peak depression of fEPSPs induced during each application of dopamine was compared and showed a significant weakening in the impact dopamine was having on synaptic transmission as it was reapplied ($F_{2, 18}$ = 5.455, P < 0.05, n = 7; **Figure 4.1C_2**). During the initial application (DA 1), responses were reduced maximally to 46.3 ± 4.4% of baseline levels. During the second application (DA 2), responses were reduced to 55.5 ± 4.0% of baseline. But by the third application, responses were reduced to only 66.4 ± 4.5% of baseline; a magnitude significantly less than the depression observed for DA 1 (Bonferroni P < 0.05). In addition, the fit of a LOWESS curve through each data set allowed the area under the curve to be determined for each application of dopamine. Similar to what was observed for the peak fEPSP depression data, the area under the curve was also reduced significantly following each successive application of dopamine ($F_{2, 18}$ = 11.04, P < 0.001, n = 7; **Figure 4.1C_3**).

To rule out the possibility that the progressive weakening in the magnitude of the dopamine-mediated depression of fEPSPs was due simply to some time-dependent run-down of responses as opposed to an actual desensitisation of dopamine receptors, a control experiment was conducted in which a single application of dopamine (100 µM for 10 minutes) was delivered at the same time (+60 minutes) as the third and final application of dopamine (DA 3) from the previous experiment (**Figure 4.1D_1**; n = 6). The data obtained during a 20-minute window for each dopamine application was then renormalised and superimposed to compare the

magnitude of the depression for the single dopamine application (with the extended baseline) and the initial dopamine application from the previous experiment (DA 1). As shown in the renormalised data in **Figure 4.1D$_2$**, there was no difference in the level of depression induced by dopamine during the two conditions. Dopamine had the same suppressive effect on fEPSPs regardless of whether it was applied quickly (after 30 minutes; DA 1) or following an extended 90-minute baseline. There was also no difference in the magnitude of the peak depression of fEPSPs when comparing the two parameters (see **Figure 4.1D$_3$**). These findings suggest that the change in magnitude of the dopamine effect following successive applications reflects a desensitisation of dopamine-binding receptors and not simply the passage of time.

Desensitisation of metabotropic receptors typically involves receptor internalisation, and this effect can persist for variable amounts of time depending on the type of receptor and where it is expressed in the brain (Tiberi *et al.*, 1996; Shenoy *et al.*, 2008; Rajagopal and Shenoy, 2018). To determine the persistence of the dopamine-mediated desensitisation of dopamine receptors in the lateral entorhinal cortex, dopamine (100 µM) was bath-applied twice for 30 minutes with a 60-minute wash between applications (see **Figure 4.2A**). Dopamine depressed synaptic responses to 38.5 ±3.8% of baseline during the initial application, and the amplitude of fEPSPs returned to baseline levels quickly (within around 10 minutes) during the initial 60-minute wash. However, although responses had returned to basal levels, a second application of dopamine had a much weaker effect on transmission. Synaptic responses were suppressed to only 56.0 ±2.1% of baseline (compared to 38.5 ±3.8%) indicating that dopamine-binding receptors were still desensitised even though 60-minutes had elapsed since initial exposure to the agonist (see **Figure 4.2A$_2$**). Data for each 30-minute application of dopamine (DA 1 and DA 2) were renormalised and superimposed to further highlight and quantify the desensitisation (see **Figure 4.2A$_3$**). The maximal depression of fEPSPs induced during each application of dopamine was compared (see **Figure 4.2A$_4$**), and the results indicate that dopamine's impact on synaptic transmission had weakened significantly during the second application (DA 2) relative to the first (DA 1; $t_{14} = 4.03$, $P < 0.01$, $n = 8$). Taken together, these findings suggest that the dopamine-mediated desensitisation of receptors induced by an initial 30-minute exposure to 100 µM dopamine might persist for at least one hour.

Interestingly, the desensitisation of dopamine receptors is reversible. Although it can persist for at least 60 minutes, the magnitude of the fEPSP depression induced by a second application of dopamine recovered fully after three hours (see **Figure 4.2B**). In a similar experiment, an initial application of dopamine for 30-min (DA 1) depressed synaptic responses to 45.1 ± 4.3% of baseline. However, there was no evidence of receptor desensitisation when the initial wash period was extended from 60-minutes to three hours. A second application of dopamine (DA 2) after this much longer delay period induced a depression of fEPSPs similar in magnitude to that of the first application (DA 1). Synaptic responses were suppressed to 44.3 ± 3.7% of baseline during the second application (compared to 45.1 ± 4.3% during DA 1) indicating that dopamine receptors were no longer desensitised three hours after initial exposure to the agonist (see **Figure 4.2B$_1$**). Data for each 30-minute application of dopamine (DA 1 and DA 2) were renormalised and superimposed to further highlight and quantify the desensitisation (see **Figure 4.2B$_2$**). The peak depression of fEPSPs induced during each application of dopamine was compared (see **Figure 4.2B$_3$**), and the results indicate that dopamine's impact on synaptic

transmission had regained its full potency after three hours (t_{20} =0.051, P = 0.959, n = 11). Taken together, these findings suggest that the desensitisation of dopamine receptors induced by an initial 30-minute exposure to 100 µM dopamine reverses within three hours.

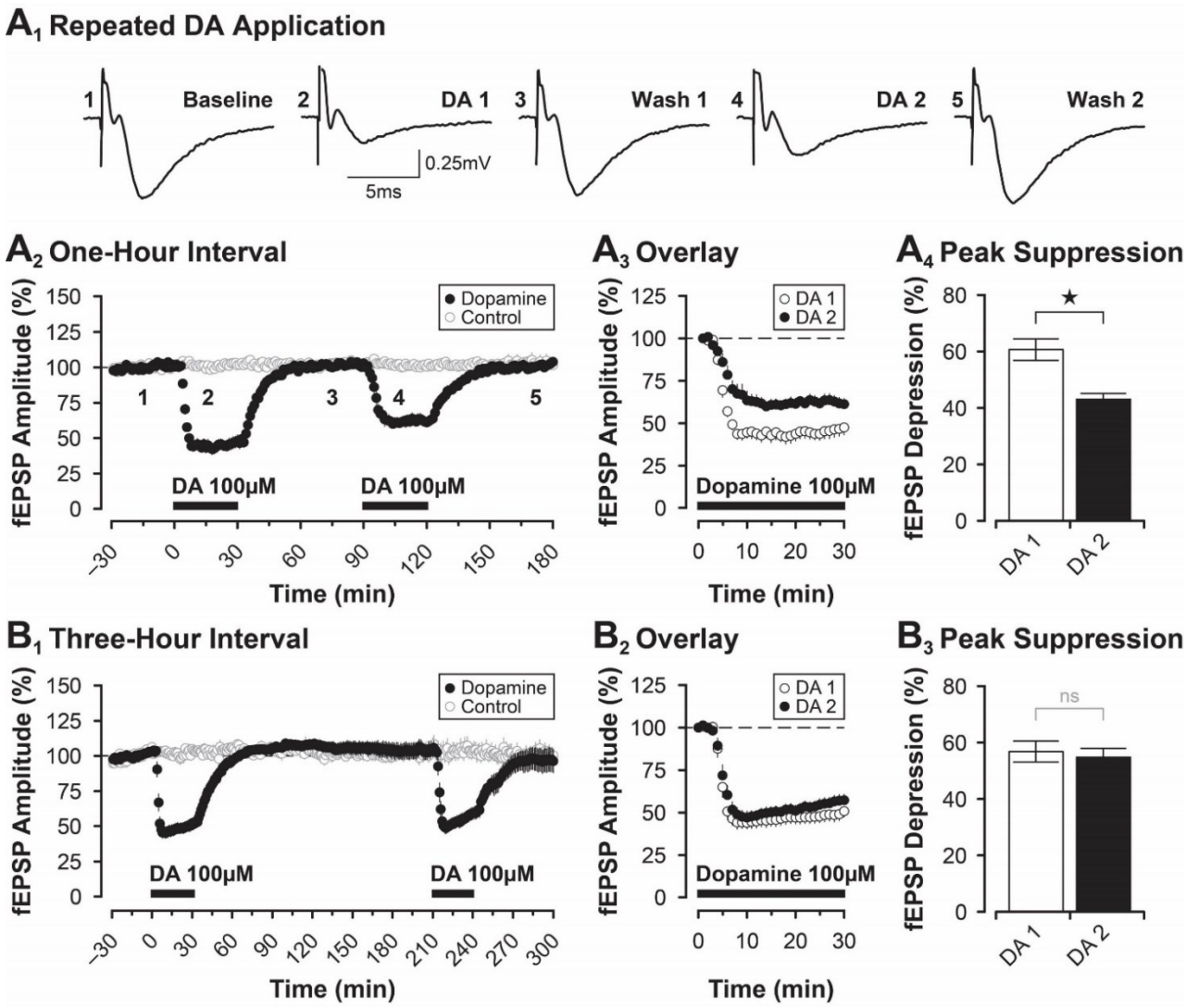

Figure 4.2. The dopamine-mediated desensitisation of metabotropic receptors is long-lasting and reversible. *(**A₁**) Representative traces recorded at different times before, during and after one of two 30-minute applications of dopamine. Numbered traces in **A₁** correspond to the timings of numbers in **A₂** highlighting the specific time points during the experiment the sample traces were recorded. (**A₂**) An initial exposure to dopamine is sufficient to trigger the lasting effect on response magnitude and attenuate the depressive effects of dopamine when applied a second time 60-minutes later. Interestingly, receptors remain in a desensitised state for at least one hour. (**A₃**) Data for each 30-minute application of dopamine (DA 1 and DA 2) shown renormalised and superimposed to further highlight and quantify the desensitisation. (**A₄**) Quantification of the mean peak fEPSP suppression comparing the first (DA 1, open circles) and second (DA 2, black circles) dopamine applications from **A₂**. (**B₁**) The desensitisation of dopamine-binding receptors is reversible. Although it can persist for at least 60 minutes, the magnitude of the fEPSP depression induced by a second application of dopamine is identical to the first when applied three hours later. (**B₂-B₃**) Conventions are the same as **A₃** to **A₄**, but for a three-hour interval between dopamine applications.*

A potential candidate mechanism to account for the desensitisation observed in the lateral entorhinal cortex may involve a GRK-mediated internalisation of dopamine receptors. Using a similar experimental design as before in which dopamine was applied to slices twice (for 30 minutes each) with a 60-minute wash in between

applications, blockers of key intracellular signals involved in metabotropic receptor internalisation were co-applied with dopamine during the initial application (DA 1). Compound 101 (CMPD101), a selective inhibitor of GRK2/3, shows a slight enhancement of synaptic efficacy although this had no significant effect on basal synaptic transmission when applied on its own, but it prevented the desensitisation of dopamine receptors when co-applied with the agonist during the initial application (**Figure 4.3A**). In the presence of CMPD101, dopamine depressed fEPSPs to 45.8 ± 2.6% of baseline during DA 1, and a second application of dopamine alone after a 60-minute wash (DA 2) induced a depression of fEPSPs that was similar in magnitude. Synaptic responses were suppressed to 46.9 ± 3.7% of baseline during the second application (compared to 45.8 ± 2.6% during DA 1) indicating that dopamine-binding receptors were no longer desensitised 60 minutes after initial exposure to CMPD101 (see **Figure 4.3A$_1$**). Data for each 30-minute application of dopamine (DA 1 and DA 2) were renormalised and superimposed to further highlight and quantify the desensitisation (see **Figure 4.2A$_2$**). The peak depression of fEPSPs induced during each application of dopamine was compared (see **Figure 4.2A$_3$**), and the results indicate that dopamine's impact on synaptic transmission had retained its full potency during DA 2 when GRK2/3 was blocked during DA 1 (t_{10} =0.249, P = 0.815, n = 6). Taken together, these findings suggest that the dopamine-mediated desensitisation of metabotropic receptors was prevented if GRK2 was blocked during the initial 30-minute exposure to 100 µM dopamine. Although dopamine-binding receptors were strongly activated by the initial 100 µM application, CMPD101 prevented GRK2/3 from phosphorylating metabotropic receptors to potentially trigger internalisation mechanisms.

To further assess the mechanisms underlying the dopamine medicated desensitisation, a potent membrane-permeable inhibitor of β-arrestin, barbadin (30 µM), was co-applied with dopamine during the initial application (DA 1). GRK mediated changes in metabotropic receptors facilitates binding of β-arrestin to initiate receptor internalisation. Preventing β-arrestin from binding to phosphorylated GPCRs with barbadin was expected to block receptor internalisation and desensitisation. Barbadin shows a slight enhancement of synaptic efficacy but had no significant effect on basal synaptic transmission when applied on its own, but it prevented the desensitisation of dopamine-binding receptors when co-applied with the agonist during the initial application (**Figure 4.3B**). In the presence of barbadin, dopamine depressed fEPSPs to 51.0 ± 9.6% of baseline during DA 1, and a second application of dopamine alone after a 60-minute wash (DA 2) induced a depression of fEPSPs that was similar in magnitude. Synaptic responses were suppressed to 53.03 ± 7.8% of baseline during the second application (compared to 51.0 ± 9.6% during DA 1) indicating that receptors were no longer desensitised 60 minutes after initial exposure to barbadin (see **Figure 4.3B$_1$**). Data for each 30-minute application of dopamine (DA 1 and DA 2) were renormalised and superimposed to further highlight and quantify the effect on transmission (see **Figure 4.2B$_2$**). The peak depression of fEPSPs induced during each application of dopamine was compared (see **Figure 4.2B$_3$**), and the results indicate that dopamine's impact on synaptic transmission had retained its full potency during DA 2 when β-arrestin activity was blocked during DA 1 (t_8 =0.164, P = 0.874, n = 5). Taken together, these data suggest that high-to-moderate concentrations of dopamine (1000 or 100 µM) applied for 10 (up to 30) minutes are sufficient to trigger GRK2- and β-arrestin-dependent internalisation of metabotropic receptors. It is possible that the desensitisation is expressed by the

internalisation of D_2-like dopaminergic receptors (see **Figure 3.12C**) that are located on sensory afferent terminals (see **Figure 3.8** and **Figure 3.9**) that terminate in layer I of the lateral entorhinal cortex.

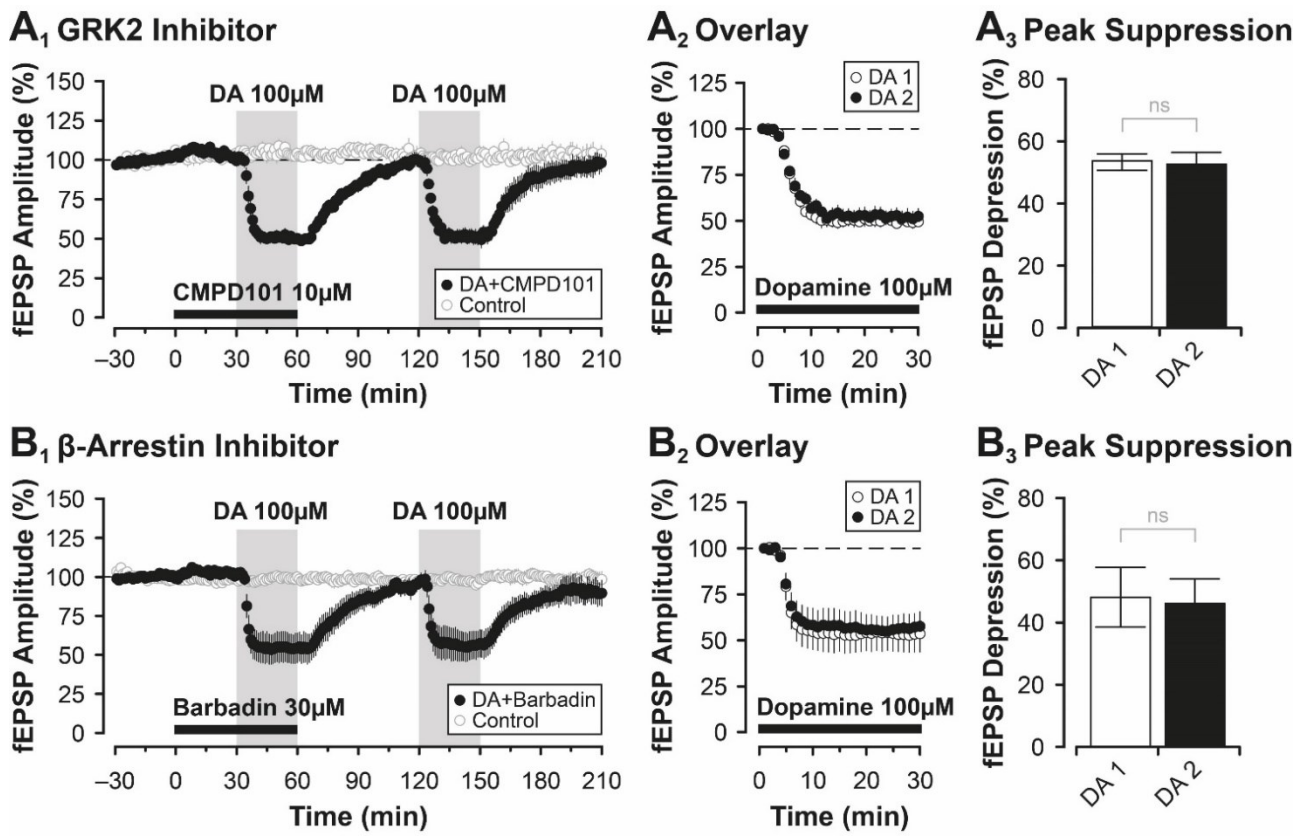

Figure 4.3. The desensitisation depends on GRK- and β-arrestin-mediated endocytosis of metabotropic receptors*. (**A1**) Pre- and co-application of the GRK inhibitor, CMPD101 (DA+CMPD101, black circles), with dopamine during the initial application prevents the desensitisation of dopamine receptors when dopamine is applied again on its own 60-minutes later. (**A2**) Overlay of dopamine applications and (**A3**) quantification of the mean peak amplitude of the fEPSP depression comparing the first (DA 1, open circles) and second (DA 2, open circles) dopamine applications. (**B1**) Pre- and co-application of the β-arrestin inhibitor, barbadin (DA+Barbadin, black circles), with dopamine during the initial application also prevents the desensitisation of dopamine receptors when dopamine is applied on its own a second time 60-minutes later. (**B2-B3**) Conventions are the same as **A2** to **A3**, but for an initial co-application of dopamine with barbadin (**B1**).*

Discussion

There is currently only sparse data available on the signalling properties of dopaminergic receptors in the superficial layers of the lateral entorhinal cortex. The presence of dopamine-rich fibres in the entorhinal cortex has been known for decades (Lindvall *et al.*, 1974; Swanson, 1982), including the laminar distribution of different dopamine receptor subtypes within the region (Köhler, Ericson and Radesäter, 1991), but little has been done to investigate how these receptors signal to modulate basal synaptic function in the superficial layers. One of the primary objectives for experiments in this chapter was to uncover the properties of dopamine-mediated desensitisation in the lateral entorhinal cortex, including the underlying mechanisms. Results of this chapter show that dopaminergic receptors in the lateral entorhinal cortex can be desensitised using several different experimental protocols that involve exposing slices to moderate or high concentrations of dopamine once or multiple times for different durations. For instance, desensitisation is evident *during* application of a high 1000 µM concentration of dopamine (**Figure 4.1A**), following *repeated short applications* of a more modest 100 µM concentration (**Figure 4.1B**), or after exposure to a *single* 100 µM concentration *for at least 30-minutes* (**Figure 4.2A$_2$**). Results also confirm that the desensitisation is not simply an artefact related to the passage of time (**Figure 4.1D$_1$**). Interestingly, the desensitisation is long-lasting and persists for at least 60 minutes (**Figure 4.3A$_2$**) and is reversible within 3 hours (**Figure 4.2B$_1$**). Experiments were also performed to uncover the mechanisms underlying the desensitisation, and experimental data from this chapter highlights how the desensitisation of metabotropic receptors is expressed via a mechanism involving the internalisation of the receptors themselves. Removal of dopamine-binding receptors from neuronal membranes *reduces* the overall magnitude of any dopamine-dependent modulation of synaptic transmission induced in the lateral entorhinal cortex. Exposure to moderate or high concentrations of dopamine recruits specific G-protein-coupled receptor kinases, GRK2/3, since blocking it with a selective inhibitor (CMPD101) prevents desensitisation (**Figure 4.3A$_1$**). Additionally, the desensitisation relies on β-arrestin, since inhibiting the formation of β-arrestin-AP2 complexes required for receptor internalisation prevents the dopamine-mediated desensitisation (**Figure 4.3B$_1$**). Taken together, these findings expand on the data collected as part of Chapter 3 and indicate that dopamine not only has potent and suppressive effects on synaptic function in the lateral entorhinal cortex, but that it also elicits persistent changes in the *availability* of dopamine-binding receptors that is dependent on past exposure to the agonist. Changes in metabotropic receptor availability will likely affect how dopamine regulates synaptic function in the lateral entorhinal cortex.

Desensitisation of metabotropic receptors is a phenomenon observed widely throughout the brain and spinal cord. It plays a key role in discriminating between qualitatively different forms of stimuli that converge at single physical location (Hao and Delmas, 2010) and is instrumental in shaping neuronal output. For example, desensitisation of D_2 receptors in the ventral tegmental area has been shown to shape firing properties of dopaminergic projection neurons, and this has dramatic effects on dopamine release in downstream targets, including the lateral entorhinal cortex (Al-Hasani *et al*., 2011). Desensitisation of dopamine-binding receptors in the lateral entorhinal cortex has not been shown previously in any published report. It is well-known that G-protein coupled receptors desensitise and internalise in response to strong stimulation, so the fact that

metabotropic receptors in the lateral entorhinal cortex, all of which are GPCRs, have the ability to desensitise is not surprising (Kim *et al.*, 2004; Al-Hasani *et al.*, 2011; Sander *et al.*, 2016). It is possible that the desensitisation is expressed by the internalisation of D_2-like dopaminergic receptors located on sensory afferent terminals that make synaptic contact with superficial layer projection neurons whose dendrites are known to ramify in layer I (Steward, 1976; Krettek and Price, 1977; Köhler, 1988; Köhler, Ericson and Radesäter, 1991; Insausti, Herrero and Witter, 1997). Activation of D_2 receptors on these terminals triggers a reduction in glutamate release and a depression in the amplitude of synaptic responses recorded in the superficial layers. However, exposing these receptors to dopamine and causing them to internalise reduces the overall magnitude of the dopamine-mediated depression of synaptic responses because the inhibitory constraint on glutamate release provided by D_2 receptors has been removed. And once the receptors are internalised, the suppressive effects of dopamine on synaptic transmission are blunted for at least one hour, perhaps longer (Williams *et al.*, 2013; Sander *et al.*, 2016). It is interesting to speculate, then, that this desensitisation may represent a novel form of *metaplasticity* in the entorhinal cortex whereby these receptors 'remember' any recent encounter they have had with dopamine. Changes in dopaminergic tone fluctuate based on many factors, and these changes in tone can either be tonic or phasic (Grace, 1991). It is likely that extracellular levels of dopamine in the lateral entorhinal cortex ebb and flow depending on intrinsic and extrinsic factors affecting behavioural state (see Caruana *et al*., 2006). As such, *previous* fluctuations in dopaminergic tone have the potential to dramatically constrain *future* regulatory functions of dopamine in the entorhinal cortex. This is something that will be explored in more detail in Chapters 5 and 6 of this thesis.

In addition to demonstrating that dopaminergic receptors desensitise in the lateral entorhinal cortex, the results of this chapter also highlight the mechanisms through which the effect is expressed. Although dopamine binds to every subtype of dopamine receptor in the brain (D_1 through to D_5), the expression of the different dopamine receptor subtypes varies dramatically across cortical layer in the entorhinal cortex (Köhler, Ericson and Radesäter, 1991). This is further complicated by the fact that different dopamine receptor subtypes also have different affinities for dopamine, with D_1 receptors expressing a low affinity for dopamine when compared to D_2 receptors (for review see Subramaniyan and Dani, 2015). It has been established previously that *both* D_1-like *and* D_2-like dopaminergic receptors can be desensitised and that GRKs and other regulatory proteins, including β-arrestin, play a key role (Tiberi *et al.*, 1996; Iwata *et al.*, 1999; Kim *et al.*, 2001). Despite this, a desensitisation of dopaminergic receptors has never been described before in the entorhinal cortex, including in the lateral division. This chapter confirms that the dopamine-mediated desensitisation of metabotropic receptors is due to the removal of these receptors from the membrane via a clathrin-mediated mechanism, similar to what has been shown previously in other brain regions (Beautrait *et al.*, 2017). This effect in the lateral entorhinal cortex is dependent on activation of GRK2/3, as well as β-arrestin. Specifically, the receptors may become internalised following phosphorylation of the GPCR complex via clathrin-mediated endocytosis (see **Figure 4.4**). As discussed, multiple dopamine receptor subtypes are present in layer II of the lateral entorhinal cortex, including D_1 and D_2 receptors (Köhler, Ericson and Radesäter, 1991). Despite both being linked to GRKs, it is possible that the these kinases may be linked to different downstream signalling cascades

and not specifically those responsible for receptor internalisation (for a review see Beaulieu and Gainetdinov, 2011). GRK2, for example, has been shown to mediate the internalisation of *both* D_1 (Tiberi *et al.*, 1996) *and* D_2 (Iwata *et al.*, 1999; Kim *et al.*, 2001) receptors, but, Tiberi *et al.* (1996) have shown that D_1 receptors can also associate with GRK2, GRK3 or GRK5, with each kinase isoform participating in a different signalling cascade. In the current study, desensitisation is linked *specifically* to GRK2/3, since the selective inhibitor for GRK2/3, CMPD101, blocked the effect. It is also dependent on receptor internalisation involving β-arrestin-AP2 interactions since the selective β-arrestin inhibitor, barbadin, prevented receptor internalisation and desensitisation. It is unclear, though, which metabotropic receptor is the one that is being internalised. Data from Chapter 3 would suggest that D_2 receptors are a potential target, but D_1 receptors as well as multiple other dopamine-binding receptors are also expressed in principal neurons in the lateral entorhinal cortex and are involved in modulating synaptic function (see **Table 2.1**; Caruana *et al*., 2006; Glovaci, Caruana and Chapman, 2014).

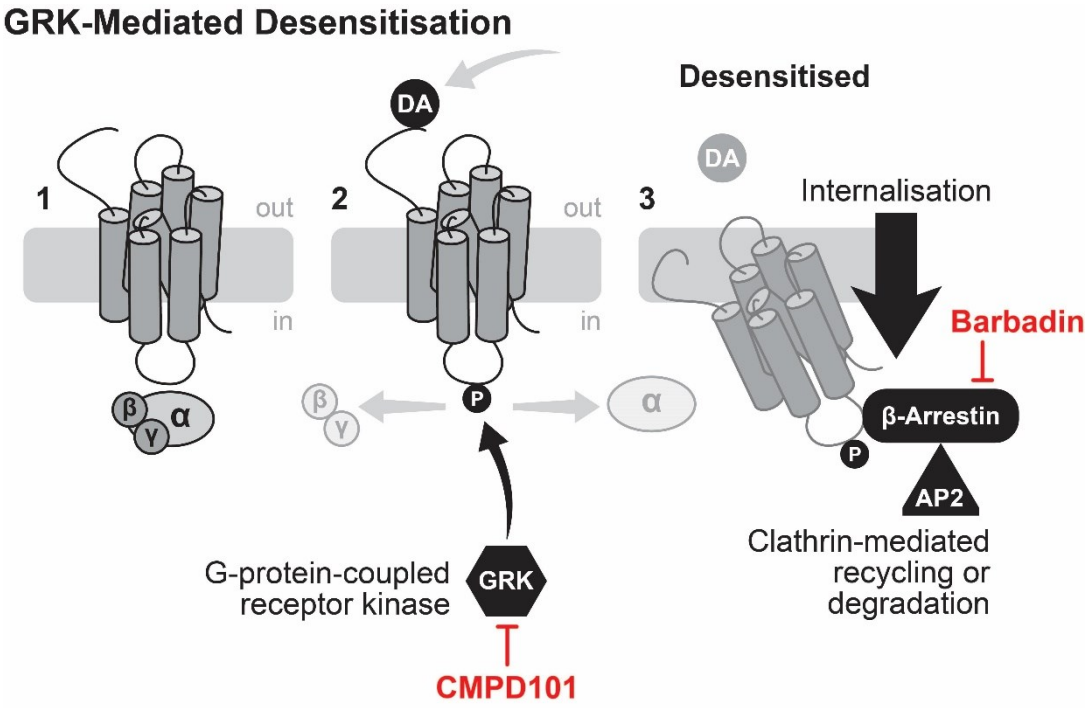

Figure 4.4. Schematic diagram for suggested mechanism of metabotropic receptor internalisation via the GRK- and clathrin-mediated pathways. *(**1**) Inactive receptor with attached G-protein becomes activated with agonists such as dopamine (DA), if too much agonist is accumulated at the synapse, (**2**) phosphorylation of the receptor via a GRK-mediated mechanism occurs, this can be blocked using GRK inhibitor, compound 101 (CMPD101) to prevent receptor desensitisation. (**3**) Following phosphorylation of the receptor, clathrin-mediated internalisation is undergone to remove the receptor from the synapse. This can be prevented using β-arrestin blocker, barbadin. Schematic diagram based on Del'Guidice et al., 2011.*

Chapter 5: Dopaminergic Modulation of LTD in the Lateral Entorhinal Cortex

Introduction

The results of previous chapters have demonstrated the potent suppressive effects of dopamine on basal synaptic function in the lateral entorhinal cortex, with peak suppressive effects occurring at a concentration of 100 µM (see **Figure 3.4A$_1$**). The suppression may be linked to a D_2 receptor-mediated reduction in glutamate release from sensory afferents that synapse with superficial layer projection neurons (see **Figure 3.8B** and **Figure 3.9A$_2$** and **Figure 3.12C$_1$**). Bath-application of an even higher 1000 µM concentration of dopamine unmasked – in real time – the innate capacity for dopamine receptors in the lateral entorhinal cortex to desensitise in response to intense activation by an agonist (see **Figure 3.4A$_1$**). Despite the continued presence of dopamine in the bathing medium, the magnitude of the effect progressively weakened the longer the agonist was applied. Further characterisation of the desensitisation showed that lower concentrations of dopamine (100 µM) were also sufficient to induce the effect (see **Figure 4.2A**), and that it was both long-lasting and reversible (see **Figure 4.2A-B**). The mechanisms underlying the expression of the desensitisation were also determined highlighting key roles for both GRK2 and β-arrestin in mediating receptor internalisation via clathrin-dependent endocytosis (see **Figure 4.3** and **Figure 4.4**). Indeed, previous literature has emphasised the importance of GRK2 in the internalisation of D_1 (Tiberi *et al.*, 1996), and in some cases D_2 (Iwata *et al.*, 1999; Kim *et al.*, 2001), receptor subtypes, but this is the first report to highlight these mechanisms in the entorhinal cortex. Yet, despite a greater understanding of how dopamine can modulate synaptic transmission, it remains largely unknown how changes in dopaminergic tone contribute to the overall sensory and mnemonic functions of the lateral entorhinal cortex. The traditional view has been that dopamine plays a significant role in dampening transmission of some sensory signals from the entorhinal cortex to the hippocampus whilst actively promoting transmission of others (Caruana *et al*., 2006). Indeed, superficial layer neurons transmit sensory information to multiple targets within the hippocampus (see **Figure 1.2**) (Deshmukh and Knierim, 2011; Tsao, Moser and Moser, 2013; Igarashi *et al.*, 2014; Basu *et al.*, 2016; Tsao *et al.*, 2018; Lee *et al.*, 2021), and dopamine may be a key regulator involved in filtering and directing the propagation of these signals to specific sites within the hippocampus (by contributing to the so-called 'gatekeeper' functions of the entorhinal cortex). In addition, activity dependent forms of synaptic plasticity are thought to play an important role in the integration of multimodal sensory signals within the superficial layers of the entorhinal cortex prior to being relayed to the hippocampus. Many different neuromodulators have been shown to regulate both the induction and expression of synaptic plasticity across many different brain regions (Otani *et al.*, 1998; Costenla *et al.*, 2001; Seamans and Yang, 2004; Vianna *et al.*, 2005; Matsuda, Marzo and Otani, 2006; Caruana *et al.*, 2007; Fink *et al.*, 2007; Mockett *et al.*, 2007), but very little is known about how dopamine may affect activity-dependent plasticity in the entorhinal cortex. Given how

potent dopamine is in suppressing basal synaptic function, it is certainly well poised to have dramatic effects on lasting forms of plasticity in sensory inputs to the superficial layers.

Multiple forms of activity-dependent plasticity are expressed at synapses in the brain, most notably long-term synaptic depression (LTD) and long-term synaptic potentiation (LTP). Increases in synaptic efficacy are a key mechanism thought to underlie memory storage in the brain whereas decreases in efficacy are thought to underlie the removal of unnecessary associations (for review see Bassi *et al*., 2019). In this chapter, the role of dopamine in modulating the induction of activity-dependent LTD in sensory inputs to the superficial layers of the lateral entorhinal cortex was explored. LTD is induced by delivering repetitive low frequency stimulation to afferent inputs over many minutes and has been observed in numerous brain regions. Interestingly, the capacity to induce LTD can vary significantly between synapse types (for review see Citri and Malenka, 2008). Both LTD and LTP have been studied extensively in the hippocampus, specifically at Schaffer collateral synapses with area CA1 (Bliss and Gardner-Medwin, 1973; Bliss and Lomo, 1973; Bliss, Lancaster and Wheal, 1983; Dudek and Bear, 1992). LTD in area CA1 of the hippocampus can be triggered by activation of mGluRs (Dudek and Bear, 1992) leading to the subsequent influx of calcium ions into the postsynaptic cell. The signalling cascade for NMDA receptor-dependent LTD is triggered by a relatively small increase in postsynaptic calcium (Dudek and Bear, 1992) sufficient to activate protein phosphatases (such as calcineurin; PP2b, and protein phosphatase 1; PP1) that dephosphorylate regulatory domains of specific AMPA receptor subunits (Lee *et al.*, 2002; Kourrich *et al.*, 2008; for review see Malenka, 1994; Malinow and Malenka, 2002). Dephosphorylation of key domains, in some instances, can downregulate the kinetic properties of existing membrane-bound AMPA receptors to reduce their functioning or lead to the internalisation and removal of the entire receptor complex from the synaptic membrane (Lee *et al*., 2002; for review see Malenka, 1994; Malinow and Malenka, 2002). As a result, there will be fewer fully functional AMPA receptors to carry depolarising current into the postsynaptic cell leading to an overall reduction in the efficacy of transmission at the synapse.

An important factor to consider when investigating LTD in vitro is the age of the brain being studied (Collingridge et al., 2010). In the present study, rats aged between postnatal days 14 and 21 were used. Research by Lee et al. (2005) on aging in male Long-Evans rats, specifically in relation to spatial behaviour and activity in Schaffer collateral synapses onto CA1 neurons in the stratum radiatum, suggests that young (6-month-old) rats exhibit NMDA receptor-dependent LTD, whereas 'aged' rats (24 months old) shift to non-NMDA receptor-dependent forms. Further work by Rajani et al. (2021) has indicated a developmental shift from NMDA receptor-dependent LTD to L-type calcium channel-dependent LTD when examining synaptic transmission in the piriform cortex of neonatal (1–2 weeks), young adult (2–3 months), and aged (20–25 months) Sprague Dawley rats. Additionally, Cheong et al. (2002) demonstrated that young (4–6-week-old) male Sprague Dawley rats exhibit only NMDA receptor-dependent LTD in both the superficial and deep layers of the medial entorhinal cortex (layers II–III and V, respectively), as blocking NMDA receptors with D-AP5 prevents LTD expression. Together, these findings suggest that NMDA receptor-dependent LTD is more prominent in younger rats (Cheong et al., 2002; Lee et al., 2005; Rajani et al., 2021).

In the entorhinal cortex, activity-dependent changes in synaptic efficacy in sensory inputs to the superficial layers may play a role in the integration and encoding of multimodal sensory representation within entorhinal cortex networks. As a result, any persistent change in the efficacy of transmission at these synapses would be expected to impact the near- to long-term propagation of specific sensory signals to the hippocampus. There are few published reports on synaptic plasticity in the entorhinal cortex. Induction of NMDA receptor-dependent LTD has been observed in both the medial division (Kourrich and Chapman, 2003; Deng and Lei, 2007) and the lateral division (Caruana *et al*., 2007), but the role of modulatory neurotransmitters, including dopamine, on regulating LTD induction and expression in the entorhinal cortex remains largely unknown. However, in a study by Caruana *et al.* (2007) rats with chronically implanted electrodes were pretreated with the selective dopamine reuptake inhibitor, GBR-12909 (10 mg/kg), just prior to the delivery of paired-pulse low frequency stimulation to induce LTD. The results showed that elevating extracellular dopaminergic tone in the entorhinal cortex *in vivo* with GBR12909 was sufficient to block induction of LTD in olfactory sensory inputs to the superficial layers of the lateral entorhinal cortex. Not only could dopamine affect synaptic plasticity in the lateral entorhinal cortex, the block of LTD was viewed as a potential mechanism responsible for shifting the encoding of sensory signals from the entorhinal cortex to the hippocampus (Caruana *et al.*, 2007).

As discussed previously, dopaminergic fibres from the VTA innervate the lateral entorhinal cortex (Fallon, Koziell and Moore, 1978; Oades and Halliday, 1987; Erickson, Sesack and Lewis, 2000; Harvey, 2020)(see **Figure 1.5**) and dopaminergic receptors (both D_1- and D_2-like receptors) are expressed in the superficial layers (Köhler, Ericson and Radesäter, 1991). As such, changes in dopaminergic tone in the lateral entorhinal cortex may play a significant role in modulating the induction and expression of LTD in the superficial layers (see Caruana *et al*., 2007). The main objective of this chapter was to further explore the role of dopamine in modulating activity-dependent LTD in sensory afferents to the superficial layers *in vitro*. Any influence of dopamine on LTD in the lateral entorhinal cortex may affect a number of key functions, including: (1) integration of signals from cortical sensory regions innervating the lateral entorhinal cortex; (2) crosstalk between deep and superficial layer feedback networks; and (3) propagation of sensory signals to various targets in the hippocampus involved in encoding an array of non-spatial sensory signals (Deshmukh and Knierim, 2011; Tsao, Moser and Moser, 2013; Igarashi *et al.*, 2014; Basu *et al.*, 2016; Tsao *et al.*, 2018; Lee *et al.*, 2021).

Materials and Methods

Electrophysiology and Pharmacology

For all field recording experiments, slices from male (95%) and female (5%) Wistar rats aged P14-21 were rested in warmed and oxygenated ACSF for at least 60 minutes after slicing just prior to experimental testing. Following the rest period, slices were transferred to the recording chamber and a bipolar stimulating electrode and glass recording electrode were placed carefully in the superficial layers of the lateral entorhinal cortex (stimulating electrode positioned to span the layer I-II border; recording electrode positioned along the layer I border with layer II; see Figure 3.3A) and responses were elicited once every 20s. Control experiments were interleaved throughout all experimental testing, and each treatment condition had its own time-matched control data to compare to. To induce LTD, 900 pairs of stimulation pulses with a 30 msec interpulse interval were delivered at a frequency of 1 Hz over 15-minutes (PP-LFS). For experiments using dopamine hydrochloride, solutions were always made fresh when required and co-administered with the antioxidant, sodium metabisulfite, to prevent degradation of dopamine in the light- and oxygen-rich environment.

Standard experiments to induce LTD in sensory inputs to the superficial layers of the lateral entorhinal cortex typical began following a 30-minute baseline period of stable fEPSP recordings, and WinLTP was used to toggle and control the delivery of the PP-LFS protocol during an experiment. Note: the stimulation intensity always remained unchanged (intensity set to evoke fEPSPs at 75% max amplitude) during delivery of the induction protocol. Following induction, the amplitude of fEPSPs in response to single test pulses was monitored once more for 60 minutes. To determine whether induction of LTD in the lateral entorhinal cortex was dependent on activation of NMDARs, the competitive NMDAR antagonist, AP5 (10 µM), was applied alone for 15-minutes and then during the 15-minute PP-LFS-induction protocol. A series of experiments were then conducted to assess whether dopamine-mediated synaptic depression and activity-dependent LTD were co-expressed at the same population of synapses. During these experiments, either activity-dependent LTD was induced first followed 60-minutes later by bath-application of 100 µM dopamine, and vice versa. Parameters for each form of synaptic depression were then analysed and compared to experimental conditions where these protocols were induced on their own. In one experiment, the ability to induce dopamine-mediated desensitisation of metabotropic receptors was assessed following induction of activity-dependent LTD at the same synapses. For this experiment, LTD was induced using the standard PP-LFS protocol. After 60-minutes, dopamine (100 µM) was bath-applied initially for 30-minutes followed by a second application of dopamine 60 minutes later. The magnitude of the dopamine-mediated suppression of fEPSPs was then compared during each application period (DA 1 versus DA 2).

To determine whether dopamine might act synergistically with activity-dependent and glutamate-mediated forms of synaptic depression to *enhance* LTD induction in the lateral entorhinal cortex, dopamine was bath-applied at a 30 µM concentration alone for 15-minutes and then together with delivery of PP-LFS to induce LTD for another 15-minutes. The amplitude of responses was then assessed for a further 60-minutes of follow-up recordings. A 30 µM concentration of dopamine was selected for use during these experiments to ensure that the maximal suppression of fEPSPs was not induced by dopamine to allow PP-LFS to potentially *augment*

the dopamine-mediated depression even further. This same experiment was then repeated, but only after dopamine receptors had been desensitised first. To accomplish this, the pairing of dopamine together with PP-LFS (as outlined above) was performed *60-minutes after* an initial application of 100 µM dopamine for 30-minutes to desensitise dopaminergic receptors. The desensitisation experiment was repeated once more, but this time with the initial desensitisation of dopaminergic receptors blocked using barbadin (30 µM).

Data Analysis

The effects of bath-applied drugs during pharmacological experiments were assessed on the amplitude of averaged synaptic responses (fEPSPs) obtained during 5- or 10-min epochs recorded at different times during an experiment (latencies specified below). In some instances, the peak change in synaptic efficacy was used, and this was determined manually for each individual experiment as the latency varied. Non-linear regression and curve fitting, when required, was performed using Prism and compared using sum-of-squares F-tests. The LTD induced on its own and together with dopamine was compared during the 15-minute induction period using the averaged peak amplitude values against time-matched control data. To track the onset of LTD in the amplitude of evoked synaptic responses during the PP-LFS protocol, the amplitude of the first stimulation pulse of each pair was averaged every minute and plotted over the 15-minute induction period. Paired-pulse ratios were calculated for each of the 900 pairs of stimulation pulses used to induce LTD, averaged every minute, and plotted. The slope of a regression line fit through each point during the 15-minute induction period assessed whether the paired-pulse ratio remained unchanged during induction. All data were expressed as the mean ± SEM and were normalised to the baseline period for plotting. Drug-induced changes in response properties were assessed with Prism using (where appropriate) paired or unpaired samples t-tests, one-way ANOVAs or repeated measures ANOVAs. Post-hoc comparisons were made using the Bonferroni method with an alpha level of $P < 0.05$.

Results

Multiple Forms of Synaptic Depression are Co-Expressed at the Same Synapses

Bath-application of 100 µM dopamine on its own induced a suppression of synaptic transmission in sensory inputs to the superficial layers (see **Figure 5.1A$_1$**). At its peak, responses were depressed significantly to 44.9 ± 6.3% of baseline by dopamine relative to untreated controls (t_{15} = 10.22, P < 0.0001, dopamine n = 7, control n = 10; **Figure 5.1A$_2$**). To assess whether activity-dependent LTD could be induced in the lateral entorhinal *in vitro*, a paired-pulse low frequency stimulation (PP-LFS) protocol was tested. Delivery of 900 pairs of stimulation pulses with an IPI of 30-msec at a frequency of 1 Hz for 15 minutes was sufficient to induce LTD in sensory inputs to the superficial layers (see **Figure 5.1B$_1$**). Synaptic responses were depressed significantly to 80.7 ± 4.9% of baseline during the last 5-minutes of the experiment compared to time-matched and unstimulated controls that remained stable at 104.8 ± 3.2% of baseline (t_{14} = 4.257, P < 0.001, LTD n = 6, control n = 10; **Figure 5.1B$_2$**).

To determine whether the same network of synapses in the lateral entorhinal cortex support both forms of synaptic depression described above, the dopamine-mediated suppression of fEPSPs was induced first followed by activity-dependent LTD one hour later. As shown in **Figure 5.1C$_1$**, bath application of 100 µM dopamine induced a suppression of fEPSPs that returned to baseline levels within around 20-minutes of washout. Following a 60-minute washout period, PP-LFS was delivered. Responses were depressed significantly to 85.3 ± 3.7% of baseline levels during the last 5-minutes of the experiment relative to controls (102.8 ± 3.1% of baseline, t_{13} = 3.632, P < 0.01, treated n = 7, control n = 8; **Figure 5.1C$_2$**), and this depression was comparable to the depression induced by PP-LFS on its own (80.7 ± 4.9% versus 85.3 ± 3.7%). These results indicate that although synapses were exposed to dopamine initially to temporarily depress transmission and to, presumably, induce desensitisation of dopamine-binding receptors, this had no effect on the capacity for these same synapses to support induction of glutamate- or metabotropic-mediated and activity-dependent LTD.

Next, the reverse experiment was conducted in which LTD was induced first prior to bath-application of dopamine. As shown in **Figure 5.1D$_1$**, PP-LFS induced LTD in sensory inputs to the superficial layers of the lateral entorhinal cortex. Subsequent bath-application of 100 µM dopamine after a 75-min follow-up period also depressed synaptic responses, though responses recovered to the same depressed level triggered by PP-LFS during the initial induction of LTD (to 78.3 ± 5.1% of baseline relative to time matched controls) when assessed at 86- to 90-minutes post-induction. Following the subsequent application and washout of dopamine, responses returned to a depressed level of 71.8 ± 9.0% of baseline during the last 5-minutes of the experiment (176- to 180-minutes), and this did not differ significantly from the initial depression induced by PP-LFS ($F_{1, 16}$ = 0.898, P = 0.357, treated n = 10, control n = 8; **Figure 5.1D$_2$**). Once activity-dependent LTD had been induced and a new baseline level set, the amplitude of fEPSPs returned to this level even after subsequent exposure to dopamine.

The time course and magnitude of the dopamine-mediated suppression of synaptic responses was compared between experiments. Data for the 30-min period prior to and during bath-application of 100 µM dopamine for data shown in **Figure 5.1A$_1$** and data from **Figure 5.1D$_1$** were renormalised and superimposed (see **Figure 5.1E$_1$**). The onset and time course of the dopamine-mediated suppression of fEPSPs were both similar

and there was no significant difference in the magnitude of the peak suppression induced by dopamine regardless of whether dopamine was applied alone or after LTD. Dopamine significantly reduced the amplitude of fEPSPs to 45.4 ± 7.2% of baseline when delivered alone and to 33.7 ± 5.1% when delivered after ($F_{2, 21}$ = 40.00, P < 0.001; control v DA before LTD, Bonferroni P < 0.0001; control v DA after LTD, Bonferroni P < 0.0001), but there was no difference in the overall magnitude of the suppression induced by dopamine regardless of when it was applied (Bonferroni P = 0.410; **Figure 5.1E$_2$**). In addition, dopamine-mediated desensitisation of metabotropic receptors was also evident during an experiment in which dopamine was applied twice to slices following induction of activity-dependent LTD. As shown in **Figure 5.1F$_1$**, PP-LFS induced LTD in sensory inputs to the superficial layers of the lateral entorhinal cortex. Once the LTD had stabilised after 75-minutes, dopamine (100 µM) was applied twice to the slices with a 60-minute wash in between each application. As before, responses returned to the new baseline level following each successive washout of dopamine. But critically, the magnitude of the fEPSP depression induced by dopamine during the second application (DA 2) was significantly smaller than it was during the first application (DA 1), and this indicates that the initial exposure to dopamine (during DA 1) was sufficient to desensitise dopamine-binding receptors. Synaptic responses evoked during each 30-minute exposure to dopamine were renormalised and superimposed in **Figure 5.1F$_2$** to better visualise the desensitisation effect. Taken together, these results demonstrate that multiple forms of synaptic depression are supported at sensory synapses in the superficial layers of the lateral entorhinal cortex. These forms of synaptic depression are mediated by different mechanisms, and so long as they are induced separately at different times during the same experiment, their effects are mutually exclusive.

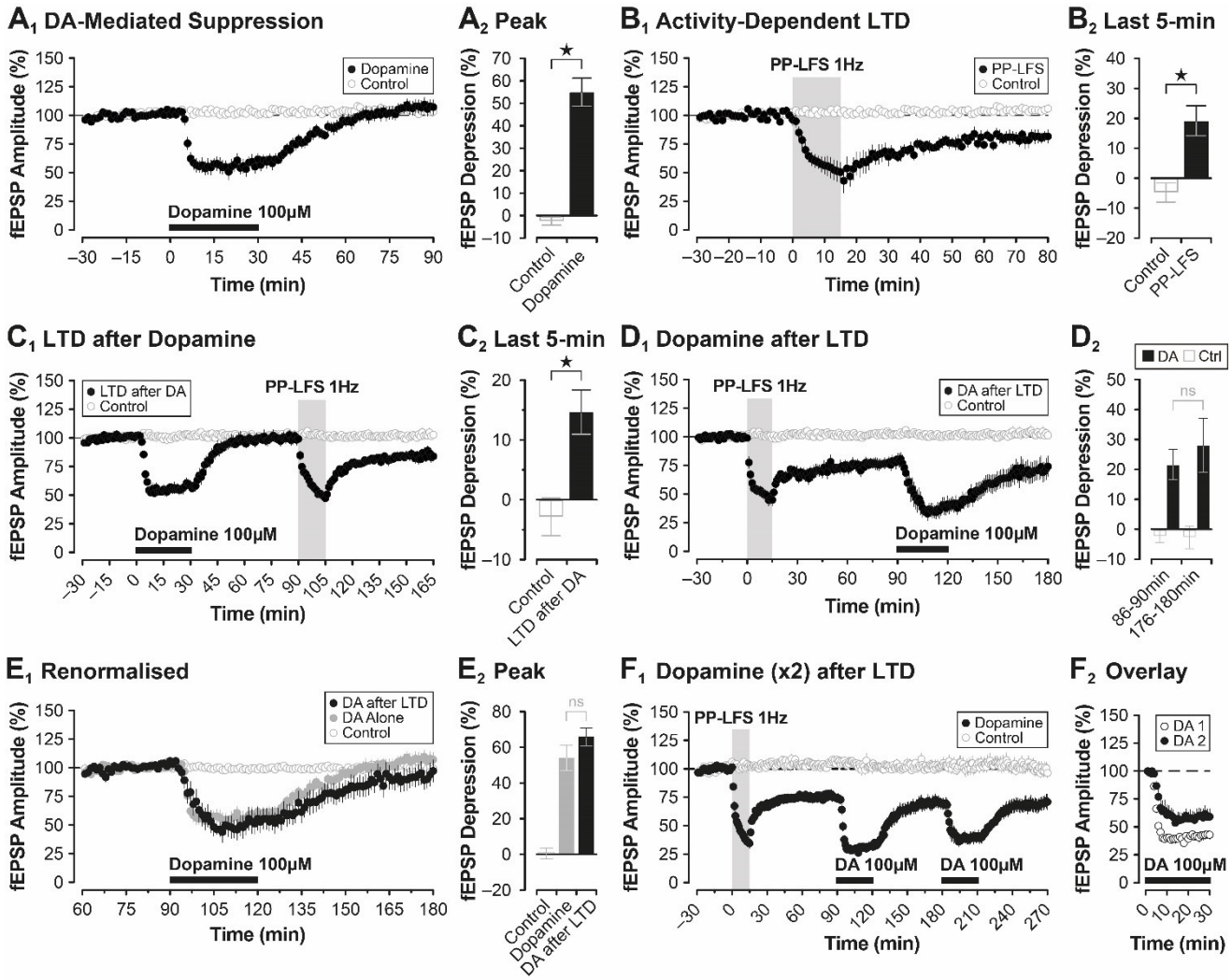

Figure 5.1. Multiple forms of synaptic depression are expressed at the same synapses in the lateral entorhinal cortex. *(**A₁**) A single applications of 100 µM dopamine has suppressive and reversible effects (filled circles) on fEPSP amplitude compared to untreated controls (open circles). (**A₂**) Quantification of the peak fEPSP depression induced by dopamine relative to controls. (**B₁**) Paired-pulse low-frequency stimulation (PP-LFS; filled circles) induces activity-dependent LTD in sensory inputs to the superficial layers of the lateral entorhinal cortex. (**B₂**) A bar plot comparing the depression of fEPSPs during the last 5-minutes of the experiment (from **B₁**) in slices that received PP-LFS (filled bar) relative to controls (open bar). (**C₁**) Previous exposure to dopamine (100 µM) does not influence the magnitude of LTD induced by PP-LFS (filled circles) when compared to untreated controls (open circles). (**C₂**) Following similar conventions as those in **B₂**, the magnitude of the LTD induced by PP-LFS during the last 5-minutes of the experiment (from **C₁**) in treated (filled bar) and untreated (open bar) slices was compared. (**D₁**) Bath-application of 100 µM dopamine followed 75-minutes after stabilisation of activity-dependent LTD. (**D₂**) Summary bar plot comparing mean fEPSP peak depression before (86-90min) and after (176-180min) dopamine application (filled bars). Following exposure to dopamine, responses return to the newly depressed baseline induced earlier by PP-LFS. (**E₁**) The depression in the amplitude of fEPSPs induced by dopamine for experiments shown in **A₁** and **D₁** were renormalised to the 30-minute period prior to dopamine application and superimposed to highlight similarities in the dopamine-mediated suppression of fEPSPs when dopamine is applied alone (DA Alone; grey circles) or after LTD was induced (DA after LTD; black circles). The onset and time course of the dopamine effect are very similar. (**E₂**) Summary bar plot comparing the mean peak depression of fEPSPs induced by dopamine alone (from **A₁**) and dopamine following PP-LFS (+105 min from **E₁**) relative to untreated controls. The magnitude of the depression is the same in both conditions. (**F₁**) A similar experiment to **D₁**, but with a second application of dopamine to confirm whether the dopamine-mediated desensitisation of metabotropic receptors is also present at these synapses. (**F₂**) Data for each 30-minute application of dopamine (DA 1 versus DA 2) are shown renormalised and superimposed to highlight the desensitisation effect.*

As demonstrated above, sensory inputs to the superficial layers of the lateral entorhinal cortex support induction of activity-dependent LTD (see **Figure 5.1B$_1$**). Indeed, a robust and long-lasting depression in the amplitude of synaptic responses was induced following delivery of PP-LFS to sensory afferents. However, it is unknown whether activity-dependent and glutamate-mediated forms of synaptic plasticity are modulated by dopamine in the lateral entorhinal cortex. During initial control experiments, delivery of PP-LFS to sensory inputs induced LTD in sensory inputs to the superficial layers (**Figure 5.2A$_2$**). Responses were depressed significantly to 83.9 ± 3.0% of baseline relative to time-matched 110-minute controls without PP-LFS (104.8 ± 3.2% of baseline; t_{21} = 4.697, P < 0.0001, LTD n = 13, control n = 10; **Figure 5.2A$_3$**). However, pairing application of dopamine together with delivery of PP-LFS *occluded* induction of LTD in the lateral entorhinal cortex (**Figure 5.2B$_2$**). A 30 µM concentration of dopamine was selected for use during these experiments to ensure that the maximal suppression of fEPSPs was not induced by dopamine to allow PP-LFS to potentially augment the dopamine-mediated depression even further. Indeed, application of 30 µM dopamine depressed the amplitude of fEPSPs during the first 15-minutes, but although fEPSPs continued to depress during PP-LFS, responses returned to baseline levels within 30 minutes of washout. During the last 5-minutes of the experiment, the average amplitude of fEPSPs was 96.6 ± 4.0% of baseline in slices that received the combined dopamine and PP-LFS treatment, and this did not differ significantly from controls (104.8 ± 3.2% of baseline; t_{16} = 1.619, P = 0.125, treated n = 8, control n = 10; **Figure 5.2B$_3$**). As such, dopamine did not enhance LTD in the lateral entorhinal cortex but instead prevented it, likely by reducing the probability of glutamate release following dopamine exposure. To confirm that induction of activity-dependent LTD in the lateral entorhinal cortex was dependent on activation of NMDA receptors, PP-LFS was delivered to sensory afferents in the presence of AP5 (10 µM). As observed in other brain regions, including area CA1 of the hippocampus, induction of activity-dependent LTD in the lateral entorhinal cortex was dependent on activation of NMDA receptors since delivery of PP-LFS in the presence of AP5 blocked induction of LTD (**Figure 5.2C**), despite PP-LFS being originally developed for mGluR-dependent LTD induction (Dudek and Bear, 1992). During the last 5-minutes of the experiment, synaptic responses were 103.9 ± 3.2% of baseline levels in slices that received the combined AP5 and PP-LFS treatment, and this did not differ significantly from controls (105.4 ± 3.3% of baseline; t_{17} = 0.321, P = 0.752, AP5 n = 8, control n = 11; **Figure 5.2C** inset). Importantly, this does not rule out the possibility that mGluR-dependent LTD is also activated during the PP-LFS protocol. Further investigation is needed to confirm this definitively.

To determine the mechanisms underlying the dopamine-mediated block of activity-dependent LTD in the lateral entorhinal cortex, the onset of LTD was assessed during the 15-minute induction period for both the control experiments to induce LTD (data from **Figure 5.2A$_2$**) and for the experiments where LTD was induced in the presence of dopamine (data from **Figure 5.2B$_2$**). The amplitude of the first response for each pulse pair delivered during PP-LFS was averaged every minute during the 15-minute induction period. Data were renormalised to the first minute and plotted, and curves fit through the averaged data points were compared. As shown in **Figure 5.2D$_1$**, although the amplitude of fEPSPs depressed progressively with each passing minute of induction for both groups, the depression was greater for controls (as LTD was induced) than it was for dopamine-treated slices, and curves fit through the data points (using a third order polynomial for best fit)

differed significantly for each group ($F_{4,157}$ = 9.347, P < 0.0001). These results suggest that synapses were responding in *qualitatively* different ways during induction for each experimental condition and that dopamine had somehow reduced the potency of the PP-LFS to induce LTD in the lateral entorhinal cortex. To explore this further, paired-pulse ratios were calculated for each of the 900 pairs of stimulation pulses used to induce LTD. These ratios were then averaged for every minute of induction, renormalised to the first minute, and plotted. As shown in **Figure 5.2D$_3$**, paired pulse ratios changed significantly over the course of the 15-minute induction period for control experiments. Specifically, at the start of induction, synapses showed paired-pulse inhibition (see also **Figure 3.8** and **Figure 3.9**), but by the end they had switched to showing paired-pulse facilitation. A regression line fit through the averaged ratio data during induction deviated significantly from zero (P < 0.001) highlighting this transition. In contrast, dopamine-treated slices showed paired-pulse facilitation throughout the entire induction period, and the magnitude of this facilitation remained unchanged as there was no deviation in the slope of a regression line fit through the averaged ratio data. The persistent paired-pulse facilitation observed in the dopamine-treated slices likely reflects a dopamine-mediated change in the release probability of glutamate from sensory afferent terminals that terminate in layer I (see **Figure 3.8** and **Figure 3.9**). A dopamine-mediated reduction in glutamate release during the induction period likely resulted in insufficient activation of postsynaptic NMDA receptors (the reduced 'potency' during induction mentioned above) required to induce LTD in the lateral entorhinal cortex. As a result, induction of LTD was blocked when PP-LFS was delivered in the presence of dopamine (see **Figure 5.2B$_2$**).

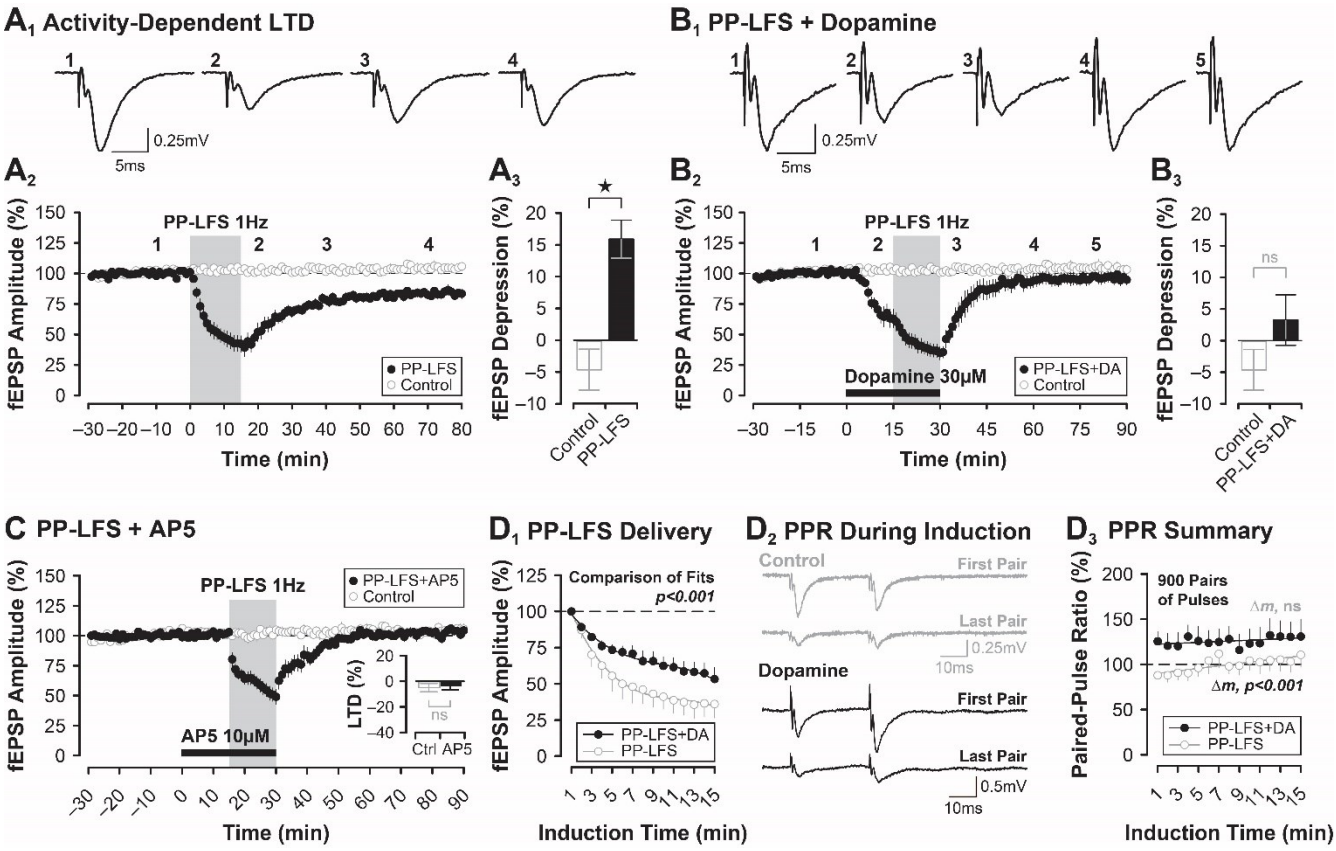

Figure 5.2. Bath-application of dopamine during PP-LFS blocks induction of LTD in the lateral entorhinal cortex*. (**A₁**) Representative fEPSP traces recorded before, during and after paired-pulse low-frequency stimulation (PP-LFS)* to induce LTD*. Numbered traces in **A₁** correspond to numbers in **A₂** highlighting the specific times during the experiment when the sample traces were recorded. (**A₂**) The change in amplitude of fEPSPs during and after PP-LFS shows the successful induction of LTD (filled circles) relative to time-matched and unstimulated controls (open circles). (**A₃**) Summary bar plot highlighting the magnitude of the LTD during the last 5-minutes of the experiment compared to controls. (**B₁**) Similar conventions as in **A₁** but for corresponding numbers in **B₂**. (**B₂**) Application of 30 μM dopamine during PP-LFS (PP-LFS+DA; filled circles) occludes LTD in the lateral entorhinal cortex relative to controls (open circles). (**B₃**) The magnitude of the LTD in treated slices was compared to controls during the last 5-min of the experiment (from B₂). (**C**) Application of the NMDA receptor antagonist, AP5 (10 μM) during PP-LFS blocks LTD. Inset in **C** highlights the block of LTD relative to controls during the last 5-minutes of the experiment. (**D₁**) The amplitude of the first response for each pulse pair delivered during PP-LFS was averaged each minute during the 15-minute induction period, renormalised, and compared. Curves fit through the data points indicate that the onset of LTD differs significantly in slices treated with dopamine during PP-LFS. (**D₂**) Sample sweeps showing paired stimulation at the start of the PP-LFS protocol and at the end. Paired-pulse inhibition is observed, initially, during control experiments to induce LTD, whereas paired stimulation shows paired-pulse facilitation in slices treated with dopamine. (**D₃**) Paired-pulse ratios were calculated for each of the 900 pairs of stimulation pulses used to induce LTD. These ratios are shown averaged for every minute of induction and renormalised to the first minute. Dopamine-treated slices (filled circles) show consistent paired-pulse facilitation throughout the entire induction period, whilst in controls, initial paired-pulse inhibition switches to paired-pulse facilitation by the end of the 15-minute induction period (open circles). The slope of a regression line deviated significantly from zero highlighting this transition.*

Desensitisation of Dopaminergic Receptors Rescues LTD in the Lateral Entorhinal Cortex

Delivering PP-LFS to sensory inputs in the presence of dopamine blocks induction of LTD in the superficial layers of the lateral entorhinal cortex (see **Figure 5.3A**). This block most likely reflects a dopamine-mediated reduction in glutamate release from presynaptic terminals during PP-LFS leading to sub-threshold activation of NMDARs to induce LTD. To test whether it is possible to *reverse* the dopamine-mediated inhibition of LTD, experiments were conducted to desensitise dopaminergic receptors first before delivering PP-LFS together with

dopamine. If dopaminergic receptors were desensitised, then enough glutamate should be released during PP-LFS to activate NMDA receptors and induce LTD. In the desensitised state, the presence of dopamine during PP-LFS was expected to have little impact on release probability due to there being fewer membrane-bound metabotropic receptors for the dopamine to bind to. To desensitise dopamine-binding receptors, dopamine (100 µM) was bath-applied on its own for 30-minutes followed by a 60-minute wash in normal ACSF. Based on results from previous experiments (see **Figure 4.2A$_2$** and **Figure 5.1F$_1$**), this treatment was expected to desensitise dopamine-binding receptors in the lateral entorhinal cortex. Next, dopamine was applied again for 30-minutes (at a lower 30 µM concentration) and PP-LFS was delivered 15-minutes into this second application of dopamine. Recordings continued for another 60-minutes in normal ACSF. As shown in **Figure 5.3B$_1$**, an initial bath-application of 100 µM dopamine was sufficient to desensitise dopamine-binding receptors and restore LTD in the lateral entorhinal cortex despite the presence of dopamine during the induction protocol. In **Figure 5.3B$_2$**, data were renormalised to the last 30-min of the initial washout just prior to delivery of PP-LFS with dopamine and superimposed with data from the previous pairing experiment for comparison (data from **Figure 5.3A**). Responses were depressed significantly to 84.77 ± 4.7% of baseline during the last 5-minutes of the experiment relative to time-matched and untreated controls (103.8 ± 3.8% of baseline; $F_{2, 20} = 5.178$, $P < 0.05$, Bonferroni $P < 0.05$, DA before LTD n = 6, control n = 9; **Figure 5.3B$_2$** inset) indicating that LTD had been induced. To confirm that dopaminergic receptors had been desensitised, the magnitude of the fEPSP depression induced by 30 µM dopamine just prior to the delivery of PP-LFS was compared for the desensitised and non-desensitised LTD experiments. Responses during the first 15-minutes of dopamine application were renormalised and superimposed for comparison. As shown in **Figure 5.3C$_1$**, the magnitude of the dopamine-mediated suppression of synaptic transmission was attenuated in slices exposed previously to dopamine. The peak suppression in the amplitude of fEPSPs induced by 30 µM dopamine did not differ significantly from controls in desensitised slices but did differ significantly in non-desensitised slices ($F_{2, 21} = 13.66$, $P < 0.001$, Bonferroni $P < 0.0001$; **Figure 5.3C$_2$**). These data indicate that the block of LTD induction in the lateral entorhinal cortex mediated by dopamine can be removed if dopamine receptors are desensitised first before delivering PP-LFS together with the agonist.

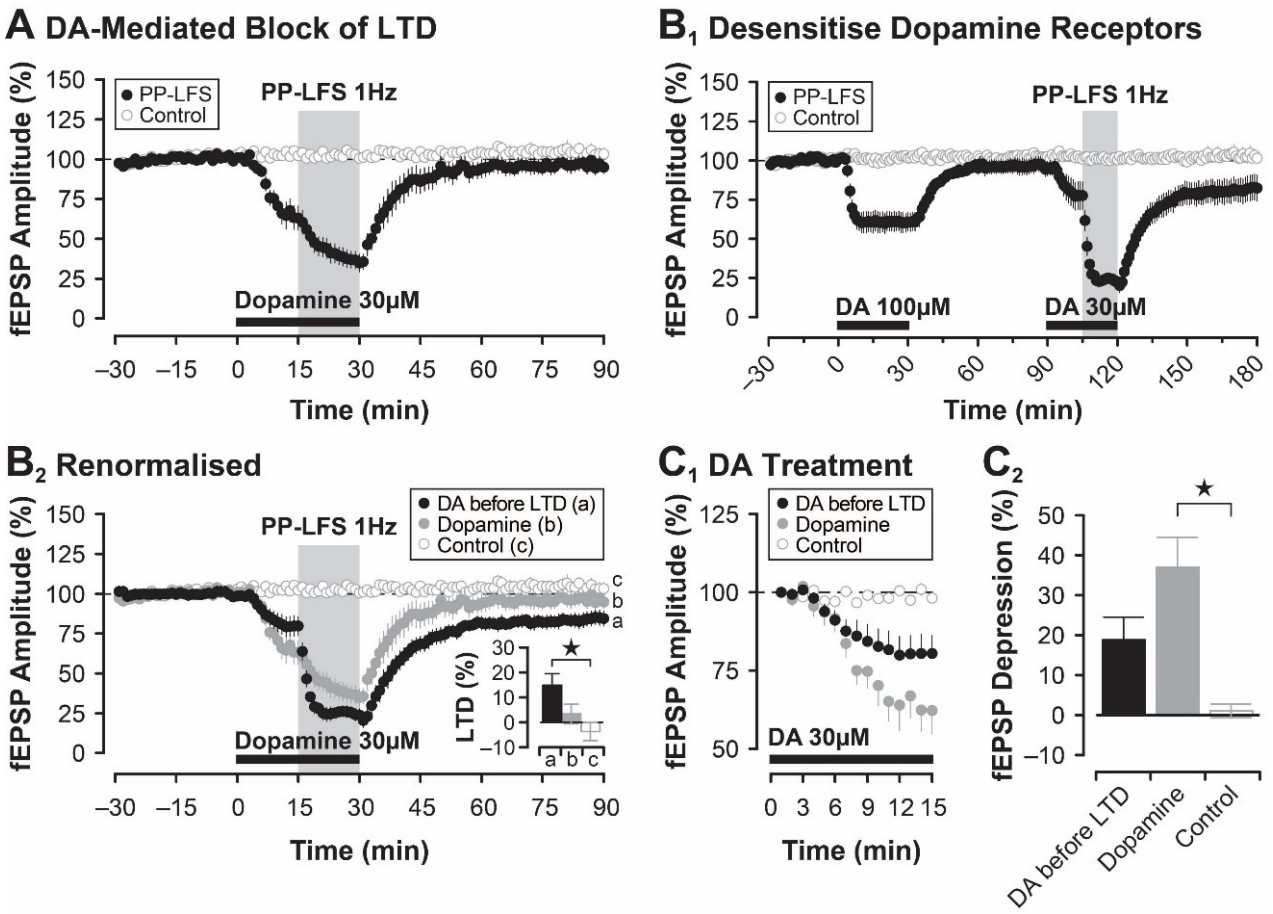

Figure 5.3. Desensitising metabotropic receptors restores LTD in the lateral entorhinal cortex despite the presence of dopamine during PP-LFS. *(**A**) Application of 30 μM dopamine during PP-LFS (PP-LFS; filled circles) blocks induction of LTD in the lateral entorhinal cortex relative to controls (open circles). (**B_1**) An initial bath-application of 100 μM dopamine to desensitise dopamine-binding receptors restores activity-dependent LTD in the lateral entorhinal cortex regardless of whether dopamine (30 μM) is applied during PP-LFS (filled circles). (**B_2**) Data from **B_1** are renormalised to the last 30-min of the initial washout just prior to delivery of PP-LFS with dopamine (a) and superimposed with data from the previous experiment shown in **A** for comparison (b). Bar plot shown in the inset highlights the significant depression in the amplitude of fEPSPs relative to controls in the desensitised slices. (**C_1**) Responses during the first 15-minutes of the dopamine application applied during PP-LFS are shown renormalised and superimposed for comparison. (**C_2**) Summary bar plot showing the peak fEPSP suppression induced by 30 μM dopamine prior to the induction of PP-LFS during each experimental condition.*

If desensitising dopamine-binding receptors in the lateral entorhinal cortex is *permissive* in allowing LTD induction despite the presence of dopamine during PP-LFS, then blocking the desensitisation effect should reinstate the capacity for dopamine to *prevent* induction of LTD. To test this, the β-arrestin inhibitor, barbadin (30 μM), was co-applied during the initial desensitising application of 100 μM dopamine. As shown previously (**Figure 4.3B_1**), this pairing successfully blocked the dopamine-mediated desensitisation of dopamine-binding receptors in the lateral entorhinal cortex. With this metabotropic receptor desensitisation blocked, the subsequent pairing of 30 μM dopamine with PP-LFS should prevent induction of LTD (as shown in **Figure 5.2B_2** and **Figure 5.3A**). Indeed, this is precisely what was observed. The full experimental timeline is shown in **Figure 5.4A**, though, there was some run-down present in averaged responses by the end of the experiment. As such, responses were renormalised to the 30-min period just prior to the second dopamine application and delivery of PP-LFS. Following this renormalisation, it is evident that blocking desensitisation of metabotropic receptors reinstates the capacity for dopamine to inhibit induction of LTD when paired with PP-LFS (**Figure 5.4B_1**). During

the last 5-minutes of the experiment, the average amplitude of fEPSPs was 96.1 ± 4.2% of baseline in slices that received the combined dopamine and PP-LFS treatment, and this did not differ significantly from time-matched controls (89.9 ± 4.5% of baseline; $F_{1, 12}$ = 1.866, P = 0.197, treated n = 8, control n = 8; **Figure 5.4B$_2$**). As such, preventing the desensitisation of metabotropic receptors with barbadin keeps slices at more 'naïve' state whereby dopamine retains its full capacity to modulate activity-dependent plasticity by constraining glutamate release during PP-LFS.

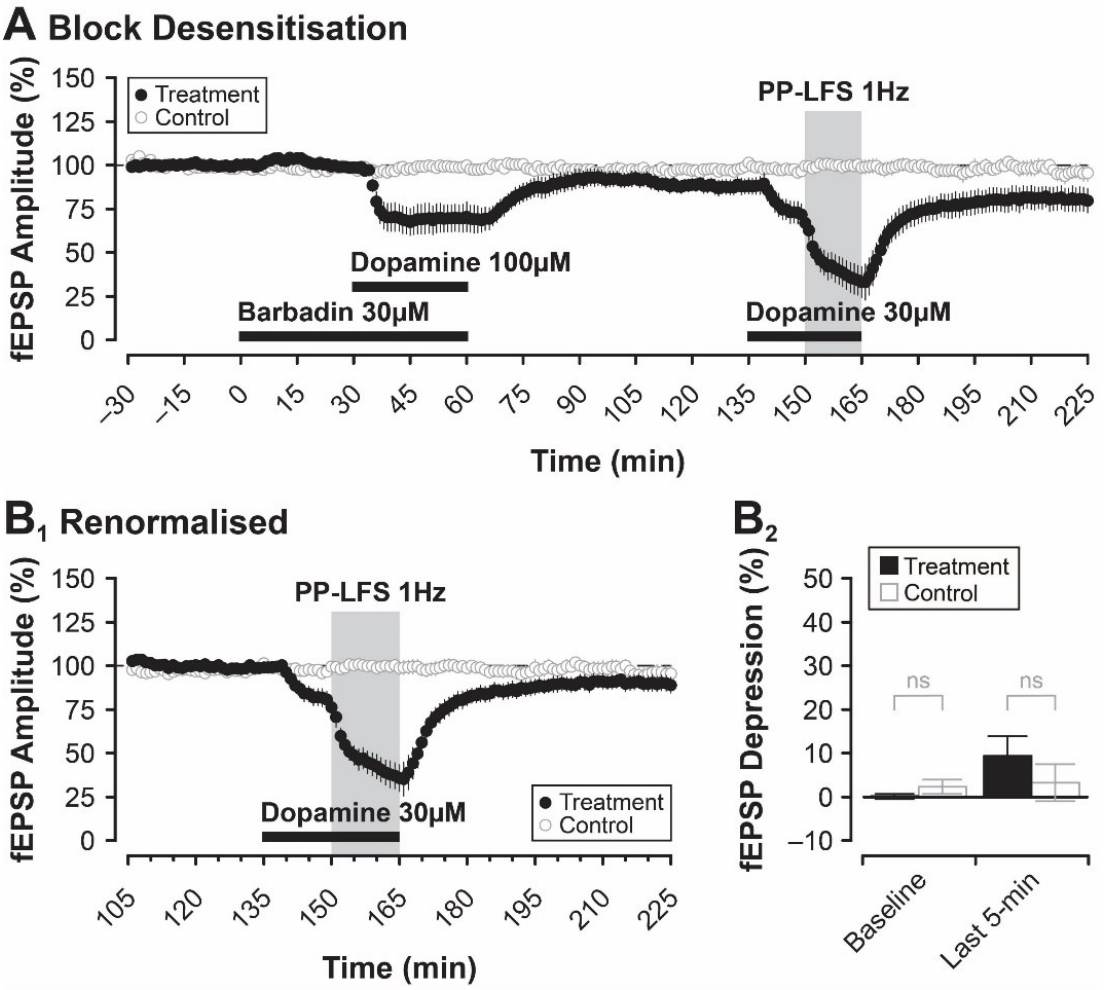

Figure 5.4. The dopamine-mediated block of LTD is restored when the initial desensitisation of metabotropic receptors is blocked by barbadin. *(**A**) The β-arrestin inhibitor, barbadin, blocks desensitisation metabotropic receptors during the initial 30-minute application of 100 µM dopamine. As such, the capacity for dopamine to block induction of LTD when applied during PP-LFS is restored. (**B$_1$**) To better visualise the restoration of the dopamine-mediated block of LTD, responses during the last 2-hours of the experiment from **A** are shown renormalised. (**B$_2$**) Summary bar plot highlighting averaged data during the last 5-minutes of the baseline (Baseline; +105 min) and last 5-minutes of the experiment comparing the depression in fEPSP amplitude in treated (filled bars) and untreated (open bars) conditions shown in **B$_1$**.*

A more in-depth view of how dopamine is mediating the expression of PP-LFS is to consider changes in paired pulse ratios during the induction period. As shown in **Figure 5.2D**, during the induction of PP-LFS alone the paired pulse ratio shifts from a paired pulse depression to a paired pulse facilitation (slope > 0, P < 0.001), whereas in the presence of dopamine, the paired pulse ratio is already elevated to paired pulse facilitation at the onset of PP-LFS with no significant change in slope, and thus preventing the induction and expression of PP-

LFS (see **Figure 5.5A$_2$**). As previously mentioned, if dopamine is applied 30-min prior to a second co-application of dopamine with PP-LFS, LTD is re-instated (see **Figure 5.3B**). Interestingly, although desensitising receptors with dopamine restores the ability for PP-LFS to induce plasticity (see **Figure 5.5B$_1$**), it does not restore the paired pulse ratio to that of paired pulse depression as seen in controls (see **Figure 5.5B$_2$**). In fact, a regression line fitted through the paired pulse ratios shows the slope is significantly different from zero and follows a negative trajectory (Y =2.072X + 164.6, $P < 0.0001$; see **Figure 5.5B$_2$,** filled circles). This could imply the changes in paired pulse ratios may be dependent on dopamine affecting change via an alternative pathway, for example, altering the activity of inhibitory responses to a elicit a block of LTD. Analysis of PP-LFS induction following the experiment shown in **Figure 5.4B$_1$** (see **Figure 5.5C**) shows that by preventing the internalisation of G-protein receptors with barbadin (30 µM), dopamine is able to once more block PP-LFS induced LTD. Paired pulse analysis of the 15-minute window of induction shows a similar pattern of activity here with the regression line fit through the averaged data deviated significantly from zero (Y = -0.1149X + 152.9, $P = 0.5383$; **Figure 5.5C$_2$,** filled circles) to that seen in dopamine experiments with unaltered G-protein sensitivity (**Figure 5.5A$_2$**, filled circles).

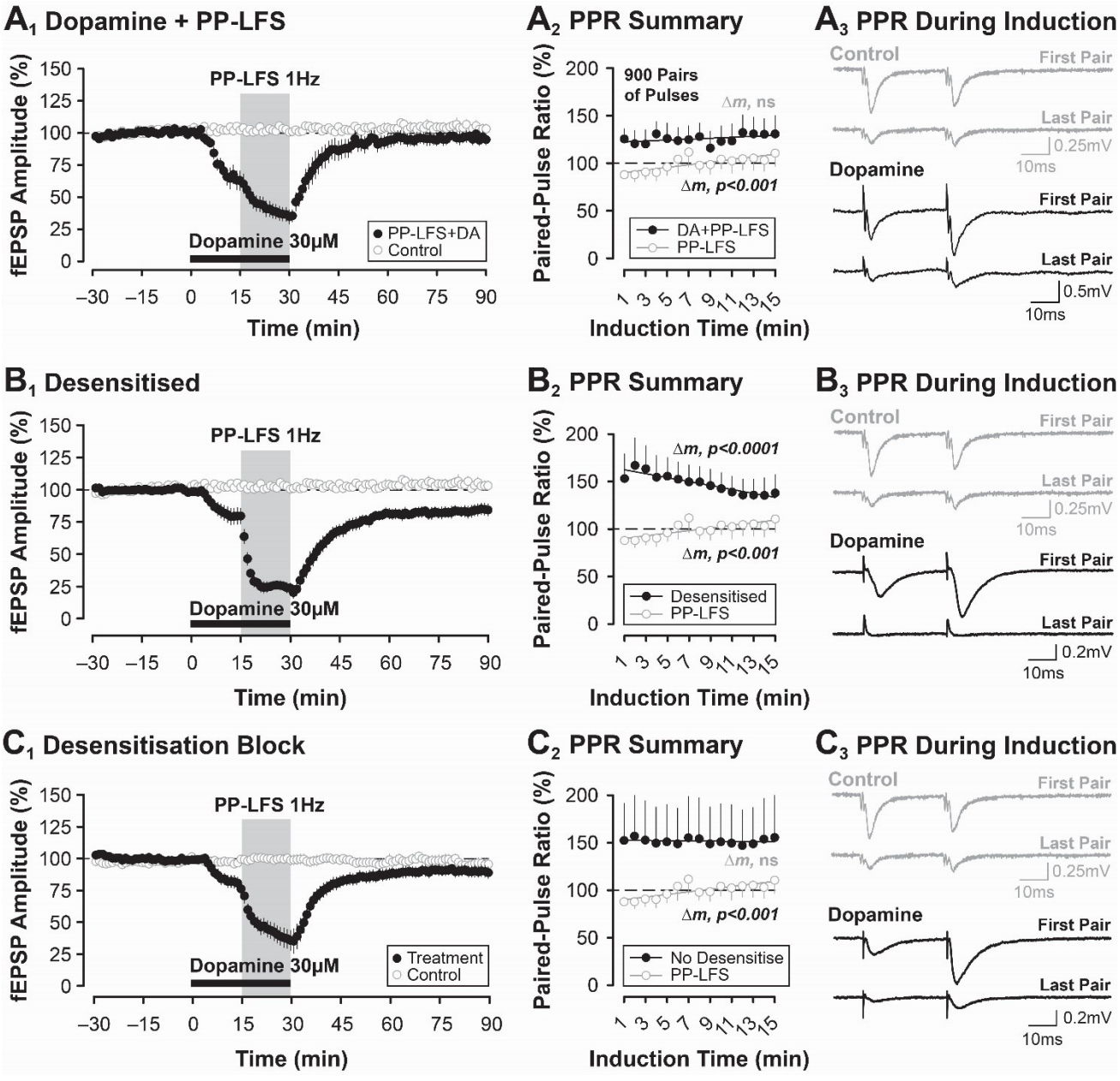

***Figure 5.5. Paired-pulse ratios are modulated by dopamine regardless of whether metabotropic receptors are desensitised**. (**A_1**) Application of 30 μM dopamine during PP-LFS (DA+PP-LFS; filled circles) blocks induction of LTD in the lateral entorhinal cortex relative to controls (open circles; Data from **Figure 5.3A**). (**A_2**) Paired-pulse ratios were calculated for each of the 900 pairs of stimulation pulses used to induce LTD and are shown averaged for every minute of induction. Dopamine-treated slices (filled circles) show consistent paired-pulse facilitation throughout the entire induction period, whilst in controls, initial paired-pulse inhibition switches to paired-pulse facilitation by the end of the 15-minute induction period (open circles). The slope of a regression line deviated significantly from zero ($P < 0.001$) highlighting this transition. (**A_3**) Sample sweeps showing paired stimulation at the start of the PP-LFS protocol and at the end. Paired-pulse inhibition is observed, initially, during control experiments to induce LTD, whereas paired stimulation shows paired-pulse facilitation in slices treated with dopamine. (**B_1**) An initial application of dopamine (100 μM) was used to desensitise metabotropic receptors, and this reinstated activity-dependent LTD in slices when PP-LFS was delivered together with a second bath-application of 30 μM dopamine (data from **Figure 5.3B_2**). (**B_2**) Interestingly, despite the desensitisation of metabotropic receptors, paired-pulse ratios did not return to basal levels. There was still notable paired-pulse facilitation observed throughout the induction period that reduced significantly throughout the course of induction (filled circles, the slope of a regression line fit through the averaged data deviated significantly from zero, $P < 0.0001$). (**B_3**) The presence of this enhanced paired-pulse facilitation is observed in sweeps taken at the start and at the end of the induction period. (**C_1**) Blocking metabotropic receptor desensitisation with barbadin (30 μM) reinstated the capacity for dopamine to block activity-dependent LTD in the lateral entorhinal cortex (data from **Figure 5.4B_1**). (**C_2**) Paired-pulse facilitation is observed throughout the induction period similar to what is shown in **A_2**, and is observed at the start and the end of the induction period (see sample sweeps in **C_3**).*

Discussion

Despite the wealth of knowledge available on activity-dependent forms of synaptic plasticity in the medial division of the entorhinal cortex (Alonso, de Curtis and Llinas, 1990; Kourrich and Chapman, 2003; Hargreaves *et al.*, 2005; Deng and Lei, 2007; Iwase, Kitanishi and Mizuseki, 2020), comparatively little is known about plasticity in the neighbouring lateral division (but see Caruana *et al*., 2007). Activity-dependent LTD of synaptic transmission is observed in numerous brain regions, including area CA1 of the hippocampus (Dudek and Bear, 1992; Collitti-Klausnitzer *et al.*, 2021), the ventral tegmental area (for review see Gerdeman *et al*., 2003) and the prefrontal cortex (Burette, Jay and Laroche, 1997; Herry, Vouimba and Garcia, 1999; Takita *et al.*, 1999; Jay, 2003), and LTD is thought to be a key physiological mechanism underlying some of the mnemonic functions of these structures (Takita *et al.*, 1999; Jay, 2003; Basu *et al.*, 2016). Moreover, modulatory neurotransmitters are known to play a critical role in regulating plasticity in these regions. In particular, the effects of dopamine on the induction and/or expression of LTD have been linked most reliably to activation of the D_1 receptor in both the prefrontal cortex (Otani *et al.*, 1998) and area CA1 of the hippocampus (Mockett *et al.*, 2007), but little is known about the contributions of different dopaminergic receptor subtypes in modulating plasticity in the superficial layers of the lateral entorhinal cortex (but see Caruana *et al*., 2007). This is surprising, given that it has been known for decades that a major branch of the mesocortical dopaminergic system innervates the lateral division (Fuxe, 1965; Lindvall *et al.*, 1974; Swanson, 1982). Thus, a major goal of this experimental chapter was to uncover links between dopamine and activity-dependent LTD in the lateral entorhinal cortex. To achieve this, a combination of both pharmacological and electrophysiological methods was applied. Results of this chapter show that LTD is readily induced in sensory afferents to the superficial layers by repetitive paired-pulse low frequency stimulation (see **Figure 5.1B_1**). This is the first report to demonstrate glutamate-mediated and NMDA receptor-dependent LTD (using a PP-LFS protocol found to induce mGluR-dependent LTD in area CA1 by Dudek and Bear (1992)) in the lateral entorhinal cortex *in vitro*, and remaining experimental work in the chapter was designed to investigate the properties of this plasticity further, especially in relation to the modulatory effects of dopamine on induction.

Multiple forms of synaptic depression are expressed in sensory inputs to the superficial layers of the lateral entorhinal cortex. In addition to the dopamine-mediated depression of synaptic transmission characterised in Chapter 3 (see **Figures 3.4** and **Figure 3.5**), these synapses also support glutamate-mediated and activity dependent LTD (see **Figure 5.1**). Each form of synaptic plasticity can be induced individually in separate experiments or co-expressed together, one before the other, in an additive but separate manner during the same experiment (see **Figure 5.1**). This is mainly because each form of synaptic depression likely involves completely different induction and expression mechanisms, so when induced in a temporally discrete way they do not influence one another. However, these forms of plasticity can interact when induced at the same time. Indeed, application of dopamine during PP-LFS blocks induction of glutamate-mediated LTD (see **Figure 5.2**), and this is consistent with findings from a previous study by Caruana *et al.* (2007) performed *in vivo*. This block most likely reflects a dopamine-mediated reduction in glutamate release from presynaptic terminals during PP-LFS leading to sub-threshold activation of NMDA receptors to induce LTD (see **Figure 5.2**). A detailed analysis of responses during the 15-minute induction period shows that, at the start of induction, paired-pulse depression is observed in control experiments when PP-LFS is delivered in the absence of any dopamine (see **Figure 5.2D**). This suggests that sensory inputs to the lateral entorhinal cortex typically form high release probability synapses with superficial layer projection neurons (for review see Thomson, 2000) and that large amounts of glutamate are released to activate postsynaptic AMPA and NMDA receptors. The subsequent influx of calcium ions into the postsynaptic neurons and activation of key protein phosphatases is critical for the induction of LTD. However, when dopamine is present during delivery of the PP-LFS protocol, the release probability of glutamate is reduced and paired-pulse facilitation is observed at these synapses (see **Figure 5.2D** & **5.5A**). This dopamine-mediated reduction in glutamate release likely results in insufficient activation of postsynaptic AMPA and NMDA receptors required for induction of LTD. Interestingly, it was possible to reverse the dopamine-mediated block of LTD by desensitising dopamine-binding receptors first before delivering PP-LFS together with dopamine (see **Figure 5.3**). With these metabotropic receptors desensitised, the presence of dopamine during PP-LFS still caused responses to elicit elevated paired pulse facilitation during the induction of PP-LFS, despite the successful expression of LTD that followed (see **Figure 5.5B**). This may be indicative of an alternative pathway, for example, perhaps involving inhibition. . Finally, blocking the desensitisation by preventing internalisation of metabotropic receptors with barbadin restored the capacity for dopamine to block induction of activity dependent LTD in the lateral entorhinal cortex (see **Figure 5.4**) and restored the paired pulse ratio during PP-LFS induction to that of baseline dopamine and PP-LFS experiments (see **Figure 5.5C**).

The properties of activity-dependent LTD expressed in the superficial layers of the lateral entorhinal cortex are similar to those observed previously in the neighbouring medial entorhinal cortex (Kourrich and Chapman, 2003; Kourrich *et al.*, 2008; Vandrey *et al.*, 2022). Using a similar PP-LFS protocol, a comparatively modest LTD was induced in sensory inputs to the superficial layers of the medial entorhinal cortex *in vitro* (Kourrich and Chapman, 2003). It is interesting to note that successful induction of LTD in the medial entorhinal cortex required significantly more experimental intervention to induce than in the lateral division. To induce LTD in the medial entorhinal cortex, local $GABA_A$ receptor-mediated inhibition had to be blocked first with bicuculine

(50 µM) prior to delivery of PP-LFS (at 0.5 Hz as opposed to the 1 Hz used here)(Kourrich and Chapman, 2003). Although induction of LTD in the medial entorhinal cortex was dependent on activation of NMDA receptors (induction was blocked with AP5), it also required significant afferent drive to induce. Specifically, stimulation intensity had to be increased temporarily during PP-LFS to overcome local inhibition in the medial division. Interestingly, there was a direct correlation between the stimulation intensity used during induction and the magnitude of the LTD induced (Kourrich and Chapman, 2003). Further experimental work by Kourrich and Chapman (2003) into the properties of LTD on the medial entorhinal cortex showed that applying the group I/II metabotropic glutamate (mGlu) receptor antagonist E4-CPG (500 µM) had no effect on the induction or expression of LTD, suggesting that group I/II mGlu receptors are not responsible for modulating PP-LFS-induced LTD in the medial division of the entorhinal cortex (Kourrich and Chapman, 2003). These findings by Kourrich and Chapman (2003) show that the properties of LTD in the medial division of the entorhinal cortex are different to those of the lateral division. It is important to note, however, that direct comparisons between studies are confounded somewhat due to differences in the rat species (Long Evans versus Wistar), age of the animals (P35 versus P14-21), recording methods (interface versus submerged) and recording temperatures (room temperature versus 32°C) used in the Kourrich and Chapman (2003) study relative to the current study. Additionally, while the use of the NMDA receptor antagonist AP5 (10 µM) blocked PP-LFS-induced LTD, suggesting NMDA receptor involvement, this study did not examine the role of mGluRs in PP-LFS-induced LTD. This remains an important consideration for further investigation.

One of the more interesting results to come from experimental work performed in this chapter is the finding that pre-exposure to dopamine can eliminate the modulatory effects of the agonist on LTD induction in the lateral entorhinal cortex. Specifically, the previous history these synapses have with dopamine can have dramatic effects on the induction and expression of future plasticity in the region. As noted in Chapter 4, extracellular dopaminergic tone fluctuates depending on the behavioural state of the animal (Hutter and Chapman, 2013; for review see Beaulieu, Espinoza and Gainetdinov, 2015), and any event that causes a sudden surge in dopamine release in the lateral entorhinal cortex has the potential to shape future encoding or integration of sensory signals entering the superficial layers. Although dopamine-mediated desensitisation of metabotropic receptors can be induced with 100 µM dopamine applied for variable amounts of time (see **Figure 4.1** and **Figure 4.2**), it is impossible to know whether behaviourally relevant events cause similar increases in dopaminergic tone within the lateral entorhinal cortex to saturate superficial layer synapses in a similar manner. Previously, it has been observed that the basal level of extracellular dopamine in the lateral entorhinal cortex measured using *in vivo* microdialysis was about 0.4 pg/10 µL (Caruana *et al*., 2006). Although the concentration of dopamine in dialysate (around 0.21 to 0.51 nM) was substantially lower than the 100 µM concentration of dopamine used to induce desensitisation here, dopamine levels are known to fall off *exponentially* with distance from the release site (for review see Cragg and Rice, 2004), and this suggests that dopamine levels in the synapse are likely to be considerably higher than in extracellular space where dialysis probes typically sample (for review see Cragg and Rice, 2004) and where excess monoamines are buffered or degraded. It is impossible to know, therefore, the precise concentration of dopamine within the synaptic cleft, but a concentration of 100 µM is not

implausible. As noted previously, changes in the surface-expression of dopaminergic receptors have dramatic effects on neuronal excitability to affect dopamine release from VTA neurons (Al-Hasani *et al*., 2011), and a similar mechanism may function in the lateral entorhinal cortex to alter synaptic transmission and plasticity. More specifically, dopamine-dependent changes in the surface expression of metabotropic receptors can directly affect glutamate release and constrain plasticity in sensory inputs to the superficial layers of the lateral entorhinal cortex. Critically, this block of plasticity can be alleviated if the modulatory effects of dopamine are removed via receptor desensitisation or internalisation. This raises the question as to whether this metabotropic receptor desensitisation represent a novel from of *metaplasticity* in the lateral entorhinal cortex. Traditionally, metaplasticity is the term used to describe the phenomenon in which activity-dependent forms of plasticity, such as LTP, are occluded at some synapses based on the previous pattern of activity (such as subthreshold stimulation) at these same synapses (Abraham and Bear, 1996). This so-called 'plasticity of synaptic plasticity' is known to involve NMDA receptors (for review see Zorumski and Izumi, 2012; Abraham, 2008), but changes in the surface expression of dopamine-binding metabotropic receptors to regulate glutamate release shown here ultimately produce very similar results. Additional work is required to characterise these dopamine-mediated metaplastic-like effects further in the lateral entorhinal cortex.

Chapter 6: Dopaminergic Modulation of LTP in the Lateral Entorhinal Cortex

Introduction

The results of experimental work described in this thesis so far indicate, collectively, that dopamine is a powerful *inhibitor* of synaptic function in the superficial layers of the lateral entorhinal cortex. In particular, the results of Chapter 3 demonstrate that dopamine induces a concentration-dependent and reversible suppression of glutamate-mediated excitatory synaptic transmission in sensory inputs that make synaptic contact with superficial layer projection neurons (see **Figure 3.4**). The depression in the amplitude of fEPSPs is not due to any dopamine-mediated change in local inhibition (see **Figure 3.10** and **Figure 3.11**), but rather to a change in the release probability of glutamate from sensory afferents that terminate in layer I (see **Figure 3.8** and **Figure 3.9**). Interestingly, although responses seemingly appear to return to baseline levels following brief exposure to dopamine, the dopamine receptors, or receptors that also bind dopamine ('dopamine-binding receptors'; see **Table 2.1**), may have been altered in a fundamental way depending on the concentration of the agonist they were exposed to (**Figure 4.1** and **Figure 4.2**). Specifically, exposure to concentrations of 100 or 1000 μM dopamine recruit activity of GRK2/3 to initiate β-arrestin-dependent internalisation of metabotropic receptors (**Figure 4.3** and **Figure 4.4**). This desensitisation changes the potency of the modulation dopamine can exert to dramatically alter future responsivity to the agonist. Dopamine not only constrains basal synaptic transmission in the lateral entorhinal cortex, but it also prevents induction of activity-dependent LTD in sensory inputs to the superficial layers. Bath-applying dopamine during PP-LFS prevents induction of LTD (**Figure 5.2**), and this is likely due to a dopamine-mediated reduction in glutamate-release leading to subthreshold activation of postsynaptic NMDA (or mGlu) receptors required for successful induction. LTD can be restored if the effects of dopamine on glutamate release during PP-LFS are attenuated. This can be accomplished by desensitising dopamine-binding receptors first by administering a 'priming' application of dopamine prior to delivering PP-LFS in the presence of the agonist (**Figure 5.3**). Preventing internalisation of metabotropic receptors during the initial desensitisation phase reinstates the dopamine-mediated block of LTD (**Figure 5.4**). To continue exploring the effects of dopamine on activity-dependent forms of synaptic plasticity in the lateral entorhinal cortex, experimental work in this chapter was conducted to characterise and assess whether dopamine influences induction and expression of LTP in sensory inputs to the superficial layers of the lateral entorhinal cortex.

Synapses within neuronal circuits throughout the medial temporal lobe are continuously modified based on experience (for review see Malenka, 1994; Malenka and Bear, 2004). In fact, activity-dependent LTP has been studied in many different brain regions, including the amygdala (Huang and Kandel, 1998), ventral tegmental area (Nugent *et al.*, 2008), cerebellum (Salin, Malenka and Nicoll, 1996) and cortex (Artola and Singer, 1987; Tsumoto, 1990; Fox, 2002). Pioneering research in the early 1970s by Bliss and Lomo (1973) showed that LTP could be induced at excitatory perforant path synapses between the entorhinal cortex and dentate gyrus of the

hippocampus. The initial discovery of LTP in the hippocampus and its potential role as a physiological substrate underlying learning and memory (Hebb, 1949) made the hippocampal formation an immensely popular region of interest in the decades that followed. Many in-depth reviews were published during this time in an attempt to keep pace with the rapid discoveries being made on a regular basis on the fundamental principles, mechanisms and signals mediating the induction, expression and maintenance of activity-dependent LTP in multiple regions of the brain (Malenka, 1994; Malenka and Bear, 2004; Sigurdsson *et al.*, 2007; Citri and Malenka, 2008; O'Dell *et al.*, 2010; Kumar, 2011; Bassi *et al.*, 2019). The induction of LTP is rapid and the effects are long-lasting. It is these properties that make LTP such an appealing candidate mechanism to underlie memory storage in the brain (Abraham *et al.*, 2002). For example, Schaffer collateral projections originating from area CA3 that make synaptic contact with the dendrites of CA1 pyramidal neurons exhibit LTP following short bursts of high frequency stimulation. Plasticity at these synapses is input specific, so only the connections activated by the high-frequency stimulation are potentiated (Bliss and Collingridge, 1993; Abraham *et al.*, 2002). The induction of LTP can be NMDA receptor-dependent or -independent, and both forms of plasticity can be induced at the same synapses depending on experimental conditions. For example, in the hippocampus, when Schaffer collateral inputs to area CA1 are exposed to high-frequency stimulation or theta-burst stimulation an NMDA receptor-dependent form of LTP is induced (Collingridge, Kehl and McLennan, 1983). The same synapses, however, can express an NMDA receptor-independent form of LTP when exposed to 200 Hz stimulation (Grover, 1998) or via activation of metabotropic glutamate receptors (Bashir *et al.*, 1993a).

AMPA and NMDA receptors mediate both excitatory synaptic transmission and synaptic plasticity (for review see Hansen *et al*., 2021), and both receptors are part of a much larger group of ionotropic glutamate receptors that also include kainate receptors. It is important to note that some ionotropic glutamate receptors, most notably NMDA receptors, do not reach full maturity until postnatal day 14 (Andersen *et al.*, 2007). A functional NMDA receptor is composed of multiple subunits in various tetrameric combinations. NMDA receptors containing GluN1 and GluN2 subunits are the most prevalent and play an important role in mediating key intracellular signals due to their calcium permeability (for review see Vyklicky *et al*., 2013). Successful activation of an NMDA receptor requires binding of four molecules: two glycine molecules and two glutamate molecules. Glycine or its agonist, D-serine, are typically found pre-bound to NMDA receptors at a glutamatergic synapse (Papouin *et al.*, 2012). This is because both compounds are found in high concentrations in the brain due to their endogenous presence in cerebrospinal fluid (Iijima *et al.*, 1978). The activation of NMDA receptors is not required for basal synaptic transmission (AMPA receptors typically fulfil this function), instead, NMDA receptors regulate induction of persistent changes in synaptic efficacy and the modification of synaptic weights. As noted, AMPA receptors are required for basal synaptic transmission. To accomplish this, glutamate must be available in high quantities in the synaptic cleft since AMPA receptors have a very low affinity for glutamate (Colquhoun, Jonas and Sakmann, 1992; Andersen *et al.*, 2007). Once bound, AMPA receptors pop open rapidly and allow the flow of sodium ions into the cell or potassium ions out (depending on the membrane potential of the neuron). However, in the presence of chronic glutamate AMPA receptors rapidly desensitise or internalise (Andersen *et al.*, 2007).

NMDA receptors play an important role in the induction of activity-dependent LTP in many brain regions, most notably in area CA1 of the hippocampus. A key feature of NMDA receptors that makes them so critical to activity-dependent forms of plasticity is their innate permeability to calcium ions. If the intracellular concentration of calcium in the postsynaptic cell exceeds a critical threshold, then LTP can be induced (for reviews see Citri and Malenka, 2008; Kumar, 2011). At rest, the channel pore of the NMDA receptor complex is blocked by a magnesium ion, and this restricts the ability of NMDA receptors to conduct sodium, potassium and calcium ions across the membrane. If, however, the membrane potential of the neuron is depolarised sufficiently, then this magnesium block is repelled. At excitatory synapses, AMPA and NMDA receptors are often co-localised. In this way, strong depolarisation provided by activation of AMPA receptors is sufficient to provide the necessary depolarisation required to alleviate the magnesium block from nearby NMDA receptors (for review see Malenka, 1994; Malinow and Malenka, 2002; Malenka and Bear, 2004; Luscher and Malenka, 2012). Full activation of NMDA receptors allows the rapid influx of calcium into the postsynaptic neuron (Bliss, Lancaster and Wheal, 1983), and depending on the concentration, calcium triggers a series of intracellular cascades that ultimately result in the induction of either LTP or LTD (Blanke and Van Dongen, 2009). For LTP induction, large calcium transients mediated by activation of NMDA receptors activate calcium/calmodulin-dependent protein kinase II (or CaMKII) to trigger an increase in the number of AMPA receptors expressed at the synapse. An increase in AMPA-mediated transmission results in a much larger postsynaptic response and enhanced efficacy at the synapse (for review see Citri and Malenka, 2008).

Activity-dependent and glutamate-mediated forms of synaptic plasticity have been observed previously in the superficial layers of both the medial and lateral divisions of the entorhinal cortex (Alonso, de Curtis and Llinas, 1990; Hanse and Gustafsson, 1992; Kourrich and Chapman, 2003; Solger *et al.*, 2004; Deng and Lei, 2007), and efferent projections originating from superficial layer neurons in the lateral division tend to support LTD exclusively when compared to efferents from the medial division (Collitti-Klausnitzer *et al.*, 2021). Moreover, Collitti-Klausnitzer *et al.* (2021) showed that long lasting changes in the strength of connections between the entorhinal cortex and hippocampus can change depending on whether synapses in the dentate gyrus were first 'primed' with stimulation at different frequencies. Few studies have assessed activity-dependent LTP in the entorhinal cortex directly, and in the few that have the experiments tended to focus on the medial division, specifically (Solger *et al.*, 2004). LTP can be induced in sensory inputs to the medial entorhinal cortex by exposing brain slices to specific neuromodulators or by delivering repetitive high frequency stimulation protocols. For example, bath application of the non-selective cholinergic agonist, carbachol, induces an LTP-like effect in the medial entorhinal cortex (Shiroma and Costa, 2015). In some instances, application of this agonist has been shown to induce a long-lasting potentiation of synaptic transmission the medial entorhinal cortex only after an initial short-lasting LTD-like effect (Yun *et al.*, 2000). Dopamine has been shown to influence synaptic transmission and plasticity at multiple synapses within neuronal circuits throughout the medial temporal lobe. For example, dopamine blocks LTP via activation of D_1 receptors in the dentate gyrus (Yanagihashi and Ishikawa, 1992) and blocks LTD via activation of D_1/D_5 receptors in area CA1 (Mockett *et al.*, 2007). However, even less is known about LTP in the lateral division of the entorhinal cortex. In the only published report, Caruana *et al.*

(2007) observed that LTP could be induced in olfactory inputs to the superficial layers of the lateral entorhinal cortex *in vivo*. In addition, enhancing extracellular dopaminergic tone in the lateral entorhinal cortex with GBR12909 prior to delivery of tetanic stimulation blocked induction of LTP in sensory inputs to the superficial layers. This is consistent with the largely suppressive effects of dopamine on synaptic function in the lateral entorhinal cortex, but more data is needed to better understand the mechanisms underlying the dopamine-mediated block of LTP in the superficial layers.

Materials and Methods

Field Potential Recordings

For all field recording experiments, slices from male (95%) and female (5%) Wistar rats aged between P14 and P21 were rested in warmed and oxygenated ACSF for at least 60 minutes after slicing just prior to experimental testing. Following the rest period, slices were transferred to the recording chamber and a bipolar stimulating electrode and glass recording electrode were placed carefully in the superficial layers of the lateral entorhinal cortex (stimulating electrode positioned to span the layer I-II border; recording electrode positioned along the layer I border with layer II; see Figure 3.3A) and responses were elicited once every 20s. Standard experiments to induce LTP in sensory inputs to the superficial layers of the lateral entorhinal cortex typically began following a 30-minute baseline period of stable fEPSP recordings, and WinLTP was used to toggle and control the delivery of the tetanic stimulation during an experiment (see below). Note: the stimulation intensity always remained unchanged (intensity set to evoke fEPSPs at 75% max amplitude) during delivery of the induction protocols. To induce LTP, several tetanic stimulation protocols were used. Two high frequency stimulation (HFS) protocols were tested (100 Hz HFS, 100 pulses delivered over 1s, repeated three times once every 10 seconds; and 200 Hz HFS, 200 pulses delivered over 1 second, only once), as well as a theta burst stimulation protocol (TBS; 10 trains consisting of 10 pulses at 100 Hz per train with an intertrain interval of 200 msec, repeated three times once every minute). Stimulation protocols were designed based on previous studies of LTP in the hippocampus and parahippocampal cortices. Superficial layer neurons in layer II/III of the medial entorhinal cortex exhibit LTP following a theta burst stimulation (10 trains of 4 pulses at 100 Hz, repeated at 5 Hz) and there is evidence to suggest that 4 pulses may not produce enough postsynaptic depolarisation to express LTP in the *stratum radiatum* in area CA1, so a total of 10 pulses was used for these experiments (Yun, Mook-Jung and Jung, 2002; Larson and Munkacsy, 2015). Short bursts of high frequency stimulation are robust paradigms used to reliably induce LTP in much of the hippocampus including the dendate gyrus, and areas CA3 and CA1 (Bliss and Lomo, 1973; Ma, Alonso and Dickson, 2008; Kumar, 2011). Control experiments were interleaved throughout all experimental testing, and each treatment condition had its own time-matched set of control data to compare to.

Experiments assessing induction of LTP in sensory inputs to the lateral entorhinal cortex began with a 30-minute baseline in normal ACSF followed by delivery of either 100 Hz HFS, 200 Hz HFS or TBS. Both short- and long-term changes in synaptic efficacy resulting from tetanic stimulation were monitored for an additional 60-minutes of follow-up recordings. To test whether NMDA receptors were required for induction, the competitive NMDA receptor antagonist, AP5 (10 µM), was added to the ACSF and present throughout the entire experiment before, during and after delivery of tetanic stimulation. Next, putative interactions between activity-dependent LTP and activity-dependent LTD at the same population of synapses were assessed. During these experiments, either tetanic stimulation was delivered prior to PP-LFS, or vice versa. To determine the role of local inhibition in the induction and expression of LTP the $GABA_A$-receptor antagonist, picrotoxin (50 µM), was added to the ACSF and present throughout the entire experiment before, during and after delivery of tetanic stimulation.

To assess whether dopamine-mediated synaptic depression and activity-dependent LTP were co-expressed at the same population of synapses, an experiment was conducted whereby activity-dependent LTP was induced first followed 30-minutes later by bath-application of 100 µM dopamine. Modulatory effects of dopamine on activity-dependent plasticity may result from the endogenous release of dopamine from dopaminergic axons still present in parahippocampal slices of the lateral entorhinal cortex. As a result, tetanic stimulation may be sufficient to drive endogenous release of dopamine from intact dopaminergic terminals preserved in the slice preparation to modulate induction of LTP. To rule out contributions of any endogenous dopamine release, dopamine-binding receptors were desensitised prior to delivery of tetanic stimulation. During these experiments, dopamine (100 µM) was applied first followed 60-minutes later by the delivery of tetanic stimulation. In other experiments, tetanic stimulation was delivered 15-minutes into a 30-minute bath application of a cocktail of both SCH-23390 (50 µM) and sulpiride (50 µM) to block both D_1-like receptors and D_2-like receptors, respectively. In this instance, SCH-23390 (50 µM) was used before its intrinsic activity at principal neurons in the superficial layers of the lateral entorhinal cortex was fully understood (see **Figure 3.12A**). The effects observed with the combined bath application of sulpiride (50 µM) and SCH-23390 (50 µM) may result from alternative receptor binding mechanisms alongside, or instead of, dopamine receptor subunit specificity (see **Table 2.1**).

To determine whether induction of activity-dependent LTP could be augmented or enhanced in sensory inputs to the superficial layers of the lateral entorhinal cortex, tetanic stimulation was delivered at the end of a 30-minute application of the non-selective adenosine receptor antagonist, caffeine (300 µM). Caffeine is one of few treatments known to reliably potentiate responses in the lateral entorhinal cortex (D Caruana unpublished observation), so potential synergistic effects between caffeine and induction of activity-dependent LTP were assessed. Finally, to determine whether induction of LTP could be enhanced by boosting NMDA receptor function, the concentration of extracellular calcium in the ACSF was raised to 10 mM for the entire experiment before, during and after delivery of tetanic stimulation. It should be noted that during these experiments, small amounts of white precipitate were observed forming in the solution. This precipitate was neither removed nor tested, and a reasonable assumption was made that calcium was fully saturated in the high-calcium (10 mM) ACSF solution. Throughout the 90-minute experiments, continuous close observation confirmed that there were no deviations in flow rate or temperature beyond normal parameters.

Whole-Cell Recordings

For all whole-cell patch clamp experiments, brain slices rested for at least 60 minutes after slicing prior to testing. For experiments measuring excitatory postsynaptic currents (EPSCs), slices were transferred to the recording chamber and a stimulating electrode was placed in layer I and a glass recording electrode, containing a potassium gluconate-based patch solution (sometimes with added biocytin), was lowered carefully into layer II and sealed onto a pre-selected neuron. Layer II neurons were preferred for these experiments to ensure consistency with methods used in previous chapters, as well as with experimental work published previously (Caruana *et al.*, 2006; Caruana and Chapman, 2008; Glovaci, Caruana and Chapman, 2014; Glovaci and Chapman,

2019). EPSCs were evoked once every 60 seconds or once every 120 seconds, and experiments began following 5 minutes of stable baseline recordings. A short, 5-minute baseline was required for these experiments since induction of LTP in whole cell recording experiments is sensitive to dialysis and washout of key intracellular signals required for induction. Tetanic stimulation was delivered after the 5-minute baseline. Neurons were clamped at -70 mV during recordings, though in some experiments the membrane potential was depolarised to 0 mV during tetanic stimulation (see below), and measures of R_s, R_m and DC monitored continuously throughout each experiment. To explore the induction and expression of LTP in single layer II neurons maintained *in vitro*, tetanic stimulation was delivered after 5-minutes of stable baseline recordings of EPSCs. WinLTP was used to toggle and control the delivery of the tetanic stimulation during an experiment. Note: the stimulation intensity always remained unchanged (intensity set to evoke fEPSPs at 75% max amplitude) during delivery of the induction protocols. In some experiments 10 mM of the calcium chelator, BAPTA, was included in the patch recording pipette to determine the role of intracellular calcium in the induction of activity-dependent LTP in the lateral entorhinal cortex.

Data Analysis

The effects of bath-applied drugs or tetanic stimulation protocols were assessed on the amplitude of averaged synaptic responses (fEPSPs or EPSCs) obtained during 5- or 10-min epochs recorded at different times during an experiment (latencies specified below). In some instances, the peak change in synaptic efficacy was used, and this was determined manually, within a strict window of +9-11 minutes post-drug wash on, for each individual experiment as the time varied. All data were expressed as the mean ± SEM and were normalised to the baseline period for plotting. Drug-induced changes in response properties were assessed with Prism using (where appropriate) paired or unpaired samples *t*-tests, one-way ANOVAs or repeated measures ANOVAs. Post-hoc comparisons were made using the Bonferroni method with an alpha level of $P < 0.05$.

Results

Tetanic Stimulation does not Induce Long-Term Potentiation in Sensory Inputs to the Lateral Entorhinal Cortex: It Induces LTD Instead

LTP is typically induced using HFS (for review see Sigurdsson *et al.,* 2007; Citri and Malenka, 2008; Kumar, 2011) or TBS protocols (Larson, Wong and Lynch, 1986; Staubli and Lynch, 1987; Abraham *et al.*, 2002). Three different tetanic stimulation protocols to induce LTP in sensory inputs to the lateral entorhinal cortex were tested here: TBS, 200 Hz HFS or 100 Hz HFS. Unexpectedly, all three protocols induced either persistent LTD or a transient suppression of synaptic transmission that returned to baseline levels during the 60-minute post-tetanus follow-up period (**Figure 6.1**), but no LTP. TBS caused an immediate reduction in the amplitude of fEPSPs post-TBS and responses remained depressed at 74.6 ± 6.5% of baseline by the end of the experiment (Last 5-min, $F_{1,20}$ = 6.571, P < 0.05, TBS n = 12, control n = 10; **Figure 6.1A**). A similar lasting depression was observed following delivery of 200 Hz HFS. Responses were weakly depressed immediately post-HFS but responses became significantly depressed at 75.6 ± 7.0% of baseline (Last 5-min, $F_{1,20}$ = 5.064, P < 0.05, HFS n = 12, control n = 10; **Figure 6.1B**), by the end of the experiment. Interestingly, delivery of 100 Hz HFS had only mild suppressive effects on transmission that returned to baseline levels by the end of the experiment ($F_{1,20}$ = 0.004, P = 0.951, HFS n = 12, control n = 10; **Figure 6.1C**). In some instances, the amplitude of the presynaptic fibre volley decreased following tetanic stimulation to induce LTP (see inset traces in **Figure 6.1B$_1$**). A tetanus-induced change in glutamate release probability could explain the absence of LTP and the expression of LTD instead. However, this is difficult to confirm, as the fibre volley reduction was inconsistent across experiments and induction protocols. Additionally, not every response had a distinct, measurable fibre volley, as it was sometimes partially occluded by the stimulation artefact. Regardless, these findings indicate that standard tetanic stimulation protocols used reliably by others to induce LTP in other regions of the brain induced LTD instead in sensory inputs to the lateral entorhinal cortex.

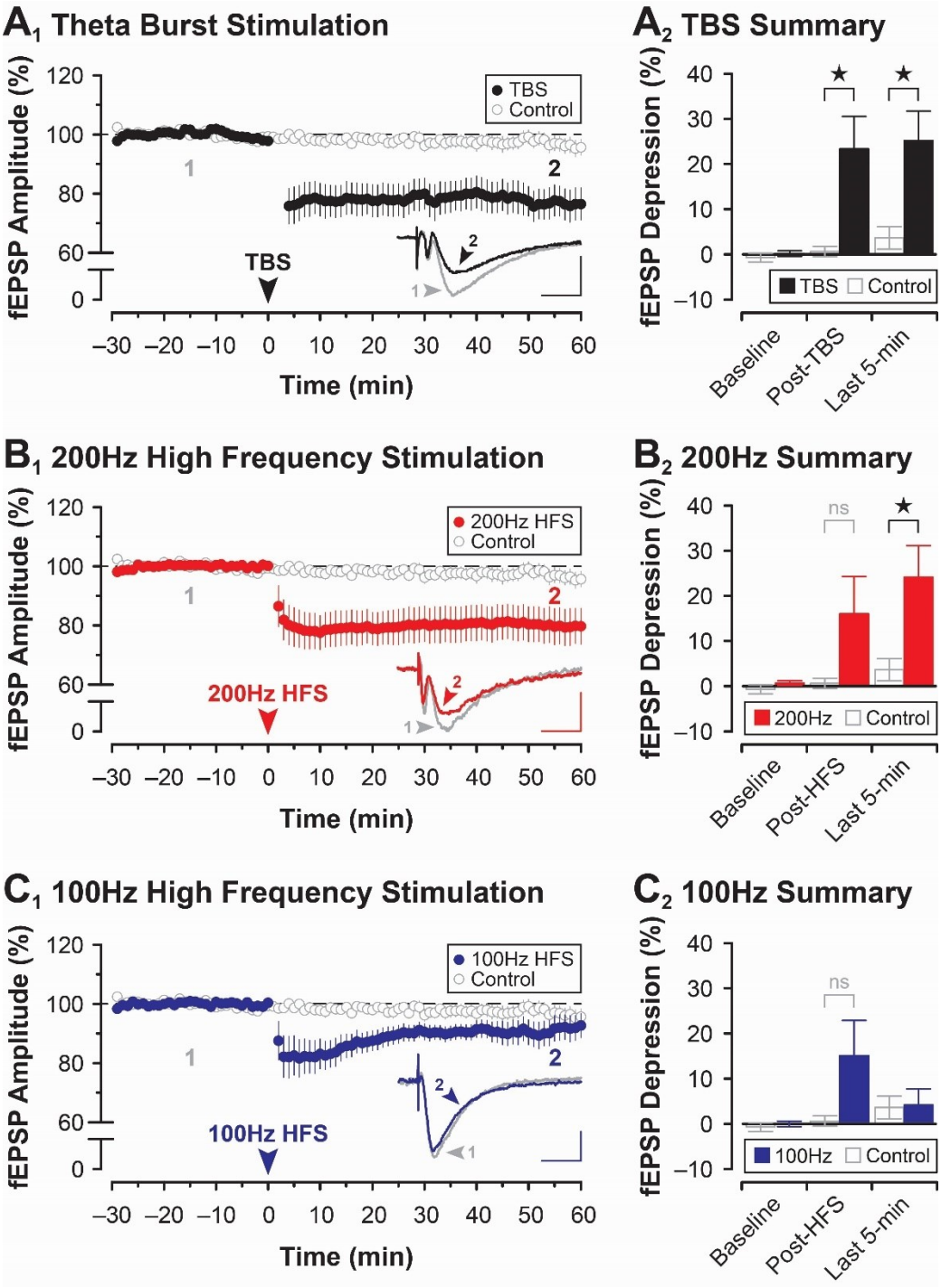

Figure 6.1. Tetanic stimulation induces LTD of evoked synaptic responses in the lateral entorhinal cortex. *(**A₁-B₁**) The amplitude of fEPSPs following theta burst stimulation (TBS; black circles, **A₁**) and 200Hz high frequency stimulation (200Hz HFS; red circles, **B₁**) is immediately depressed and remains so throughout the rest of the experiment compared to untreated controls (open circles). (**A₂-C₂**) Summary bar plots highlighting the depression of fEPSPs relative to controls at three different time points during the experiments (Baseline, Post-TBS/Post-HFS and Last 5-min). (**C₁**) The amplitude of fEPSPs was not changed significantly following 100 Hz HFS (blue circles) compared to untreated controls (open circles). Insets in **A₁**, **B₁** and **C₁** are representative fEPSP traces recorded before and after TBS (grey and black, **A₁**), 200 Hz HFS (grey and red, **B₁**) or 100 Hz HFS (grey and blue, **C₁**). Numbered traces correspond to numbers on the respective graph, highlighting the specific times during the experiment when the sample traces were recorded. Scale bar: 0.2 mV / 5 ms.*

Interestingly, tetanic stimulation also induced LTD-like effects in whole-cell recordings of EPSCs from layer II neurons directly in the lateral entorhinal cortex. During these experiments, two different induction protocols were tested under varying conditions, resulting in three distinct experimental setups. Given TBS was the most effective tetanus during previous field recording experiments (see **Figure 6.1A**), it was also tested here

at typical resting membrane potential (-70 mV). In a separate set of experiments, a similar design was used, but a 200 Hz HFS protocol was tested. Finally, delivery of 200 Hz HFS with neurons clamped at 0 mV (as opposed to -70 mV) during the tetanus was also tested. Clamping neurons at 0 mV during tetanic stimulation is a method used frequently during whole-cell recordings to depolarise the postsynaptic cell in order to help alleviate the magnesium block from NMDA receptors. Similar to results of field recording experiments summarised above, TBS and 200 Hz HFS protocols did not induce LTP in sensory inputs to layer II neurons; they seemed to induce LTD instead (**Figure 6.2**). Delivery of TBS induced a similar LTD-like effect in sensory inputs to layer II neurons. Responses were reduced to 52.0 ± 10.4% of baseline 60 minutes post-TBS induction, this differs significantly from the time-matched controls ($F_{1,10}$ = 7.545, P < 0.05, TBS n = 4, control n = 8; **Figure 6.2A**). Delivery of 200 Hz HFS at resting membrane potential (-70 mV) induced significant LTD of synaptic transmission as responses were depressed to 47.9 ± 5.5% of baseline at the end of the experiment ($F_{1,12}$ = 5.189, P < 0.05, HFS n = 6, control n = 8; **Figure 6.2B**). When 200 Hz HFS was delivered whilst neurons were depolarised to 0 mV during the tetanus responses were reduced to 41.8 ± 19.2% of baseline at the end of the experiment, but did not differ significantly from controls ($F_{1,9}$ = 2.822, P = 0.127, HFS n = 3, control n = 8; **Figure 6.2C**). However, due to the low sample size for 200 Hz HFS on neurons clamped at 0 mV, these data should not be considered reliable. Based on results from these two data sets (excluding 200 Hz at 0 mv), 200 Hz HFS and TBS protocols are not sufficient to induce activity-dependent LTP in sensory inputs to the lateral entorhinal cortex but instead seem to induce a persistent depression of synaptic transmission. A short 5-minute baseline period is typically used in whole-cell patch-clamp experiments to induce activity-dependent plasticity, as pipette dialysis removes many proteins and signalling molecules necessary for successful induction. It is unclear whether the activity-dependent LTD induced by tetanic stimulation undergoes a similar washout or whether dialysis contributes to the shift from LTP to LTD. However, this seems unlikely given the extracellular data in **Figure 6.1**, where dialysis is not a factor.

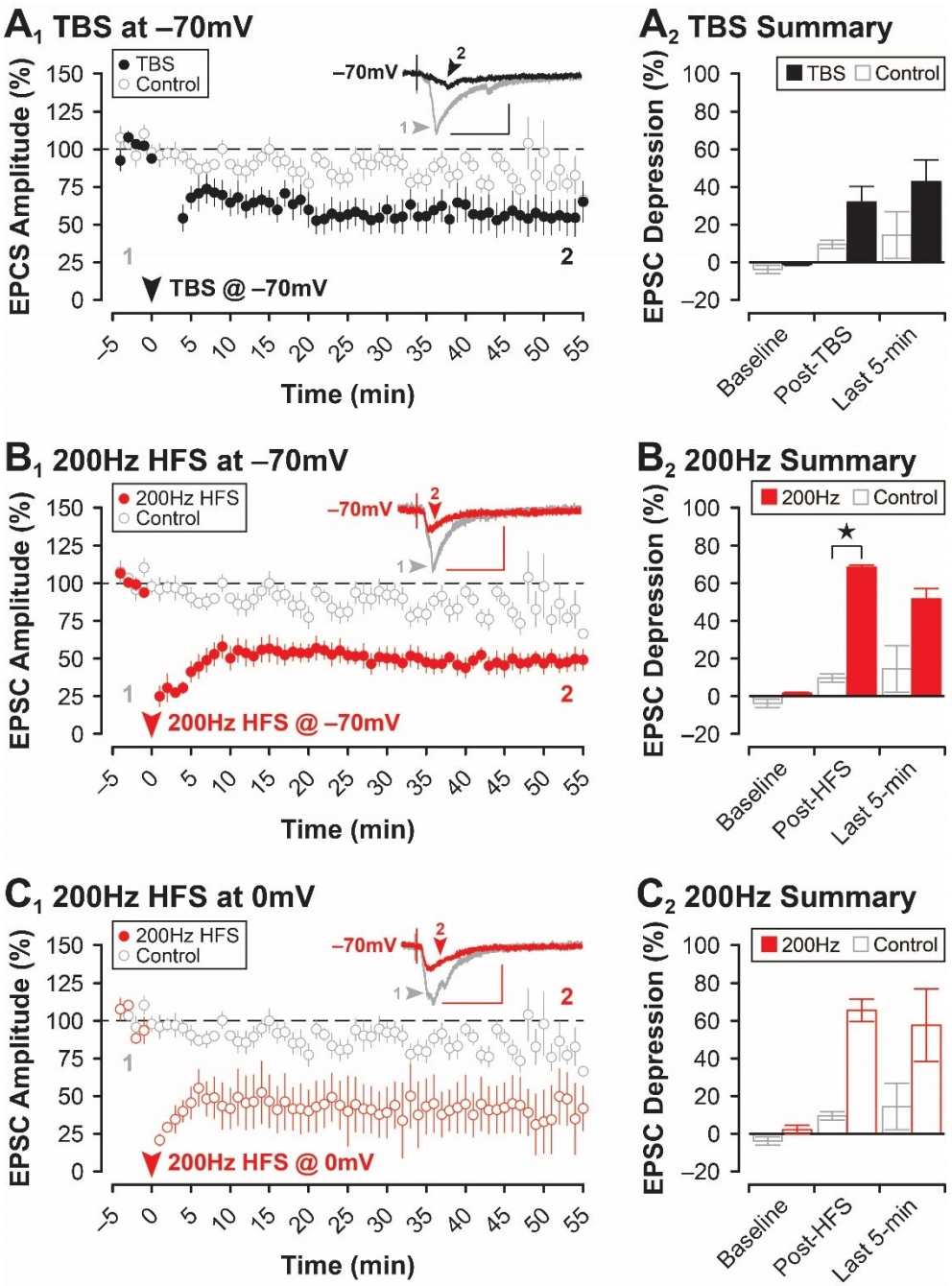

Figure 6.2. Tetanic stimulation induces LTD in individual layer II projection neurons. *(**A₁-B₁**) At resting membrane potential (-70 mV), excitatory postsynaptic current (EPSCs) are suppressed following the induction of 200 Hz HFS (filled red circles, **B₁**), this depression is not significant for EPSCs following the induction of TBS (black circles, **A₁**), compared to time-matched controls (open circles). (**A₂-C₂**) Summary bar plots highlighting the depression of fEPSPs (filled bars) relative to controls (open bars) at three different time points during the experiment (Baseline, Post-TBS/Post-HFS and Last 5-min). (**C₁**) If the neuron is depolarised to 0 mV during delivery of 200 Hz HFS (open red circles), evoked EPSCs are not significantly depressed compared to time-matched controls (open circles). Insets on **A₁**, **B₁** and **C₁** are representative fEPSP traces recorded before and after the induction of TBS (grey and black, **A₁**) or 200 Hz HFS (grey and red, **B₁** and **C₁**). Numbered traces correspond to numbers on the graph below, highlighting the specific times during the experiment when the sample traces were recorded. Scale bar: 100 pA / 25 ms.*

Tetanus-Induced LTD in the Lateral Entorhinal Cortex Depends on activation of NMDA Receptors and an Elevation in Intracellular Calcium

To investigate whether induction of tetanus-induced LTD in the lateral entorhinal cortex required activation of NMDA receptors, the competitive NMDA receptor antagonist, AP5 (10 μM), was added to the perfusate and was present throughout the entire experiment before, during and after delivery of tetanic stimulation. For these experiments, a TBS protocol was used as it elicited the most reliable LTD of synaptic transmission during previous field and whole cell recording experiments (see **Figure 6.1A and 6.2A**). Indeed, induction of LTD by delivering TBS was blocked in the presence of AP5 (**Figure 6.3A**). Although synaptic responses were depressed significantly after TBS to 81.5 ± 8.8% of baseline ($F_{2, 28}$ = 5.060, P < 0.05, Bonferroni P < 0.001, TBS n = 7, control n = 9; **Figure 6.3A**), responses quickly recovered to baseline levels (to 94.8 ± 2.6% during the last 5-minutes of the experiment) and did not differ significantly from time matched controls (Bonferroni P = 0.999). In addition, loading cells with the calcium chelator, BAPTA (10 mM), also blocked the LTD-like effect induced following delivery of TBS (Figure 6.3B). There was no significant reduction in the amplitude of synaptic responses following delivery of TBS during whole-cell experiments ($F_{2, 28}$ = 2.168, P = 0.1332, TBS n = 9, control n = 7; **Figure 6.3B**).

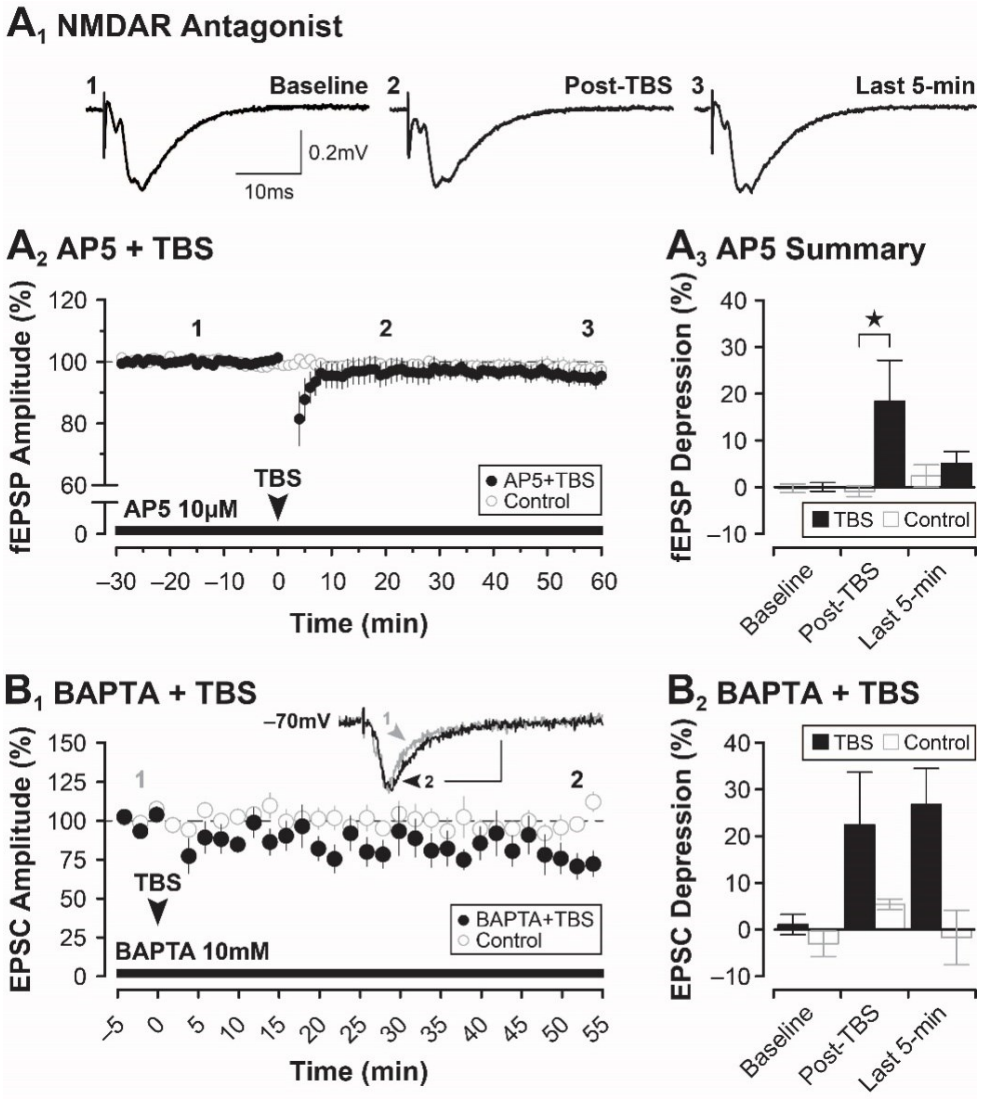

Figure 6.3. Induction of tetanus-induced LTD depends on NMDA receptors and intracellular calcium. *(**A₁**) Representative fEPSP traces recorded before and after TBS induction. Numbered traces in **A₁** correspond to numbers in **A₂** highlighting the specific times during the experiment when the sample traces were recorded. (**A₂**) Blocking NMDA receptors with AP5 (10 μM) prevents TBS from depressing the amplitude of fEPSPs (filled circles) relative to unstimulated and untreated controls (open circles). (**A₃**) Summary bar plot highlighting the depression of fEPSPs (filled bars) at three different time points during the experiment (Baseline, Post-TBS and Last 5-min) compared to time matched controls (open bars). (**B₁**) In whole cell preparations, adding the calcium chelator, BAPTA (10 mM), to the recording electrode solution (BAPTA+TBA; filled circles) prevents TBS-induced induction of LTD relative to untreated controls (open circles). Inset: representative synaptic currents recorded before and after TBS induction. Numbered traces in the inset correspond to numbers above the data graph in **B₁** highlighting the specific times during the experiment when the sample traces were recorded. (**B₂**) Conventions are the same as **A₃** but for BAPTA + TBS experiments. Scale bar: 100 pA/ 25 ms.*

To test whether tetanus-induced LTD and standard PP-LFS-mediated LTD recruit similar or overlapping expression mechanisms in the lateral entorhinal cortex, experiments were performed whereby TBS was delivered to slices first, followed later by PP-LFS (and vice versa). If both stimulation protocols recruit the same expression mechanism, then inducing LTD with one protocol first would be expected to occlude any further depression induced by the other protocol later during the same experiment. Following a 30-minute baseline, TBS was delivered to slices and significant LTD was induced (**Figure 6.4A**). Once the TBS-mediated LTD had stabilised after about 30-minutes, PP-LFS was delivered. By the end of the TBS-mediated LTD (Pre-PP-LFS), responses were depressed to 88.9 ± 2.8% of baseline, but responses were depressed even further following delivery of PP-LFS. By the end of the experiment, responses were depressed to 78.2 ± 3.5% following PP-LFS,

and this depression was significantly greater than the depression induced previously by TBS alone ($F_{2, 32}$ = 12.59 P < 0.0001, Bonferroni P < 0.001, stim n = 10, control n = 8; **Figure 6.4A$_2$**). These data, alone would suggest that the LTD induced by TBS and the LTD induced by PP-LFS recruit *different* mechanisms for their expression, however, as shown in **Figure 6.4A$_3$** and **A$_4$** the average response amplitudes, when renormalised to 30-min prior to PP-LFS, are *not* depressed further and instead return to the newly depressed baseline following the initial TBS protocol (to 87.76 ± 3.05% of baseline, t_{16} = 2.014, P = 0.4227, n = 8; **Figure 6.4A$_4$**), thus suggesting they may recruit *similar* mechanisms for their expression. Delivering PP-LFS first before TBS seemed to have had a different effect (**Figure 6.4B**). During this experiment, PP-LFS was delivered first and induced significant LTD in sensory inputs to the superficial layers of the lateral entorhinal cortex ($F_{2, 28}$ = 6.937, P < 0.01; Bonferroni P < 0.001, stim n = 10, control n = 6; **Figure 6.4B$_2$**). The LTD stabilised within about 60-minutes of follow-up recording, and by the end of this period (Pre-TBS) responses were depressed to 85.1 ± 3.6% of baseline. Interestingly, subsequent delivery of TBS had no additional impact on the magnitude of LTD observed. By the end of the experiment, responses were depressed to 90.8 ± 5.7% following TBS, and this depression was not significantly greater than the depression induced previously by PP-LFS alone, during the last 5-mins (Bonferroni P < 0.375; **Figure 5.1B$_1$** vs **6.4B$_1$**). Upon further analysis, by renormalising the data in **Figure 6.4B$_1$** to 30-min prior to TBS induction and plotting it separately (see **Figure 6.4B$_3$** & **B$_4$**), the responses appear to be increasing in amplitude, linearly. In fact, after 60 minutes the responses have increased significantly to 108.28 ± 3.75 of baseline (t_{14} = 2.179, P < 0.05, n = 10; **Figure 6.4B$_4$**). In contrast to data shown in **Figure 6.4A**, these results suggest that the two stimulation protocols may recruit *overlapping* mechanisms.

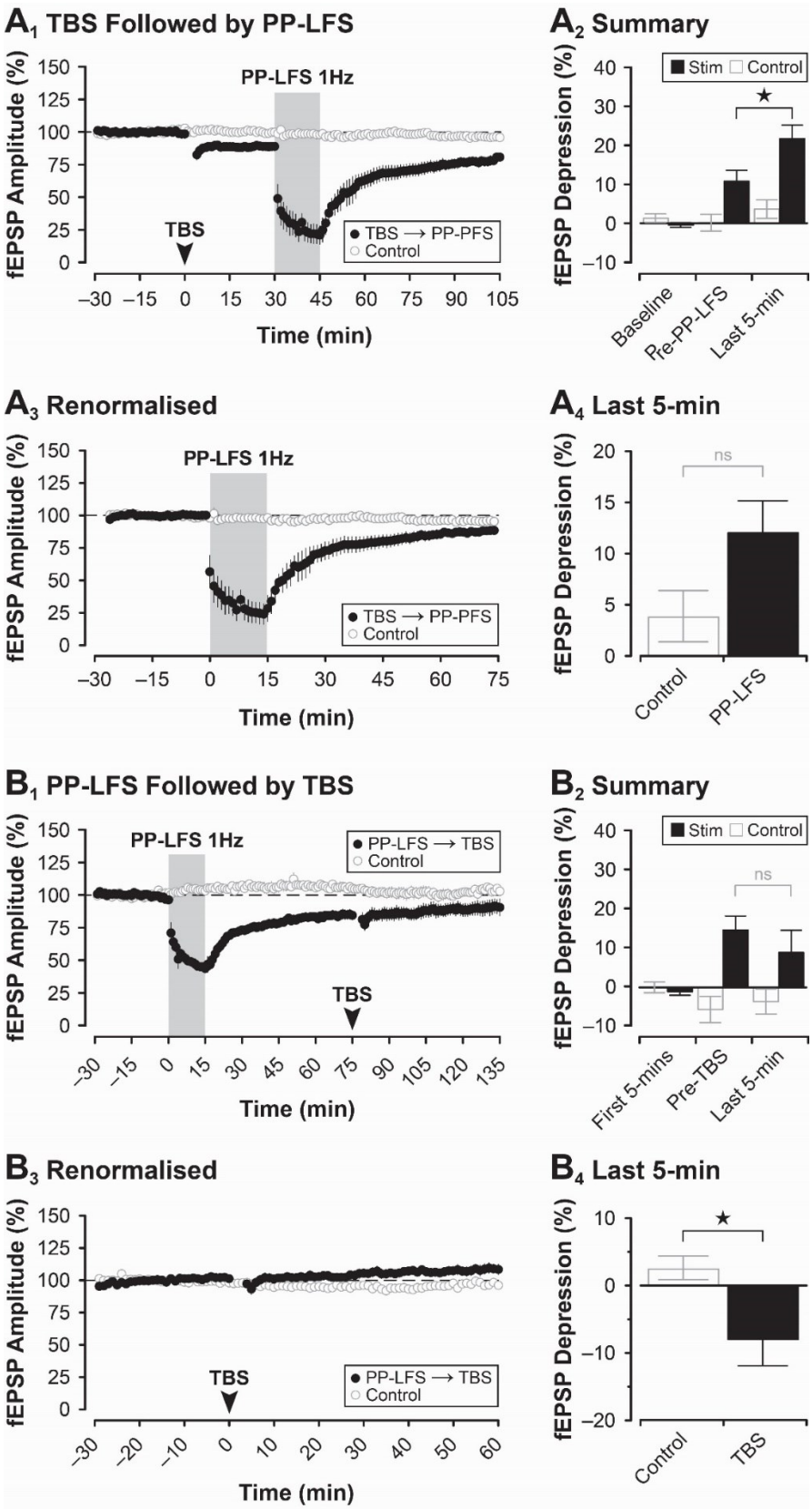

Figure 6.4. Expression of LTD induced by TBS or PP-LFS may involve overlapping mechanisms. *(**A$_1$**) Amplitude of fEPSPs following TBS-induced LTD are further suppressed following paired-pulse low-frequency stimulation (PP-LFS) leading to an even larger LTD effect (TBS→PP-LFS; filled circles) compared to untreated controls (open circles). (**A$_2$**) Summary bar plot highlighting the depression of fEPSPs (filled bars) at three different time points during the experiment (Baseline, Pre-PP-LFS and Last 5-min) compared to time matched controls (open bars). (**A$_3$**) However, renormalising the PP-LFS data to the period of stable LTD induced by TBS indicates that any additional depression induced by PP-LFS may have been occluded. (**A$_4$**) Comparing the magnitude of the depression induced by PP-LFS to time-matched controls during the last 5-minutes of the experiment shows no significant difference in the amplitude of fEPSPs recorded in the lateral entorhinal cortex. (**B$_1$**) The amplitude of fEPSPs following PP-LFS-induced LTD return to the 'new' LTD baseline following TBS induction; there is no change in the magnitude of the depression induced by PP-LFS or TBS (PP-LFS→TBS; filled circles)*

*relative to untreated controls (open circles). (**B_2**) Summary bar plot highlighting the fEPSP depression (filled bars) at three different time points (Baseline, Pre-TBS and Last 5-min), relative to time-matched controls (open bars). (**B_3**) Renormalising the TBS data to the period of LTD induced by PP-LFS during the 30-minute period prior to the tetanus indicates that any additional depression induced by TBS was occluded. (**B_4**) Interestingly, there was a significant potentiation of synaptic responses relative to controls when assessed during the final 5-minutes of the experiment. This suggests that induction of activity-dependent LTD with PP-LFS prior to the delivery of tetanic stimulation may restore the capacity for some activity-dependent LTP to be induced at these synapses.*

Tetanus-induced LTD is NMDA receptor-dependent (see **Figure 6.3A**) and requires an increase in levels of intracellular calcium for induction (see **Figure 6.3B**). The next series of experiments assessed whether tetanus-induced changes in local inhibition also contributed to the persistent depression of synaptic transmission in the lateral entorhinal cortex. Indeed, an activity-dependent *enhancement* in local inhibition may help to suppress responses during tetanic stimulation leading to reduced NMDA receptor activation and subsequent recruitment of phosphatases to induce LTD, as opposed to kinases to induce LTP. As shown in **Figure 6.5**, blocking fast $GABA_A$-mediated as well as $GABA_C$ receptor mediated inhibition with picrotoxin (50 μM) before, during and after tetanic stimulation (either TBS, *n* = 7, control *n* = 10, **Figure 6.5A**; 200 Hz HFS, *n* = 6, control *n* = 10, **Figure 6.5B**; or 100 Hz HFS, *n* = 5, control *n* = 10, **Figure 6.5C**), was sufficient to *prevent* induction of LTD in sensory inputs to the superficial layers, but it was not sufficient to induce LTP. An alternative explanation could also be that LTP was induced in picrotoxin, compensating for the LTD. Regardless of the protocol delivered, responses quickly returned to baseline and did not differ significantly from time-matched control experiments at any time point assessed.

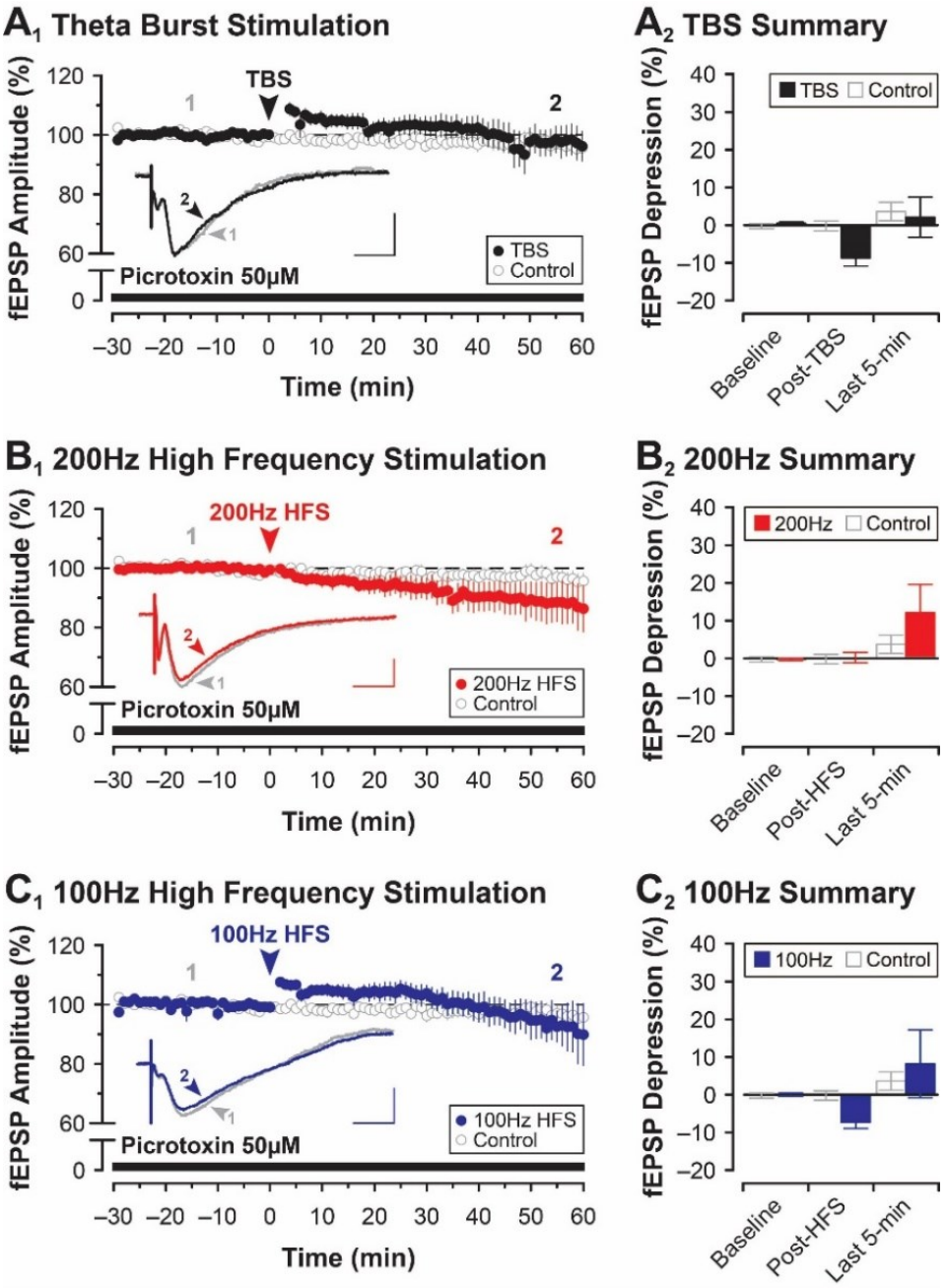

Figure 6.5. HFS and TBS may elicit their suppressive effects via changes in local inhibition. *(**A₁-C₁**) Tetanus-induced changes in fEPSP amplitude following delivery of TBS (black circles, **A₁**), 200 Hz HFS (red circles, **B₁**) or 100 Hz HFS (blue circles, **C₁**) are abolished when GABA receptors are blocked by picrotoxin (50 μM) relative to untreated controls (open circles). This suggests involvement of GABA receptors in the induction and/or expression of TBS- and HFS-induced LTD. Insets: representative fEPSP traces recorded before and after the induction of TBS (grey and black, **A₁**), 200 Hz HFS (grey and red, **B₁**) or 100 Hz HFS (grey and blue, **C₁**). Numbered traces correspond to numbers above the scatter plots highlighting the specific times during the experiment when the sample traces were recorded. (**A₂-C₂**) Summary bar plots highlighting the fEPSP depression at three different time points (Baseline, Post-tetanus and Last 5-min) relative to time-matched controls for TBS (filled black bars **A₂**), 200 Hz HFS (filled red bars, **B₂**) or 100 Hz HFS (filled blue bars, **C₂**) experiments. Scale bar: 0.2 mV / 5 ms.*

Dopaminergic Modulation of Tetanus-Induced LTD

To determine whether dopamine-mediated synaptic depression and tetanus-mediated LTD were co-expressed at the same population of synapses in the lateral entorhinal cortex, LTD was induced first by delivering tetanic stimulation (TBS) followed 30-minutes later by bath-application of 100 μM dopamine. As shown in **Figure 6.6A₁**, delivery of TBS induced a significant depression of synaptic responses that stabilised within 30-minutes.

Responses were depressed significantly to 83.0 ± 4.3% of baseline by the end of this 30-minute period relative to time-matched controls ($F_{2, 18}$ = 13.91, P < 0.001, Bonferroni P < 0.0001, treated n = 3, control n = 8; **Figure 6.6A$_2$**). Subsequent bath-application of 100 µM dopamine after the initial 30-minute follow-up period also depressed synaptic responses, and responses recovered to the same depressed level triggered by TBS during the initial induction of LTD. Following the subsequent application and washout of dopamine, responses returned to a depressed level of 75.2 ± 3.2% of baseline during the last 5-minutes of the experiment, and this did not differ significantly from the initial depression induced by TBS (Bonferroni P = 0.141; **Figure 6.6A$_2$**). Once tetanic stimulation had induced LTD and set a new baseline, the amplitude of fEPSPs returned to this level even after subsequent exposure to 100 µM dopamine.

Modulatory effects of dopamine on activity-dependent plasticity may result from the endogenous release of dopamine from dopaminergic axons still present in parahippocampal slices of the lateral entorhinal cortex. As a result, tetanic stimulation may be sufficient to drive endogenous release of dopamine from intact dopaminergic terminals preserved in the slice preparation to modulate presynaptic glutamate release to affect induction of LTP. To rule out contributions of any endogenous dopamine release, dopaminergic receptors were desensitised first prior to delivery of tetanic stimulation. It was expected that desensitising dopaminergic receptors would produce a similar effect to using a combination of dopamine receptor antagonists. As such, any modulatory role of dopamine would be removed during delivery of the tetanus a short time later. To desensitise dopaminergic receptors during these experiments, dopamine (100 µM) was bath-applied on its own for 30-minutes followed by a 60-minute wash in normal ACSF. Based on results from previous experiments (see **Figure 4.2A$_2$** and **Figure 5.1F$_1$**), this treatment was expected to desensitise dopamine-sensitive receptors in the lateral entorhinal cortex (see **Table 2.1** for dopamine-binding receptor types). Next, TBS was delivered to slices, and recordings continued for an additional 60-minutes. As shown in **Figure 6.6B$_1$**, bath application of an initial 100 µM application of dopamine caused a transient suppression of synaptic responses that returned to near baseline levels within about 30-minutes of washout. After 60-minutes of washout, TBS was delivered. Interestingly, induction of LTD was blocked, and responses did not differ significantly from time-matched control experiments at any time point assessed (**Figure 6.6B**). This block was even more evident when responses during the last 90-minutes of the experiment were renormalised to account for the slight run-down observed in the recordings ($F_{2, 24}$ = 1.920, P = 0.168, treated n = 8, control n = 6; **Figure 6.6C**). These data suggest that under basal and non-desensitised conditions activation of dopaminergic receptors *facilitates* induction of LTD in the lateral entorhinal cortex following delivery of the theta-burst stimulation. This may reflect a dopamine-mediated change in glutamate release during the tetanus to constrain NMDA receptor activity leading to LTD as opposed to LTP.

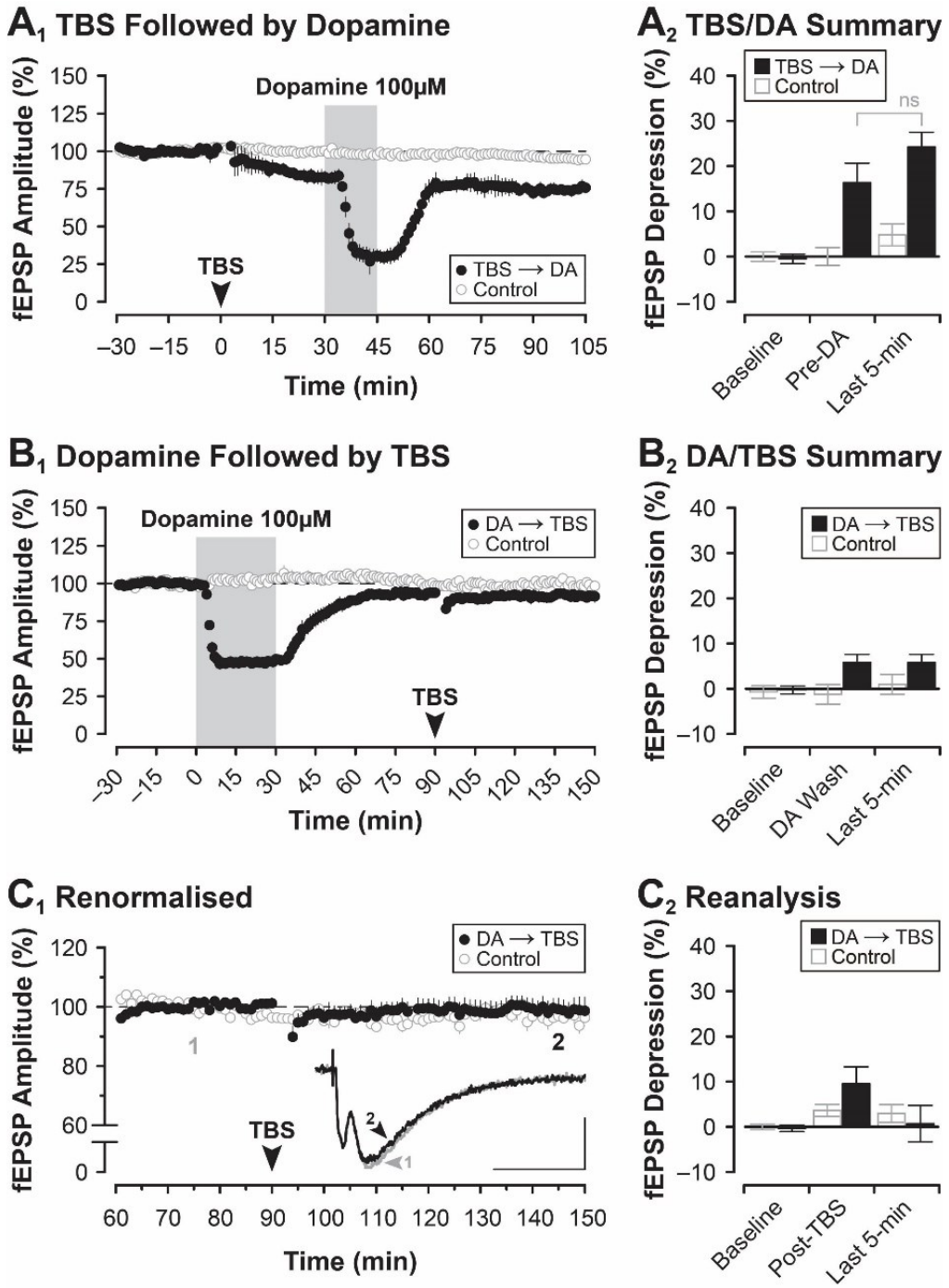

Figure 6.6. Previous dopamine-mediated desensitisation of metabotropic receptors blocks tetanus-induced LTD*. (**A₁**) The amplitude of fEPSPs following TBS-induced LTD are reversibly suppressed by dopamine (100 µM) and return to the 'new' depressed baseline (TBS→DA; filled circles) and not the original baseline prior to TBS induction relative to untreated controls (open circles). (**A₂**) Summary bar plot highlighting the depression of fEPSPs induced by TBS and dopamine (filled bars) at three different time points (Baseline, Pre-DA, and Last 5-min) relative to time-matched controls (open bars). (**B₁**) The amplitude of fEPSPs following dopamine-mediated desensitisation of dopaminergic receptors and subsequent delivery of TBS (DA→TBS; filled circles) compared to untreated controls (open circles). Responses show that LTD is not induced by the tetanus when dopaminergic receptors are desensitised. (**B₂**) Summary bar plot highlighting the fEPSP depression (filled bars) at three different time points (Baseline, DA Wash and Last 5-min), relative to time-matched controls (open bars). (**C₁**) Data from **B₁** renormalised to 30-minutes prior to TBS induction to highlight the lack of fEPSP depression (filled circles) compared to untreated controls (open circles). Inset: representative fEPSP traces recorded before and after TBS induction. Numbered traces correspond to the numbers on the graph highlighting specific times during the experiment when the sample traces were recorded. (**C₂**) Summary bar plot highlighting the renormalised fEPSP depression (filled bars) at three different time points (Baseline, Post-TBS and Last 5-min) compared to time-matched controls (open bars). Scale Bar: 0.2 mv / 5 ms.*

In the previous experiment, dopamine was applied once at the start of testing to desensitise dopaminergic receptors. This was expected to have a similar effect as treating slices with various dopaminergic receptor antagonists to block their activity. In the next experiment, tetanic stimulation was delivered 15-minutes into a 30-minute bath application of a cocktail of both SCH-23390 (a D_1-like receptor antagonist; 50 μM) and sulpiride (a D_2-like receptor antagonist; 50 μM) to block both D_1-like receptors and D_2-like receptors, respectively (see **Table 2.1**). This was done to confirm the results of the previous desensitisation experiment, but this time in the presence of dopaminergic receptor antagonists. As shown in **Figure 6.7A**, delivery of TBS induces LTD in sensory inputs to the lateral entorhinal cortex as opposed to LTP (data shown in **Figure 6.7A** taken from **Figure 6.1A**). To test whether TBS was driving endogenous release of dopamine from dopaminergic fibres present in slices to constrain LTP induction and facilitate LTD induction, TBS was delivered 15-minutes into bath-application of both SCH-23390 and sulpiride. Interestingly, the combined antagonists did not block the long-term depression induced by tetanic stimulation (see **Figure 6.7B$_1$**). Synaptic responses were depressed significantly to 85.5 ± 6.4% of baseline relative to controls (104.4 ± 3.7% of baseline) during the last 5-min of the experiment (t_{15} = 2.642, P < 0.05, TBS n = 8, control n = 9; **Figure 6.7B$_2$**). Interestingly, the initial depression following delivery of the tetanus seems larger in **Figure 6.7B$_2$** compared to **Figure 6.7A$_1$**. This may be due to an antagonist-induced depression in the amplitude of fEPSPs. Note how responses started to depress about half-way into the application of the antagonists in **Figure 6.7B$_2$** and showed a partial recovery to the depressed level not observed in the control TBS condition (**Figure 6.7A$_1$**). These data are also not consistent with the desensitisation data shown in **Figure 6.6B-C** and the results suggest that TBS was ineffective at altering endogenous dopamine release to affect induction of LTD in the lateral entorhinal cortex. There are several explanations to account for the discrepancy in results. Firstly, desensitisation may be more effective than a cocktail of antagonists in blocking activity at dopamine-binding metabotropic receptors (see **Table 2.1**). Secondly, the concentrations of the antagonists used may not have been high enough to outcompete the bolus of dopamine released by tetanic stimulation for binding sites on the receptors. Regardless, additional work is required to determine whether dopaminergic signalling plays a role in the tetanus-induced LTD observed in the lateral entorhinal cortex.

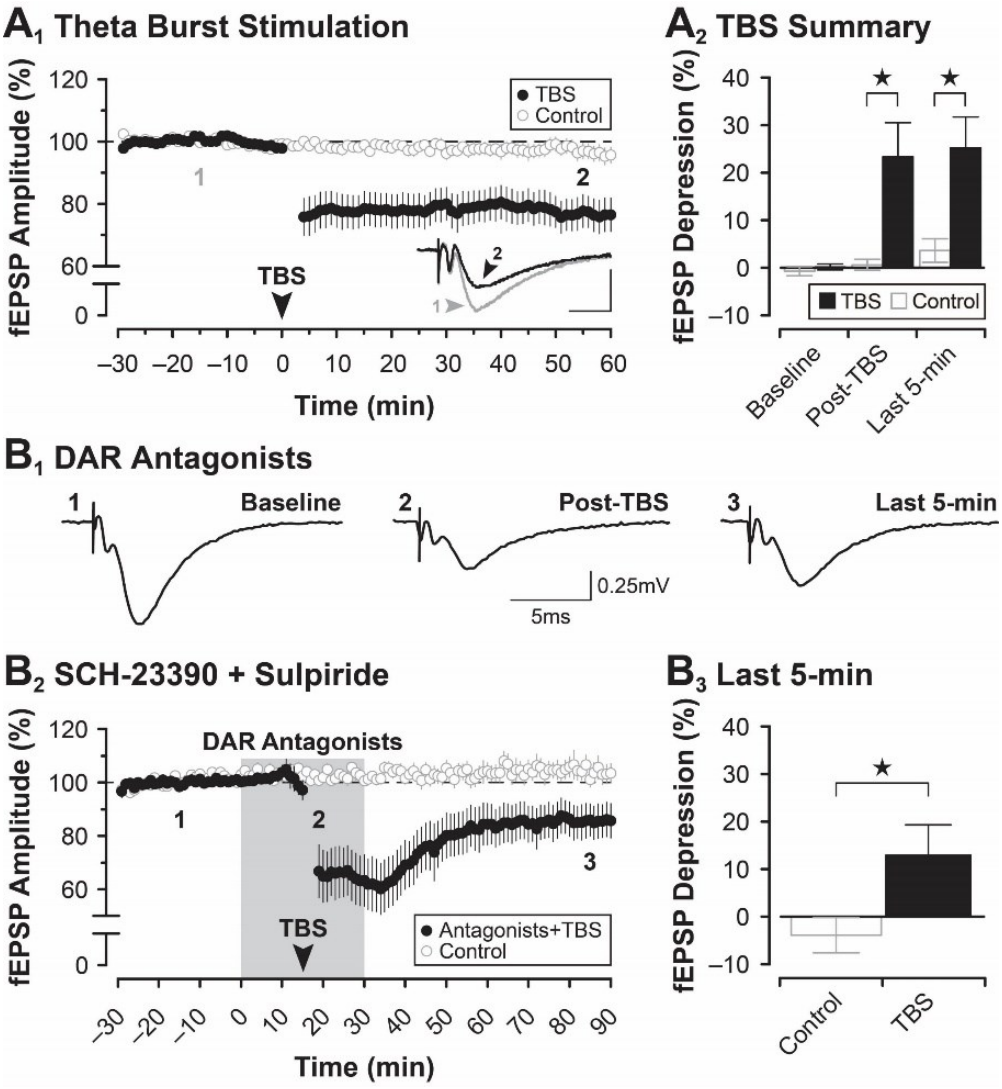

Figure 6.7. Blocking receptors with SCH-23390 and sulpiride has no effect on the LTD induced by TBS*. (**A₁-A₂**) Data from **Figure 6.1A₁-A₂** (identical conventions) highlighting the depression of fEPSPs induced by TBS in sensory inputs to the superficial layers of the lateral entorhinal cortex. (**B₁**) Representative fEPSP traces before and after the induction of TBS. Numbered traces in **B₁** correspond to the numbers in **B₂** highlighting the specific times during the experiments when these sample traces were recorded. (**B₂**) Applying specific D_1- and D_2-like dopamine receptor antagonists, sulpiride (50 µM) and SCH-23390 (50 µM), before, during and after delivery of TBS induces a lasting LTD of fEPSPs (filled circles) relative to untreated and unstimulated controls (open circles). (**B₃**) Quantification of the mean fEPSP suppression during the last 5-min comparing treated (filled bar) and untreated (open bar) conditions.*

Enhancing Excitability to Facilitate LTP Induction

Several factors, including tetanus-inducted changes in local inhibition and/or changes in dopaminergic-tone to affect glutamate release, may be working in parallel to *constrain* induction of LTP and *promote* induction of LTD in sensory inputs to the lateral entorhinal cortex. As such, treatments to overcome some of these suppressive constraints may help to increase excitability and facilitate successful induction of LTP using standard tetanic stimulation protocols. To determine whether induction of activity-dependent LTP could be augmented or enhanced in sensory inputs to the superficial layers of the lateral entorhinal cortex, tetanic stimulation was delivered at the end of a 30-minute application of the non-selective adenosine receptor antagonist, caffeine (300 µM). A 300 µM concentration was selected as it effectively binds to all adenosine receptor types with K_D values of 12, 2.4, 13 and 80 µM for A_1, A_{2A}, A_{2B} and A_3 receptors, respectively (see **Table 2.1**; Froestl, Muhs and

Pfeifer, 2012). Exposure to caffeine is one of very few experimental manipulations known to reliably potentiate basal synaptic transmission in the *lateral* entorhinal cortex (D Caruana unpublished observation), so potential synergistic effects between caffeine and induction of activity-dependent LTP were assessed. It was predicted that increasing synaptic excitability with caffeine would help boost NMDA receptor activation and promote induction of LTP following tetanic stimulation, rather than the induction of LTD. As shown in **Figure 6.8A$_1$**, bath-application of 300 μM caffeine on its own potentiated basal synaptic transmission in sensory inputs to the superficial layers of the lateral entorhinal cortex. The amplitude of fEPSPs were enhanced in the presence of the antagonist, and responses returned to baseline levels within about 10 to 15 minutes of washout (**Figure 6.8A$_1$**). During the peak facilitation, the amplitude of fEPSPs was enhanced significantly to 132.8 ± 10.4% of baseline relative to time-matched and untreated controls (100.8 ± 0.5% of baseline, $F_{2, 24} = 15.71$, $P < 0.0001$, Bonferroni $P < 0.05$, Caffeine $n = 4$, control $n = 10$; **Figure 6.8A$_2$**). In the next experiment, caffeine (300 μM) was applied once more for 30-minutes, but at the end of the application when responses were significantly enhanced by caffeine, TBS was delivered. Interestingly, synaptic responses were still depressed by the tetanus relative to controls despite being delivered during a period of enhanced transmission ($F_{2, 32} = 11.11$, $P < 0.001$, Bonferroni $P < 0.05$, treated $n = 8$, control $n = 10$; see **Figure 6.8B$_1$**). By the end of the experiment, responses were suppressed to 94.2 ± 6.3% of baseline relative to controls (104.7 ± 3.5% of baseline), but this depression was not statistically significant (Bonferroni $P = 0.522$), and the magnitude of this depression was significantly smaller than the LTD induced by TBS alone, $t_7 = 3.02$, $P < 0.05$ (compare **Figure 6.8B$_1$** to **Figure 6.1A$_1$**). Taken together, these results suggest that enhancing synaptic transmission with caffeine is enough to prevent the induction of LTD, however it may not be sufficient to augment excitability and promote induction of LTP in the lateral entorhinal cortex.

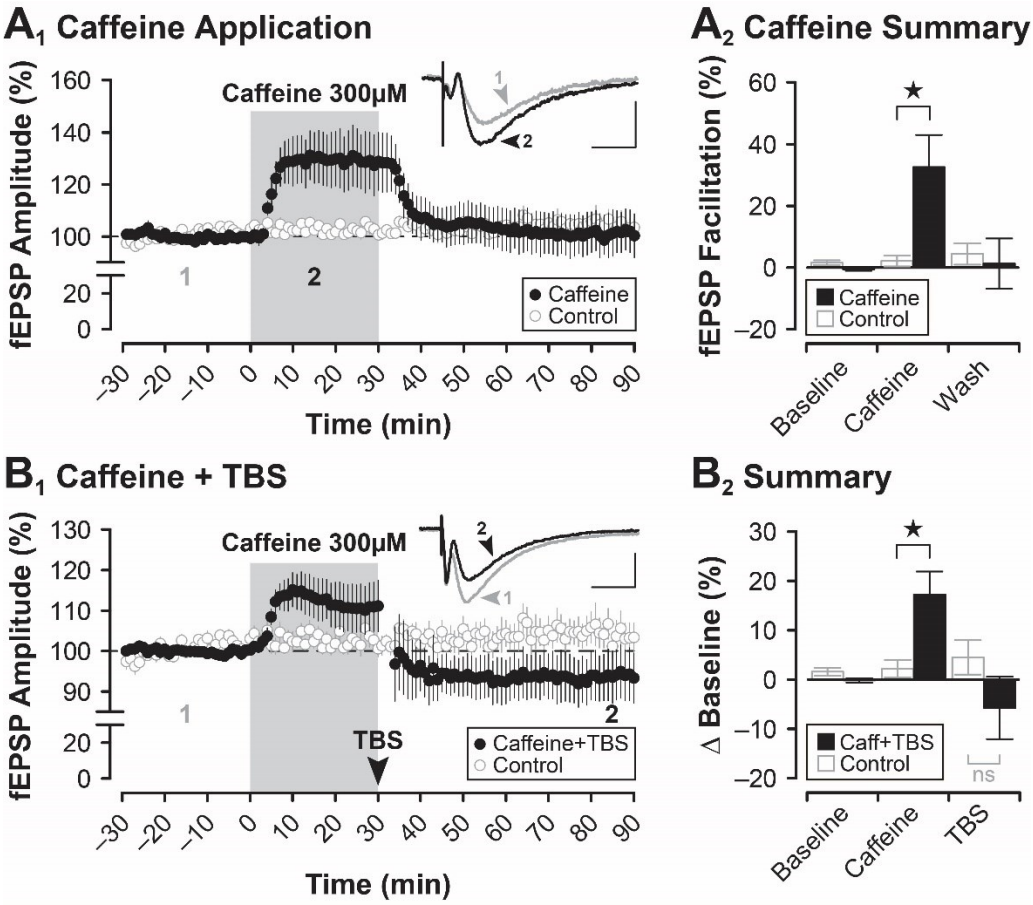

Figure 6.8. Enhancing synaptic excitability with caffeine does not promote induction of LTP in the lateral entorhinal cortex*. (**A₁**) Data highlighting the facilitation of fEPSPs induced by the broad-spectrum nonselective adenosine receptor antagonist, caffeine (300 µM; filled circles), relative to untreated controls (open circles). (**A₂**) Summary bar plot highlighting the facilitation of fEPSPs (filled bars) at three different time points (Baseline, Caffeine and Wash) compared to time-matched controls. (**B₁**) Potentiating fEPSP responses using 300 µM caffeine prior to TBS induction blocks LTD induction (filled circles) relative to untreated and unstimulated controls (open circles). (**B₂**) Bar plot summary highlighting the change in fEPSP amplitude relative to baseline (filled bars) at three different time points (Baseline, Caffeine and TBS) compared to controls. Insets for **A₁** and **B₁** show representative fEPSP traces recorded before and during bath-application of 300 µM caffeine (**A₁**) or before and after tetanic stimulation (**B₁**). Numbered traces correspond to the numbers on the respective data graphs highlighting specific times during the experiments when the sample traces were recorded. Scale Bar: 0.2 mV / 5 ms.*

The degree to which NMDA receptors are activated plays a critical role in determining whether certain forms of activity-dependent synaptic plasticity are induced successfully in the lateral entorhinal cortex. As shown previously in this thesis, dopamine-mediated changes in the release probability of glutamate can dramatically influence induction of LTD during PP-LFS (see **Figure 5.3B**). Similar constraints on NMDA receptor function may be at work here to shift the balance from LTP induction to LTD induction during tetanic stimulation of sensory inputs to the superficial layers. To target NMDA receptors more selectively and boost their function, experiments were performed in high calcium (elevated from 2 mM to 10 mM in the perfusate) before, during and after tetanic stimulation to induce LTP in the lateral entorhinal cortex. As shown in **Figure 6.9A₂**, delivery of TBS in high calcium ACSF induced a transient potentiation in the amplitude of fEPSPs in the lateral entorhinal cortex that decayed back to baseline levels by the end of the experiment. Indeed, immediately following delivery of TBS, responses were potentiated significantly to 123.3 ± 7.7% of baseline relative to time-matched and unstimulated controls (100.2 ± 1.3% of baseline, $F_{2,34}$ = 6.458, P < 0.01, Bonferroni P < 0.01, TBS n = 9, control n

= 10; **Figure 6.9B**). However, this potentiation did not persist past 40-minutes post-TBS, and responses returned to baseline levels by the end of the experiment (to 100.8 ± 3.8% of baseline, Bonferroni *P* = 1.00; **Figure 6.9B**). Although the potentiation induced by TBS only persisted for a short period of time, it was still the first time any activity-dependent potentiation was observed in sensory inputs to the lateral entorhinal cortex *in vitro* during experiments conducted as part of this thesis. These data suggest, then, that multiple factors may be working to constrain synaptic excitability and prevent activation of NMDA receptors to limit the induction and expression of activity-dependent LTP in the lateral entorhinal cortex. This is not the only possible explanation, since elevated calcium levels increase presynaptic neurotransmitter release, the results seen here could be due to a larger bolus of residual Ca^{2+} ions being present in extracellular space of the 10 mM solution compared to the 2 mM solution to occupy high-affinity calcium buffers in order to retain a high (net) level of freely available Ca^{2+} ions (Catterall and Few, 2008).

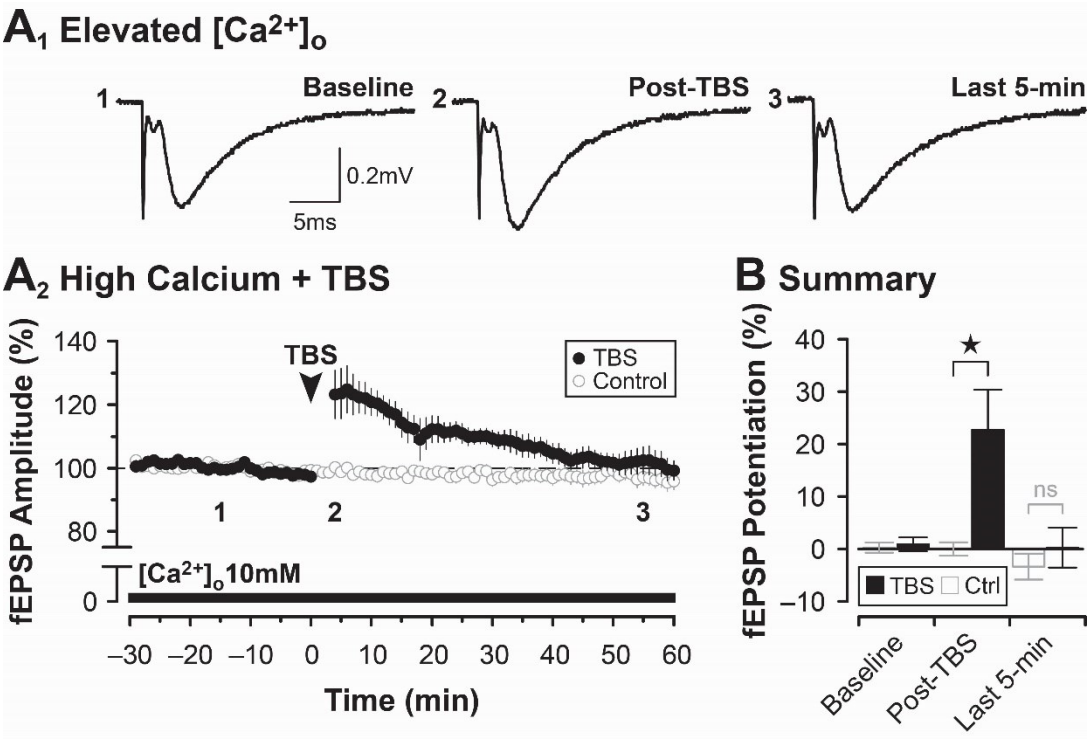

Figure 6.9. Increasing extracellular levels of calcium restores the ability to potentiate responses with tetanic stimulation in the lateral entorhinal cortex*. (**A₁**) Representative fEPSPs recorded before and after TBS induction. Numbered traces in **A₁** correspond to the numbers in **A₂** highlighting the specific times the traces were recorded during the experiment. (**A₂**) Delivery of TBS in high calcium (10 mM) induces a potentiation of synaptic responses that persists for around 40-minutes before returning to baseline (filled circles) relative to untreated controls (open circles). (**B**) Bar plot summary of the fEPSP potentiation (filled bars) at three different time point during the experiment (Baseline, Post-TBS and Last 5-min) relative to time-matched controls (open bars).*

Discussion

Throughout this thesis, as well as in previous literature, results highlight how sensory inputs to the superficial layers of the lateral entorhinal cortex can be modulated by a number of complex factors (de Curtis and Llinas, 1993; Caruana *et al.*, 2006; Liu, 2020; Vyleta and Snyder, 2021). Indeed, dopamine may have bidirectional and concentration-dependent effects on transmission (Caruana *et al.*, 2006), but at concentrations ≥100 µM dopamine triggers the internalisation of its own receptors with long-lasting and powerful effects on transmission (**Figure 4.2** and **Figure 4.3**). In Chapter 5 the results show that dopamine, when co-applied *during* PP-LFS induction, blocks induction of LTD (**Figure 5.2B$_1$-B$_2$**) likely through a mechanism involving a dopamine-mediated reduction in glutamate release from afferent sensory terminals (**Figure 5.2D**). This block of LTD is dopamine receptor-dependent since desensitising the receptors first prior to delivery of PP-LFS in the presence of the agonist reinstates induction (**Figure 5.3B$_1$**). Results of the current chapter build on the results of previous chapters and provide critical new insights into the properties of activity-dependent plasticity in the superficial layers. Although sensory inputs to the superficial layers of the lateral entorhinal cortex support LTP in awake and freely behaving rats *in vivo* (Caruana *et al.*, 2007), induction of LTP at these same synapses in brain slices maintained *in vitro* has proven to be surprisingly elusive. As a result, the priorities of this chapter had to change to focus on factors contributing to the limited induction and expression of LTP in the lateral entorhinal cortex. Virtually *every attempt* to induce LTP during experimental work conducted in this chapter failed (but see **Figure 6.9**). Interestingly, a consistent and long-lasting *depression* of synaptic transmission was induced instead (**Figure 6.1** and **Figure 6.2**). This form of LTD is both NMDA receptor-dependent and calcium-dependent (**Figure 6.3**). Recruitment of local inhibition during tetanic stimulation may play a significant role in limiting LTP induction (**Figure 6.5**), along with release of endogenous dopamine from preserved dopaminergic terminals in the slice triggered by the stimulation trains (**Figure 6.6B-C**). These factors may be working in parallel to *constrain* induction of LTP whilst simultaneously *promoting* induction of LTD in sensory inputs to the lateral entorhinal cortex. The common target underlying the shift in the direction of plasticity may be the NMDA receptor. The degree to which NMDA receptors are activated during tetanic stimulation will have a dramatic effect on levels of postsynaptic calcium and whether kinases or phosphatases are recruited. Tetanus-induced changes in local inhibition or in dopamine-mediated glutamate release have the potential to affect activation of NMDA receptors. Targeting NMDA receptors more selectively to boost their function directly by enhancing the ionic driving force acting on NMDA-mediated calcium transients (via high calcium in the bathing medium) was the only manipulation that was permissive in allowing tetanic stimulation to induce a potentiation of synaptic efficacy, and not LTD, in the lateral entorhinal cortex (**Figure 6.9**).

Activity-dependent forms of synaptic plasticity typically depend on activation of NMDA receptors (Alonso, de Curtis and Llinas, 1990; Hanse and Gustafsson, 1992; Kourrich and Chapman, 2003; Solger *et al.*, 2004; Deng and Lei, 2007), though a number of other factors have been shown to contribute. Results from a study utilising the isolated whole guinea pig brain preparation *ex vivo* showed that monosynaptic projections from the piriform (primary olfactory) cortex that synapse with superficial layer projection neurons in the lateral entorhinal cortex support both NMDA-dependent and NMDA-independent forms of synaptic plasticity. (de

Curtis and Llinas, 1993). Additionally, activity-dependent LTD in sensory inputs to the superficial layers of the *medial* entorhinal cortex *in vitro* are also NMDA receptor-dependent (Kourrich and Chapman, 2003). Results from Chapter 5 and Chapter 6 of this thesis highlight how activity-dependent forms of plasticity in the lateral division of the entorhinal cortex, such as PP-LFS LTD (**Figure 5.2C**) and tetanus-induced LTD (**Figure 6.3**), also depend on activation of NMDA receptors, though, it is important to note that this does preclude the existence of any non-NMDA-dependent factors from contributing to the induction of activity-dependent forms of plasticity in the superficial layers. In addition, the mechanisms involved in the expression of LTD may differ in the lateral entorhinal cortex. During experiments where TBS was administered 30-minutes before delivery of PP-LFS the results show mixed effects: TBS induced an initial depression that was not changed by the PP-LFS protocol (**Figure 6.4A**). These data suggest that the two forms of LTD recruit simialr mechanisms for their expression. However, it should be noted that a similar experiment where the order in which the stimulation protocols were delivered was reversed had a much different outcome. Specifically, the initial induction of LTD induced by PP-LFS occluded subsequent LTD induced by TBS and instead resulted in a linear increase in response amplitude to a significant level after 60 minutes (**Figure 6.4B**) suggesting expression of both forms of LTD involved a similar yet distinct underlying mechanism.

Induction of LTD in the lateral entorhinal cortex is both reliable and robust, but this is not the case for induction of LTP. The failure of tetanic stimulation to induce activity-dependent LTP at superficial layer synapses may be due constraints imposed by inhibitory interneurons present in the superficial layers (Nilssen *et al.*, 2018). Activation of local inhibitory networks during tetanic stimulation may play a role in constraining synaptic excitability to limit depolarisation and prevent activation of postsynaptic NMDA receptors required for induction of LTP. Indeed, although blocking fast inhibitory transmission with picrotoxin does not restore the capacity for superficial layer synapses to support LTP, it does prevent induction of LTD (see **Figure 6.5**). As such, it appears that superficial layer networks are downregulated during bursts of tetanic stimulation leading to changes in the direction of the plasticity induced. As noted above, induction of LTP is successful in piriform cortex inputs to the lateral division of the entorhinal cortex in awake rats *in vivo* (Caruana *et al*., 2007). This raises the question as to why LTP can be induced in the lateral entorhinal cortex *in vivo* but not in brain slices maintained *in vitro*. The reason for the discrepancy could simply be due to differences in inhibitory tone between the two experimental paradigms. In awake rats, levels of inhibition are likely very different than they are in slices prepared for *in vitro* recordings (Fischl and Weisz, 2020) with conditions much more favourable to induction of LTP. This is not to say that inhibition is the only factor critical to induction of LTP in the lateral entorhinal cortex. As Caruana *et al*. (2007) have shown, blocking the reuptake of dopamine with GBR12909 prevents induction of LTP. As such, dopamine also plays a key role in mediating activity-dependent synaptic plasticity in sensory inputs to the superficial layers. Another possible explanation to account for the lack of LTP in slices could be due to endogenous dopamine release during tetanic stimulation from dopaminergic fibres preserved in the parahippocampal slice preparation. Afferent dopaminergic fibres originating from the VTA are densely packed in layer I and layer II of the lateral entorhinal cortex (see **Figure 1.5**). Indeed, desensitising dopaminergic

receptors reverses the LTD induced by tetanic stimulation (**Figure 6.6B-C**) suggesting that dopamine may also play a role in limiting activity-dependent LTP in the lateral entorhinal cortex *in vitro*.

Very few manipulations enhance synaptic excitability in the lateral entorhinal cortex, with the only exception being the facilitation of synaptic responses by low concentrations of dopamine (1 to 10 µM; Caruana *et al*., 2006; Caruana and Chapman, 2008). Given that no facilitation of synaptic responses was observed at these concentrations in the present study (see **Figure 3.1**), additional methods had to be developed to overcome the suppressive constraints on activity-dependent plasticity to facilitate successful induction of LTP. To determine whether induction of activity-dependent LTP could be augmented or enhanced in sensory inputs to the superficial layers of the lateral entorhinal cortex, the nonselective adenosine receptor antagonist, caffeine, was used as a method to enhance synaptic transmission and boost excitability in lateral entorhinal cortex networks. Exposure to caffeine is one of very few experimental manipulations known to reliably potentiate basal synaptic transmission in the *lateral* entorhinal cortex (D Caruana unpublished observation), so potential synergistic effects between caffeine and induction of activity-dependent LTP were assessed. It has been shown previously that adenosine suppresses the excitability of LII stellate neurons in the medial division of the entorhinal cortex via activation of A_1 receptors (Li *et al.*, 2011). As such, blocking adenosine receptors with caffeine was predicted to have the opposite effect. In the current study 300 µM caffeine significantly enhanced synaptic transmission (see **Figure 6.8A**), however experiments have shown lower concentrations of caffeine were not sufficient to induce any change in fEPSP amplitude evoked in superficial layer neurons of the lateral entorhinal cortex (D Caruana unpublished observation). Caffeine (300 µM) was then used as a method to boost excitability and maximise NMDA receptor activation during tetanic stimulation to induce LTP. Unfortunately, this was not the case as tetanic stimulation induced LTD even though synaptic excitability had been augmented with caffeine (see **Figure 6.8B**) It is also important to note that caffeine has other targets at concentrations above 100 µM. Namely, it is able to increase calcium release from internal stores via activation of calcium channels on the endoplasmic reticulum and sarcoplasmic reticulum resulting in the efflux of calcium ions out of the cell to manipulate neurotransmission (Reddy *et al.*, 2024). Reddy *et al.* (2024) also report caffeine at 300 µM is able to act as an antagonist of $GABA_A$ receptors via weak binding to benzodiazepine receptors and via alterations of the chloride (Cl^-) ion transport function of these receptors (Cooper, Safran and Eberhardt, 2004). Indeed, both caffeine (300 µM) and picrotoxin (50 µM) are able to inhibit Cl^-linked $GABA_A$ receptors and results from **Figures 6.8B** and **6.5A$_1$** show a block in TBS-induced LTD when co-applied. It is important to consider the possibility that GABA receptors are involved in the induction and/or expression of TBS-induced LTD in the superficial layers of the lateral entorhinal cortex. Indeed, picrotoxin is specific to $GABA_A$ and $GABA_C$ receptors but it is not known to bind to $GABA_B$ at all, caffeine also doesn't bind to $GABA_B$ receptors. However, $GABA_{A\text{-}C}$ are all found in the entorhinal cortex (Couve, Moss and Pangalos, 2000; Deng *et al.*, 2009) and the activation of $GABA_B$ receptors elicits strong inhibitory control over superficial layer neurons in the medial entorhinal cortex via the same GPCR proteins as those linked to dopamine receptors (Deng *et al.*, 2009; Schwenk *et al.*, 2016; Porcu *et al.*, 2021). Future work would be needed to address the involvement of $GABA_B$ receptors in the suppression seen following theta-burst stimulation. Altogether, it may not be the direct effect of any one component on any one receptor

eliciting the results seen, instead, a complex multifactor mechanism could be at play here involving calcium and/or inhibitory control.

Hippocampal area CA2 is another brain region known to be resistant to activity-dependent LTP. More specifically, the Schaffer collateral projections that synapse onto the CA2 dendrites do not support induction of LTP (Zhao *et al*., 2007; Caruana, Alexander and Dudek, 2012; Dasgupta *et al*., 2020). Subsequent work by Simons *et al.* (2009) demonstrated that this resistance was due to the intrinsic capacity of CA2 neurons to buffer and extrude excessive amounts of intracellular calcium, such as those required to support induction of LTP. To overcome these mechanisms and facilitate induction of LTP in area CA2 of the hippocampus, Simons *et al*. (2009) performed slice experiments in high extracellular calcium to overwhelm the buffering and extrusion mechanisms in CA2 neurons and permit induction of NMDA-dependent LTP at Schaffer collateral synapses. A similar approach was undertaken in this current study. Indeed, increasing levels of extracellular calcium from 2 mM to 10 mM was sufficient to allow successful induction of a transient potentiation of synaptic responses in sensory inputs to the superficial layers of the lateral entorhinal cortex that persisted for about 40 minutes (see **Figure 6.9**). This potentiation of fEPSPs induced by tetanic stimulation in the presence of high concentration of extracellular calcium suggests that projection neurons in the superficial layers of the lateral entorhinal cortex may also be endowed with similar high intrinsic buffering and extrusion mechanisms to those observed in pyramidal neurons in area CA2 of the hippocampus (Simons *et al*., 2009). Further experimental work is required to uncover these mechanisms, but these results indicate that the lateral entorhinal cortex can, indeed, support LTP *in vitro*, and that many factors converge to constrain induction outright or toggle synapses to support LTD as opposed to LTP.

Chapter 7: General Discussion

The main aim of this thesis was to further the current knowledge and understanding of the modulation of synaptic function by dopamine in the superficial layers of the lateral entorhinal cortex and to achieve this, a series of objectives was set out (see 'Aims and objectives' in Chapter 1). The confirmation and extension of previous knowledge regarding dopaminergic function on basal synaptic transmission in the superficial layers of the lateral entorhinal cortex has been achieved here along with novel findings of a long-lasting reversible dopamine-mediated desensitisation of metabotropic receptors. By characterising this extremely robust dopamine-mediated desensitisation we were able to show it lasts between 60 and 180 minutes regardless of the presence or absence of basal synaptic transmission via a clathrin-mediated internalisation mechanism linked to the activation of β-arrestin. Further work is required to determine the precise receptors that are targeted since dopamine is not the only metabotropic receptor capable of internalisation mechanisms. Perhaps through targeted radioligand binding or fluorescence-linked immune assays with follow-up imaging techniques (Koenig, 2004) before and after dopamine-mediated desensitisation of the superficial layer neurons of the lateral entorhinal cortex would aid in the comparison of surface expression of specific receptors eliciting effects seen following desensitisation. The study then explored the properties of synaptic plasticity, including long-term depression and potentiation, in the superficial layer neurons of the lateral entorhinal cortex. This was achieved through a series of carefully designed electrophysiology experiments, which demonstrated that activity-dependent long-term depression elicited by PP-LFS is both reliable and readily induced. It is also shown that the PP-LFS induced LTD is dependent on NMDA receptor function and influenced heavily by the activation of dopamine-binding metabotropic receptors during induction. Interestingly this very similar to the properties of TBS-induced LTD, since LTP was not expressed in the superficial layers of the lateral entorhinal cortex by well-established electrical stimulation patterns (see **Figure 6.1**; Malenka, 1994; Malenka and Bear, 2004; Sigurdsson *et al.*, 2007; Citri and Malenka, 2008; O'Dell *et al.*, 2010; Kumar, 2011; Bassi *et al.*, 2019). Once it became apparent that the lateral entorhinal cortex is seemingly resistant to LTP *in vitro,* the objective transformed from investigating the properties of LTP, to investigating the properties of TBS-induced LTD and the *lack* of LTP. This was achieved following a series of strategically designed electrophysiological experiments to show TBS-induced LTD is reliant on NMDA receptors and the presence of calcium at the synapse and could be influenced by a change in GABAergic or dopaminergic tone. Investigating the role of dopamine in modulating PP-LFS- and TBS-induced LTD on the superficial layers of the lateral entorhinal cortex showed a direct interaction between suppression caused by dopamine and LTD. It went further to show that this interaction can be 'rescued' by desensitising the effected receptors using dopamine exposure prior to patterned stimulation protocols. Therefore, although the resulting receptors may not be dopaminergic themselves, they are readily influenced by changes in dopaminergic tone. Further work is needed to identify and characterise the exact receptors and mechanisms that are influencing the induction and expression of LTD via PP-LFS and TBS patterned stimulation,

perhaps via a multi-faceted approach incorporating ligand-binding assays with fluorescent imaging techniques at critical points during the experiment.

The entorhinal cortex plays a pivotal role in the formation of new memories by integrating sensory information, including olfactory, auditory and visual representations, and transmitting it through the hippocampal circuit (Burwell *et al.*, 2004; Deshmukh and Knierim, 2011). Dysfunction in the entorhinal cortex can lead to conditions such as medial temporal lobe epilepsy in humans (Bragin *et al.*, 1999; Kemppainen, Jolkkonen and Pitkanen, 2002; Thompson *et al.*, 2006; for review see Vismer *et al.*, 2015), and it is one of the first regions where neurons degenerate in the early stages of Alzheimer's dementia (Van Hoesen *et al.*, 2000). Recent evidence also suggests a correlation between maladaptive dopaminergic signalling in the entorhinal cortex and major depression (Thiele *et al*., 2016; Cook *et al*., 2017). Therefore, determining the factors influencing the excitability of entorhinal cortex projection neurons, as well as the mechanisms underlying the integration of sensory information within superficial layer circuits, is essential for understanding how the entorhinal cortex contributes to human cognition. Indeed, modulatory neurotransmitters are well-poised to play a strategic role in regulating both the integration and the propagation of all sensory signals that pass through both the medial and lateral divisions of the entorhinal cortex (Stanton and Sejnowski, 1989; for review see Burwell, 2000; Jones and McHugh, 2011; Knierim *et al*., 2014). Despite the well-established existence of dopaminergic projections to the superficial layers of the lateral entorhinal cortex (see **Figure 1.5**; Fallon , Koziell, and Moore, 1978; Swanson , 1982; Oades and Halliday, 1987), surprisingly little research has been undertaken to understand *why* dopaminergic fibres innervate this region (Akil and Lewis, 1994; Harvey, 2020), *how* dopamine modulates synaptic integration and neuronal excitability within the superficial layers, or *what* downstream effects this neuromodulation may induce on processing by targets in the hippocampus (see **Figure 1.2**; Burwell and Amaral, 1998b; Agster and Burwell, 2013; for review, see Jones and McHugh, 2011).

Results of this thesis suggest that the neurotransmitter dopamine may play a central role in regulating the integration of multimodal sensory inputs within lateral entorhinal cortex circuits to affect the propagation of highly processed sensory signals to the hippocampus during the encoding of new declarative memories. As noted, the lateral division of the entorhinal cortex receives dense dopaminergic innervation from the ventral tegmental area (**Figure 1.5**; Fallon , Koziell, and Moore, 1978; Swanson , 1982; Oades and Halliday, 1987), and previous research has shown that dopamine has powerful effects on the excitability and responsiveness of superficial layer projection neurons that provide the hippocampus with its primary source of sensory innervation (Caruana and Chapman, 2008; Harvey, 2020). In the current study, application of dopamine or apomorphine to parahippocampal slices of lateral entorhinal cortex maintained *in vitro* had potent *suppressive* effects on synaptic transmission across a wide range of concentrations (**Figure 3.4** and **Figure 3.6**), and this effect was mediated, in part, by a reduction in glutamate release from sensory afferent terminals that make synaptic contact with superficial layer neurons (**Figure 3.8B** and **Figure 3.9A**). High concentrations of dopamine caused a rapid and persistent desensitisation of dopamine-binding receptors (**Figure 4.1A**), and synapses exposed repeatedly to dopamine responded differentially to each successive exposure (**Figure 4.1B** and **Figure 4.2A**). This

desensitisation was dependent on activity of GRK2 to initiate β-arrestin-dependent desensitisation of metabotropic receptors, likely due to internalisation (**Figure 4.3** and **Figure 4.4)** to dramatically alter future responsivity of sensory synapses to the agonist. Interestingly, increasing dopaminergic tone during stimulation to induce activity-dependent LTD prevented its induction (**Figure 5.2B**), and this was caused by a dopamine-induced change in the release probability of glutamate from presynaptic terminals on sensory afferents projecting to the superficial layers (**Figure 5.2D**). When attempting to assess potential interactions between dopamine and glutamate-mediated LTP in the lateral entorhinal cortex it was observed that superficial layer projection neurons were *resistant* to the induction of LTP, and that tetanic stimulation induced a rapid form of NMDAR- and calcium-dependent LTD instead of LTP (**Figure 6.1**, **Figure 6.2** and **Figure 6.3**). Inhibition of glutamatergic (**Figure 6.5**) tone and elevations in dopaminergic (**Figure 6.6**) tone were shown to play a permissive role in the induction of this novel form of LTD, and the short-term excitability of basal synaptic transmission following high-frequency stimulation in the lateral entorhinal cortex could be partly rescued by increasing the concentration of calcium in the bathing medium (**Figure 6.9**). Taken together, the findings of this thesis point to multiple mechanisms through which exposure to dopamine may modulate sensory and mnemonic processing in the medial temporal lobe by regulating basal synaptic transmission and activity-dependent plasticity in the lateral entorhinal cortex.

No Evidence for Bidirectional Effects of Dopamine on Synaptic Transmission

The findings of this thesis align closely with existing literature (Caruana *et al.*, 2006; Caruana *et al.*, 2007; Caruana and Chapman, 2008) and substantially enhance our understanding of how dopamine influences basal synaptic function and plasticity in the lateral entorhinal cortex. A notable inconsistency identified in the current results, which differs markedly from previous studies, is that dopamine suppressed basal synaptic transmission at *every* concentration tested. (see **Figure 3.4**). Previously, dopamine has been shown to have concentration-dependent and *bidirectional* effects on synaptic transmission in sensory inputs to the superficial layers of the lateral entorhinal cortex (Caruana *et al.*, 2006; Caruana and Chapman, 2008; Glovaci, Caruana and Chapman, 2014). Specifically, high concentrations of dopamine (50 to 100 µM) suppressed responses whereas low concentrations (1 to 10 µM) significantly enhanced them. This bidirectionality in responsiveness to dopamine was thought to be a hallmark feature of the neurotransmitter in the region. There could be several reasons for this disparity. Firstly, the species of rats used between studies differed, and previous research has shown that performance on spatial and non-spatial learning and memory tasks varies significantly between different rodent species (Harker and Whishaw, 2002). As such, dopamine may have differential effects on transmission depending on the species from which the brain slices were prepared. Secondly, the slices used in the current thesis were obtained from rats that were much younger than those used by Caruana *et al.* (2006), and previous work has shown that the maturation of ionotropic glutamate receptors differs depending on the age of the animal (Andersen *et al*., 2007; for review see Egbenya, Aidoo and Kyei, 2021). Finally, recordings by Caruana *et al.* (2006) were performed at room temperature (around 20 °C). In contrast, the current study was performed

on slices maintained closer to physiological temperature (30 to 32 °C). Changes in bath temperature during slice recording experiments can elicit differential effects on synaptic responses when using the same drug. For example, in area CA1 of the hippocampus, the synthetic cannabinoid, WIN55,212-2, was shown to selectively inhibit paired-pulse depression of population spikes when recorded at 28 to 30 °C. However, the same drug elicited the opposite effect at a much higher temperature (35 °C; Al-Hayani and Davies, 2002). It was proposed that the reversal of cannabinoid influence on paired-pulse depression was due to an increase in GABA uptake at higher bath temperatures (Al-Hayani and Davies, 2002). As such, differences in any one of these key parameters may account for the discrepancy in the results observed between studies.

Resistance to Activity-Dependent LTP

Another interesting finding to come from this thesis is the observation that superficial layer projection neurons in the lateral entorhinal cortex are seemingly *resistant* to induction of activity-dependent LTP. This is notable for two reasons. Firstly, there are relatively few regions of the brain that are resistant to activity-dependent forms of LTP, one is the cerebellum (Frisch *et al.*, 2000; Locatelli *et al*., 2001; for review see Hansel, Linden and D'Angelo, 2001), and another is area CA2 of the hippocampus (Zhao *et al.*, 2007; Simons *et al.*, 2009; Caruana, Alexander and Dudek, 2012). Secondly, tetanic stimulation induced a novel form of NMDAR- and calcium-dependent LTD in the lateral entorhinal cortex. The same brief tetanic stimulation protocols used elsewhere to induce LTP (Chapman, Perez and Lacaille, 1998; Yun, Mook-Jung and Jung, 2002; Park *et al.*, 2014; Locatelli *et al.*, 2021) reliably induced LTD in the lateral entorhinal cortex instead. Typically, induction of canonical activity-dependent LTD requires repetitive low frequency stimulation delivered over many minutes (Stanton and Sejnowski, 1989; Tsumoto, 1990; Caruana, Warburton and Bashir, 2011; for review see Malenka and Bear, 2004). The LTD induced by tetanic stimulation in the lateral entorhinal cortex is enigmatic for just how *rapidly* it can be induced – a single train delivered at 200 Hz is sufficient for induction (see **Figure 6.1B**). This may represent a novel form of LTD in the entorhinal cortex that is completely unique to the lateral division. It is also possible that superficial layer projection neurons possess specific physiological adaptations that render them immune to LTP and more susceptible to LTD. In the hippocampus, previous research has shown that CA2 pyramidal neurons are resistant to activity-dependent LTP because of their intrinsic capacity to buffer and extrude excessive amounts of intracellular calcium (Simons *et al.*, 2009). To overcome these mechanisms and facilitate induction of LTP in area CA2 of the hippocampus, Simons *et al.* (2009) performed slice experiments in high extracellular calcium to overwhelm the buffering and extrusion mechanisms to facilitate induction of NMDA-dependent LTP at Schaffer collateral synapses. A similar approach was undertaken in this current study and a transient potentiation of synaptic responses in sensory inputs to the superficial layers of the lateral entorhinal cortex was induced that persisted for about 40 minutes (see **Figure 6.9**). Although it is tempting to conclude that *all* projection neurons in the lateral entorhinal cortex possess similar calcium handling mechanisms as CA2 neurons to limit plasticity, it is unlikely given the diverse array of neuronal phenotypes expressed in the superficial layers (see **Figure 3.1** and **Figure 3.2**). Indeed, some neurons may possess such

intrinsic adaptations, but a more reasonable explanation may be that a combination of factors, including tetanus induced changes in local inhibition and endogenous levels of dopamine, function to limit plasticity in the lateral entorhinal cortex.

Dopamine-Mediated Desensitisation of Dopaminergic Receptors

A noteworthy discovery in this thesis is the demonstration of how prior dopaminergic activity at synapses in the superficial layers of the lateral entorhinal cortex can influence dopamine's future ability to modulate transmission at these same synapses (see **Figure 4.1** and **Figure 4.2**). Prolonged exposure to dopamine and the subsequent desensitisation of dopaminergic receptors can have potent effects on any dopamine-dependent modulation of synaptic function long after the initial exposure. This phenomenon stems from a dopamine-mediated desensitisation of dopamine-binding receptors, suggestive of a novel form of metaplasticity in the region. Traditionally, metaplasticity refers to alterations in activity-dependent synaptic plasticity following previous synaptic activity at the same synapses, such as subthreshold stimulation (Abraham and Bear, 1996). The results of this thesis demonstrate that alterations in the surface expression of dopaminergic receptors are sufficient to yield comparable outcomes.

In the lateral entorhinal cortex, it is likely that the dopamine-mediated desensitisation is expressed partly by the internalisation of D_2-like dopaminergic receptors (see **Figure 3.12C**). Activation of D_2 receptors by dopamine, when the receptors are in their naïve and non-desensitised state, results in a D_2 receptor-mediated reduction in glutamate release and a net suppression of synaptic transmission. However, if those same synapses had been exposed to a moderate concentration of dopamine within the past hour, some of the receptors would have become desensitised, thereby reducing the overall magnitude of subsequent dopamine-mediated suppression of synaptic transmission. Endogenous fluctuations in dopaminergic tone can be based on multiple factors and expressed by either tonic or phasic release of dopamine from terminals in various target regions (Grace, 1991). In awake rats, for example, extracellular concentrations of dopamine in the lateral entorhinal cortex vary depending on the intrinsic and extrinsic factors affecting behavioural state (Caruana *et al.*, 2006). In this way, past exposure to dopamine has the potential to affect dopamine's future ability to modulate synaptic function during behaviours that engage mesocortical inputs to the lateral entorhinal cortex.

Dopamine, the Lateral Entorhinal Cortex and Affective Disorders

In humans, the entorhinal cortex is the first structure to show evidence of degeneration in Alzheimer's dementia and this suggests that the cognitive impairments associated with the onset of the disease result, in part, from a loss of cells in this region (Van Hoesen *et al.*, 2000). The degeneration of neurons in the entorhinal cortex effectively isolates the hippocampus from its cortical sensory input and this has profound consequences for sensory and mnemonic processing. Interestingly, the deterioration of the entorhinal cortex in Alzheimer's

dementia typically occurs in a laminar fashion with neurofibrillary tangles first appearing in layer II during the initial stages of the disease and then progressing to the deeper layers as the pathology worsens (Beall and Lewis, 1992; for review see Fu, Hardy and Duff, 2018). The initial degeneration observed in layer II may underlie the early cognitive impairments associated with the disease because it is layer II neurons that give rise to the perforant path projection to the hippocampus thereby providing the hippocampal formation with the bulk of its sensory innervation. Similar memory impairments are also observed in other neurodegenerative disorders that have effects on the entorhinal cortex, including argyrophilic grain disease and Pick's disease (Dickson, 1998; Ferrer, Santpere and van Leeuwen, 2008). Initial memory impairments linked to entorhinal cortex dysfunction may result, in part, from disease-related changes in midbrain dopaminergic signalling, or possibly via acetylcholine receptor signalling, in the superficial layers of the lateral entorhinal cortex.

Interestingly, evidence is mounting that dopaminergic signalling in the entorhinal cortex may be impaired in affective disorders, such as major depression, and that this impairment is linked to some of the sensory, cognitive and hedonic symptoms indicative of the disorder (Thiele *et al.*, 2016; Cook *et al.*, 2017). A recent study used small animal PET imaging to assess regional glucose metabolism (a reliable marker of neuronal activity) in the temporal lobes of a valid and well-characterised model of human depression, the Flinders Sensitive Line (FSL) rat (Overstreet and Wegener, 2013; Thiele *et al.*, 2016). The results showed that there was a significant and persistent *hypometabolism* observed in the entorhinal cortex, and this underlying change in neural activity was related to long-term deficits in memory acquisition and consolidation in FSL rats (Thiele *et al.*, 2016). Moreover, a subsequent study by the same group showed that FSL rats suffered from impaired olfactory processing and were less motivated to explore novelty, both indicative of a dysfunctional entorhinal cortex linked to depression (Cook *et al.*, 2017). Taken together, the findings of these two reports suggest that the hypometabolism and downregulation of entorhinal cortex function observed in FSL rats underlies the detrimental effects on olfactory sensory processing and memory encoding mediated by the entorhinal cortex, and alterations in basal dopaminergic signalling in FSL rats may play a significant *causal* role.

Major depressive disorder is one of the most common psychiatric diseases affecting roughly 250-310 million people worldwide (Evaluation., 2019). The disease is characterised by a diverse range of symptoms, such as loss of interest in most activities, anhedonia, feelings of despair and hopelessness, pervasive pessimism about the future, and suicidal thoughts or tendencies. Established treatments, including psychotherapy, electroconvulsive therapy and pharmacological treatment, are known to be effective in only about 80% of patients, and novel experimental approaches, such as deep brain stimulation, have been shown to produce symptomatic relief among formally treatment-resistant and depressed individuals (Overstreet and Wegener, 2013; Thiele *et al.*, 2016). In preclinical settings, several animal models for depression have been developed that have been central to increasing understanding of the brain systems, receptor substrates and signalling pathways linked to the disease. Since the initial conception of the strain, Flinders Sensitive Line (FSL) rats have been used extensively as a valid animal model of depression (Overstreet and Wegener, 2013; Thiele *et al.*, 2016; Cook *et al.*, 2017). Physiological factors associated with clinical depression displayed by FSL rats include decreased BDNF

levels in the hippocampus, reduced serotonin synthesis, changes in basal levels of serotonin and dopamine in the nucleus accumbens, altered neuropeptide Y levels, and a hyperactive hypothalamic-pituitary-adrenal stress axis (Overstreet and Wegener, 2013). Key behavioural deficits and changes seen in the FSL strain include reduced mobility in the Forced Swim Test and Open Field Test, reduced appetite and weight, altered sleep patterns, increased passive response to stress, increased aggression, and immune abnormalities that are observed in depressed individuals (Overstreet and Wegener, 2013; Thiele *et al.*, 2016; Cook *et al.*, 2017). Thus, the FSL rat model of depression exhibits many behavioural, neurochemical and pharmacological features that have been reported in depressed individuals, and FSL rats have been extremely effective in studies assessing the effectiveness of novel antidepressant drugs currently under active development. As such, future experimental work should utilise this well-defined and validated animal model of brain disease to increase understanding of the role the entorhinal cortex plays in the aetiology of major depression.

Depression is a heterogeneous mental disorder covering a multitude of symptoms. Different neurotransmitters and neurocircuitry contribute to its pathology and its expression. As anhedonia and the lack of motivation are key symptoms of depression, the reward system, and in particular the function and regulation of the ventral tegmental area's ascending dopaminergic projections via the medial forebrain bundle to the nucleus accumbens and the prefrontal cortex, have come into the spotlight recently (Thiele *et al.*, 2016). Very little is known, though, regarding the role these same dopaminergic inputs to the entorhinal cortex may play in affective or neurodegenerative disorders. Given the anatomical connectivity between the ventral tegmental area and entorhinal cortex, midbrain dopaminergic inputs to the lateral entorhinal cortex are well-poised to modulate the output activity of the lateral entorhinal cortex (Akil and Lewis, 1994; Caruana *et al.*, 2006; Caruana and Chapman, 2008; Glovaci, Caruana and Chapman, 2014). However, it is currently unknown whether it is an underlying dysfunction in ventral tegmental area projections to target structures, including the entorhinal cortex, that affects dopamine release or a primary pathology in how entorhinal cortex neurons respond to dopaminergic signals that contributes to the hypometabolism observed in the entorhinal cortex of FSL rats. The putative interplay between the ventral tegmental area and entorhinal cortex, in the context of models of depression, remain to be determined.

Cognitive disturbances in depressed individuals can involve both learning difficulties and memory loss, and memory impairments on tasks which depend on the entorhinal cortex are observed in FSL rats (Cook *et al.*, 2017). The entorhinal cortex and hippocampus are involved in numerous cognitive functions, including spatial navigation, memory acquisition and memory consolidation (Caruana *et al.*, 2006; Caruana and Chapman, 2008; Deshmukh and Knierim, 2011; Glovaci, Caruana and Chapman, 2014). More specifically, the entorhinal cortex encodes general spatial/directional/temporal data, but also data about the objects/items in the immediate environment (Deshmukh and Knierim, 2011). These streams of information are then relayed to the hippocampus which links it together with data pertaining to spatial and temporal context (Deshmuk and Knierim, 2011; Burwell, 2000). Communication and information flow between the entorhinal cortex and hippocampus is essential, and any dysfunction in this process will have immediate and short-term implications on behavioural

output, as well as on long-term information processing, including the formation of new declarative memories. The results of this thesis provide further evidence to show how dopamine contributes to the physiology underlying these important cognitive functions.

Pharmacological treatments that are effective in producing relief in individuals suffering from major depression typically target the serotonergic and noradrenergic systems, but as noted above recent work has shifted focus to include the diffuse dopaminergic neuromodulatory system, too. Despite the array of commercially-available antidepressant drugs, the search for novel therapeutic targets and specific drugs remains of critical importance for several reasons: (1) most depressed patients are not adequately treated with a single drug therapy; (2) current antidepressants, even when effective, are often discontinued because of unpleasant side effects, including sexual dysfunction, nausea, weight gain and precipitation of a manic phase; (3) current antidepressants have a slow onset of a clinical response (2 to 4 weeks) that prolongs suffering and can result in dire consequences for patients with suicidal thoughts; and (4) all antidepressants currently carry a warning for their ability to increase suicidal thoughts in a small percentage of adolescents and young adults. The findings of this current thesis may provide a novel therapeutic target – *the lateral entorhinal cortex* – to help drive future drug development and discovery in the treatment of major depression.

Bibliography

Abraham, W. C. 2008. Metaplasticity: tuning synapses and networks for plasticity. *Nat Rev Neurosci,* 9**,** 387.

Abraham, W. C. & Bear, M. F. 1996. Metaplasticity: the plasticity of synaptic plasticity. *Trends Neurosci,* 19**,** 126-30.

Abraham, W. C., Logan, B., Greenwood, J. M. & Dragunow, M. 2002. Induction and experience-dependent consolidation of stable long-term potentiation lasting months in the hippocampus. *J Neurosci,* 22**,** 9626-34.

Abraham, W. C., Mason-Parker, S. E. & Logan, B. 1996. Low-frequency stimulation does not readily cause long-term depression or depotentiation in the dentate gyrus of awake rats. *Brain Res,* 722**,** 217-21.

Adell, A. 2020. Brain NMDA Receptors in Schizophrenia and Depression. *Biomolecules,* 10.

Agster, K. L. & Burwell, R. D. 2013. Hippocampal and subicular efferents and afferents of the perirhinal, postrhinal, and entorhinal cortices of the rat. *Behav Brain Res,* 254**,** 50-64.

Aittoniemi, J., Jensen, M. O., Pan, A. C. & Shaw, D. E. 2023. Desensitization dynamics of the AMPA receptor. *Structure,* 31**,** 724-34.

Akaike, N., Hattori, K., Oomura, Y. & Carpenter, D. O. 1985. Bicuculline and picrotoxin block gamma-aminobutyric acid-gated Cl- conductance by different mechanisms. *Experientia,* 41**,** 70-1.

Akil, M. & Lewis, D. A. 1994. The distribution of tyrosine hydroxylase-immunoreactive fibers in the human entorhinal cortex. *Neuroscience,* 60**,** 857-74.

Al-Hasani, R., Foster, J. D., Metaxas, A., Ledent, C., Hourani, S. M., Kitchen, I. & Chen, Y. 2011. Increased desensitization of dopamine D(2) receptor-mediated response in the ventral tegmental area in the absence of adenosine A(2A) receptors. *Neuroscience,* 190**,** 103-11.

Al-Hayani, A. & Davies, S. N. 2002. Effect of cannabinoids on synaptic transmission in the rat hippocampal slice is temperature-dependent. *Eur J Pharmacol,* 442**,** 47-54.

Alcaro, A., Huber, R. & Panksepp, J. 2007. Behavioral functions of the mesolimbic dopaminergic system: an affective neuroethological perspective. *Brain Res Rev,* 56**,** 283-321.

Alonso, A., De Curtis, M. & Llinas, R. 1990. Postsynaptic Hebbian and non-Hebbian long-term potentiation of synaptic efficacy in the entorhinal cortex in slices and in the isolated adult guinea pig brain. *Proc Natl Acad Sci USA,* 87**,** 9280-4.

Amaral, D. G. & Witter, M. P. 1995. Hippocampal Formation. *In:* Paxinos, G. (ed.) *The Rat Nervous System.* 2nd ed. London: Academic Press.

Andersen, P., Morris, R., Amaral, D., Bliss, T. & O'keefe, J. 2007. *The hippocampus book,* Oxford; New York, Oxford University Press. pp. 17-9, 213-4, 224, 410.

Ang, Z. Y., Boddy, M., Liu, Y. & Sunderland, B. 2016. Stability of apomorphine in solutions containing selected antioxidant agents. *Drug Des Devel Ther,* 10**,** 3253-65.

Annese, J., Schenker-Ahmed, N. M., Bartsch, H., Maechler, P., Sheh, C., Thomas, N., Kayano, J., Ghatan, A., Bresler, N., Frosch, M. P., Klaming, R. & Corkin, S. 2014. Postmortem examination of patient H.M.'s brain based on histological sectioning and digital 3D reconstruction. *Nat Commun,* 5**,** 3122.

Arbuthnott, G. W. & Wickens, J. 2007. Space, time and dopamine. *Trends Neurosci,* 30**,** 62-9.

Arroyo-Garcia, L. E., Vazquez-Roque, R. A., Diaz, A., Trevino, S., De La Cruz, F., Flores, G. & Rodriguez-Moreno, A. 2018. The Effects of Non-selective Dopamine Receptor Activation by Apomorphine in the Mouse Hippocampus. *Mol Neurobiol,* 55**,** 8625-36.

Arshadi, C., Gunther, U., Eddison, M., Harrington, K. I. S. & Ferreira, T. A. 2021. SNT: a unifying toolbox for quantification of neuronal anatomy. *Nat Methods,* 18**,** 374-7.

Artola, A. & Singer, W. 1987. Long-term potentiation and NMDA receptors in rat visual cortex. *Nature,* 330**,** 649-52.

Atkinson, R. C. & Shiffrin, R. M. 2024. Reprint of: Human memory: A proposed system and its control processes. *J. Mem. Lang.,* 136.

Avital, A., Ram, E., Maayan, R., Weizman, A. & Richter-Levin, G. 2006. Effects of early-life stress on behavior and neurosteroid levels in the rat hypothalamus and entorhinal cortex. *Brain Res Bull,* 68**,** 419-24.

Baez, M. V., Cercato, M. C. & Jerusalinsky, D. A. 2018. NMDA Receptor Subunits Change after Synaptic Plasticity Induction and Learning and Memory Acquisition. *Neural Plast,* 2018**,** 5093048.

Baiano, M., Perlini, C., Rambaldelli, G., Cerini, R., Dusi, N., Bellani, M., Spezzapria, G., Versace, A., Balestrieri, M., Mucelli, R. P., Tansella, M. & Brambilla, P. 2008. Decreased entorhinal cortex volumes in schizophrenia. *Schizophr Res,* 102**,** 171-80.

Barrios, F. A., Gonzalez, L., Favila, R., Alonso, M. E., Salgado, P. M., Diaz, R. & Fernandez-Ruiz, J. 2007. Olfaction and neurodegeneration in HD. *Neuroreport,* 18**,** 73-6.

Barron, H. C. 2020. Neural inhibition for continual learning and memory. *Curr Opin Neurobiol,* 67**,** 85-94.

Bashir, Z. I., Bortolotto, Z. A., Davies, C. H., Berretta, N., Irving, A. J., Seal, A. J., Henley, J. M., Jane, D. E., Watkins, J. C. & Collingridge, G. L. 1993a. Induction of LTP in the hippocampus needs synaptic activation of glutamate metabotropic receptors. *Nature,* 363**,** 347-50.

Bashir, Z. I., Jane, D. E., Sunter, D. C., Watkins, J. C. & Collingridge, G. L. 1993b. Metabotropic glutamate receptors contribute to the induction of long-term depression in the CA1 region of the hippocampus. *Eur J Pharmacol,* 239**,** 265-6.

Bassi, M. S., Iezzi, E., Gilio, L., Centonze, D. & Buttari, F. 2019. Synaptic Plasticity Shapes Brain Connectivity: Implications for Network Topology. *Int J Mol Sci,* 20.

Basu, J., Zaremba, J. D., Cheung, S. K., Hitti, F. L., Zemelman, B. V., Losonczy, A. & Siegelbaum, S. A. 2016. Gating of hippocampal activity, plasticity, and memory by entorhinal cortex long-range inhibition. *Science,* 351.

Batallan-Burrowes, A. A. & Chapman, C. A. 2018. Dopamine suppresses persistent firing in layer III lateral entorhinal cortex neurons. *Neurosci Lett,* 674**,** 70-4.

Beall, M. J. & Lewis, D. A. 1992. Heterogeneity of layer II neurons in human entorhinal cortex. *J Comp Neurol,* 321**,** 241-66.

Beaulieu, J. M., Espinoza, S. & Gainetdinov, R. R. 2015. Dopamine receptors - IUPHAR Review 13. *Br J Pharmacol,* 172**,** 1-23.

Beaulieu, J. M. & Gainetdinov, R. R. 2011. The physiology, signaling, and pharmacology of dopamine receptors. *Pharmacol Rev,* 63**,** 182-217.

Beautrait, A., Paradis, J. S., Zimmerman, B., Giubilaro, J., Nikolajev, L., Armando, S., Kobayashi, H., Yamani, L., Namkung, Y., Heydenreich, F. M., Khoury, E., Audet, M., Roux, P. P., Veprintsev, D. B., Laporte, S. A. & Bouvier, M. 2017. A new inhibitor of the beta-arrestin/AP2 endocytic complex reveals interplay between GPCR internalization and signalling. *Nat Commun,* 8.

Behuet, S., Cremer, J. N., Cremer, M., Palomero-Gallagher, N., Zilles, K. & Amunts, K. 2019. Developmental Changes of Glutamate and GABA Receptor Densities in Wistar Rats. *Front Neuroanat,* 13**,** 100.

Beneyto, M., Kristiansen, L. V., Oni-Orisan, A., Mccullumsmith, R. E. & Meador-Woodruff, J. H. 2007. Abnormal glutamate receptor expression in the medial temporal lobe in schizophrenia and mood disorders. *Neuropsychopharmacology,* 32**,** 1888-902.

Bertolino, M., Vicini, S. & Costa, E. 1989. Kynurenic acid inhibits the activation of kainic and N-methyl-D-aspartic acid-sensitive ionotropic receptors by a different mechanism. *Neuropharmacology,* 28**,** 453-7.

Besnard, J., Ruda, G. F., Setola, V., Abecassis, K., Rodriguiz, R. M., Huang, X. P., Norval, S., Sassano, M. F., Shin, A. I., Webster, L. A., Simeons, F. R., Stojanovski, L., Prat, A., Seidah, N. G., Constam, D. B., Bickerton, G. R., Read, K. D., Wetsel, W. C., Gilbert, I. H., Roth, B. L. & Hopkins, A. L. 2012. Automated design of ligands to polypharmacological profiles. *Nature,* 492**,** 215-20.

Blanke, M. L. & Van Dongen, A. M. J. 2009. Activation Mechanisms of the NMDA Receptor. *In:* Van Dongen, A. M. (ed.) *Biology of the NMDA receptor.* Boca Raton, Florida: CRC Press/Taylor & Francis.

Bliss, T. V. & Collingridge, G. L. 1993. A synaptic model of memory: long-term potentiation in the hippocampus. *Nature,* 361**,** 31-9.

Bliss, T. V. & Gardner-Medwin, A. R. 1973. Long-lasting potentiation of synaptic transmission in the dentate area of the unanaestetized rabbit following stimulation of the perforant path. *J Physiol,* 232**,** 357-74.

Bliss, T. V., Lancaster, B. & Wheal, H. V. 1983. Long-term potentiation in commissural and Schaffer projections to hippocampal CA1 cells: an in vivo study in the rat. *J Physiol,* 341**,** 617-26.

Bliss, T. V. & Lomo, T. 1973. Long-lasting potentiation of synaptic transmission in the dentate area of the anaesthetized rabbit following stimulation of the perforant path. *J Physiol,* 232**,** 331-56.

Boling, W. W. 2018. Surgical Considerations of Intractable Mesial Temporal Lobe Epilepsy. *Brain Sci,* 8.

Bourne, J. A. 2001. SCH 23390: the first selective dopamine D1-like receptor antagonist. *CNS Drug Rev,* 7**,** 399-414.

Boyson, S. J., Mcgonigle, P. & Molinoff, P. B. 1986. Quantitative autoradiographic localization of the D1 and D2 subtypes of dopamine receptors in rat brain. *The Journal of Neuroscience,* 6**,** 3177-88.

Bozzi, Y. & Borrelli, E. 2013. The role of dopamine signaling in epileptogenesis. *Front Cell Neurosci,* 7**,** 157.

Bragin, A., Engel, J., Jr., Wilson, C. L., Fried, I. & Mathern, G. W. 1999. Hippocampal and entorhinal cortex high-frequency oscillations (100--500 Hz) in human epileptic brain and in kainic acid--treated rats with chronic seizures. *Epilepsia,* 40**,** 127-37.

Breathnach, A. S. & Goldby, F. 1954. The amygdaloid nuclei, hippocampus and other parts of the rhinencephalon in the porpoise (Phocaena phocaena). *J Anat,* 88**,** 267-91.

Briggs, C. A., Pollock, N. J., Frail, D. E., Paxson, C. L., Rakowski, R. F., Kang, C. H. & Kebabian, J. W. 1991. Activation of the 5-HT1C receptor expressed in Xenopus oocytes by the benzazepines SCH 23390 and SKF 38393. *Br J Pharmacol,* 104**,** 1038-44.

Broadbent, D. E. 1958. *Perception and Communication*, Pergamon Press. pp. 240-243.

Buccafusco, J. J., Letchworth, S. R., Bencherif, M. & Lippiello, P. M. 2005. Long-lasting cognitive improvement with nicotinic receptor agonists: mechanisms of pharmacokinetic-pharmacodynamic discordance. *Trends Pharmacol Sci,* 26**,** 352-60.

Burette, F., Jay, T. M. & Laroche, S. 1997. Reversal of LTP in the hippocampal afferent fiber system to the prefrontal cortex in vivo with low-frequency patterns of stimulation that do not produce LTD. *J Neurophysiol,* 78**,** 1155-60.

Burwell, R. D. 2000. The parahippocampal region: corticocortical connectivity. *Ann N Y Acad Sci,* 911**,** 25-42.

Burwell, R. D. & Amaral, D. G. 1998a. Cortical afferents of the perirhinal, postrhinal, and entorhinal cortices of the rat. *J Comp Neurol,* 398**,** 179-205.

Burwell, R. D. & Amaral, D. G. 1998b. Perirhinal and postrhinal cortices of the rat: interconnectivity and connections with the entorhinal cortex. *J Comp Neurol,* 391**,** 293-321.

Burwell, R. D., Saddoris, M. P., Bucci, D. J. & Wiig, K. A. 2004. Corticohippocampal contributions to spatial and contextual learning. *J Neurosci,* 24**,** 3826-36.

Canto, C. B. & Witter, M. P. 2012a. Cellular properties of principal neurons in the rat entorhinal cortex. I. The lateral entorhinal cortex. *Hippocampus,* 22**,** 1256-76.

Canto, C. B. & Witter, M. P. 2012b. Cellular properties of principal neurons in the rat entorhinal cortex. II. The medial entorhinal cortex. *Hippocampus,* 22**,** 1277-99.

Canto, C. B., Wouterlood, F. G. & Witter, M. P. 2008. What does the anatomical organization of the entorhinal cortex tell us? *Neural Plast,* 2008**,** 381243.

Carboni, A. A. & Lavelle, W. G. 2000. Ultrastructural characterizations of olfactory pathway neurons in layer II of the entorhinal cortex in monkey. *Acta Otolaryngol,* 120**,** 424-31.

Caruana, D. A., Alexander, G. M. & Dudek, S. M. 2012. New insights into the regulation of synaptic plasticity from an unexpected place: hippocampal area CA2. *Learn Mem,* 19**,** 391-400.

Caruana, D. A. & Chapman, C. A. 2008. Dopaminergic suppression of synaptic transmission in the lateral entorhinal cortex. *Neural Plast,* 2008**,** 1-14.

Caruana, D. A. & Dudek, S. M. 2020. Adenosine A1 Receptor-Mediated Synaptic Depression in the Developing Hippocampal Area CA2. *Front Synaptic Neurosci,* 12**,** 21.

Caruana, D. A., Reed, S. J., Sliz, D. J. & Chapman, C. A. 2007. Inhibiting dopamine reuptake blocks the induction of long-term potentiation and depression in the lateral entorhinal cortex of awake rats. *Neurosci Lett,* 426**,** 6-11.

Caruana, D. A., Sorge, R. E., Stewart, J. & Chapman, C. A. 2006. Dopamine has bidirectional effects on synaptic responses to cortical inputs in layer II of the lateral entorhinal cortex. *J Neurophysiol,* 96**,** 3006-15.

Caruana, D. A., Warburton, E. C. & Bashir, Z. I. 2011. Induction of activity-dependent LTD requires muscarinic receptor activation in medial prefrontal cortex. *J Neurosci,* 31**,** 18464-78.

Catterall, W. A. & Few, A. P. 2008. Calcium channel regulation and presynaptic plasticity. *Neuron,* 59**,** 882-901.

Cercato, M. C., Vazquez, C. A., Kornisiuk, E., Aguirre, A. I., Colettis, N., Snitcofsky, M., Jerusalinsky, D. A. & Baez, M. V. 2016. GluN1 and GluN2A NMDA Receptor Subunits Increase in the Hippocampus during Memory Consolidation in the Rat. *Front Behav Neurosci,* 10**,** 242.

Chapman, C. A. & Lacaille, J. C. 1999. Intrinsic theta-frequency membrane potential oscillations in hippocampal CA1 interneurons of stratum lacunosum-moleculare. *J Neurophysiol,* 81**,** 1296-307.

Chapman, C. A., Perez, Y. & Lacaille, J. C. 1998. Effects of GABA(A) inhibition on the expression of long-term potentiation in CA1 pyramidal cells are dependent on tetanization parameters. *Hippocampus,* 8**,** 289-98.

Chauhan, P., Jethwa, K., Rathawa, A., Chauhan, G. & Mehra, S. 2021. The Anatomy of the Hippocampus. *In:* Pluta, R. (ed.) *Cerebral Ischemia.* Brisbane (AU).

Chen, A. P. F., Malgady, J. M., Chen, L., Shi, K. W., Cheng, E., Plotkin, J. L., Ge, S. & Xiong, Q. 2022. Nigrostriatal dopamine pathway regulates auditory discrimination behavior. *Nat Commun,* 13**,** 5942.

Chen, Z., Fujii, S., Ito, K., Kato, H., Kaneko, K. & Miyakawa, H. 1995. Activation of dopamine D1 receptors enhances long-term depression of synaptic transmission induced by low frequency stimulation in rat hippocampal CA1 neurons. *Neurosci Lett,* 188**,** 195-8.

Christie, B. R. & Abraham, W. C. 1992. Priming of associative long-term depression in the dentate gyrus by theta frequency synaptic activity. *Neuron,* 9**,** 79-84.

Citri, A. & Malenka, R. C. 2008. Synaptic plasticity: multiple forms, functions, and mechanisms. *Neuropsychopharmacology,* 33**,** 18-41.

Collingridge, G. L., Kehl, S. J. & Mclennan, H. 1983. Excitatory amino acids in synaptic transmission in the Schaffer collateral-commissural pathway of the rat hippocampus. *J Physiol,* 334**,** 33-46.

Collingridge, G. L., Peineau, S., Howland, J. G. & Wang, Y. T. 2010. Long-term depression in the CNS. *Nat Rev Neurosci,* 11**,** 459-73.

Collingridge, G. L., Volianskis, A., Bannister, N., France, G., Hanna, L., Mercier, M., Tidball, P., Fang, G., Irvine, M. W., Costa, B. M., Monaghan, D. T., Bortolotto, Z. A., Molnar, E., Lodge, D. & Jane, D. E. 2013. The NMDA receptor as a target for cognitive enhancement. *Neuropharmacology,* 64**,** 13-26.

Collitti-Klausnitzer, J., Hagena, H., Dubovyk, V. & Manahan-Vaughan, D. 2021. Preferential frequency-dependent induction of synaptic depression by the lateral perforant path and of synaptic potentiation by the medial perforant path inputs to the dentate gyrus. *Hippocampus,* 31**,** 957-81.

Colquhoun, D., Jonas, P. & Sakmann, B. 1992. Action of brief pulses of glutamate on AMPA/kainate receptors in patches from different neurones of rat hippocampal slices. *J Physiol,* 458**,** 261-87.

Cook, A., Pfeiffer, L. M., Thiele, S., Coenen, V. A. & Dobrossy, M. D. 2017. Olfactory discrimination and memory deficits in the Flinders Sensitive Line rodent model of depression. *Behav Processes,* 143**,** 25-9.

Coombs, I. D. & Cull-Candy, S. G. 2021. Single-channel mechanisms underlying the function, diversity and plasticity of AMPA receptors. *Neuropharmacology,* 198**,** 108781.

Cooper, M., Safran, M. & Eberhardt, M. 2004. Caffeine consumption among adults on benzodiazepine therapy: United States 1988-1994. *Psychol Rep,* 95**,** 183-91.

Corkin, S. 2014. *Permanent present tense: the man with no memory, and what he taught the world*, Basic Books. pp. 221-3.

Corkin, S., Amaral, D. G., Gonzalez, R. G., Johnson, K. A. & Hyman, B. T. 1997. H. M.'s medial temporal lobe lesion: findings from magnetic resonance imaging. *J Neurosci,* 17**,** 3964-79.

Costenla, A. R., Lopes, L. V., De Mendonca, A. & Ribeiro, J. A. 2001. A functional role for adenosine A3 receptors: modulation of synaptic plasticity in the rat hippocampus. *Neurosci Lett,* 302**,** 53-7.

Couve, A., Moss, S. J. & Pangalos, M. N. 2000. GABAB receptors: a new paradigm in G protein signaling. *Mol Cell Neurosci,* 16**,** 296-312.

Cowan, N. 2008. What are the differences between long-term, short-term, and working memory? *Prog Brain Res,* 169**,** 323-38.

Cragg, S. J. & Rice, M. E. 2004. DAncing past the DAT at a DA synapse. *Trends Neurosci,* 27**,** 270-7.

Dasgupta, A., Lim, Y. J., Kumar, K., Baby, N., Pang, K. L. K., Benoy, A., Behnisch, T. & Sajikumar, S. 2020. Group III metabotropic glutamate receptors gate long-term potentiation and synaptic tagging/capture in rat hippocampal area CA2. *Elife,* 9.

De Curtis, M. & Llinas, R. R. 1993. Entorhinal cortex long-term potentiation evoked by theta-patterned stimulation of associative fibers in the isolated in vitro guinea pig brain. *Brain Res,* 600**,** 327-30.

Deng, P. Y. & Lei, S. 2007. Long-term depression in identified stellate neurons of juvenile rat entorhinal cortex. *J Neurophysiol,* 97**,** 727-37.

Deng, P. Y., Xiao, Z., Yang, C., Rojanathammanee, L., Grisanti, L., Watt, J., Geiger, J. D., Liu, R., Porter, J. E. & Lei, S. 2009. GABA(B) receptor activation inhibits neuronal excitability and spatial learning in the entorhinal cortex by activating TREK-2 K+ channels. *Neuron,* 63**,** 230-43.

Deshmukh, S. S. & Knierim, J. J. 2011. Representation of non-spatial and spatial information in the lateral entorhinal cortex. *Front Behav Neurosci,* 5**,** 69.

Dickerson, B. C. & Eichenbaum, H. 2010. The episodic memory system: neurocircuitry and disorders. *Neuropsychopharmacology,* 35**,** 86-104.

Dickson, C. T., Magistretti, J., Shalinsky, M. H., Fransen, E., Hasselmo, M. E. & Alonso, A. 2000. Properties and role of I(h) in the pacing of subthreshold oscillations in entorhinal cortex layer II neurons. *J Neurophysiol,* 83**,** 2562-79.

Dickson, D. W. 1998. Pick's disease: a modern approach. *Brain Pathol,* 8**,** 339-54.
Dorst, M. & Vervaeke, K. 2024. A low-cost perfusion heating system for slice electrophysiology. *Sci Rep,* 14**,** 28521.
Dossani, R. H., Missios, S. & Nanda, A. 2015. The Legacy of Henry Molaison (1926-2008) and the Impact of His Bilateral Mesial Temporal Lobe Surgery on the Study of Human Memory. *World Neurosurg,* 84**,** 1127-35.
Dudek, S. M., Alexander, G. M. & Farris, S. 2016. Rediscovering area CA2: unique properties and functions. *Nat Rev Neurosci,* 17**,** 89-102.
Dudek, S. M. & Bear, M. F. 1992. Homosynaptic long-term depression in area CA1 of hippocampus and effects of N-methyl-D-aspartate receptor blockade. *Proc Natl Acad Sci USA,* 89**,** 4363-7.
Egbenya, D. L., Aidoo, E. & Kyei, G. 2021. Glutamate receptors in brain development. *Childs Nerv Syst,* 37**,** 2753-8.
Eichenbaum, H., Yonelinas, A. P. & Ranganath, C. 2007. The medial temporal lobe and recognition memory. *Annu Rev Neurosci,* 30**,** 123-52.
Erhardt, S., Olsson, S. K. & Engberg, G. 2009. Pharmacological manipulation of kynurenic acid: potential in the treatment of psychiatric disorders. *CNS Drugs,* 23**,** 91-101.
Erickson, S. L., Sesack, S. R. & Lewis, D. A. 2000. Dopamine innervation of monkey entorhinal cortex: postsynaptic targets of tyrosine hydroxylase-immunoreactive terminals. *Synapse,* 36**,** 47-56.
Evaluation., I. F. H. M. A. 2019. *Global Health Data Exchange* [Online]. Available: http://ghdx.healthdata.org/gbd-results-tool [Accessed 27/05/2024].
Falck, B., Hillarp, N. A., Thieme, G. & Torp, A. 1962. Fluorescence of catechol amines and related compounds condensed with formaldehyde. *Brain Res Bull,* 9**,** 11-5.
Falcon-Moya, R. & Rodriguez-Moreno, A. 2021. Metabotropic actions of kainate receptors modulating glutamate release. *Neuropharmacology,* 197**,** 108696.
Fallon, J. H., Koziell, D. A. & Moore, R. Y. 1978. Catecholamine innervation of the basal forebrain. II. Amygdala, suprarhinal cortex and entorhinal cortex. *J Comp Neurol,* 180**,** 509-32.
Ferrer, I. 2009. Early involvement of the cerebral cortex in Parkinson's disease: convergence of multiple metabolic defects. *Prog Neurobiol,* 88**,** 89-103.
Ferrer, I., Santpere, G. & Van Leeuwen, F. W. 2008. Argyrophilic grain disease. *Brain,* 131**,** 1416-32.
Feuerbach, D., Loetscher, E., Neurdin, S. & Koller, M. 2010. Comparative pharmacology of the human NMDA-receptor subtypes R1-2A, R1-2B, R1-2C and R1-2D using an inducible expression system. *Eur J Pharmacol,* 637**,** 46-54.
Fink, A. E., Sarinana, J., Gray, E. E. & O'dell T, J. 2007. Activity-dependent depression of local excitatory connections in the CA1 region of mouse hippocampus. *J Neurophysiol,* 97**,** 3926-36.
Fischl, M. J. & Weisz, C. J. C. 2020. In Vitro Wedge Slice Preparation for Mimicking In Vivo Neuronal Circuit Connectivity. *J Vis Exp*.
Fox, K. 2002. Anatomical pathways and molecular mechanisms for plasticity in the barrel cortex. *Neuroscience,* 111**,** 799-814.
France, G., Volianskis, R., Ingram, R., Bannister, N., Rotharmel, R., Irvine, M. W., Fang, G., Burnell, E. S., Sapkota, K., Costa, B. M., Chopra, D. A., Dravid, S. M., Michael-Titus, A. T., Monaghan, D. T., Georgiou, J., Bortolotto, Z. A., Jane, D. E., Collingridge, G. L. & Volianskis, A. 2022. Differential regulation of STP, LTP and LTD by structurally diverse NMDA receptor subunit-specific positive allosteric modulators. *Neuropharmacology,* 202**,** 108840.
Franco, R., Garrigos, C. & Lillo, J. 2024. The Olfactory Trail of Neurodegenerative Diseases. *Cells,* 13.
Frisch, C., Dere, E., Silva, M. A., Godecke, A., Schrader, J. & Huston, J. P. 2000. Superior water maze performance and increase in fear-related behavior in the endothelial nitric oxide synthase-deficient mouse together with monoamine changes in cerebellum and ventral striatum. *J Neurosci,* 20**,** 6694-700.
Froestl, W., Muhs, A. & Pfeifer, A. 2012. Cognitive enhancers (nootropics). Part 1: drugs interacting with receptors. *J Alzheimers Dis,* 32**,** 793-887.
Fu, H., Hardy, J. & Duff, K. E. 2018. Selective vulnerability in neurodegenerative diseases. *Nat Neurosci,* 21**,** 1350-8.
Fuxe, K. 1965. Evidence for the existence of monoamine neurons in the central nervous system. *Zeitschrift fr Zellforschung und Mikroskopische Anatomie,* 65**,** 573-96.

Fyhn, M., Molden, S., Witter, M. P., Moser, E. I. & Moser, M. B. 2004. Spatial representation in the entorhinal cortex. *Science,* 305**,** 1258-64.

Gao, S. H., Tao, Y., Zhu, Y., Huang, H., Shen, L. L. & Gao, C. Y. 2022. Activation of Dopamine D2 Receptors Alleviates Neuronal Hyperexcitability in the Lateral Entorhinal Cortex via Inhibition of HCN Current in a Rat Model of Chronic Inflammatory Pain. *Neurosci Bull,* 38**,** 1041-56.

Gerdeman, G. L., Partridge, J. G., Lupica, C. R. & Lovinger, D. M. 2003. It could be habit forming: drugs of abuse and striatal synaptic plasticity. *Trends Neurosci,* 26**,** 184-92.

Glanzer, M. & Cunitz, A. R. 1966. Two storage mechanisms in free recall. *J Verb Learn Verb Behav,* 5**,** 351-60.

Glovaci, I., Caruana, D. A. & Chapman, C. A. 2014. Dopaminergic enhancement of excitatory synaptic transmission in layer II entorhinal neurons is dependent on D(1)-like receptor-mediated signaling. *Neuroscience,* 258**,** 74-83.

Glovaci, I. & Chapman, C. A. 2015. Activation of Phosphatidylinositol-Linked Dopamine Receptors Induces a Facilitation of Glutamate-Mediated Synaptic Transmission in the Lateral Entorhinal Cortex. *PLoS One,* 10**,** 1-19.

Glovaci, I. & Chapman, C. A. 2019. Dopamine induces release of calcium from internal stores in layer II lateral entorhinal cortex fan cells. *Cell Calcium,* 80**,** 103-11.

Goldman-Rakic, P. S. 1996. Regional and cellular fractionation of working memory. *Proc Natl Acad Sci U S A,* 93**,** 13473-80.

Goldman-Rakic, P. S. 1999. The "psychic" neuron of the cerebral cortex. *Ann N Y Acad Sci,* 868**,** 13-26.

Goldman-Rakic, P. S. & Selemon, L. D. 1997. Functional and anatomical aspects of prefrontal pathology in schizophrenia. *Schizophr Bull,* 23**,** 437-58.

Gonon, F. 1997. Prolonged and extrasynaptic excitatory action of dopamine mediated by D1 receptors in the rat striatum in vivo. *J Neurosci,* 17**,** 5972-8.

Gonzalez, J., Morales, I. S., Villarreal, D. M. & Derrick, B. E. 2014. Low-frequency stimulation induces long-term depression and slow onset long-term potentiation at perforant path-dentate gyrus synapses in vivo. *J Neurophysiol,* 111**,** 1259-73.

Goutman, J. D. & Calvo, D. J. 2004. Studies on the mechanisms of action of picrotoxin, quercetin and pregnanolone at the GABA rho 1 receptor. *Br J Pharmacol,* 141**,** 717-27.

Grace, A. A. 1991. Phasic versus tonic dopamine release and the modulation of dopamine system responsivity: a hypothesis for the etiology of schizophrenia. *Neuroscience,* 41**,** 1-24.

Grover, L. M. 1998. Evidence for postsynaptic induction and expression of NMDA receptor independent LTP. *J Neurophysiol,* 79**,** 1167-82.

Guo, J. Y., Ragland, J. D. & Carter, C. S. 2019. Memory and cognition in schizophrenia. *Mol Psychiatry,* 24**,** 633-42.

Gusel'nikova, V. V. & Korzhevskiy, D. E. 2015. NeuN As a Neuronal Nuclear Antigen and Neuron Differentiation Marker. *Acta Naturae,* 7**,** 42-7.

Hajos, N., Ellender, T. J., Zemankovics, R., Mann, E. O., Exley, R., Cragg, S. J., Freund, T. F. & Paulsen, O. 2009. Maintaining network activity in submerged hippocampal slices: importance of oxygen supply. *Eur J Neurosci,* 29**,** 319-27.

Hanse, E. & Gustafsson, B. 1992. Long-term Potentiation and Field EPSPs in the Lateral and Medial Perforant Paths in the Dentate Gyrus In Vitro: a Comparison. *Eur J Neurosci,* 4**,** 1191-201.

Hansel, C., Linden, D. J. & D'angelo, E. 2001. Beyond parallel fiber LTD: the diversity of synaptic and non-synaptic plasticity in the cerebellum. *Nat Neurosci,* 4**,** 467-75.

Hansen, K. B., Wollmuth, L. P., Bowie, D., Furukawa, H., Menniti, F. S., Sobolevsky, A. I., Swanson, G. T., Swanger, S. A., Greger, I. H., Nakagawa, T., Mcbain, C. J., Jayaraman, V., Low, C. M., Dell'acqua, M. L., Diamond, J. S., Camp, C. R., Perszyk, R. E., Yuan, H. & Traynelis, S. F. 2021. Structure, Function, and Pharmacology of Glutamate Receptor Ion Channels. *Pharmacol Rev,* 73**,** 298-487.

Harding, S. D., Armstrong, J. F., Faccenda, E., Southan, C., Alexander, S. P. H., Davenport, A. P., Spedding, M. & Davies, J. A. 2024. The IUPHAR/BPS Guide to PHARMACOLOGY in 2024. *Nucleic Acids Res,* 52**,** D1438-D49.

Hargreaves, E. L., Rao, G., Lee, I. & Knierim, J. J. 2005. Major dissociation between medial and lateral entorhinal input to dorsal hippocampus. *Science,* 308**,** 1792-4.

Harker, K. T. & Whishaw, I. Q. 2002. Place and matching-to-place spatial learning affected by rat inbreeding (Dark-Agouti, Fischer 344) and albinism (Wistar, Sprague-Dawley) but not domestication (wild rat vs. Long-Evans, Fischer-Norway). *Behav Brain Res,* 134**,** 467-77.

Harvey, L., A. 2020. *Dopaminergic modulation of superficial layer projection neuron excitability in the lateral entorhinal cortex.* MPhil, Keele University.
Hasbi, A., O'dowd, B. F. & George, S. R. 2010. Heteromerization of dopamine D2 receptors with dopamine D1 or D5 receptors generates intracellular calcium signaling by different mechanisms. *Curr Opin Pharmacol,* 10**,** 93-9.
Hasselmo, M. E. 2006. The role of acetylcholine in learning and memory. *Curr Opin Neurobiol,* 16**,** 710-5.
Hasselmo, M. E., Fransen, E., Dickson, C. & Alonso, A. A. 2000. Computational modeling of entorhinal cortex. *Ann N Y Acad Sci,* 911**,** 418-46.
Hattori, T., Takada, M., Moriizumi, T. & Van Der Kooy, D. 1991. Single dopaminergic nigrostriatal neurons form two chemically distinct synaptic types: possible transmitter segregation within neurons. *J Comp Neurol,* 309**,** 391-401.
Hausdorff, W. P., Caron, M. G. & Lefkowitz, R. J. 1990. Turning off the signal: desensitization of beta-adrenergic receptor function. *FASEB J,* 4**,** 2881-9.
Herry, C., Vouimba, R. M. & Garcia, R. 1999. Plasticity in the mediodorsal thalamo-prefrontal cortical transmission in behaving mice. *J Neurophysiol,* 82**,** 2827-32.
Hirano, S. 2021. Clinical implications for dopaminergic and functional neuroimage research in cognitive symptoms of Parkinson's disease. *Mol Med,* 27**,** 40.
Ho, B. C., Andreasen, N. C., Ziebell, S., Pierson, R. & Magnotta, V. 2011. Long-term antipsychotic treatment and brain volumes: a longitudinal study of first-episode schizophrenia. *Arch Gen Psychiatry,* 68**,** 128-37.
Huang, S. & Uusisaari, M. Y. 2013. Physiological temperature during brain slicing enhances the quality of acute slice preparations. *Front Cell Neurosci,* 7**,** 48.
Huang, Y. Y. & Kandel, E. R. 1998. Postsynaptic induction and PKA-dependent expression of LTP in the lateral amygdala. *Neuron,* 21**,** 169-78.
Hutter, J. A. & Chapman, C. A. 2013. Exposure to cues associated with palatable food reward results in a dopamine D(2) receptor-dependent suppression of evoked synaptic responses in the entorhinal cortex. *Behav Brain Funct,* 9**,** 37.
Igarashi, K. M., Lu, L., Colgin, L. L., Moser, M. B. & Moser, E. I. 2014. Coordination of entorhinal-hippocampal ensemble activity during associative learning. *Nature,* 510**,** 143-62.
Iijima, K., Takase, S., Tsumuraya, K., Endo, M. & Itahara, K. 1978. Changes in free amino acids of cerebrospinal fluid and plasma in various neurological diseases. *Tohoku J Exp Med,* 126**,** 133-50.
Insausti, R., Herrero, M. T. & Witter, M. P. 1997. Entorhinal cortex of the rat: cytoarchitectonic subdivisions and the origin and distribution of cortical efferents. *Hippocampus,* 7**,** 146-83.
Ireland, D. R. & Abraham, W. C. 2009. Mechanisms of group I mGluR-dependent long-term depression of NMDA receptor-mediated transmission at Schaffer collateral-CA1 synapses. *J Neurophysiol,* 101**,** 1375-85.
Isaacson, S. H., Hauser, R. A., Pahwa, R., Gray, D. & Duvvuri, S. 2023. Dopamine agonists in Parkinson's disease: Impact of D1-like or D2-like dopamine receptor subtype selectivity and avenues for future treatment. *Clin Park Relat Disord,* 9**,** 100212.
Iwase, M., Kitanishi, T. & Mizuseki, K. 2020. Cell type, sub-region, and layer-specific speed representation in the hippocampal-entorhinal circuit. *Sci Rep,* 10**,** 1407.
Iwata, K., Ito, K., Fukuzaki, A., Inaki, K. & Haga, T. 1999. Dynamin and rab5 regulate GRK2-dependent internalization of dopamine D2 receptors. *Eur J Biochem,* 263**,** 596-602.
Jay, T. M. 2003. Dopamine: a potential substrate for synaptic plasticity and memory mechanisms. *Prog Neurobiol,* 69**,** 375-90.
Jones, M. W. & Mchugh, T. J. 2011. Updating hippocampal representations: CA2 joins the circuit. *Trends Neurosci,* 34**,** 526-35.
Kamalova, A. & Nakagawa, T. 2021. AMPA receptor structure and auxiliary subunits. *J Physiol,* 599**,** 453-69.
Kelly, E., Bailey, C. P. & Henderson, G. 2008. Agonist-selective mechanisms of GPCR desensitization. *Br J Pharmacol,* 153, Suppl 1**,** 379-88.
Kemp, A. & Manahan-Vaughan, D. 2004. Hippocampal long-term depression and long-term potentiation encode different aspects of novelty acquisition. *Proc Natl Acad Sci USA,* 101**,** 8192-7.
Kemp, N. & Bashir, Z. I. 1999. Induction of LTD in the adult hippocampus by the synaptic activation of AMPA/kainate and metabotropic glutamate receptors. *Neuropharmacology,* 38**,** 495-504.
Kemppainen, S., Jolkkonen, E. & Pitkanen, A. 2002. Projections from the posterior cortical nucleus of the amygdala to the hippocampal formation and parahippocampal region in rat. *Hippocampus,* 12**,** 735-55.

Kim, K. M., Valenzano, K. J., Robinson, S. R., Yao, W. D., Barak, L. S. & Caron, M. G. 2001. Differential regulation of the dopamine D2 and D3 receptors by G protein-coupled receptor kinases and beta-arrestins. *J Biol Chem,* 276**,** 37409-14.

Kim, O. J., Gardner, B. R., Williams, D. B., Marinec, P. S., Cabrera, D. M., Peters, J. D., Mak, C. C., Kim, K. M. & Sibley, D. R. 2004. The role of phosphorylation in D1 dopamine receptor desensitization: evidence for a novel mechanism of arrestin association. *J Biol Chem,* 279**,** 7999-8010.

Kitamura, T., Pignatelli, M., Suh, J., Kohara, K., Yoshiki, A., Abe, K. & Tonegawa, S. 2014. Island cells control temporal association memory. *Science,* 343**,** 896-901.

Klein, A. S., Donoso, J. R., Kempter, R., Schmitz, D. & Beed, P. 2016. Early Cortical Changes in Gamma Oscillations in Alzheimer's Disease. *Front Syst Neurosci,* 10**,** 1-11.

Kloosterman, F., Van Haeften, T. & Lopes Da Silva, F. H. 2004. Two reentrant pathways in the hippocampal-entorhinal system. *Hippocampus,* 14**,** 1026-39.

Knierim, J. J., Neunuebel, J. P. & Deshmukh, S. S. 2014. Functional correlates of the lateral and medial entorhinal cortex: objects, path integration and local-global reference frames. *Philos Trans R Soc Lond B Biol Sci,* 369**,** 1-7.

Koenig, J. A. 2004. Assessment of Receptor Internalization and Recycling. *In:* Willars, G. B.and Challiss, R. a. J. (eds.) *Receptor Signal Transduction Protocols.* Totowa, NJ: Humana Press.

Köhler, C. 1988. Intrinsic connections of the retrohippocampal region in the rat brain: III. The lateral entorhinal area. *J Comp Neurol,* 271**,** 208-28.

Köhler, C., Ericson, H. & Radesäter, A. 1991. Different laminar distributions of dopamine D1 and D2 receptors in the rat hippocampal region. *Neuroscience Letters,* 126**,** 107-9.

Koles, L., Kato, E., Hanuska, A., Zadori, Z. S., Al-Khrasani, M., Zelles, T., Rubini, P. & Illes, P. 2016. Modulation of excitatory neurotransmission by neuronal/glial signalling molecules: interplay between purinergic and glutamatergic systems. *Purinergic Signal,* 12**,** 1-24.

Kook, S. Y., Jeong, H., Kang, M. J., Park, R., Shin, H. J., Han, S. H., Son, S. M., Song, H., Baik, S. H., Moon, M., Yi, E. C., Hwang, D. & Mook-Jung, I. 2014. Crucial role of calbindin-D28k in the pathogenesis of Alzheimer's disease mouse model. *Cell Death Differ,* 21**,** 1575-87.

Kourrich, S. & Chapman, C. A. 2003. NMDA receptor-dependent long-term synaptic depression in the entorhinal cortex in vitro. *J Neurophysiol,* 89**,** 2112-9.

Kourrich, S., Glasgow, S. D., Caruana, D. A. & Chapman, C. A. 2008. Postsynaptic signals mediating induction of long-term synaptic depression in the entorhinal cortex. *Neural Plast,* 2008**,** 840374.

Kovalenko, A. A., Zakharova, M. V., Zubareva, O. E., Schwarz, A. P., Postnikova, T. Y. & Zaitsev, A. V. 2021. Alterations in mRNA and Protein Expression of Glutamate Receptor Subunits Following Pentylenetetrazole-induced Acute Seizures in Young Rats. *Neuroscience,* 468**,** 1-15.

Krettek, J. E. & Price, J. L. 1977. Projections from the amygdaloid complex and adjacent olfactory structures to the entorhinal cortex and to the subiculum in the rat and cat. *J Comp Neurol,* 172**,** 723-52.

Kumar, A. 2011. Long-Term Potentiation at CA3-CA1 Hippocampal Synapses with Special Emphasis on Aging, Disease, and Stress. *Front Aging Neurosci,* 3**,** 7.

Kuzhikandathil, E. V. & Oxford, G. S. 2002. Classic D1 dopamine receptor antagonist R-(+)-7-chloro-8-hydroxy-3-methyl-1-phenyl-2,3,4,5-tetrahydro-1H-3-benzazepine hydrochloride (SCH23390) directly inhibits G protein-coupled inwardly rectifying potassium channels. *Mol Pharmacol,* 62**,** 119-26.

Larson, J. & Lynch, G. 1986. Induction of synaptic potentiation in hippocampus by patterned stimulation involves two events. *Science,* 232**,** 985-8.

Larson, J. & Munkacsy, E. 2015. Theta-burst LTP. *Brain Res,* 1621**,** 38-50.

Larson, J., Wong, D. & Lynch, G. 1986. Patterned stimulation at the theta frequency is optimal for the induction of hippocampal long-term potentiation. *Brain Res,* 368**,** 347-50.

Lee, J. Y., Jun, H., Soma, S., Nakazono, T., Shiraiwa, K., Dasgupta, A., Nakagawa, T., Xie, J. L., Chavez, J., Romo, R., Yungblut, S., Hagihara, M., Murata, K. & Igarashi, K. M. 2021. Dopamine facilitates associative memory encoding in the entorhinal cortex. *Nature,* 598**,** 321-6.

Lee, S., Goodchild, S. J. & Ahern, C. A. 2012. Local anesthetic inhibition of a bacterial sodium channel. *J Gen Physiol,* 139**,** 507-16.

Lee, S. H., Liu, L., Wang, Y. T. & Sheng, M. 2002. Clathrin adaptor AP2 and NSF interact with overlapping sites of GluR2 and play distinct roles in AMPA receptor trafficking and hippocampal LTD. *Neuron,* 36**,** 661-74.

Leitner, F. C., Melzer, S., Lutcke, H., Pinna, R., Seeburg, P. H., Helmchen, F. & Monyer, H. 2016. Spatially segregated feedforward and feedback neurons support differential odor processing in the lateral entorhinal cortex. *Nat Neurosci,* 19**,** 935-44.

Li, P., Snyder, G. L. & Vanover, K. E. 2016. Dopamine Targeting Drugs for the Treatment of Schizophrenia: Past, Present and Future. *Curr Top Med Chem,* 16**,** 3385-403.

Li, Y., Fan, S., Yan, J., Li, B., Chen, F., Xia, J., Yu, Z. & Hu, Z. 2011. Adenosine modulates the excitability of layer II stellate neurons in entorhinal cortex through A1 receptors. *Hippocampus,* 21**,** 265-80.

Li, Z., Ma, Y., Dong, B., Hu, B., He, H., Jia, J., Xiong, M., Xu, T., Xu, B. & Xi, W. 2023. Functional magnetic resonance imaging study on anxiety and depression disorders induced by chronic restraint stress in rats. *Behav Brain Res,* 450**,** 114496.

Lindvall, O., Björklund, A., Moore, R. Y. & Stenevi, U. 1974. Mesencephalic dopamine neurons projecting to neocortex. *Brain Research,* 81**,** 325-31.

Lingenhohl, K. & Finch, D. M. 1991. Morphological characterization of rat entorhinal neurons in vivo: soma-dendritic structure and axonal domains. *Exp Brain Res,* 84**,** 57-74.

Lipton, P., Aitken, P. G., Dudek, F. E., Eskessen, K., Espanol, M. T., Ferchmin, P. A., Kelly, J. B., Kreisman, N. R., Landfield, P. W., Larkman, P. M. & Et Al. 1995. Making the best of brain slices: comparing preparative methods. *J Neurosci Methods,* 59**,** 151-6.

Lisman, J. E., Pi, H. J., Zhang, Y. & Otmakhova, N. A. 2010. A thalamo-hippocampal-ventral tegmental area loop may produce the positive feedback that underlies the psychotic break in schizophrenia. *Biol Psychiatry,* 68**,** 17-24.

Liu, S. 2020. Dopamine Suppresses Synaptic Responses of Fan Cells in the Lateral Entorhinal Cortex to Olfactory Bulb Input in Mice. *Front Cell Neurosci,* 14**,** 181.

Liu, Z., Sun, W., Ng, Y. H., Dong, H., Quake, S. R. & Südhof, T. C. 2024. The cortical amygdala consolidates a socially transmitted long-term memory. *Nature,* 632**,** 366-74.

Locatelli, F., Soda, T., Montagna, I., Tritto, S., Botta, L., Prestori, F. & D'angelo, E. 2021. Calcium Channel-Dependent Induction of Long-Term Synaptic Plasticity at Excitatory Golgi Cell Synapses of Cerebellum. *J Neurosci,* 41**,** 3307-19.

Lohman, A. H. M. & Lammers, H. J. 1963. The nuclear configuration of the anterior olfactory lobe. *Acta Anatomica,* 53**,** 11-27.

Lohse, M. J., Benovic, J. L., Codina, J., Caron, M. G. & Lefkowitz, R. J. 1990. beta-Arrestin: a protein that regulates beta-adrenergic receptor function. *Science,* 248**,** 1547-50.

Lopez-Rojas, J., De Solis, C. A., Leroy, F., Kandel, E. R. & Siegelbaum, S. A. 2022. A direct lateral entorhinal cortex to hippocampal CA2 circuit conveys social information required for social memory. *Neuron,* 110**,** 1559-72 e4.

Lopez, F., Miller, L. G., Greenblatt, D. J., Kaplan, G. B. & Shader, R. I. 1989. Interaction of caffeine with the GABAA receptor complex: alterations in receptor function but not ligand binding. *Eur J Pharmacol,* 172**,** 453-9.

Lowe, J. D., Sanderson, H. S., Cooke, A. E., Ostovar, M., Tsisanova, E., Withey, S. L., Chavkin, C., Husbands, S. M., Kelly, E., Henderson, G. & Bailey, C. P. 2015. Role of G Protein-Coupled Receptor Kinases 2 and 3 in mu-Opioid Receptor Desensitization and Internalization. *Mol Pharmacol,* 88**,** 347-56.

Luscher, C. & Malenka, R. C. 2012. NMDA receptor-dependent long-term potentiation and long-term depression (LTP/LTD). *Cold Spring Harb Perspect Biol,* 4**,** 1-15.

Ma, L., Alonso, A. & Dickson, C. T. 2008. Differential induction of long-term potentiation in the horizontal versus columnar superficial connections to layer II cells of the entorhinal cortex. *Neural Plast,* 2008**,** 814815.

Majlath, Z., Torok, N., Toldi, J. & Vecsei, L. 2016. Memantine and Kynurenic Acid: Current Neuropharmacological Aspects. *Curr Neuropharmacol,* 14**,** 200-9.

Malenka, R. C. 1994. Synaptic plasticity in the hippocampus: LTP and LTD. *Cell,* 78**,** 535-8.

Malenka, R. C. & Bear, M. F. 2004. LTP and LTD: an embarrassment of riches. *Neuron,* 44**,** 5-21.

Malenka, R. C. & Nicoll, R. A. 1999. Long-term potentiation--a decade of progress? *Science,* 285**,** 1870-4.

Malinow, R. & Malenka, R. C. 2002. AMPA receptor trafficking and synaptic plasticity. *Annu Rev Neurosci,* 25**,** 103-26.

Marder, C. P. & Buonomano, D. V. 2003. Differential effects of short- and long-term potentiation on cell firing in the CA1 region of the hippocampus. *J Neurosci,* 23**,** 112-21.

Martel, J. C. & Gatti Mcarthur, S. 2020. Dopamine Receptor Subtypes, Physiology and Pharmacology: New Ligands and Concepts in Schizophrenia. *Front Pharmacol,* 11**,** 1003.
Matsuda, Y., Marzo, A. & Otani, S. 2006. The presence of background dopamine signal converts long-term synaptic depression to potentiation in rat prefrontal cortex. *J Neurosci,* 26**,** 4803-10.
Mccutcheon, J. E. & Marinelli, M. 2009. Age matters. *Eur J Neurosci,* 29**,** 997-1014.
Meriney, S. D. & Fanselow, E. E. 2019. Monoamine Transmitters. *Synaptic Transmission.*
Meunier, M., Bachevalier, J., Mishkin, M. & Murray, E. A. 1993. Effects on visual recognition of combined and separate ablations of the entorhinal and perirhinal cortex in rhesus monkeys. *J Neurosci,* 13**,** 5418-32.
Meyerson, J. R., Chittori, S., Merk, A., Rao, P., Han, T. H., Serpe, M., Mayer, M. L. & Subramaniam, S. 2016. Structural basis of kainate subtype glutamate receptor desensitization. *Nature,* 537**,** 567-71.
Milior, G., Di Castro, M. A., Sciarria, L. P., Garofalo, S., Branchi, I., Ragozzino, D., Limatola, C. & Maggi, L. 2016. Electrophysiological Properties of CA1 Pyramidal Neurons along the Longitudinal Axis of the Mouse Hippocampus. *Sci Rep,* 6**,** 38242.
Millan, M. J., Newman-Tancredi, A., Quentric, Y. & Cussac, D. 2001. The "selective" dopamine D1 receptor antagonist, SCH23390, is a potent and high efficacy agonist at cloned human serotonin2C receptors. *Psychopharmacology (Berl),* 156**,** 58-62.
Miller, G. M. 2011. The emerging role of trace amine-associated receptor 1 in the functional regulation of monoamine transporters and dopaminergic activity. *J Neurochem,* 116**,** 164-76.
Milner, B. 1972. Disorders of learning and memory after temporal lobe lesions in man. *Clin Neurosurg,* 19**,** 421-46.
Milner, B., Corkin, S. & Teuber, H. L. 1968. Further analysis of the hippocampal amnesic syndrome: 14-year follow-up study of H.M. *Neuropsychologia,* 6**,** 215-34.
Mingote, S., Chuhma, N., Kusnoor, S. V., Field, B., Deutch, A. Y. & Rayport, S. 2015. Functional Connectome Analysis of Dopamine Neuron Glutamatergic Connections in Forebrain Regions. *J Neurosci,* 35**,** 16259-71.
Missale, C., Nash, S. R., Robinson, S. W., Jaber, M. & Caron, M. G. 1998. Dopamine receptors: from structure to function. *Physiol Rev,* 78**,** 189-225.
Mockett, B. G., Guevremont, D., Williams, J. M. & Abraham, W. C. 2007. Dopamine D1/D5 receptor activation reverses NMDA receptor-dependent long-term depression in rat hippocampus. *J Neurosci,* 27**,** 2918-26.
Moser, E. I., Kropff, E. & Moser, M. B. 2008. Place cells, grid cells, and the brain's spatial representation system. *Annu Rev Neurosci,* 31**,** 69-89.
Moult, P. R., Correa, S. A., Collingridge, G. L., Fitzjohn, S. M. & Bashir, Z. I. 2008. Co-activation of p38 mitogen-activated protein kinase and protein tyrosine phosphatase underlies metabotropic glutamate receptor-dependent long-term depression. *J Physiol,* 586**,** 2499-510.
Nahum-Levy, R., Lipinski, D., Shavit, S. & Benveniste, M. 2001. Desensitization of NMDA receptor channels is modulated by glutamate agonists. *Biophys J,* 80**,** 2152-66.
Neve, K. A., Seamans, J. K. & Trantham-Davidson, H. 2004. Dopamine receptor signaling. *J Recept Signal Transduct Res,* 24**,** 165-205.
Newman-Tancredi, A., Cussac, D., Audinot, V., Nicolas, J. P., De Ceuninck, F., Boutin, J. A. & Millan, M. J. 2002a. Differential actions of antiparkinson agents at multiple classes of monoaminergic receptor. II. Agonist and antagonist properties at subtypes of dopamine D(2)-like receptor and alpha(1)/alpha(2)-adrenoceptor. *J Pharmacol Exp Ther,* 303**,** 805-14.
Newman-Tancredi, A., Cussac, D., Quentric, Y., Touzard, M., Verriele, L., Carpentier, N. & Millan, M. J. 2002b. Differential actions of antiparkinson agents at multiple classes of monoaminergic receptor. III. Agonist and antagonist properties at serotonin, 5-HT(1) and 5-HT(2), receptor subtypes. *J Pharmacol Exp Ther,* 303**,** 815-22.
Nilssen, E. S., Doan, T. P., Nigro, M. J., Ohara, S. & Witter, M. P. 2019. Neurons and networks in the entorhinal cortex: A reappraisal of the lateral and medial entorhinal subdivisions mediating parallel cortical pathways. *Hippocampus,* 29**,** 1238-54.
Nilssen, E. S., Jacobsen, B., Fjeld, G., Nair, R. R., Blankvoort, S., Kentros, C. & Witter, M. P. 2018. Inhibitory Connectivity Dominates the Fan Cell Network in Layer II of Lateral Entorhinal Cortex. *J Neurosci,* 38**,** 9712-27.

Nugent, F. S., Hwong, A. R., Udaka, Y. & Kauer, J. A. 2008. High-frequency afferent stimulation induces long-term potentiation of field potentials in the ventral tegmental area. *Neuropsychopharmacology,* 33**,** 1704-12.

Nyberg, L., Mcintosh, A. R. & Tulving, E. 1998. Functional brain imaging of episodic and semantic memory with positron emission tomography. *J Mol Med (Berl),* 76**,** 48-53.

Nyberg, L. & Tulving, E. 1996. Classifying Human Long-term Memory: Evidence from Converging Dissociations. *EJCP,* 8**,** 163-84.

O'dell, T. J., Connor, S. A., Gelinas, J. N. & Nguyen, P. V. 2010. Viagra for your synapses: Enhancement of hippocampal long-term potentiation by activation of beta-adrenergic receptors. *Cell Signal,* 22**,** 728-36.

O'keefe, J. & Dostrovsky, J. 1971. The hippocampus as a spatial map. Preliminary evidence from unit activity in the freely-moving rat. *Brain Res,* 34**,** 171-5.

O'keefe, J. & Nadel, L. 1978. *The hippocampus as a cognitive map,* Oxford, UK, Oxford University Press.

Oades, R. D. & Halliday, G. M. 1987. Ventral tegmental (A10) system: neurobiology. 1. Anatomy and connectivity. *Brain Res,* 434**,** 117-65.

Otani, S., Blond, O., Desce, J. M. & Crepel, F. 1998. Dopamine facilitates long-term depression of glutamatergic transmission in rat prefrontal cortex. *Neuroscience,* 85**,** 669-76.

Otmakhova, N. A. & Lisman, J. E. 1999. Dopamine Selectively Inhibits the Direct Cortical Pathway to the CA1 Hippocampal Region. *J Neurosci,* 19**,** 1437-45.

Overstreet, D. H. & Wegener, G. 2013. The flinders sensitive line rat model of depression--25 years and still producing. *Pharmacol Rev,* 65**,** 143-55.

Papouin, T., Ladepeche, L., Ruel, J., Sacchi, S., Labasque, M., Hanini, M., Groc, L., Pollegioni, L., Mothet, J. P. & Oliet, S. H. 2012. Synaptic and extrasynaptic NMDA receptors are gated by different endogenous coagonists. *Cell,* 150**,** 633-46.

Park, P., Volianskis, A., Sanderson, T. M., Bortolotto, Z. A., Jane, D. E., Zhuo, M., Kaang, B. K. & Collingridge, G. L. 2014. NMDA receptor-dependent long-term potentiation comprises a family of temporally overlapping forms of synaptic plasticity that are induced by different patterns of stimulation. *Philos Trans R Soc Lond B Biol Sci,* 369**,** 20130131.

Paxinos, G. & Watson, C. 2007. *The rat brain in stereotaxic coordinates,* Amsterdam; Boston, Academic Press/Elsevier.

Porcu, A., Mostallino, R., Serra, V., Melis, M., Sogos, V., Beggiato, S., Ferraro, L., Manetti, F., Gianibbi, B., Bettler, B., Corelli, F., Mugnaini, C. & Castelli, M. P. 2021. COR758, a negative allosteric modulator of GABA(B) receptors. *Neuropharmacology,* 189**,** 108537.

Pralong, E. & Jones, R. S. 1993. Interactions of dopamine with glutamate- and GABA-mediated synaptic transmission in the rat entorhinal cortex in vitro. *Eur J Neurosci,* 5**,** 760-7.

Premont, R. T. & Gainetdinov, R. R. 2007. Physiological roles of G protein-coupled receptor kinases and arrestins. *Annu Rev Physiol,* 69**,** 511-34.

Price, J. L. & Powell, T. P. 1971. Certain observations on the olfactory pathway. *J Anat,* 110**,** 105-26.

Purves, D. 2018. *Neuroscience,* New York, Oxford University Press.

Qi-Lytle, X., Sayers, S. & Wagner, E. J. 2023. Current Review of the Function and Regulation of Tuberoinfundibular Dopamine Neurons. *Int J Mol Sci,* 25**,** 1-15.

Qian, H. & Dowling, J. E. 1994. Pharmacology of novel GABA receptors found on rod horizontal cells of the white perch retina. *J Neurosci,* 14**,** 4299-307.

Rajagopal, S. & Shenoy, S. K. 2018. GPCR desensitization: Acute and prolonged phases. *Cell Signal,* 41**,** 9-16.

Ran, I., Gkogkas, C. G., Vasuta, C., Tartas, M., Khoutorsky, A., Laplante, I., Parsyan, A., Nevarko, T., Sonenberg, N. & Lacaille, J. C. 2013. Selective regulation of GluA subunit synthesis and AMPA receptor-mediated synaptic function and plasticity by the translation repressor 4E-BP2 in hippocampal pyramidal cells. *J Neurosci,* 33**,** 1872-86.

Reddy, V. S., Shiva, S., Manikantan, S. & Ramakrishna, S. 2024. Pharmacology of caffeine and its effects on the human body. *European Journal of Medicinal Chemistry Reports,* 10**,** 100138.

Richfield, E. K., Penney, J. B. & Young, A. B. 1989. Anatomical and affinity state comparisons between dopamine D1 and D2 receptors in the rat central nervous system. *Neuroscience,* 30**,** 767-77.

Roalf, D. R., Quarmley, M., Calkins, M. E., Satterthwaite, T. D., Ruparel, K., Elliott, M. A., Moore, T. M., Gur, R. C., Gur, R. E., Moberg, P. J. & Turetsky, B. I. 2017. Temporal Lobe Volume Decrements in Psychosis Spectrum Youths. *Schizophr Bull,* 43**,** 601-10.

Roda, A. R., Serra-Mir, G., Montoliu-Gaya, L., Tiessler, L. & Villegas, S. 2022. Amyloid-beta peptide and tau protein crosstalk in Alzheimer's disease. *Neural Regen Res,* 17**,** 1666-74.

Rosenkranz, J. A. & Johnston, D. 2006. Dopaminergic regulation of neuronal excitability through modulation of Ih in layer V entorhinal cortex. *J Neurosci,* 26**,** 3229-44.

Rozov, A., Zilberter, Y., Wollmuth, L. P. & Burnashev, N. 1998. Facilitation of currents through rat Ca2+-permeable AMPA receptor channels by activity-dependent relief from polyamine block. *J Physiol,* 511**,** 361-77.

Salin, P. A., Malenka, R. C. & Nicoll, R. A. 1996. Cyclic AMP mediates a presynaptic form of LTP at cerebellar parallel fiber synapses. *Neuron,* 16**,** 797-803.

Sander, C. Y., Hooker, J. M., Catana, C., Rosen, B. R. & Mandeville, J. B. 2016. Imaging Agonist-Induced D2/D3 Receptor Desensitization and Internalization In Vivo with PET/fMRI. *Neuropsychopharmacology,* 41**,** 1427-36.

Savasta, M., Dubois, A. & Scatton, B. 1986. Autoradiographic localization of D1 dopamine receptors in the rat brain with [3H]SCH 23390. *Brain Research,* 375**,** 291-301.

Schindelin, J., Arganda-Carreras, I., Frise, E., Kaynig, V., Longair, M., Pietzsch, T., Preibisch, S., Rueden, C., Saalfeld, S., Schmid, B., Tinevez, J. Y., White, D. J., Hartenstein, V., Eliceiri, K., Tomancak, P. & Cardona, A. 2012. Fiji: an open-source platform for biological-image analysis. *Nat Methods,* 9**,** 676-82.

Schmitz, D., Gloveli, T., Empson, R. M. & Heinemann, U. 1998. Comparison of the effects of serotonin in the hippocampus and the entorhinal cortex. *Mol Neurobiol,* 17**,** 59-72.

Schroder, T. N., Haak, K. V., Jimenez, N. I. Z., Beckmann, C. F. & Doeller, C. F. 2015. Functional topography of the human entorhinal cortex. *Elife,* 4.

Schultz, S. A., Gordon, B. A., Mishra, S., Su, Y., Perrin, R. J., Cairns, N. J., Morris, J. C., Ances, B. M. & Benzinger, T. L. S. 2018. Widespread distribution of tauopathy in preclinical Alzheimer's disease. *Neurobiol Aging,* 72**,** 177-85.

Schwenk, J., Perez-Garci, E., Schneider, A., Kollewe, A., Gauthier-Kemper, A., Fritzius, T., Raveh, A., Dinamarca, M. C., Hanuschkin, A., Bildl, W., Klingauf, J., Gassmann, M., Schulte, U., Bettler, B. & Fakler, B. 2016. Modular composition and dynamics of native GABAB receptors identified by high-resolution proteomics. *Nat Neurosci,* 19**,** 233-42.

Scoville, W. B. & Milner, B. 1957. Loss of recent memory after bilateral hippocampal lesions. *J Neurol Neurosurg Psychiatry,* 20**,** 11-21.

Seamans, J. K. & Yang, C. R. 2004. The principal features and mechanisms of dopamine modulation in the prefrontal cortex. *Prog Neurobiol,* 74**,** 1-58.

Shenoy, S. K., Xiao, K., Venkataramanan, V., Snyder, P. M., Freedman, N. J. & Weissman, A. M. 2008. Nedd4 mediates agonist-dependent ubiquitination, lysosomal targeting, and degradation of the beta2-adrenergic receptor. *J Biol Chem,* 283**,** 22166-76.

Sheppard, O. & Coleman, M. 2020. Alzheimer's Disease: Etiology, Neuropathology and Pathogenesis. *In:* Huang, X. (ed.) *Alzheimer's Disease: Drug Discovery.* Brisbane (AU).

Shiroma, L. O. & Costa, V. P. 2015. 56 - Parasympathomimetics. *In:* Shaarawy, T. M., Sherwood, M. B., Hitchings, R. A.and Crowston, J. G. (eds.) *Glaucoma (Second Edition).* W.B. Saunders.

Sigurdsson, T., Doyere, V., Cain, C. K. & Ledoux, J. E. 2007. Long-term potentiation in the amygdala: a cellular mechanism of fear learning and memory. *Neuropharmacology,* 52**,** 215-27.

Simons, S. B., Escobedo, Y., Yasuda, R. & Dudek, S. M. 2009. Regional differences in hippocampal calcium handling provide a cellular mechanism for limiting plasticity. *Proc Natl Acad Sci USA,* 106**,** 14080-4.

Sneyers, F., Speelman-Rooms, F., Verhelst, S. H. L., Bootman, M. D. & Bultynck, G. 2024. Cellular effects of BAPTA: Are they only about Ca(2+) chelation? *Biochim Biophys Acta Mol Cell Res,* 1871**,** 119589.

Solger, J., Wozny, C., Manahan-Vaughan, D. & Behr, J. 2004. Distinct mechanisms of bidirectional activity-dependent synaptic plasticity in superficial and deep layers of rat entorhinal cortex. *Eur J Neurosci,* 19**,** 2003-7.

Solodkin, A. & Van Hoesen, G. W. 1996. Entorhinal cortex modules of the human brain. *J Comp Neurol,* 365**,** 610-7.

Staff, N. P., Jung, H. Y., Thiagarajan, T., Yao, M. & Spruston, N. 2000. Resting and active properties of pyramidal neurons in subiculum and CA1 of rat hippocampus. *J Neurophysiol,* 84**,** 2398-408.

Stanton, P. K. & Sejnowski, T. J. 1989. Associative long-term depression in the hippocampus induced by hebbian covariance. *Nature,* 339**,** 215-8.

Staubli, U. & Lynch, G. 1987. Stable hippocampal long-term potentiation elicited by 'theta' pattern stimulation. *Brain Res,* 435**,** 227-34.
Stenkamp, K., Heinemann, U. & Schmitz, D. 1998. Dopamine suppresses stimulus-induced field potentials in layer III of rat medial entorhinal cortex. *Neuroscience Letters,* 255**,** 119-21.
Steward, O. 1976. Topographic organization of the projections from the entorhinal area to the hippocampal formation of the rat. *J Comp Neurol,* 167**,** 285-314.
Strauch, C. & Manahan-Vaughan, D. 2020. Orchestration of Hippocampal Information Encoding by the Piriform Cortex. *Cereb Cortex,* 30**,** 135-47.
Subramaniyan, M. & Dani, J. A. 2015. Dopaminergic and cholinergic learning mechanisms in nicotine addiction. *Ann N Y Acad Sci,* 1349**,** 46-63.
Sunanda, Meti, B. L. & Raju, T. R. 1997. Entorhinal cortex lesioning protects hippocampal CA3 neurons from stress-induced damage. *Brain Research,* 770**,** 302-6.
Sundqvist, M., Holdfeldt, A., Wright, S. C., Moller, T. C., Siaw, E., Jennbacken, K., Franzyk, H., Bouvier, M., Dahlgren, C. & Forsman, H. 2020. Barbadin selectively modulates FPR2-mediated neutrophil functions independent of receptor endocytosis. *Biochim Biophys Acta Mol Cell Res,* 1867**,** 118849.
Suzuki, W. A., Zola-Morgan, S., Squire, L. R. & Amaral, D. G. 1993. Lesions of the perirhinal and parahippocampal cortices in the monkey produce long-lasting memory impairment in the visual and tactual modalities. *J Neurosci,* 13**,** 2430-51.
Swanson, L. W. 1982. The projections of the ventral tegmental area and adjacent regions: A combined fluorescent retrograde tracer and immunofluorescence study in the rat. *Brain Research Bulletin,* 9**,** 321-53.
Taber, K. H., Black, D. N., Porrino, L. J. & Hurley, R. A. 2012. Neuroanatomy of dopamine: reward and addiction. *J Neuropsychiatry Clin Neurosci,* 24**,** 1-4.
Tahvildari, B. & Alonso, A. 2005. Morphological and electrophysiological properties of lateral entorhinal cortex layers II and III principal neurons. *J Comp Neurol,* 491**,** 123-40.
Takita, M., Izaki, Y., Jay, T. M., Kaneko, H. & Suzuki, S. S. 1999. Induction of stable long-term depression in vivo in the hippocampal-prefrontal cortex pathway. *Eur J Neurosci,* 11**,** 4145-8.
Thiele, S., Spehl, T. S., Frings, L., Braun, F., Ferch, M., Rezvani, A. H., Furlanetti, L. L., Meyer, P. T., Coenen, V. A. & Dobrossy, M. D. 2016. Long-term characterization of the Flinders Sensitive Line rodent model of human depression: Behavioral and PET evidence of a dysfunctional entorhinal cortex. *Behav Brain Res,* 300**,** 11-24.
Thompson, S. E., Ayman, G., Woodhall, G. L. & Jones, R. S. 2006. Depression of glutamate and GABA release by presynaptic GABAB receptors in the entorhinal cortex in normal and chronically epileptic rats. *Neurosignals,* 15**,** 202-15.
Thomson, A. M. 2000. Facilitation, augmentation and potentiation at central synapses. *Trends Neurosci,* 23**,** 305-12.
Tiberi, M., Nash, S. R., Bertrand, L., Lefkowitz, R. J. & Caron, M. G. 1996. Differential regulation of dopamine D1A receptor responsiveness by various G protein-coupled receptor kinases. *J Biol Chem,* 271**,** 3771-8.
Tikhonov, D. B. & Zhorov, B. S. 2017. Mechanism of sodium channel block by local anesthetics, antiarrhythmics, and anticonvulsants. *J Gen Physiol,* 149**,** 465-81.
Ting, J. T., Daigle, T. L., Chen, Q. & Feng, G. 2014. Acute brain slice methods for adult and aging animals: application of targeted patch clamp analysis and optogenetics. *Methods Mol Biol,* 1183**,** 221-42.
Tsao, A., Moser, M. B. & Moser, E. I. 2013. Traces of experience in the lateral entorhinal cortex. *Curr Biol,* 23**,** 399-405.
Tsao, A., Sugar, J., Lu, L., Wang, C., Knierim, J. J., Moser, M. B. & Moser, E. I. 2018. Integrating time from experience in the lateral entorhinal cortex. *Nature,* 561**,** 57-62.
Tsumoto, T. 1990. Long-term potentiation and depression in the cerebral neocortex. *Jpn J Physiol,* 40**,** 573-93.
Tulving, E. & Donaldson, W. 1972. *Organization of memory,* New York, Academic Press. pp. 382-402.
Vago, D. R., Bevan, A. & Kesner, R. P. 2007. The role of the direct perforant path input to the CA1 subregion of the dorsal hippocampus in memory retention and retrieval. *Hippocampus,* 17**,** 977-87.
Van Aerde, K. I. & Feldmeyer, D. 2015. Morphological and physiological characterization of pyramidal neuron subtypes in rat medial prefrontal cortex. *Cereb Cortex,* 25**,** 788-805.
Van Hoesen, G. W., Augustinack, J. C., Dierking, J., Redman, S. J. & Thangavel, R. 2000. The parahippocampal gyrus in Alzheimer's disease. Clinical and preclinical neuroanatomical correlates. *Ann N Y Acad Sci,* 911**,** 254-74.

Van Strien, N. M., Cappaert, N. L. & Witter, M. P. 2009. The anatomy of memory: an interactive overview of the parahippocampal-hippocampal network. *Nat Rev Neurosci,* 10**,** 272-82.
Vandrey, B., Armstrong, J., Brown, C. M., Garden, D. L. F. & Nolan, M. F. 2022. Fan cells in lateral entorhinal cortex directly influence medial entorhinal cortex through synaptic connections in layer 1. *Elife,* 11**,** 1-30.
Vandrey, B., Garden, D. L. F., Ambrozova, V., Mcclure, C., Nolan, M. F. & Ainge, J. A. 2020. Fan Cells in Layer 2 of the Lateral Entorhinal Cortex Are Critical for Episodic-like Memory. *Curr Biol,* 30**,** 169-75.
Vesikansa, A., Sallert, M., Taira, T. & Lauri, S. E. 2007. Activation of kainate receptors controls the number of functional glutamatergic synapses in the area CA1 of rat hippocampus. *J Physiol,* 583**,** 145-57.
Vianna, E. P., Ferreira, A. T., Dona, F., Cavalheiro, E. A. & Da Silva Fernandes, M. J. 2005. Modulation of seizures and synaptic plasticity by adenosinergic receptors in an experimental model of temporal lobe epilepsy induced by pilocarpine in rats. *Epilepsia,* 46, Suppl 5**,** 166-73.
Vismer, M. S., Forcelli, P. A., Skopin, M. D., Gale, K. & Koubeissi, M. Z. 2015. The piriform, perirhinal, and entorhinal cortex in seizure generation. *Front Neural Circuits,* 9**,** 27.
Voss, L. J., George, S. A. & Sleigh, J. W. 2012. Testing neocortical slice viability in non-perfused no-magnesium artificial cerebrospinal fluid solutions. *J Neurosci Methods,* 204**,** 273-5.
Vyleta, N. P. & Snyder, J. S. 2021. Prolonged development of long-term potentiation at lateral entorhinal cortex synapses onto adult-born neurons. *PLoS One,* 16**,** 1-16.
Warburton, E. C., Glover, C. P., Massey, P. V., Wan, H., Johnson, B., Bienemann, A., Deuschle, U., Kew, J. N., Aggleton, J. P., Bashir, Z. I., Uney, J. & Brown, M. W. 2005. cAMP responsive element-binding protein phosphorylation is necessary for perirhinal long-term potentiation and recognition memory. *J Neurosci,* 25**,** 6296-303.
Warburton, E. C., Koder, T., Cho, K., Massey, P. V., Duguid, G., Barker, G. R., Aggleton, J. P., Bashir, Z. I. & Brown, M. W. 2003. Cholinergic neurotransmission is essential for perirhinal cortical plasticity and recognition memory. *Neuron,* 38**,** 987-96.
Ward, J. 2020. *The Student's Guide to Cognitive Neuroscience,* London, New York, Routledge, Taylor & Francis Group. pp. 265-7.
Waugh, N. C. & Norman, D. A. 1965. Primary memory. *Psychological Review,* 72.
Weiner, D. M., Levey, A. I., Sunahara, R. K., Niznik, H. B., O'dowd, B. F., Seeman, P. & Brann, M. R. 1991. D1 and D2 dopamine receptor mRNA in rat brain. *Proc Natl Acad Sci USA,* 88**,** 1859-63.
Wightman, R. M. & Robinson, D. L. 2002. Transient changes in mesolimbic dopamine and their association with 'reward'. *J Neurochem,* 82**,** 721-35.
Williams, J. T., Ingram, S. L., Henderson, G., Chavkin, C., Von Zastrow, M., Schulz, S., Koch, T., Evans, C. J. & Christie, M. J. 2013. Regulation of mu-opioid receptors: desensitization, phosphorylation, internalization, and tolerance. *Pharmacol Rev,* 65**,** 223-54.
Winters, B. D. & Bussey, T. J. 2005. Removal of cholinergic input to perirhinal cortex disrupts object recognition but not spatial working memory in the rat. *Eur J Neurosci,* 21**,** 2263-70.
Witter, M. P. & Amaral, D. G. 2004. Hippocampal Formation. *In:* Paxinos, G. (ed.) *The Rat Nervous System.* 3rd ed. London: Elsevier Science & Technology. pp. 635-704.
Witter, M. P., Doan, T. P., Jacobsen, B., Nilssen, E. S. & Ohara, S. 2017. Architecture of the Entorhinal Cortex A Review of Entorhinal Anatomy in Rodents with Some Comparative Notes. *Front Syst Neurosci,* 11**,** 46.
Wong, J. H., Muthuraju, S., Reza, F., Senik, M. H., Zhang, J., Mohd Yusuf Yeo, N. a. B., Chuang, H. G., Jaafar, H., Yusof, S. R., Mohamad, H., Tengku Muhammad, T. S., Ismail, N. H., Husin, S. S. & Abdullah, J. M. 2019. Differential expression of entorhinal cortex and hippocampal subfields alpha-amino-3-hydroxy-5-methyl-4-isoxazolepropionic acid (AMPA) and N-methyl-D-aspartate (NMDA) receptors enhanced learning and memory of rats following administration of Centella asiatica. *Biomed Pharmacother,* 110**,** 168-80.
Wouterlood, F. G., Mugnaini, E. & Nederlof, J. 1985. Projection of olfactory bulb efferents to layer I GABAergic neurons in the entorhinal area. Combination of anterograde degeneration and immunoelectron microscopy in rat. *Brain Res,* 343**,** 283-96.
Wyllie, D. J., Livesey, M. R. & Hardingham, G. E. 2013. Influence of GluN2 subunit identity on NMDA receptor function. *Neuropharmacology,* 74**,** 4-17.
Wyllie, D. J. A. & Bowie, D. 2022. Ionotropic glutamate receptors: structure, function and dysfunction. *J Physiol,* 600**,** 175-9.

Yanagihashi, R. & Ishikawa, T. 1992. Studies on long-term potentiation of the population spike component of hippocampal field potential by the tetanic stimulation of the perforant path rats: effects of a dopamine agonist, SKF-38393. *Brain Res,* 579**,** 79-86.

Yang, C. R., Seamans, J. K. & Gorelova, N. 1996. Electrophysiological and morphological properties of layers V-VI principal pyramidal cells in rat prefrontal cortex in vitro. *J Neurosci,* 16**,** 1904-21.

Yeung, J. H. Y., Walby, J. L., Palpagama, T. H., Turner, C., Waldvogel, H. J., Faull, R. L. M. & Kwakowsky, A. 2021. Glutamatergic receptor expression changes in the Alzheimer's disease hippocampus and entorhinal cortex. *Brain Pathol,* 31**,** e13005.

Yoo, H. S., Jeon, S., Chung, S. J., Yun, M., Lee, P. H., Sohn, Y. H., Evans, A. C. & Ye, B. S. 2018. Olfactory dysfunction in Alzheimer's disease- and Lewy body-related cognitive impairment. *Alzheimers Dement,* 14**,** 1243-52.

Yun, S. H., Cheong, M. Y., Mook-Jung, I., Huh, K., Lee, C. J. & Jung, M. W. 2000. Cholinergic modulation of synaptic transmission and plasticity ln entorhinal cortex and hippocampus of the rat. *Neuroscience,* 97**,** 671-6.

Yun, S. H., Mook-Jung, I. & Jung, M. W. 2002. Variation in effective stimulus patterns for induction of long-term potentiation across different layers of rat entorhinal cortex. *J Neurosci,* 22**,** 1-5.

Zhang, X. M. & Luo, J. H. 2013. GluN2A versus GluN2B: twins, but quite different. *Neurosci Bull,* 29**,** 761-72.

Zhao, M., Choi, Y. S., Obrietan, K. & Dudek, S. M. 2007. Synaptic plasticity (and the lack thereof) in hippocampal CA2 neurons. *J Neurosci,* 27**,** 12025-32.

Zhou, Y., Zhang, Y., Zhao, D., Yu, X., Shen, X., Zhou, Y., Wang, S., Qiu, Y., Chen, Y. & Zhu, F. 2024. TTD: Therapeutic Target Database describing target druggability information. *Nucleic Acids Res,* 52**,** D1465-D77.

Zipursky, R. B., Reilly, T. J. & Murray, R. M. 2013. The myth of schizophrenia as a progressive brain disease. *Schizophr Bull,* 39**,** 1363-72.

Zola-Morgan, S., Squire, L. R., Amaral, D. G. & Suzuki, W. A. 1989. Lesions of perirhinal and parahippocampal cortex that spare the amygdala and hippocampal formation produce severe memory impairment. *J Neurosci,* 9**,** 4355-70.

Zola-Morgan, S., Squire, L. R., Clower, R. P. & Rempel, N. L. 1993. Damage to the perirhinal cortex exacerbates memory impairment following lesions to the hippocampal formation. *J Neurosci,* 13**,** 251-65.

Zorumski, C. F. & Izumi, Y. 2012. NMDA receptors and metaplasticity: mechanisms and possible roles in neuropsychiatric disorders. *Neurosci Biobehav Rev,* 36**,** 989-1000.

Appendices

Appendix A

Year	Medial Entorhinal Cortex	Lateral Entorhinal Cortex
2021	18	7
2020	18	5
2019	10	7
2018	19	6
2017	22	5
2016	16	3
2015	19	4
2014	17	3
2013	16	8
2012	12	4
TOTAL	**167**	**52**
AVERAGE	**16.7**	**5.2**

Table A1. Search results from 2012 to 2021 for search terms 'medial entorhinal cortex' compared to 'lateral entorhinal cortex' in title. *Source: National Library of Medicine*